Can the voluntary drive to a paretic muscle be estimated from the myoelectric signal during stimulation?

Runhan Luo

A thesis submitted in partial fulfilment
of the requirements for the degree of
Doctor of Philosophy
of the
Department of Medical Physics and Bioengineering
University College London

Supervisor: Prof. Nick Donaldson
Second supervisor: Dr. Anne Vanhoestenberghe

May 2013

Official declaration

I, Runhan Luo, confirm that the work presented in this thesis is my own. Where information has been derived from other sources, I confirm that this has been indicated in the thesis.

Acknowledgment

Many people say that the PhD will make you a different person, well, I agree with them. The last four years I spent in the Implanted Devices Group (IDG) has made me a better person. Finishing this PhD is one of the most challenging tasks I have ever done, and this would not have been possible without the guidance and the help of several individuals who in one way or another contributed and extended their valuable assistance in the preparation and completion of this study.

First and foremost, I would like to record my gratitude to my supervisor Professor Nick Donaldson for his supervision, advice, and guidance from the very early stage of this research as well as giving me extraordinary experiences throughout the work. His engineer intuition and broad knowledge have exceptionally inspired my growth as a student, a researcher and an engineer. I could not imagine having a better supervisor for my PhD study.

I was extraordinarily fortunate in having my colleagues and friends from the IDG whose advice, encouragement and support will never be forgotten. You made my life full of joy.

I would like to thank all the “healthy” subjects who contribute their legs to this project, thank you for not complaining when I demand higher stimulation intensities.

Special acknowledgement to my husband, Zhenhua, who has been really patient to me for the past 4 years (most of the time). He sacrificed a lot of his leisure time taking care of an irritable yet fragile person especially in the final days of the writing up. Words fail me to express my appreciation to his love and persistent confidence in me.

My parents, thank you for your unquestioningly support and unconditional love, for giving me the strength and conviction to complete this journey. It is not very common for the Chinese to say the word “love”, but I want you to know that I love you and it is great to be your daughter.

I was 5-week pregnant when I had the PhD viva, so technically my baby attend the viva with me. Although I haven’t met you yet, my son or daughter, I want you to know that I love you and I hope one day when you read this, you will feel proud of your mom.

Abstract

Patients with SCI (Spinal Cord Injury) sometimes recover lost function after using FES (Functional Electrical Stimulation). This phenomenon, known as the *carry-over effect*, is not fully understood. One theory used to explain this mechanism is that electrical stimulation of the peripheral nerve causes antidromic action potentials to reach the anterior horn cells at the same time that the patient's voluntary effort to activate the paralysed muscles is activating these cells. This may reinforce the motor pathways and consequently restore voluntary control of the muscles. However, the theory has never been properly tested and testing requires a method of measuring the voluntary drive. This project aims to find out whether it is possible to estimate the voluntary drive from measured myoelectric signals.

The project is based on an FES cycling system. A key feature of the system is that it adjusts the stimulation intensity relating to the corresponding voluntary drive to the same muscle. As the required FES cycling system did not exist prior to undertaking this project, a large part of the thesis discusses the building of the necessary electronic instrumentation, the design of the feedback control loop, development of the software program to record and process the data and identifying appropriate statistical tools to analyse the experimental data. Experiments were carried out both to test this apparatus and to investigate two techniques estimate the voluntary drive. Although the study only tested on able-bodied subjects, it would be possible to establish similar protocols for SCI patients.

In paretic muscles, the weak voluntary contraction produces an EMG response. The EMG signal measured in this way cannot be used directly as an indication of the voluntary drive because of the presence of stimulus artefact and reflexes which contaminate the EMG signal. Two methods were investigated to estimate the voluntary drive from the recorded EMG. Initially a time domain method was tested using RMS EMG extracted from a range of time windows following the stimulation pulse. This approach was unsatisfactory because the large variations seen in the RMS EMG amplitudes for the same power output as well as the low sensitivity of it to the change of power output. A frequency domain approach was then tested using coherence between co-contracting muscles. In the beginning it was encouraging to see that the area under the coherence curve in the selected frequency band reflected changes in the power output level. However, further tests showed that this area was also greatly influenced by exercise time, becoming unpredictable after 3 minutes. In conclusion, neither of the two methods of using the myoelectric signal from muscles under stimulation is practical for the estimation of voluntary drive in the proposed experiments.

TABLE OF CONTENTS

List of Figures

Chapter 2

Chapter 3

Chapter 4

Chapter 5

Chapter 6

Chapter 7

Chapter 8

Appendix

List of Tables

List of equations

Abbreviations

AB	Able Bodied
AC	Alternating Current
AFO	Ankle-foot Orthoses
AH	Anterior Horn
AISA	American Impairment Scale Association
AP	Action Potential
BF	Bicep Femoris
CC	Current Conveyor
CM	Common Mode
CMRR	Common Mode Rejection Ratio
CNS	Central Nervous System
DAQ	Data Acquisition
DC	Direct Current
DD	Double Differential
EEG	Electroencephalograph
EMG	Electromyograph
FES	Functional Electrical Stimulation
FFT	Fast Fourier Transform
GUI	Graphical User Interface
IDG	Implanted Device Group
ISCI	Incomplete Spinal Cord Injury
LTP	Long-term Potentiation
MEG	Magnetoencephalograph
MUAP	Motor Unit Action Potential
MVC	Maximum Voluntary Contraction
NINDS	National Institute of Neurological Disorders and Strok

NL	Non-linear
ODFS	Odstock Dropped Foot Stimulator
PCB	Printed Circuit Board
PCI	Physiological Cost Index
PH	Posterior Horn
PNS	Peripheral Nervous System
RF	Rectus Femoris
RMS	Root Mean Square
SEMG	Surface Electromyograph
SCI	Spinal Cord Injury
SD	Single Differential
SENIAM	Surface Electromyography for the Non-Invasive Assessment of Muscles
TA	Tibialis Anterior
TDC	Top Dead Centre
VL	Vastus Lateralis
VM	Vastus Medialis

CHAPTER 1 THESIS OUTLINE

There are 8 chapters in this thesis, structured as shown in Table 1. 1.

Table 1. 1: Thesis lay out.

	Chapters							
Content	1	2	3	4	5	6	7	8
Outline								
Literature review								
Hardware development								
Voluntary drive estimation (two methods)								
Disucssions, conclusions and future work								

In chapter 2, the structure of the spinal cord, spinal cord injury, and, the anatomy and physiology of skeletal muscles are introduced, along with a brief introduction to FES. The chapter then carries on introducing the concept of neuroplasticity which supports the finding of motor relearning and carry over effect found after FES treatment. An important hypothesis suggested by Rushton (Rushton, 2003) is adapted as a possible explanation to the mechanism behind the carry-over effect. In the end of this chapter, a brief description of the proposed FES cycling system is described.

Chapter 3 discusses the Electromyogram and various signal processing techniques used to analyse it, as are frequently seen in the literature. An important aspect of the thesis is highlighted, namely the problems encountered when trying to interpret EMG signals captured under stimulation. When an active muscle is stimulated, there are stimulus artefact and other physiological effects which continue after the stimulation pulse has come to an end, contaminating the recorded EMG activity. These physiological effects are also considered to be artefacts in this thesis and consequently have to be removed before the EMG signals could be analysed. Another factor that may influence the interpretation of the recorded EMG signals is muscle fatigue. Therefore a general review of muscle fatigue, as well as a review of muscle fatigue during cycling, under stimulation, are presented in this chapter. The muscle activation range during cycling is considered and a few commercially available FES cycling systems are discussed. Towards the end of the chapter, a more detailed description of the FES cycling system, developed for this study, is given.

The development of the FES cycling system required the design and construction of assorted apparatus. This is the focus of Chapter 4. The apparatus discussed includes: differential EMG amplifiers, blankable EMG amplifiers, a fast recovery EMG amplifier, isolation amplifiers,

stimulators, and a commutator. These devices were designed specifically for this project. Other apparatus, which were originally built for different applications, were modified for our purposes. This included the tricycle, the shaft encoder, the EMG amplifier with current conveyor, the biphasic stimulator and the TACX ergotrainer. The constructed EMG amplifiers were tested and the influence of the stimulation artefact on their measured outputs compared. Some of the EMG amplifiers were selected for use in an experiment to investigate the muscle activation range of the quadriceps during tricycling.

The main body of the thesis is presented in chapters 5 through 7. These chapters present two different methods, used to estimate the voluntary drive, as well as an experimental evaluation of both methods. The relevant literature (especially for Chapter 6 and 7), as well as any further modifications that have to be made to the apparatus, during experimental investigation of the two methods, are discussed in the relevant chapters. This is so that the reader is presented with information relevant to the matter currently under discussion.

In chapter 5, the time domain method is discussed. This method is a simple approach to estimating the voluntary activity by recording the RMS amplitude of the EMG signal during a short time interval, referred to as a window, after the stimulus pulse. The method was tested in 5 neurologically intact subjects. It was shown that, with an appropriate choice of window, the measured EMG is highly correlated to the RMS EMG before the stimulation. This was considered to be a good representation of the voluntary drive. We proceeded to examine the relationship of such signals with the subject's exertion required to maintain a steady cycling cadence against different effort levels.

A different approach, using a frequency domain analysis, is then considered (Chapter 6). This new method uses coherence. Coherence is found between EMG data recorded from muscles that work synergistically. Coherence in the range of the β band is considered to be related to the common motor drive to the skeletal muscles from the motor cortex. It is therefore proposed to use the coherence in the β band as a possible estimation of the subject's voluntary drive. This coherence method, offers advantages over the time domain method, as the frequency component of the stimulation artefact is different from that of the frequency band defined the coherence of interest. The influence of changes in effort level on the coherence is investigated.

Chapter 7 evaluates coherence as a control signal in a real time environment. A control box, designed for controlling the stimulation intensity via software written in LABVIEW, is constructed. A new program is written to record the raw EMG signals, calculate the coherence and adjust the

stimulation intensity to one of the five stimulation levels set by the control box. An experimental investigation of changes in coherence against effort level, in realtime, is presented.

Chapter 8 concludes the thesis with a discussion, bringing together the important findings of this study. A summary of the major achievements and critical reviews of the methods are given. Possible directions for future research are also highlighted.

CHAPTER 2: ESSENTIAL PHYSIOLOGY AND MOTOR RELEARNING

2.1 Introduction

People with incomplete spinal cord lesions and other conditions causing paralysis in the legs, are often forced to use wheelchairs. The lack of leg exercise causes medical complications (fractures, pressure sores, heart disease). FES, which produces contractions in weak or paralysed muscles after SCI, has been seen to reduce the risk of developing these medical complications (Kjaer, 2000). In these patients, appropriately-timed stimulation can dramatically improve functions, for example, correcting foot-drop while walking (Liberson, 1961; Taylor 1999) or improving grasping force following stroke (Prochazka, 1997).

This project aims to develop a Functional Electrical Stimulation (FES) cycling system that can effectively exercise the paralysed muscles of Spinal Cord Injury (SCI) patients and provide therapeutic benefits. In this chapter, the essential physiology and the fundamentals of FES and FES-induced functional recovery are introduced.

2.2 The spinal cord anatomy

The human nervous system is often divided into the Central Nervous System (CNS) and the Peripheral Nervous System (PNS). The CNS contains the brain and the spinal cord; it is the controlling part of the nervous system that gives commands to the rest of the body. The PNS composes all the nerves after they have left the spinal cord, these nerves constitute a communication network that deliver the commands from CNS to the rest of the body as well as carry the information from the body back to the CNS. The PNS breaks off into two divisions, the autonomic and somatic nervous systems. The autonomic nervous system includes all of the neural pathways that result in involuntary actions, i.e. it functions below the level of consciousness. Somatic nervous system includes all of the voluntary control of the body movements via skeletal muscles. For the interest of this project, only the Somatic nervous system is considered.

The anatomy of the spinal cord provides essential knowledge to understand the anatomical terms used later when introducing the relevant neurophysiology. The spinal cord is a long, tubular cord surrounded by the bony vertebral column. The vertebrae consist of 33 segments. Pairs of spinal nerves arise from the spinal cord and leave the vertebrae through a hole in each vertebra called the intervertebral foramina. Based on their exit levels, the spinal nerves can be divided into four groups (Conn, 2003). The 5 sacral and 4 coccygeal vertebrae are often considered together as they are fused together to form 1 bone called the sacrum. These spinal nerves are responsible for transmitting information between the muscles, organs, trunk and the brain. Depending on their functions, these nerves are divided into sensory and motor nerves.

The sensory nerves carry information from the body going up towards the brain and motor nerves carry information from the brain down to the body (Watson et al., 2008)

Figure 2. 1 shows the cross section of the spinal cord. The grey butterfly-shaped are in the centre of the cord is the grey matter. It consists of cell bodies of interneurons and motoneurons (motor neuron). Projections of the grey matter are called horns, the ventral one is called the anterior horn (AH) and the dorsal one is called posterior horn (PH). The AH contains motoneurons that affect the movements of the muscles while the PH receives information regarding touch and sensation. The white matter is located outside of the grey matter towards the edge of the spinal cord. It consists of nerve fibres entering from dorsal roots; nerve fibres exiting to ventral roots; and millions of longitudinally oriented fibres. These longitudinally oriented fibres are mostly myelinated and are grouped into "columns or tracts". There are six ascending tracts and four descending tracts which are responsible for carrying information either up or down the spinal cord.

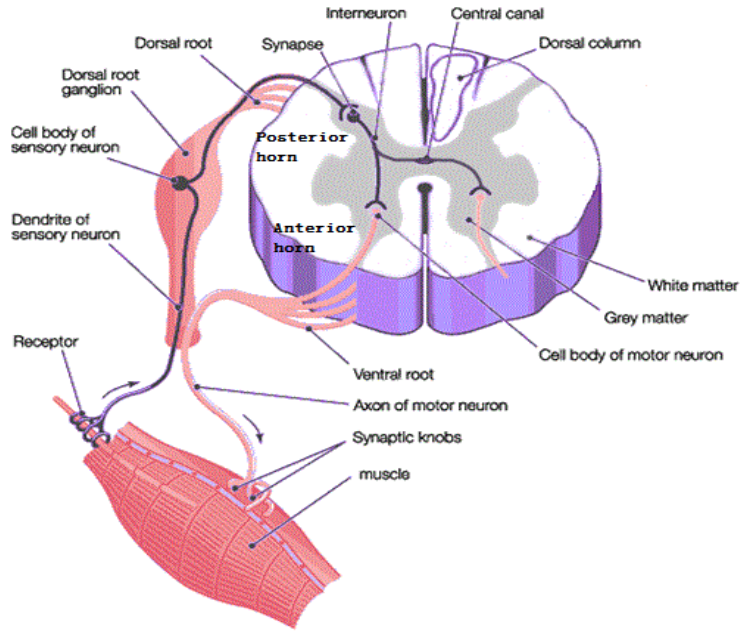

Figure 2. 1:Cross section of the spinal cord with the dorsal (posterior) and ventral (anterior) roots, modified from (Yvonnes neuropsychology pictures, 2011).

2.3 Spinal cord reflex pathways

If we take a closer look at the posterior root (or dorsal root), the neuron in Figure 2. 1 represents one of the many neurons that are inside the posterior root, all these neurons are sensory neurons which bring information to the spinal cord. The neurons have their cell bodies located in a discrete cluster known as the dorsal root ganglion. The neuron goes into the spinal cord at the

posterior location and enters the posterior horn of the grey matter. At the end of the sensory neuron, there is a synapse. A synapse is a structure that permits a neuron to pass electrical or chemical signal to another cell. It is also the key structure that neuroplasticity might occur (see 2.7). Between the sensory neuron and the synapse, there are a large number of neurons called interneurons which are not leaving or entering the CNS. These interneurons, which are also called “connector neurons”, form connections between other neurons. There is another synapse between the interneuron and the motoneuron whose cell body is in the anterior horn of the grey matter. The motoneurons travel through the anterior root carry the motor information from the spinal cord to the body. All the motor neurons exit the spine via the anterior root (ventral root). The inflow and outflow of the sensory and motor neurons join together to form the spinal nerve.

2.4 Spinal cord injury

A Spinal Cord Injury (SCI) is damage or trauma to the spinal cord that results in loss or impaired functions causing reduced mobility or feeling (Harvey, 2008). It has a devastating effect on the patient and their family. There are three dominating causes for Spinal Cord Injury (SCI): road traffic accidents, domestic & industrial accidents and sports injuries (Grundy & Russell, 1986). The majority of SCI patients are aged 16 – 30years, with a male:female ratio of 4:1 (Lindsay et al., 2010) There are currently 11 SCI centres in UK designed to receive and treat SCI patients. During the year 2000, reports show that there were 666 new patients’ admissions to the SCI centres in UK (Apparelyzed spinal cord injury peer support, 2010). This does not include anyone treated acutely in the general hospitals.

The effects of SCI depend on the type of injury and the level of the injury. There are different ways to define a SCI. It can be classified with the American Impairment Scale Association (AISA) Classification, as AISA A, B, C, D or E shown in Table 2. 1.

Table 2. 1: AISA Impairment Scale reproduced from AISA (AISA, 2013).

ASIA Grade	Level of Impairment
A	No motor or sensory function preserved in the lowest sacral segments (S4 and S5)
B	Sensory but no motor function preserved, including the lowest sacral segments (S4-S5)
C	Motor function present below the injury, but the strengths of more than half of the key muscles are graded < 3 of 5
D	Motor function present below the injury, but the strengths of more than half of the key muscles are graded ≥ 3 of 5
E	Motor and sensory functions in key muscles and dermatomes are normal

Alternatively; SCI can be divided into two types of injury - complete and incomplete (Grundy & Russell, 1986). A complete lesion means that there is no function below the level of the injury; no sensation and no voluntary movement. Both sides of the body are equally affected and the patient cannot feel anything below the lesion. However, this definition is difficult to apply to all situations as SCI can be very complicated and different depending on each trauma. For example, some patients may have zones of partial preservation of sensory and/or motor functions below

the lesion; or the patients may initially have no function below the injury level but gradually recovers some motor or sensory function. Therefore it is hard to define whether an injury is complete or incomplete. These facts were taken into consideration when the AISA (American Impairment Scale Association) Committee forms the regulation in 1992 which they indicate that if a person has no motor and sensory function in the anal and perineal region representing the lowest sacral cord (S4-S5), he is a complete ("ASIA | American Spinal Injury Association website," accessed 2010).

Since 2010, the most frequent neurologic category at discharge of persons reported to the database is incomplete tetraplegia (40.6%), followed by incomplete paraplegia (18.7%), complete paraplegia (18.0%) and complete tetraplegia (11.6%). Less than 1% of persons experienced complete neurologic recovery by hospital discharge (National Spinal Cord Injury Statistical Centre, 2013). An incomplete lesion means that there are some functions remaining below the lesion. An incomplete SCI patient may have sensations of the body below the injury level. In some cases one side of the body may function better than the other. Some muscle functions, like voluntary muscle control may be preserved. Incomplete SCI is more common than complete. This is largely because medical team now follow more efficient procedures to reduce further damage from occurring, allowing an injury to become “complete”. The proposed FES cycling system target at the incomplete SCI patients with some intact motoneurons below the lesions.

Injury to the spinal cord triggers a series of biological events that unfold within seconds and proceed for months or even years. Understanding the progression of the spinal cord injury, including the biochemical reactions and pathways that are involved in the process, enables people to control and to influence its progression, hence to preserve the regenerative potential of the spinal cord with perhaps maximum possibility, for improvement and development of therapies.

There are three phases of SCI response that occur after injury: the acute, secondary, and chronic injury processes (Tator 1995; Tator 1996; Tator 1998). Most of the patients in the acute injury phase were treated by the emergency medical service during, where steroids (like methylprednisolone) were given to reduce inflammation as well as to reduce the extent of permanent paralysis (Bracken, 2012). The secondary and chronic injury processes generally make better therapeutic targets as they occur in the later stages of injury. The major systems in the body including the nervous system, the immune system and the vascular system respond to injury dynamically. Although some injurious responses heal and promote the recovery of function, others leave a wave of tissue damage that expands well beyond the original site of injury (Liverman, 2005).

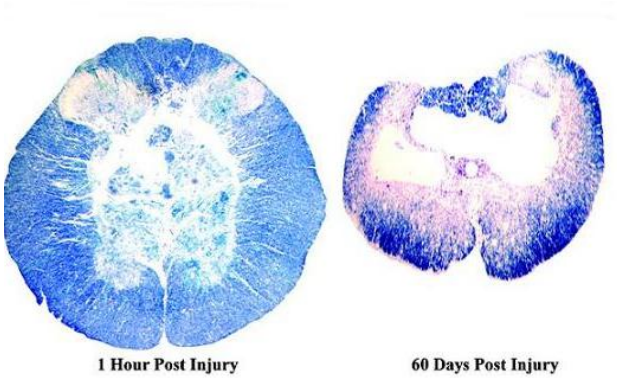

Figure 2. 2: Full cross section of a damaged spinal cord showing tissue loss after the injury. It is stained with a blue myelin stain (luxol fast blue), so the white matter is blue and the grey matter is pinker, reprinted from (Hulsebosch 2002).

The left picture of Figure 2. 2 is the cross section of a rodent contusion model of SCI, with a necrotic core surrounded by histologically normal-appearing myelinated fibres and portions of grey matter from both dorsal and ventral horns. Irreversible damage has already happened here immediately after the initial impact in the central core region which causes massive cell death. After that, the lesion grows in size from the initial core of cell death and the cell loss continues radially in all directions over time. By 60 days post-SCI, there remains only a thin rim of white matter as shown in the right picture (Hulsebosch 2002). What needs to be noted here is the absence of motor and sensory function below the injury site does not necessarily mean that there are no axons that cross the injury site. More precisely, there are fewer axons crossing the lesion. Cell bodies under the lesion which are isolated from the brain for incomplete SCI still have neurological functions but may no longer be controlled by the brain. This is an important foundation to support the hypothesis of our project as explained later in 2.10.

2.5 Anatomy and Physiology of skeletal muscles

Muscles are the tissues which convert chemical energy into mechanical energy (Basmajian, 1962). All muscles regardless of their type are specialized for contractions; these contractions produce various types of movements in the body. There are three types of muscle tissues in the human body: smooth, cardiac and skeletal muscles. The focus of this project is the skeletal muscle which is made up of long muscle fibres, terminated at each end by tendinous material attached to the bone. Skeletal muscles are used to create movement by contraction and generally contract voluntarily, hence also called voluntary muscle. The functional unit in the voluntary muscle is the Motor Unit (MU), which is the combination of an alpha motoneuron (α-motoneuron) and the set of muscle fibres it innervates (Basmajian, 1962). When initiating a voluntary movement, the brain sends signals in the forms of Action Potentials (APs) through the spinal cord to the motor unit. One AP descending the motoneuron causes all the muscle fibres in one motor unit to contract almost simultaneously to generate a twitch and in normal muscle activity, streams of Aps cause tetanic contractions (Basmajian, 1962). MU recruitment is the progressive activation

of a muscle by successive recruitment of MUs to accomplish increasing gradations of contractile force (Ounjian et al., 1991). The recruitment of the MUs when performing a task follows the Henneman's size principle, which states that MUs are recruited in order of increasing size (Henneman et al., 1965). Such a mechanism uses the most fatigue-resistant muscle fibres most often and holds more fatigable fibres in reserve until needed to achieve higher forces thereby minimising the development of fatigue.

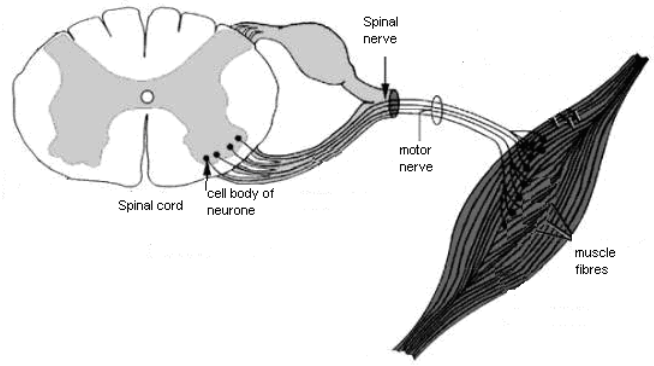

Figure 2. 3: Schematic of a motor unit. (Modified picture from (Basmajian, 1962)).

2.6 Functional Electrical Stimulation (FES)

The activation of muscles using electrical stimulation of the relative peripheral nerve has a long history. There was a lot interest in electrical stimulation for treating diseases in the 18th century in England. In 1756, electrical therapists in Shrewsbury hospital treated a woman's rheumatic pain in her right arm with electrical shock (Fara, 2003). John Wesley and his fellow physicians used electricity to treat illnesses "of the nervous kind" (Fara, 2003). Yet today many people still consider Luigi Galvani as the father of electrophysiology (Dibner, 1971). He first observed motion after applying electrical wires to leg muscles severed from the body of frogs in 1777 (Cambridge, 1977). In 1831, Michael Faraday showed that electrical currents could stimulate nerves to create active movement (Cambridge, 1977). Later electrical stimulation was used to stimulate the peroneal nerve in the leg in an effort to correct foot drop in patients with stroke-related hemiplegia (Liberson, 1961). In 1967, FES was formally described as "electrical stimulation of muscle deprived of nervous control with a view of providing muscular contraction and producing a functionally useful moment" (Gracanin, 1984). Since then, FES has been used in the upper and lower extremities to achieve functional movements like grasping, knee joint movement, standing and walking (Hausdorff & Durfee, 1991; Keith & Peckham, 1988; Mangold & Keller, 2004; Popovic & Keller, 2001; Popovic et.al, 2005). In terms of control strategy, these researches all used conventional open loop systems. These open loop systems are designed to perform certain motor tasks with pre-programed stimulation patterns and intensity i.e. the applied stimulation

was not modulated by any feedback. They activate the muscle in an unnatural way – all the muscle fibres contract at the same time which results in early muscle fatigue.
In more recent years, closed-loop FES has become a more active field in rehabilitation engineering (Cozean et al., 1988; Fields, 1987; Francisco et al. , 1998). Closed-loop FES systems require controllers with inputs of the ongoing changes in the system. This usually involves sensors like accelerometer, gyroscope, or goniometer which provide measurement of the current state of the system. One major advantage of such a closed loop FES system is that it responds to any disturbances that may happen. In other words, it has the ability to regulate any errors in the system by analysing the feedback signal. These processed feedback signals are fed back to the controller to further modulate the stimulation.

Depending on the severity of the injury, different control signals recorded from the patients could be used to achieve functional movements. There are two types of signals represent the popular choices of feedback signals used in research field, Electroencephalogram (EEG) and EMG (see 3.2). If we consider the pathway of a muscle movement. The brain initiates the process by sending command though the spinal cord to the muscles. People with high level lesions (C4 or above) whose spinal cords can no longer carry signals to their limbs might still be able to complete the initiation phase in their brains, this EEG can be used as the control signal to trigger a neuroprostheses to carry out the movement. An experiment carried out by Chapin and Moxon used microwires implanted in the motor cortex area of the brain to record brain-wave activity, which was then relayed to a computer that analysed the data, predicted the movement, and sent the command to a robotic arm (Chapin & Moxon, 1999). A device such as this could be used to control a wheelchair, a prosthetic limb, or even a patient's own arms and legs with stimulators.

On the other hand, because of the lesion in the spinal cord, the nerves to activate the muscles can no longer receive command from the brain. The pathway from the AH cell to the MU is intact and it is still capable of giving contractions, which can be demonstrated by measuring its EMG, but it is no longer under voluntary control due to the damage to the spinal cord injury. The measured EMG signal, or the voluntary effort of the subject is trying to use the muscles can also be used in closed-loop control of FES. Adopting EMG for FES application has a long history (see 3.10), but this method is not so popular due to some limitations. Most FES applications aim to achieve functional movements for paralysed people who have lost the voluntary control of their muscles. For people with SCI, it is not always possible to acquire EMG signals from the selected muscles, therefore careful patient selection should be performed before the trials. As described in 2.4, incomplete SCI patients with some intact lower motoneurones can benefit from EMG controlled FES. Also, when recording EMG from the same muscle that is being stimulated, the stimulation interferes the EMG signal therefore making it very difficult to interpret (see 3.5). Despite the difficulties of EMG controlled FES systems, adopting EMG for FES control can also exhibit some advantages, since the user activates the same muscles as being stimulated. This

might lead to a natural way for the user to control their neural prosthesis. Some researchers reported a carry-over effect after using such EMG-controlled FES systems (see 2.8), which lead to another possible benefit of FES – functional recovery. This functional recovery is often considered as a result of motor relearning. To understand this mechanism, the fundamentals of motor neuroplasticity and motor relearning are introduced in the following sections.

2.7 Neuroplasticity

Plasticity of the nervous system has long been an important theme in psychology and neurosciences. It was first introduced by James (James, 1890) in his book, *The principles of psychology*, where he states: "An acquired habit is nothing but a new pathway of discharge formed in the brain…nervous tissue seems endowed with a very extraordinary degree of plasticity… Plasticity means the possession of a structure weak enough to yield to an influence, but strong enough not to yield all at once." That is, an existing neuronal pathway can be reinforced gradually with past experience.

The term "neuroplasticity" is a fundamental concept in neuroscience: it is possible because of the ability of neurons to rearrange their anatomical and functional connectivity and properties in response to input change in the nervous system (Shaw & McEachern, 2013). Each neuron is a cell that forms contacts with other neurons. Based on the neuron doctrine, Tanzi and Ramon y Cajal independently proposed that the brain plasticity probably takes place at the junctions between neurons (Ramon y Cajal, 1893; Tanzi, 1893). Later Sherrington named these junctions synapses (Sherrington, 1906). The idea that the brain is composed of interconnected neurons and that a change in behaviour is mediated by a change in cellular and synaptic properties continues to serve as the basis for theories concerning neuroplasticity.

Neuroplasticity could be described by Hebbian rules as first described by Daniel Hebb:

When an axon of cell A is near enough to excite cell B and repeatedly or persistently takes part in firing it, some growth process or metabolic change takes place in one or both cells such that A's efficiency, as one of the cells firing B is increased.

–Hebb (Hebb, 1950)

Hebb assumed that synaptic function is strengthened by coactivation of a presynaptic fibre and its postsynaptic neurone. The synaptic transmission from a presynaptic fibre, *a*, to its postsynaptic neurone, *b*, increases in efficiency when excitation occurs concurrently and repeatedly in both elements (Hebb, 1950). The first clues for the molecular basis of how a nervous system can display neuroplasticity and adapt its motor behaviour was found in the invertebrate sea-slug Aplysia California by Eric Kandel and his group (Eisenstadt et al., 1973; Frazier, 1967; Klein & Kandel, 1978; Kriegstein, Castellucci, & Kandel, 1974). Changes in synaptic properties were shown to occur after the Aplysia California had acquired a memory. This led to the discovery of long-term potentiation (LTP) in the mammalian hippocampus 1973 by Bliss and

Lomo (Bliss & Lomo, 1973), which provided a molecular mechanism for neuroplasticity that obeys Hebbian principles. Hebbian principle provides a framework that governs neuroplasticity, allowing synapses to retain a memory of previous activity. The synapse that features concomitant activation of pre-and postsynaptic elements is now termed a Hebbian synapse.

Hebb-type synapses have since been discovered in many species and in many locations. They have been of particular interest in the brain, in the context of learning and memory. The underlying mechanism is thought to be LTP, which is originally described in the hippocampus of the rabbit (Bliss & Lomo, 1973). It was later identified as a phenomenon occurring in many areas of the mammalian CNS, including the anterior horn of the spinal cord (Pockett & Figurov, 1993). Pockett and FIgurov applied stimulation at 100Hz to the dorsal horn-intermediate nucleus region of transverse slices of rat spinal cords and found LTP in 25% of slices. The long-term changes lasted at least 2.5 hours. This suggests that the synapses between pyramidal tract axon and the anterior horn cell may indeed be a modifiable Hebb-type synapse.

2.8 Motor learning

Learning is behavioural modification resulting from experience (Thompson, 1967). Novel motor skills are learned through repetitive practice and, once acquired, persist long after training stops (Karni et al., 1995; Luft & Buitrago, 2005). There are few universally agreed definitions of motor learning, the broadest definition is: a lasting change in motor performance shaped by prior experience. It is also described by Krakauer in more detail:

"Motor learning does not need to be rigidly defined in order to be effectively studied. Instead it is better thought of as a fuzzy category that includes skill acquisition, motor adaptation, such as prism adaptation, and decision making, that is, the ability to select the correct movement in the proper context. A motor skill is the ability to plan and execute a movement goal."

-Krakauer (Krakauer, 2006)

A key feature from the definition and description of motor learning is that it involves changes in motor performance, and motor performance (outcome) can be measured in a number of different ways depending on the goal. The mechanisms underlying motor control and the acquisition of motor tasks are complex and not yet fully understood.

2.8.1 Motor learning at synaptic level

Earlier studies have shown that long-lasting learning induces an increase in the efficacy of synapses in the primary motor cortex, the persistence of which is associated with retention of the task (Harms & Rioult-Pedotti, 2008; Rioult-Pedotti et al., 2007). Researchers in University of California have demonstrated that new connections begin to form between brain cells almost immediately as animals learn a new task (Xu et al., 2009). They trained mice to reach through a slot to get a seed repeatedly and imaged the same apical dendrites of pyramidal neurons in various cortical regions during and after motor learning, using transcranial two-photon

microscopy. The formation of new structures called "dendritic spines" that grow on pyramidal neurons in the motor cortex. The dendritic spines form synapses with other nerve cells. At those synapses, the pyramidal neurons receive input from other brain regions involved in motor memories and muscle movements. The growth of new dendritic spines is followed by selective elimination of pre-existing spines, so that the overall density of spines returned to the original level. The new spines induced during learning are preferentially stabilized during subsequent training and endure long after training stops. Practice of novel, but not previously learned, tasks further promotes dendritic spine formation in adulthood. Their findings reveal that rapid, but long-lasting, synaptic reorganization is closely associated with motor learning (Xu et al., 2009).

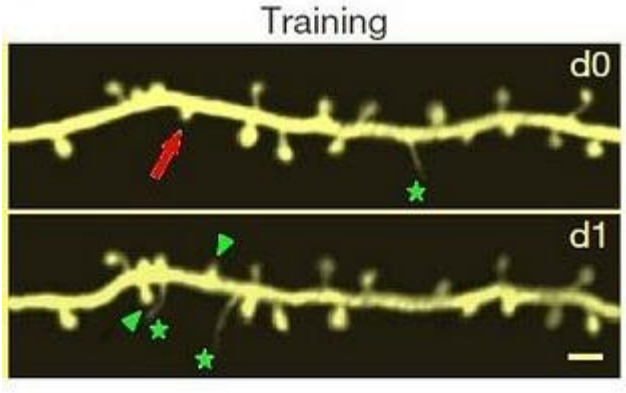

Figure 2. 4: Enhanced spine dynamics of a neuron: the little blobs above and below are individual dendritic spines. The top image shows the cell before training, and the bottom image is the same neuron 24 hours later, after skill learning. Several new dendritic spines have grown and a few old dendritic spines have disappeared reprinted from (Xu et al., 2009)

2.8.2 Motor learning after SCI

In addition to Hebb's idea described in 2.7, Gordon Allport introduces the "auto-association theory" described as follows:

"If the inputs to a system cause the same pattern of activity to occur repeatedly, the set of active elements constituting that pattern will become increasingly strongly interassociated. That is, each element will tend to turn on every other element. To put it another way, the pattern as a whole will become 'auto-associated."

-Allport (Allport, 1985)

In other words, it is possible to "re-associate" the synaptic connections by repeatedly performing the same task. This idea was extended firstly by Carr and Shepherd in 1987 as part of their 'Motor Relearning Approach' (Carr & Shepherd, 1987, 1990, 1997) and later by Shumway-Cook and Woollacott in their 'Task-Oriented Approach' (Shumway-Cook & Woollacott, 2007). They proposed the key feature of learning motor tasks is intense, well-structured and active practice which is task- and context-specific. Task- and context-specific practice implies practice of precisely the task which needs to be learned. Often patients with newly acquired spinal cord

injury are unable to perform motor tasks because they lack skill. That is, they do not know how to move optimally with their paralysis. Daily motor tasks like rolling in bed or standing now require novel patterns of muscle activation. However, by repeating these tasks, either with the help of trained physiotherapists or with the aid of neuroprostheses, the patients can master these novel motor tasks. The synaptic connections which were once lost or weakened could be restored or strengthened, hence promoting functional recovery. These motor tasks need to be learnt with repetitious practice.

Electrical stimulation induced goal-oriented repetitive movements could also promote motor relearning. Among all the other applications, EMG-controlled electrical stimulation time locked to repetitive movements has demonstrated improvement in motor impairment (Francisco et al., 1998). Such FES systems with designed repetitive exercised are now used together with traditional physiotherapy. Selected systems are reviewed in 3.12.

2.9 The carry-over effect

As supported by the National Institute of Neurological Disorders and Stroke (NINDS), FES is often used in “retraining neural circuits to restore body functions” (NINDS, accessed 2010). By constantly repeating a lost function using FES, it is possible to retrain the neural circuit of the patients to relearn the function (Chae & Fang, 2001; Cozean et al., 1988; Fields, 1987; Khaslavskaia & Sinkjaer, 2005). The carry-over effect was first reported by Liberson in 1961: “On several occasions we observed, after training with the electrophysiologic brace, patients acquired the ability of dorsiflexing the foot by themselves, although the period of spontaneous activity were only transitory (Liberson et al. 1961).” It was also reported by many other researchers: Chae (Chae, 2008) suggested that repetition of goal-oriented active movement could promote motor-relearning in his work with hemiparetic patients using neuromuscular electrical stimulation; Stefancis found more normal pattern of muscle activation with increased reciprocal inhibition and low amplitude in previously silent muscles in more than half of his 15 hemiplegic subjects which he believed to be “central reprogramming mechanism” (Stefancis, 1976). Here we are going to talk about three examples, each representing a scale of impairment, from the least paralysed (foot drop stimulator user) to incomplete spinal cord injury patient (Fitzwater and FES cycling) then to the most server complete spinal cord injury (Reeve). They were all treated with electrical devices and managed to demonstrate some recovery after the treatment which was believed to be “carry-over effect”.

The foot drop stimulator acts as a walking aid to correct dropped foot which is a condition often seen with stroke, multiple sclerosis, ISCI, brain injury and other neurologic diseases. A successful example of this application is the Odstock Dropped Foot Stimulator (ODFS). The device uses single-channel stimulation with surface electrodes to correct dropped foot (Taylor et al., 1999). The stimulation is synchronised to the gait cycle by using a pressure-sensitive switch in the shoe sole. When the patient lifts his heel, the pressure on the switch is reduced which triggers the stimulation and causes the tibialis anterior (TA) to contract hence lifting the foot and completing

the swinging phase (Taylor et al., 1999). With prolonged use, patient can receive benefits like improved balance during walking, reduced spasticity of quadriceps, increased the range of motion of ankle and improved walking gait.

In a large study with 151 ODFS users who had been using the device for an average of 4.5 months, increase in walking speed and effort was found in some patients (Taylor et al., 1999). The patients were asked to complete six 10-metre walking trials with randomized chance of being stimulated. A 10% increase in walking speed and decrease in effort without stimulation was considered to be positive. This was assessed by Physiological Cost Index (PCI) = (walking heart rate—resting heart rate)/walking speed. Over 50% of stroke and SCI users had achieved this. This outcome was considered to be a demonstration of the carry-over effect.

In a pilot study of FES cycling at the Implanted Device Group (IDG) in University College London (UCL), Fitzwater who has an incomplete lesion at T11/12 participated (Donaldson et al., 2000). An 8-channel stimulator was used to provide stimulations pulse at 20Hz with pulse period up to 500μs on 8 muscle groups (4 from each leg). Two switches were used to control the stimulation. One switch controlled left quadriceps and right Hamstring and the other one controlled the right quadriceps and left Hamstring. The stimulator was operated by Fitzwater himself, so he was aware when the stimulation was going to happen to which muscle groups either for a push or pull action to complete the pedalling action. So it was very likely that he was voluntarily trying to use the corresponding muscles while stimulating them. He received near-isometric exercise to increase endurance and to perform FES cycling. After training for an average of 21 minutes per day for 15 months, Fitzwater was able to cycle on tarmac level at 7.7km/h for 12km. Recovery of voluntary strength and natural leg function was found besides the increased muscle thickness. This recovery of voluntary function has allowed him to walk short distances with one crutch, to pick things up from the floor more easily and for his left leg to move itself when it becomes uncomfortable (he has residual sensation). This was believed to be the first report on FES cycling promoted neuromuscular re-education with improved voluntary leg function, and was a successful demonstration of carry-over effect.

If we consider the case of Christopher Reeve, who was completely paralysed and partially recovered five to seven years after his injury. It is believed his improved function was the result of vigorous physical activity. He began exercising the year he was injured. It was then after five years that he first noticed that he could voluntarily move his index finger. An intense exercise program was planned for him including daily electrical stimulation of his arms, quadriceps, hamstrings and other muscle groups to increase muscle mass. He also did FES cycling three times a week under the supervision of Dr. McDonald at Washington University (McDonald, 2004). As shown by the scientific literature on SCI patients (McDonald & Becker, 2002), most recovery will occur in the first six months after injury and generally complete within two years. Reeve's case has demonstrated it is possible to achieve functional recovery even after 5 years. Reeve and McDonald suggested that the activities that he had been doing may have 'awakened' dormant nerve pathways. It seems likely those axons in the cord that were spared by the injury, and were

dormant after the injury, were utilised during the electrical therapy. It was not possible in a single experiment to know just what did occur in his nervous system, however, a mechanism behind such recovery was hypothesised.

2.10 The hypothesis

An explanation is needed to help researchers understand the mechanism behind the carry-over effect. The carry-over effect after FES leads to a presumption that FES may somehow promote adaptive changes in brain or spinal cord hence may result in functional recovery (Rushton, 2003). It is necessary to understand the mechanism of change that happens to the spinal cord when the nerve is being stimulated. Stimulation of a peripheral nerve during muscle contraction has many consequences as APs are launched bi-directionally in each of the stimulated axons. Orthodromic APs in the motor fibres result in a direct muscle twitch (M wave); antidromically propagated APs in the same fibres may collide with naturally occurring APs and result in mutual annihilation. IThey cannot propagate passed each other because the fibre just behind an AP is in its refractory period. This mutual annihilation is called collision blocking and it contributes to the silent period seen immediately after the M wave.

Rushton (Rushton, 2003) has suggested a mechanism for the change in the spinal cord:

"FES combined with coincident voluntary effort through a damaged motor system, could help to promote restorative synaptive modifications at anterior horn cell level."

In other words, the recovery of the lost functions may only happen if the electrical stimulation is combined with simultaneous voluntary effort. This would explain why the foot-drop stimulator is successful in promoting functional recovery in some patients but not all of them. Some patients may be stimulated while not trying to contract the muscle (i.e. they just let the stimulator to activate the muscles); others may try to contract the muscle voluntarily to work together with the stimulator, therefore may receive this carry-over effect.

In some cases, when the antidromic AP reaches the motoneuron cell bodies, a small portion of the mortor neurons backfire and an orthodromic wave travels back down the nerve towards the muscle. The reflected stimulus evokes a small proportion of the muscle fibres causing a small response called F wave.

Restoration of Hebb synapse

As explained in 2.8.1, Hebb synapses are modifiable and would be strengthened if pre-synaptic firing coincided with or was shortly followed by post-synaptic discharge. Following the SCI, the activity in the pyramidal tract is significantly reduced which leads to "de-correlation" of the pre-synaptic and post-synaptic activities. This "unsynchronisation" of pre and post synaptic activities further weaken the Hebb synapses in anterior horn. Rushton hypothesised that the stimulation of peripheral nerves coinciding with voluntary effort of the muscle provided an

artificial way of synchronising pre and post synaptic activities, hence encouraging restorative modifications of the Hebb synapses in the AH. This suggested mechanism is illustrated in Figure 2. 5.

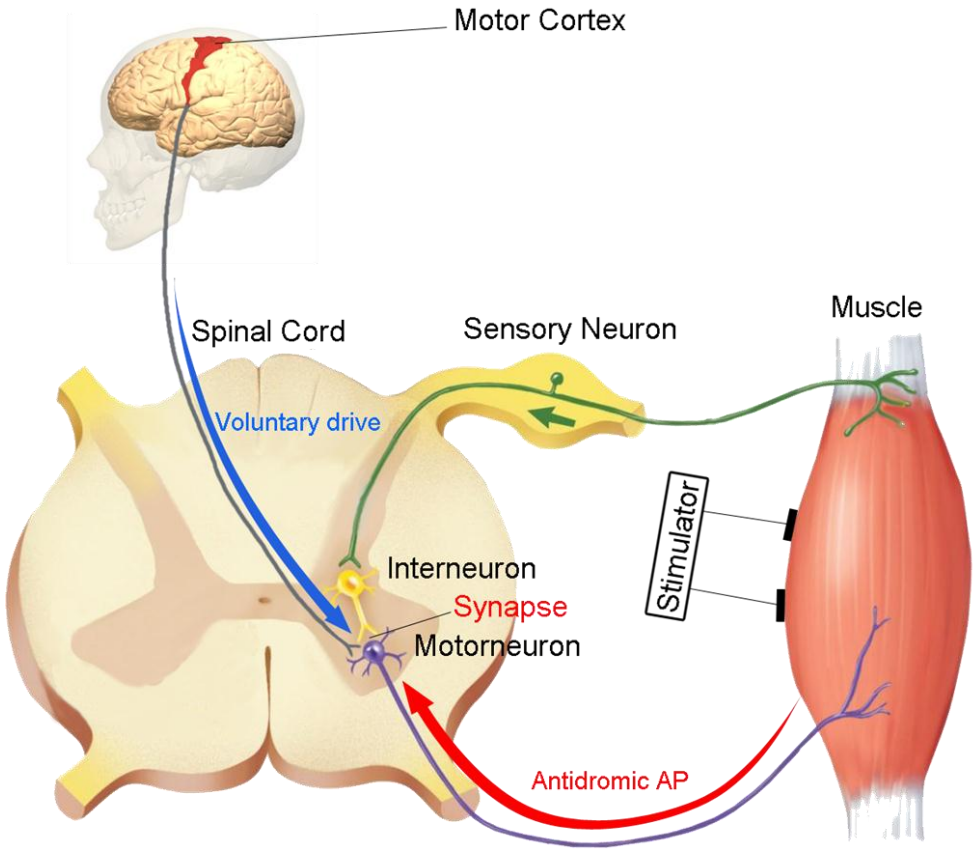

Figure 2. 5: Mechanism for the hypothesis.

2.11 The choice of FES system

We propose to design a FES system that allows testing of Rushton's hypothesis. However, the required electronic devices need to be designed and constructed, which is not a simple undertaking. Consequently the scale of this project is limited to the first step in testing the hypothesis, namely to build a FES system in which the stimulation intensity is controlled by a signal representing the voluntary EMG. Even this first step consists of two parts:

1. Building a FES system with all the essential apparatus.

2. Finding a method to measure the subject's voluntary drive during FES.

There are a broad range of FES systems we could choose to base our system on. Aside from FES being used to allow standing and walking for paraplegics and hand grasping for tetraplegics, many bioengineers have investigate the benefits offered by FES cycling for these patients. FES cycling was first demonstrated in 1980s (Petrofsky et al., 1983; Kern et al., 1985). Since then, it

has been developed to encourage frequent exercise and has shown various physiological benefits such as improvements in cardiopulmonary fitness (Petrofsky et al., 1992), increased muscle mass and bone density (Frotzler et al., 2008), reduced spasticity (Janssen et al., 1998), increased metabolic and neural factors (Griffin et al., 2008).

Adaptation of EMG control for FES cycling is possible in patients with residual voluntary effort. As reviewed earlier in 2.9, there is some evidence that FES cycling may promote the recovery of voluntary strength and natural leg functions for patient with incomplete spinal cord injury, if they make a voluntary attempt to pedal the tricycle while being stimulated (Donaldson et al., 2000). This agrees with Rushton's hypothesis that the voluntary effort together with the artificial AP which makes the muscle contract may bring about the re-learning process. Therefore an EMG controlled tricycle may encourage the use of their voluntary effort and thus have greater benefit than passive cycling.

As explained in 2.10, the functional recovery will only work if the electrical stimulation (and the antidromic activity it generates) is combined with simultaneous voluntary effort. The proposed FES system needs to provide a way of ensuring synchronised voluntary effort and stimulation in the affected population of AH cells. Therefore the FES cycling system we build should only stimulate when the subject is making a voluntary effort to cycle. Therefore it is important to find a signal that represents the subject's voluntary drive from the same muscle that is being stimulated. The difficulty of finding such a signal is explained in the next chapter.

CHAPTER 3: MUSCLE FUNCTION AND STIMULATION

3.1 Introduction

In this chapter, the fundamentals of EMG and EMG signals under stimulation are introduced first. With the understanding of stimulus artefact and the M wave being the obstacle in interpreting EMG signal under stimulation, we will then proceed to review the various methods used in the literature to eliminate them. There are also other reflexes found in EMG signals when stimulating the muscle, namely H and F reflexes. The origins of these reflexes and their possible influence on the voluntary drive estimation are also discussed. When stimulating the muscles to perform functional movements, the muscles can get fatigue more quickly than natural movements. The possible reasons for this as well as the fatigue model during cycling are introduced. Towards the end of this chapter, four commercial FES cycling systems in the market are reviewed. Their design and control methods of these FES cycling systems are described and compared to the proposed FES cycling system in 3.13.

3.2 The Electromyogram (EMG)

As reviewed in 2.5, the basic functional unit of the muscles is the MU. Apart from being the force generating elements of the movements, the MU is also a source of electrical signals. When a single motor unit contracts via a voluntary action potential, the electrical impulse is called a muscle unit action potential, or MUAP. When an entire muscle is contracted, the individual MUAPs are superimposed onto one another in a signal known as the electromyogram, or EMG, of the muscle (see Figure 3. 1). The study of muscle electrical signals is called Electromyography. EMG can be recorded using electrodes, either invasively (needle electrode) or non-invasively (surface electrodes). The needle electrodes are more frequently used with deep muscle or localized tissue while the surface electrodes are convenient for superficial muscles. Surface EMG is preferred for this project. The surface EMG is a stochastic signal, with usable frequencies in the range of 5-500Hz and dominating frequencies from 50-150Hz (Figure 3. 2), due to the unsynchronised nature of the MUAPs firing. These signals are generally range from several hundred μV to a few mV hence requiring amplification.

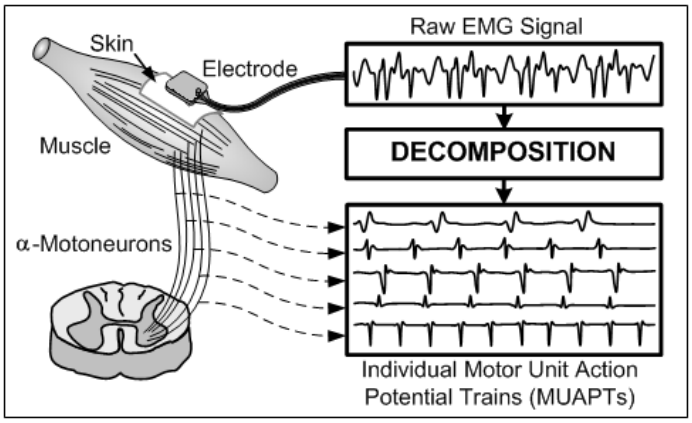

Figure 3. 1: Composition of EMG signal, reprinted from (De Luca & Adam 2006).

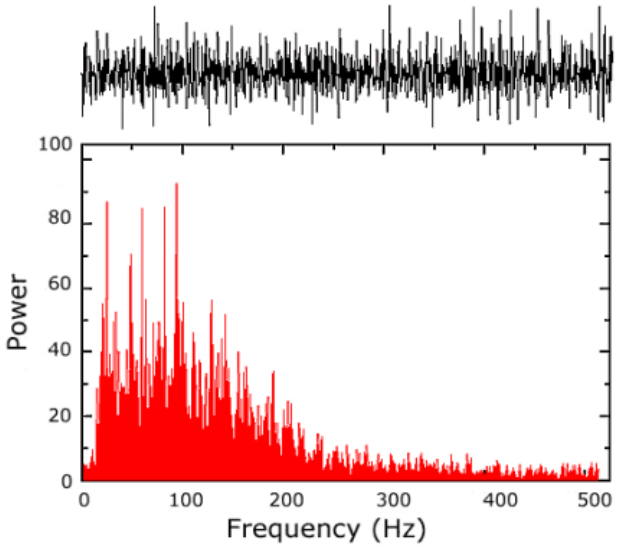

Figure 3. 2: Frequency spectrum of the EMG signal detected from the TA muscle during a constant force isometric contraction, reprinted from (De Luca 2002).

3.3 EMG signal detection and processing

EMG signals are small and need to be recorded using EMG amplifiers. Natural EMG appears to be a random noise-like signal whose amplitude varies with the amount of the muscle activity. It is desirable to obtain an EMG signal that contains the maximum amount of information from the EMG signal and the minimum contamination from electrical noise. Various signal processing techniques are used to maximise the signal-to-noise ratio. Bandpass filters with a pass band at 20-500Hz and a roll-off slope at 40dB/decade are normally selected to filter the EMG signal. The reason of the lower passband is that the surface-detected signal often shows slow variations due to the movement artefacts and instability of the electrode-skin interface, these unwanted signals are usually in the frequency range of 0-20Hz (De Luca et al., 2006)

Figure 3. 3 shows the EMG signal recorded from Biceps during voluntary contraction. We can see that the amplitude of the EMG signal increases as the subject began to contract the muscle harder and soon diminished when the subject stopped contracting the muscle. The sample rate was 2000 samples/s so the entire contraction lasted about 4s. The raw EMG does not provide much information and normally signal processing techniques are required.

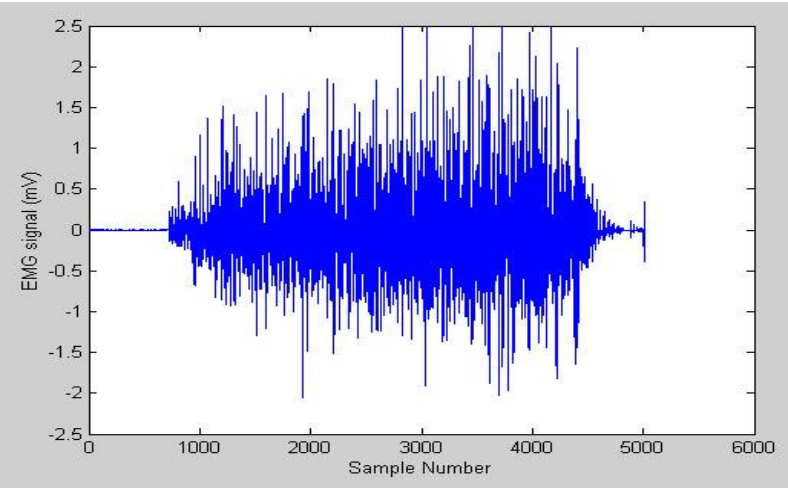

Figure 3. 3: EMG signal recorded from biceps during voluntary contraction, sample rate 1000 samples/s.

There are many signal processing techniques that are used with EMG signals. The most common ones are: full-wave rectification (absolute value of the entire signal), linear envelope (low-pass filtering of the full-wave rectified signal), root mean square (square the signal, take the mean of it in a timed window, then take the square root), integrated EMG (area under the rectified curve for the entire activity or for preset time or amplitude values), and frequency analysis (normally involves of using fast Fourier analysis and looking at the power density spectrum). Depending on the application, these processing techniques may be used alone or together.
EMG obtained from SCI patients can be very different from AB subjects, in terms of much lower amplitude and narrowed frequency band.

3.4 Decomposition of EMG signal during stimulation

The EMG signal obtained when there is electrical stimulation is different from that obtained when there is none. It also depends on whether the subject is trying to use the muscle. By comparing the different signals, it is possible identify the EMG component which corresponds to the voluntary effort of the patient as shown in Figure 3. 4. In picture A, there is no muscle activity. In picture B, when a person with normal neurological function relaxes his muscle, with stimulation, there is the actual stimulus artefact and then there is the M wave. Picture C: When a person with normal neurological function consciously contracts his muscles, without stimulation, there is voluntary effort which represents the subject trying to use his muscle. Picture D: When

he consciously contracts his muscle, with stimulation, there is a stimulus artefact, the M wave as well as the voluntary effort.

Basically, when a contracted muscle is electrically stimulated, there are two artefacts we need to consider before we could study the voluntary effort: the stimulus artefact and the M-wave. Both the stimulus artefact and the M wave are independent of the voluntary activity we are trying to measure. The stimulus artefact is in the form of large spikes due to the stimulation voltage being picked up by the recording electrodes to measure the EMG signal in mV (Yeom et al., 2004). The M-wave is the compound muscle action potential due to the synchronous firing of motor units; it is the response of muscle fibres to the stimulation pulse. The M-wave depends on many factors including stimulation intensity, muscle fatigue and the contraction levels of the muscle (Merletti et al., 1992). It can be used as an indicator of the number of muscle units contracted, or the strength of the contraction. This data can therefore be used to evaluate the effectiveness of electrode placement on a muscle (see 3.7). However, in order to use voluntary EMG signals as a control mechanism for stimulating the same muscle, the M-wave is of no concern and appears as an artefact.

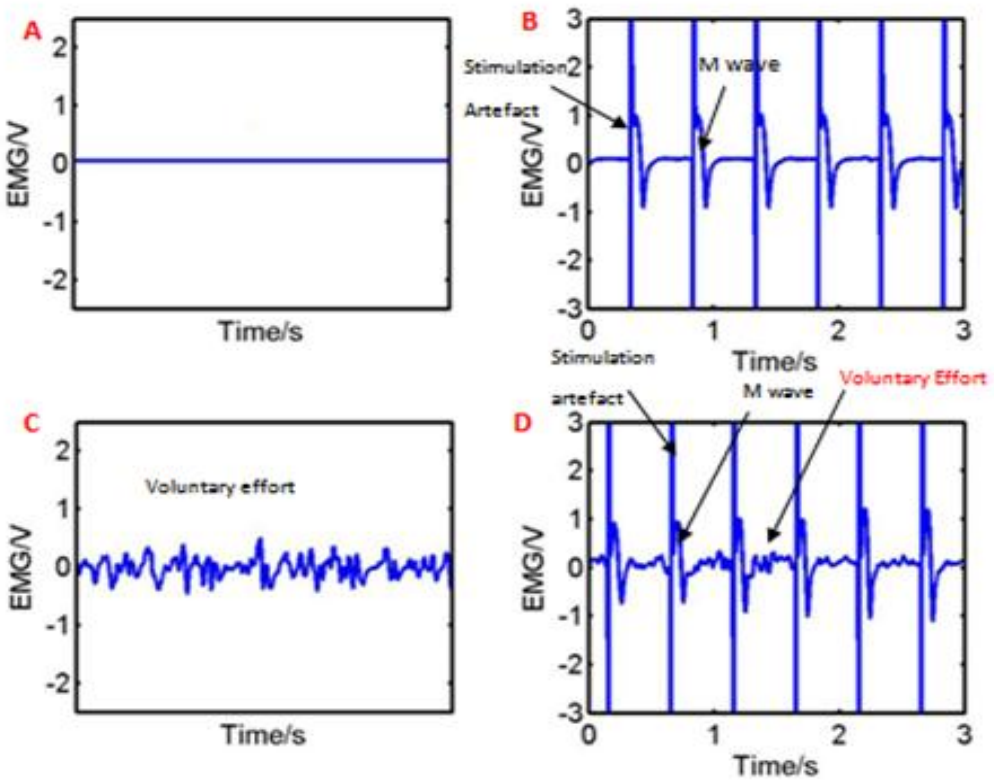

Figure 3. 4: EMG recorded from the tibialis anterior muscle of an able-bodied person.

3.5 Stimulus artefact

3.5.1 Understanding the stimulus artefact

The stimulus artefact is a large spike followed by an exponential decay. The amplitude and time constant of the exponential decay is dependent on several factors including amplifier design, electrode orientation, stimulation type and electrode–skin interface (McGill & Cummins, 2007).

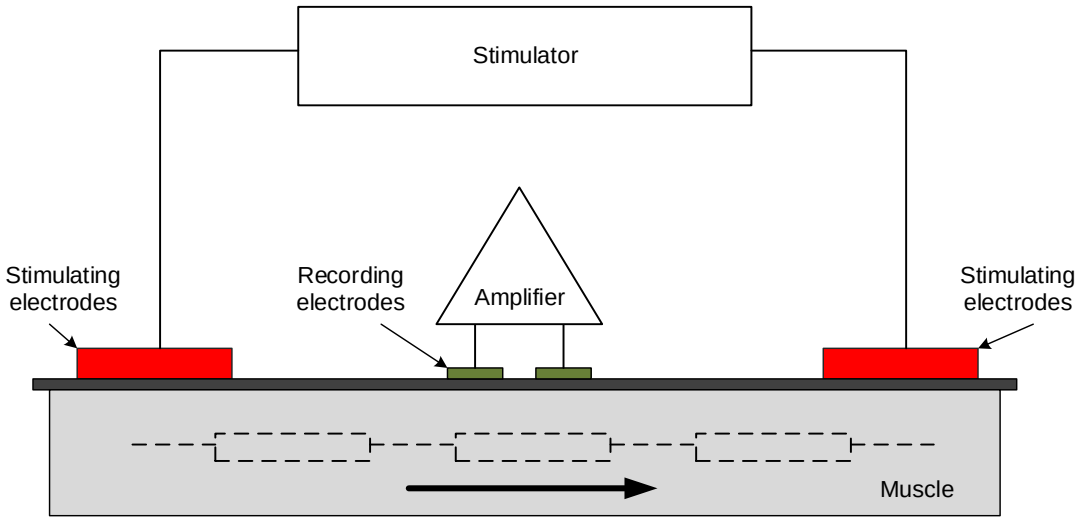

Figure 3. 5: Electrode configuration: the recording electrodes are placed between stimulating electrodes.

When recording from a muscle that is being stimulated, the first problem that arises is the amplifier saturation. During a stimulation pulse, current will flow between the stimulating electrodes, through the volume resistance of the tissue within the body. The volume resistance can be considered as a potential divider (see Figure 3. 5). The input to the amplifier equals to the potential difference across the resistance below the recording electrodes. If the amplifier had infinite voltage range and infinite bandwidth, the output would always look like the input. However, in practice the amplifier only behaves linearly for a limited range of input and output voltages. The maximum and minimum values of the output voltage are determined by the supply rails between which the amplifier operates. If the input voltage is sufficiently large to drive the amplifier output outside of this range, the amplifier is said to be saturated (Sedra & Smith, 1997). After removing the input overdrive it takes a finite amount of time for the output to return from saturation to linear operation.

The voltage difference produced between the recording electrodes is the major source of the stimulus artefact. The amplitude of the voltage difference decreases as the distance between the stimulating and recording sites is increased. Furthermore, the distance between the two sites will affect the conduction latency period (see Figure 3. 6). The conduction latency period is considered to be the delay between the stimulus artefact and the M wave. If the recording site is

sufficiently far away from the stimulus location, then the stimulus artefact and the M wave will not overlap. In the case where the recording electrodes are placed between the stimulating electrodes, the M-wave usually starts directly after the stimulation pulse. This can result in the two responses overlapping (Harding, 1991).

3.5.2 The problem

One major difficulty of using EMG signal for control is the presence of the large stimulus artefact. High gain, sensitive EMG amplifiers are designed to capture the small EMG signals but not to handle the large stimulation voltage. The large stimulation current passes through recording electrodes can easily saturate a conventional EMG amplifier. The EMG amplifier then requires time to recover to its normal working state, by which time the EMG signal of interest may no longer be acquired. Furthermore, the M wave comes after the stimulus artefact and must extend for part of the stimulation period (Yeom et al., 2004).These artefacts often distort the wanted voluntary EMG signal hence it is necessary to eliminate them.

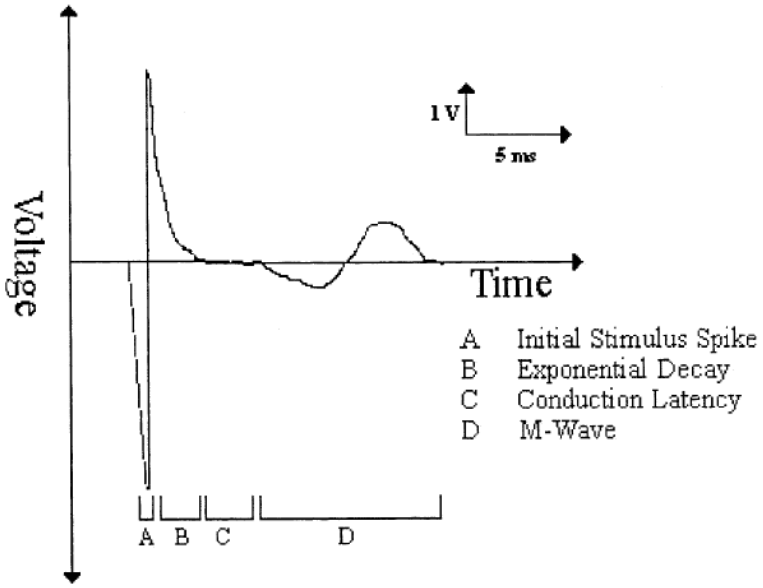

Figure 3. 6: A closer look of the stimulus artefact and M wave

3.5.3 Ways to supress the stimulus artefact

Stimulus artefact suppression and cancellation has a long history. Techniques to achieve this have been investigated ever since electrical stimulation was used together with EMG signal recording. Stimulus artefact was mentioned in the scientific literature by Guld as far back as 1959 (Guld, 1959). In 1965, Coombs suggested several methods of reducing the influence of the stimulus artefact (Coombs, 1965). Further suggestions for reducing the artefact were published during the 1970s (Babb et al., 1978) followed by discussions on the nature of the artefacts and a review of the available removal methods (McGill & Cummins, 2007). Generally, there are two broad categories of these techniques: hardware-based methods and software-based methods.

Hardware-based methods

It would be amplifier saturation that causes it. So by preventing the amplifier from saturating in the first place, you eliminate the artefact. The hardware-based methods often involve implementing a specialized circuit design or experimental configuration. Modifications to the conventional differential amplifiers are essential to provide both protection to the amplifier and clear recording. The idea is to block the stimulus artefact while keeping the EMG signal intact. It was firstly achieved by using a sample and hold circuitry (Roby and Lettich 1975; Freeman 1971; Babb et al., 1978).

The sample and hold circuit is capable of sampling the input signal while applying a gain and switching to a hold mode during stimulation whereby the previous signal is held constant during the blanking period. The hold mode is usually triggered by an external pulse from the stimulator. The output of this circuit differs from the input only due to a "flat spot" where the stimulus artefact normally would occur (Freeman, 1971). An example of such a circuit is shown in the blankable EMG amplifier design in 4.3.4. The major disadvantage of using these blanking circuits is that the length of the blanking signal is usually fixed by a potentiometer, which can lead to undesirable blanking lengths should the stimulation parameters (frequency, pulse width, amplitude) change (O'Keeffe & Lyons, 2001).

In 1978, Walker and Kimura suggested a direct-coupled amplifier with feedback design that allows fast recovery from stimulation pulses (Walker & Kimura, 1978). Thorsen adapted the idea and designed a fast recovery myoelectric amplifier (4.3.3) (Thorsen, 2002). Such a fast-recovery amplifying circuit contains different feedback loops and a DC amplifier in order to decrease the number of capacitors in the circuitry which result in the extended duration of stimulus artefacts. An integrator feedback loop is used to eliminate the DC offset from the surface electrodes and is the only capacitor in the circuit where significant charge could be stored. In order to achieve fast recovery, a control circuit detects if the DC amplifier output exceeds a saturation limit (during stimulation) and subsequently opens a feedback loop. Once the stimulation pulse is completed, and the output is below the saturation limit, the feedback loop closes and the amplifier is returned to baseline.

Software-based methods

The software-based methods mainly involve post-signal processing techniques or real-time analysis by computers or signal processors. The former has the advantages of flexibility and no time constraints while the latter can be used in real-time closed loop applications. Both methods use algorithms either to "subtract" the stimulus artefact or to filter it. The subtraction method was firstly used in 1977 by Kovacs in his studies of peripheral nerves (Zsolt et al., 1979). In 1996, Hines et al. introduced a simple method of replacing the stimulus artefact in EMG signal by a constant amplitude EMG signal equal to the mean EMG 25ms before and after the artefact (Hines et al., 1996). Others attempted to subtract a mean stimulus artefact from the original signal (Hashimoto, 2002; Nakamura et al., 1990; Wichmann, 2000). More complex methods in this category include fitting models to the stimulus artefact and subsequently subtracting it.

Nevertheless, these methods aim to replace/remove the parts of the recorded signal that stimulus artefacts occupy; data loss could happen during this process (as decisions on the duration of the artefact may be arbitrary).

The filtering methods, on the other hand, try to maintain the integrity of the recorded data. There are numerous filters described in the literature from simple-passive filtering (Solomonow et al., 1985) to complicated adaptive filtering (McCallum & Grieve 2002), linear prediction filters to non-linear adaptive filtering (Grieve et al., 2000). The characteristic of the filters depends on the nature of the EMG signal and can be used either alone or in conjunction with other methods (Whittington et al., 2005).

To summarise, the possible methods for post-processing stimulus artefact removal are endless, each with their own advantages and disadvantages. For the purpose of this project, real-time stimulus artefact suppression is required for the feedback control loop therefore limiting the number of appropriate methods. Various methods of artefact suppressions are introduced throughout the thesis (hardware in chapter 4, software in chapter 5).

3.6 Other muscle reflexes

A muscle reflex, or reflex action, is a fast, involuntary muscle contraction. A reflex action differs from the normal muscle contraction as the brain does not initiate the contraction. The time it takes for a reflex action to occur, after an external stimulus, is much less than what it would take for a voluntary action to occur. This is because the muscle contraction response is initiated at the spinal cord, through reflex pathways. By the time the stimulus reaches the brain, the muscle contraction has already responded to the stimulus. A typical example of the muscle reflex is a tendon jerk. In 1906, Sharrington demonstrated that the quadriceps jerk in the cat could be abolished by dorsal root section, hence confirming the nature of the reflex response (Sherrington, 1906). When recording EMG signals during surface electrical stimulation, there are a few reflexes that may be present, among which two of the late responses H reflex and F wave are reviewed here in more detail (Shin, 2003).

3.6.1 H reflex

In 1926 Paul Hoffman found that low intensity stimulation of the tibial nerve in the popliteal fossa could produce a reflex contraction of the triceps surae muscles without direct activation of the muscle via the α-motoneurones. The reflex had a latency of 28-35ms and was believed to be an electrically elicited analogue of the tendon jerk. The H reflex, which is named after Hoffman, occurs because the group Iα fibres are larger than the α-motoneurones. Therefore, at very low stimulation intensities, these sensory fibres may be the first ones to be activated. However, as the stimulation intensity increases, the axons of α-motoneurones are stimulated and a direct muscle response (M-wave) is elicited 3-6ms after the onset of stimulation. If we increase the stimulation intensity further to supramaximal, the H-reflex will diminish. The reasons are: 1. Antidromic firing of motor fibres renders the motoneurones refractory to the reflex input and 2.

The antidromic motor volley collides with the orthodromic reflex volley set up by the Iα input. The H-reflex can be obtained in many muscles, Figure 3. 7 shows the evoked potentials by stimulation of the medial nerve with pulses of increasing amplitude (the stimulus artefact increases with stimulus intensity.

H-reflex is analogous to the mechanically induced spinal stretch reflex. The primary difference between the H-reflex and the spinal stretch reflex is that the H-reflex bypasses the muscle spindle, and, therefore, is a valuable tool in assessing modulation of monosynaptic reflex activity in the spinal cord. Although stretch reflex gives just qualitative information about muscle spindles and reflex activity; if the purpose of the test is to compare performances from different subjects, H-reflex should be used. In such a case latencies (in ms) and amplitudes (in mV) of H-wave can be compared.

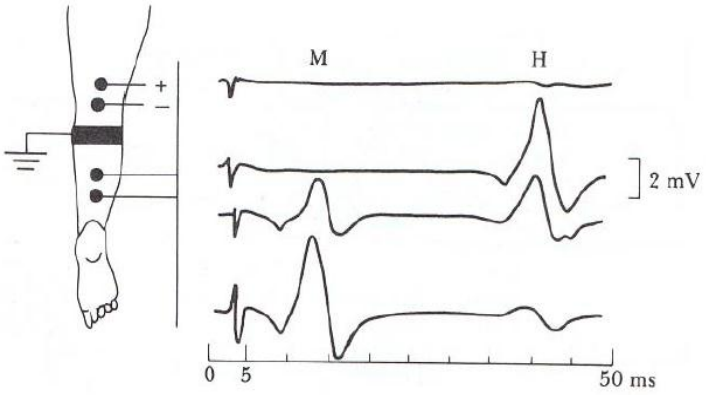

Figure 3. 7: Recording the H-reflex from the popliteal fossa. The M-wave amplitude is seen to increase as the H-wave amplitude decreases. As the stimulus increases the M-wave increases. There is a point of minimal stimulus where the M-wave is absent and the H-wave is maximal (Lenman & Ritchie, 1987).

3.6.2 F wave

The F-wave is one of the late responses produced by antidromic activation of motoneurons by supramaximal stimulation. The name F wave was used for the first time by Magladery and McDougal in 1950 (Magladery et.al, 1951), when considering the intrinsic muscles of the foot. Unlike the H wave, a strong electrical stimulus (supramaximal stimulation) is applied to the skin surface above the distal portion of a nerve when observing the F-wave. When the antidromic stimulus reaches the motor neuron cell bodies, a small proportion of motor neurones are re-excited by the antidromic impulse causing the production of an orthodromic action potential which travels back down the nerve towards the muscle. This reflected stimulus evokes a small proportion of the muscle fibres, causing a small response called the F-wave. Only about 2% of axons backfire with each stimulus (Basmajian, 1962). Because a different population of anterior horn cells is stimulated every time, each F wave has a slightly different shape, amplitude and latency. The minimal F wave latency is typically 25-32ms in the upper extremities, and 45-56ms in the lower extremities (Basmajian, 1962).

3.7 Crosstalk

Crosstalk is defined in the literature (Knaflitz et al., 1988; De Luca & Merletti, 1988) as the measurement of EMG in a given muscle, when the signal itself originates in a different muscle. This is problematic as it can lead to "an erroneous conclusion of coactivation among different muscles when only one muscle is active" (Merletti et al., 1992), particularly in the case of muscles that are close to each other (Farina et al., 2002), such as the Quadriceps which we will be recording from in future experiments. The type of electrode used to record the EMG greatly influences the amount of crosstalk present in the measurements (De Luca & Merletti, 1988). Muscle activity recorded using intramuscular electrodes is mostly unaffected by crosstalk. This is due to the small detection volume associated with these types of electrodes. Surface electrodes have a much larger detection volume which provide more information of the activation of an entire muscle, but can lack selectivity and are more susceptible to crosstalk. Anatomical conditions also affect the likelihood of crosstalk being present. The thicker the layer of subcutaneous fat covering the muscles below the recording electrodes, the more prevalent the presence of crosstalk in the measurements (Farina et al., 2004; Solomonow et al., 1994).

3.7.1 Evaluation of the crosstalk in quadriceps

The Quadriceps are of particular interest to us as they will be used in the experiments described in chapters 5-7. A multi-electrode detection system is usually used to access the percentage of crosstalk in muscles. It captures two signals, a single differential (SD) signal and a double differential (DD) signal, as shown in Figure 3. 8. According to Koh and Grabiner (Koh & Grabiner, 1993), the DD detection system has a smaller pick-up volume than the SD detection system, which causes it to have greater selectivity. Merletti et al. state that a signal generated below the detection electrodes (i.e. a true measurement of muscle activation), would produce a SD and a DD signal of roughly the same amplitude; while a signal generated far from the detection electrodes (i.e. a crosstalk signal), would produce a DD signal of much smaller amplitude than the SD signal (Merletti et al., 1992). This was shown experimentally when stimulation of VL resulted in an M-wave being measured in VM using the SD detection system, but not with the DD detection system, even though both systems measured an M-wave of similar amplitude in VL. The two authors, Knaflitz et al. (Knaflitz et al., 1988) and Farina et al. (Farina et al., 2002) both used similar SD and DD detection systems to characterise crosstalk in the thigh. The peak-to-peak amplitude of the M-waves were then used to calculate a percentage of the SD M-wave amplitude measured in the stimulated muscle that would appear as crosstalk in the adjacent non-stimulated muscle. The results are shown in Table 3. 1.

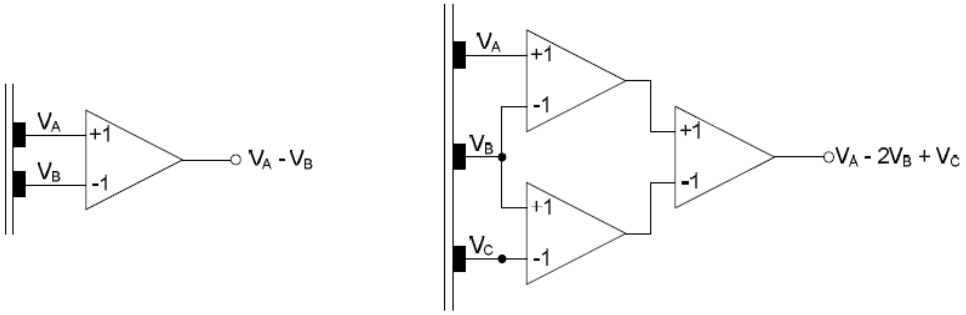

(a) Single differential. (b) Double differential.

Figure 3. 8: Detection systems for assessing crosstalk, replotted from (Merletti et al., 1992) and (Koh & Grabiner, 1993)

Table 3. 1: Comparison of crosstalk percentage in the adjacent quadriceps by two authors

Stimulated muscle	Percentage SD signal attributed to crosstalk		
	VL	RF	VM
Maximum percentage, [Knaflitz etal.,1988]			
VL	-	18.2	7.7
VM	10.7	8.6	-
Mean ± Standard Error, [Farina et al.,2002]			
VL	-	24.1 ± 5.4	12.8 ± 3.5
RF	12.3 ± 1.6	-	17.8 ± 11.3
VM	19.3 ± 4.2	20.3 ± 4.7	-

It appears from the results that, when using a SD detection system, the EMG recorded in the non-stimulated muscles of the quadriceps will partially be attributed to crosstalk. 7.7% - 24.1% of the peak-to-peak amplitude of the M-wave recorded in the stimulated muscle may appear in the M-wave recorded in the non-stimulated muscle. Yet both studies have used selective stimulation by placing surface stimulating electrodes on the motor point of the muscle, there was still an M-wave present in some of the DD signals of the non-stimulated muscle, although with a reduced amplitude. It is questionable how selective the stimulation methods used by the two groups are. Farina et al. (Farina et al., 2002) say that "...controversies exist in the literature, because of confusion about the sources of signal that are mostly responsible for crosstalk". The issue of crosstalk is complicated and one could only try to minimise the influence. The quadriceps will be in the future experiments, therefore selective stimulation of the muscles is important. A European standard for surface electrode placement is followed to ensure the correct position of the electrodes ((SENIAM, 2010) (see Appendix D: Guidelines of electrode placement for the 4 muscles used in this project (SENIAM, 2010)).

3.8 EMG and force relationship

Our study requires an estimation of the subject's voluntary drive to the muscles using surface EMG (SEMG). This voluntary drive signal would then be used to control the stimulation intensity applied to the muscles, consequently changing the force generated by the muscles. The EMG is expected to be related to the force output, however, this relationship would not necessarily be linear. Nonetheless, as long as the relationship is consistent, thereby producing a reliable prediction to be used in the control algorithm.

The voluntary contraction of the muscles produces two phenomena that can easily be measured using noninvasive methods, namely, the force and the EMG. The relationship between surface EMG and generated force has been examined in several studies. Lippold (Lippold, 1952), Close (Close, 1972) & Bigland-Ritchie (Bigland-Ritchie, 1981a) suggest that there is a linear relationship between integrated EMG and tension; while Zuniga & Simons (Zuniga & Simons, 1969) and Vrendenbregt & Rau (Vredenbregt & Rau, 1973) suggested a non-linear relationship exists. An opinion that has been more accepted in the field is that the relationship between EMG and force can be "linear" or "non-linear", depending on different conditions (Basmajian, 1962). The reason for this apparent contradiction is most likely due to the fact that the EMG-force relationship, for SEMG, is influenced by a number of factors, namely, the MU recruitment and firing rate properties, the crosstalk from adjacent muscles (see 3.7), the relative location of the slow-twitch and fast-twitch muscles, the size and position of the electrodes and the interaction between agonist-antagonist muscles (Basmajian, 1962).

It is generally accepted that muscle fibre types can be broken down into two main types: slow twitch (Type I) muscle fibres and fast twitch (Type II) muscle fibres. At low exercise intensities, slow twitch fibres are recruited because they have the lowest threshold for recruitment. The fast twitch fibres are better at generating short bursts of strength or speed. The fast twitch fibres generally have higher fibre diameters (Polgar & Johnson, 1973) and the AP generated by a single muscle fibre is proportional to its fibre diameter. Therefore these fast twitch fibres result in higher EMG amplitudes. The amplitude of the MUAP that contributes to the surface EMG is a function of the distance between the active fibres and the detection electrodes: the greater the distance, the smaller the amplitude. Therefore, the relative location of the fast twitch fibres and electrodes positions affects the SEMG. Most of the commercial surface electrodes have sizes ranging of 20-90mm (diameter), therefore for large muscles like the leg muscles we are targeting; the number of motor units recorded by electrodes will be less than the total number of motor units that are firing simply because the electrodes cannot pick up all of the motor units.

The interaction between the agonist and antagonist muscles during muscle contractions is also an important consideration. The relationship between the force and EMG of an agonist muscle cannot be analysed without interpreting the antagonist muscle. Sometimes the joints are stiffened to isolate the interactions. In a dynamic movement like cycling, which requires cooperation between the agonist and antagonist muscles (see 3.11), the EMG-force relationship

can be altered by many factors including the joint angle, limb position and pain sensation(Lawrence & De Luca, 1983).

For our purposes, it is necessary to understand the EMG and force relationship in cycling. Several studies have reported that a progressive increase in EMG of the knee extensor muscles occurs during a high-intensity cycling exercise (Housh et al., 2000; Petrofsky, 1979; Saunders et al., 2000). Housh et al. found a significant increase in EMG activity of VM during a high intensity cycling trial at 80-95% peak power output (PPO) (Housh et al., 2000). Similar results were obtained by Petrofsky at 60-100% PPO (Petrofsky, 1979). Ryan and Gregor‘s work (Ryan & Gregor, 1992), which shares some similarity with us, monitors EMG signals of 10 lower extremity muscles during cycling at constant cadence and constant load. The EMG signals are averaged to find the general patterns of these muscles when generating constant force. Their work provided useful information in the control of these muscle functions during cycling, however, no influence of the load change was experimentally investigated. Limited conclusions concerning the EMG/force relationship during cycling can be made from the literature because of methodological differences which include electrode placement and experimental design. However, these provide some insights towards carefully designed experiments in Chapter 5 with RMS EMG’s relationship to the effort level and pedal force are studied during cycling with variable load at constant cadence.

3.9 Muscle Fatigue

Muscle fatigue has been defined as the “failure to maintain the required or expected force” by physiologist and health specialists since 1981 (Edwards, 1981). The failure point is when a particular task cannot be performed or maintained at a specific time. Fatigue here is considered as an event occurring at or over an identifiable period of time. However, some engineers and physical scientists argue that before this failure point happens, the muscle is already fatigued. Fatigue, in this perspective, is a time-dependent progressive process from the onset of the muscle contraction (Basmajian, 1962). An example of this would be the task of maintaining a muscle contraction constant for as long as possible. Throughout the task, the involved muscles are continuously fatiguing, but at some instant in time the failure point will occur when the desired force output may no longer be maintained and fatigue becomes observable. Therefore the fatigue should be an ongoing process with regard to physiological and biochemical changes (De Luca, 1984; Merletti et al., 1990).

Muscle fatigue is a complex phenomenon encompassing various causes. It could be result from inadequacies in any parts of the motor command pathway and is divided into two groups: central (associated with the central nervous system) and peripheral (neuromuscular junction and muscle itself) (Merletti & Parker, 2004). The central factors of fatigue comprise decreases in the voluntary activation of the muscle, which is due to decreases in the number of recruited motor units and their discharge rate. The peripheral factors of muscle fatigue include alterations in

neuromuscular transmission and muscle action potential propagation and decreases in the contractile strength of the muscle fibres (Boyas & Guevel, 2011).

3.9.1 Assessment of muscle fatigue

Fatigue itself is difficult to assess as it is not a physical variable to measure. Instead, physical variables relate to fatigue should be measured: force, torque or power produced by the muscle; angular velocity of joints; oxygen or blood flow in the muscle and variables associated to the EMG signal such as RMS amplitudes or median frequency. Both mechanical and biological measurements have been used in the literature for assessment of the muscle fatigue, with analysis of the EMG signal being studied intensively in the field.

Surface EMG has been used by many scientists to evaluate muscle fatigue (Camic et al., 2010; Chen, Hsueh, & He, 2008; Cifrek et al., 2009; De Luca, 1984; Garcia et al., 2010; González-Izal et al., 2012; Kattla & Lowery, 2010; Merletti et al., 1990; So etal., 2005). Their experiments mostly focused on isometric contractions to simplify the real life dynamic movements. An important characteristic of the SEMG signals recorded during isometric contractions is that the changes in the frequency domain can be assumed to be independent of time, so the SEMG signal can be assumed to be stationary (Farina, 2006). Therefore the traditional frequency-based techniques, such as Fourier transforms (FT) or discrete fast Fourier transforms (FFT) can be used to determine changes in the power spectral content of the SEMG signals. In 1912, Piper observed a progressive “slowing” of EMG during isometric voluntary sustained contractions which shifts the spectral components of surface EMG toward lower frequencies (Piper, 1907). Since then, a few attempts were made to identify a single parameter to represent the frequency shift resulted from the muscle fatigue and a “ratio” was found to be closely related to it. This ratio of the RMS of the low-frequency components to the RMS of the high frequency components has been used by several researchers (Bellemare & Grassino, 1982; Bigland-Ritchie, 1981; Eberstein & Beattie, 1985). The separation of the low and high frequency bands can be chosen from the median-frequency (the frequency at which the power density spectrum is divided into two regions with equal power), the mean-frequency (average frequency) and the mode frequency (the frequency of the peak of the spectrum). The main attraction of the ratio parameter is that it presents dramatic changes in value of the frequency shift.

The difficulties in interpreting SEMG signals in static contractions are amplified in dynamic cases. There are other factors that affect SEMG signals during dynamic tasks that differ from those recording during static conditions (Farina, 2006). The joint movements tend to cause a shift of the underlying muscle fibres with respect to the recording electrodes. In addition, rapid changes in the motor unit recruitment and muscle force cause a faster change in the SEMG signal. The ratio technique was found to be sensitive to the shape of the EMG signal spectrum, making it unsuitable for dynamic movements (Stulen & DeLuca, 1981). Therefore the traditional frequency techniques may not be appropriate for extracting information from the SEMG signal for dynamic movements and more complex techniques are needed. The assumption that fatigue-induced

changes that are measured during isometric contractions can be applied to dynamic contractions is questionable (Cheng and Rice, 2005).

3.9.2 The influence of muscle fatigue on cycling

In the literature, the influence of fatigue on cycling was evaluated from different aspects. Some focus on the possible changes in the timing of muscle activation and show that the timing of onset and offset of EMG activation is not altered by fatigue (Knaflitz & Molinari, 2003; Sarre & Lepers, 2005). Others study the possible changes in muscle recruitment pattern and coordinations during prolonged exercises. Sanderson and Black (Sanderson & Black, 2003) showed an alteration in the mechanical pattern in an exhaustive cycling exercise (i.e. a reduced force application during the recovery phase with an increase in force during the propulsive phase). With a more detailed study to evaluate the muscular activities at different phases during cycling, Dorel and Drouet (Dorel & Drouet, 2009) were able to provide a detailed review of the RMS EMG changes with crank angles of 10 lower limb muscles. Their results showed that alterations occur in patterns of force application during exhaustive cycling. These alterations suggested that some adjustments were made in the coordination of muscles with the occurrence of fatigue.

Psek and Cafarelli (Psek & Cafarelli, 1993) examined the activation of antagonist muscles under fatigue conditions and found that fatigue of the VL muscle was associated with the activation of the BF muscle, which acts as an antagonist in knee extension movement. These results strongly suggest that muscle coordination is modified with fatigue as well as the existence of a possible compensation effect between muscles that involved in the same task. Duc and Hautier studied EMG/torque ratio changes of four lower limb muscles (VM, RF, BF and gastrocnemius) during 30 minute cycling time-trial (TT) on a ergotrainer with nine male competitive cyclists (Grappe et al., 2005; Hautier et al., 2000). EMG of the four muscles as well as the torque was recorded for 10s with 5 minutes of break in between during constant load cycling at the maximum speed possible. EMG/toque ratio of RF and VM are expressed as a percentage of the value at the 5th minute as show in Figure 3. 9. A slight decreasing tendency is seen with time for RF and VM until around 20s when further decrement of RF is accompanied by an increase in VM. This result show the potential compensation relationship between RF and VM pair. Therefore an important point they made was that when under intensive cycling at constant velocity, EMG/torque ratio of the prime cycling muscles may decrease after fatigue when increased activity were recorded from other muscles (Hautier et al., 2000). This natural compensation was reported in the previous studies to compensate contractile loss (Greig et al., 1985; Kirsch & Rymer, 1987).

As mentioned earlier in 3.9.1, fatigue can also be assessed in the frequency domain. Von Tscharner (von Tscharner, 2002) adopted a time–frequency analysis and used it in EMG recorded during cycling. Shifting of the frequency components were found to occur with fatigue at certain periods during the revolution. Thus the spectral changes are likely to reflect a systematic change of motor unit recruitment pattern with pedal position and with fatigue (von Tscharner, 2002).

This brings awareness to us since the coherence method being examined in Chapter 6 and 7 is based on the frequency analysis of the EMG from cocontracting muscles.

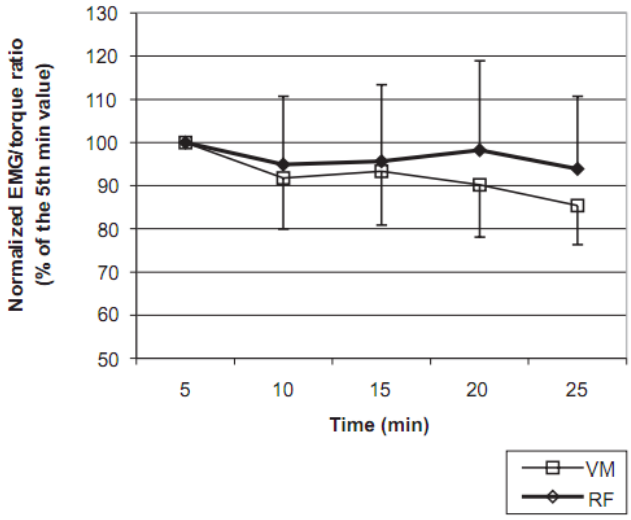

Figure 3. 9: EMG/torque ratio changes with time, normalised to the 5th minute for VM and RF (Duc et al., 2005).

Stimulated muscle generally fatigue quicker than the same response initiated voluntary. The higher the stimulation frequency, the faster the muscle fatigues (Benton et al., 1981). The influence of FES on muscle fatigue is not addressed further as continuous stimulation is not used on subjects in this project.

3.10 EMG controlled closed-loop FES systems

Benefits and difficulties of closed-loop FES systems with feedback were briefly introduced in 2.6. Here we focus at EMG controlled FES systems. EMG has been used in FES applications for more than 25 years. In 1965, Vodovnik et al. used EMG as a control signal for FES of paralyzed muscles (Vodovnik & Long, 2008). In the 1980s, Graupe et al. (Graupe et al., 1988) studied the possibility of using above-lesion voluntary EMG signals of the upper trunk to control the stimulation of the below-lesion leg muscles for walking. They designed a computer program to identify muscle contractions in the upper body that indicate the desire to take a step forward with either the right or left foot. Their results showed patients' ability to take steps, with the help of a walker, with only 1 misactivation of leg muscles per 100 steps. In 1996, Scott et al. (Scott, Peckham, & Kilgore, 1996) performed a similar study using the voluntary EMG signals of the sternocleidomastoid muscles to control an FES system for hand grasping of tetraplegics. These studies have demonstrated the capability of controlling stimulation via voluntary EMG signals from non-paralysed muscles. As repeatedly mention throughout this chapter, it is difficult to use EMG from the same muscle that is being stimulated as a control signal to the FES system. Chae (Chae, 2001) developed such a finger flexion/extension exercise system with EMG-triggered stimulation from the same muscle as shown in Figure 3. 10. The system was tested on three

stroke patients and the electrodes were implanted percutaneously. The recorded EMG was rectified and integrated firstly. If the processed signal exceeds a preset threshold, the stimulator outputs a train of pulses. As long the threshold was maintained, the stimulation continued. The large stimulation artefact and evoked EMG signal were blocked by a sampling gate and thus did not adversely affect the operation of the circuit. Note the stimulation intensity is not controlled by the process EMG, the EMG signal only controls the ON/OFF of the stimulation. The functional recovery of the three patients were evaluated by Fugl-Meyer score (use to assess physical performance) and only minimal to modest improvement was observed.

Futami et al. attempted to modulate the stimulation to a muscle with EMG measured from the same muscle (Futami et al. 2005). They reported a clinical application of EMG-driven stimulation system used for knee extension of incomplete paralysed patients. Figure 3. 11 shows the timing diagram of their work. The “protection” is a gating circuit used to protect the input stage of the EMG amplifier. It is turned on when there is a stimulation pulse and off during the EMG sampling periods. The EMG sampling periods are the 20ms windows selected between the stimuli. The stimulation frequency is at 20Hz, so there is 50ms between the pulses, the rest of the time are occupied by the stimulation pulse and a resting period after it. This method was tested on three hemiplegia patients who could do slow crutch-walking. The EMG-driven FES was used to aid their walking with a crutch. Unfortunately, the results were oral feedback from the subjects like: “this is helpful”, therefore the feedback was subjective and its statistical significance is unknown.

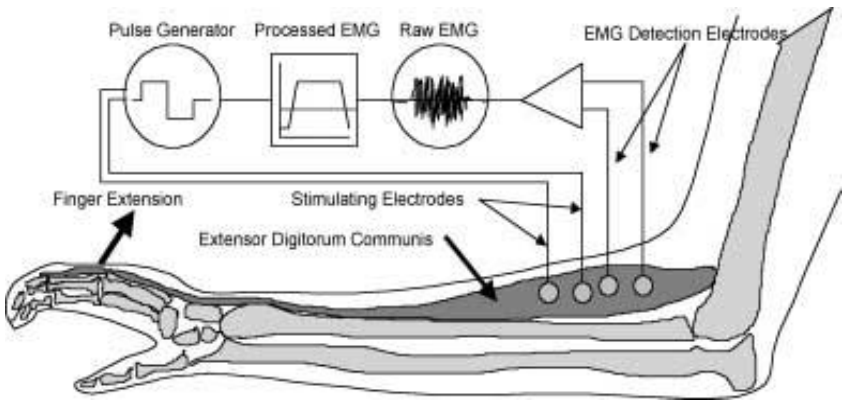

Figure 3. 10: Schematic representation of EMG-controlled NMES-mediated finger flexion/extension exercise (Chae, 2001). Subject’s voluntary EMG is detected by intramuscular electrodes. The EMG is firstly rectified and then integrated to check if it exceeds a preset threshold to trigger the stimulator.

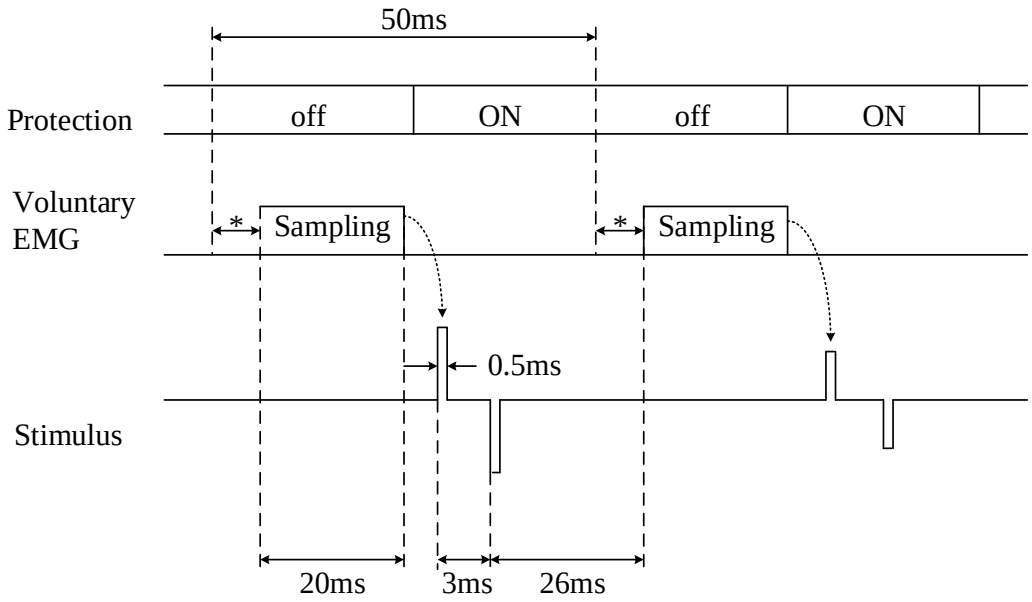

Figure 3. 11: Timing diagram of control strategy of the knee extension system, reproduced from (Futami et al., 2005)

Apart from the previous work of our group (Norton et al. , 2004), the only literature about EMG controlled FES cycling is the worked carried out by Chen (Chen et al., 2008). It is found that many experimental details are absent from the paper and it is not a well-established system, therefore it is not reviewed in details here.

3.11 Muscle activation during cycling

Cycling requires the cooperation of most muscles in the human body. The upper human body is responsible for balance and posture while the lower body muscles generate the power. Muscles involve in cycling work in a coordinated way; some work together whilst others work in a sequence in order to maximize energy transfer from the cyclist to the bike (So et al., 2005). The eight key leg muscles involved in cycling are illustrated in Figure 3. 12 and their roles in cycling are summarised in Table 3. 2.

The large number of muscles used in cycling are utilised in the form of agonist and antagonist. An agonist is a prime mover that makes a motion, such as contracting a limb while the antagonist muscle performs a motion that is the opposite of what the agonist did (MacIntosh, et al., 2006). The antagonist and agonist are usually found on opposite sides of a joint. Depending on the action that is performed, each muscle serves as the agonist at some times and as the antagonist at other times. These muscles can be also be divided into two types: the muscles that span a single joint (monoarticular) and the ones that span two (biarticular) or more joints. The first can be considered to be power producers, whereas the second type is responsible for the fine regulation of the net moments about the joints (Jacob et al., 1993). Research has shown that the biarticular muscles serve different purposes at different phases of cycling. For example, the Rectus Femoris assists flexion of the hip during the recovery phase, but it also supports knee

extension in the propulsive phase (Eisner et al., 1999). A similar pattern was also observed for the gastrocnemius; during the recovery phase, it functioned as a knee flexor, but during the propulsive phase, it worked as an ankle stabilizer (Burke, 1995). These functions of the muscles enable the optimization of intermuscular coordination for the best efficiency. The muscles used in FES cycling were reviewed by Cash (Cash, 2000) as shown in Table 3. 2. The table also distinguishes the muscles as being either mono- or bi-articular.

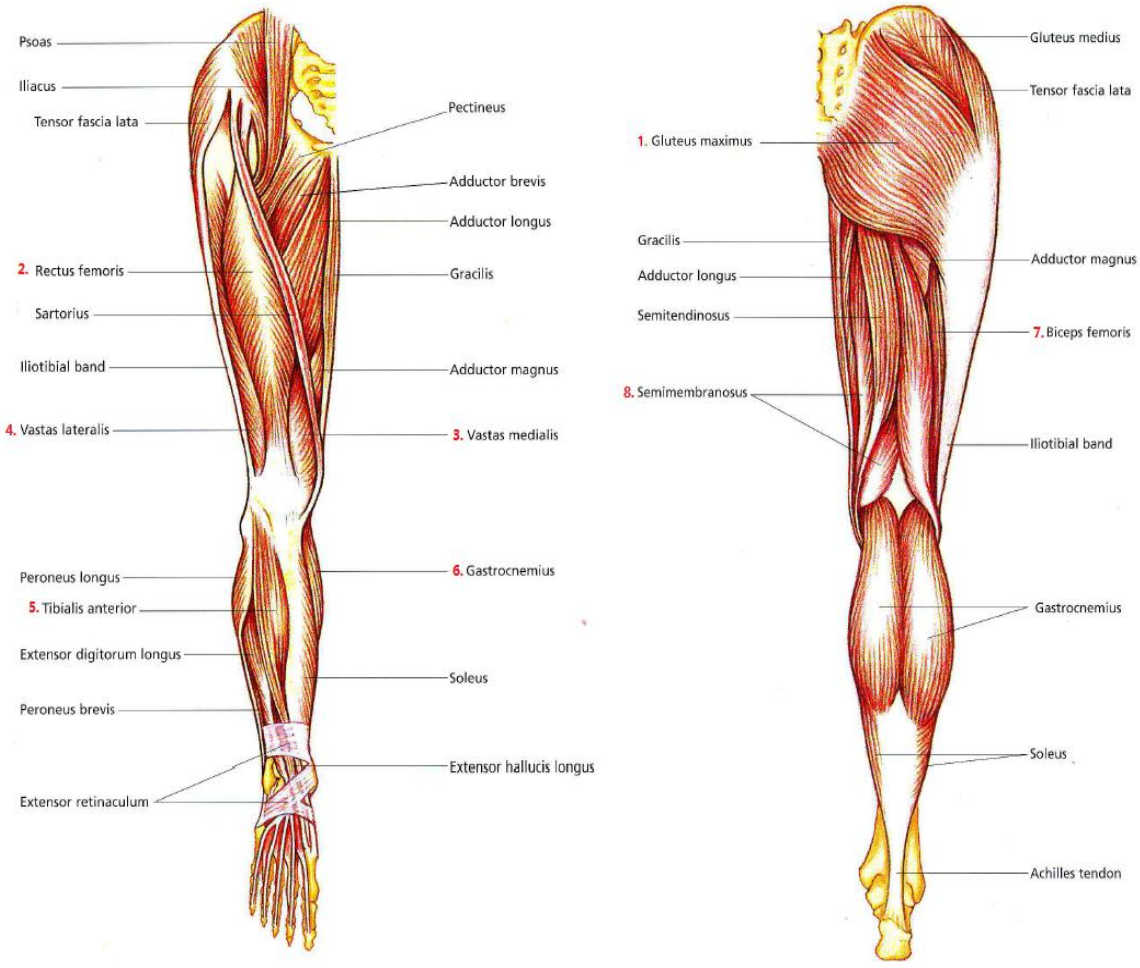

Figure 3. 12: Superficial muscles of the human anterior and posterior leg, reproduced from (Cash, 2000), with added labels of the eight muscles that were tested by different authors: 1-Gluteus maximus (GM); 2-rectus femoris (RF); 3-vastus medialis (VM); 4-vastus lateralis (VL); 5-tibialis anterior (TA); 6-gastrocnemius (G); 7-biceps femoris (BF); 8-semimembranosus (S).

In the literature, many different patterns of muscle activity during cycling (bicycle) were discussed (Desipres, 1974; Faria & Cavanagh, 1978; Gregor et al., 1981; Houtz & Fischer, 1959) with different protocols.

Figure 3. **13** shows a comparison of 4 different regions of muscle activity from the literature where the black areas indicate the regions of muscle activity. Discrepancies are seen among the plots which could be resultant from different experimental setups including foot-to pedal positions, types of shoes worn, seat height, applied load, habit of cycling, different analysis criteria used (the criteria to determine the muscle activation timing).There are various ways to determine the onsets of muscle contraction, several studies used criteria like the earliest detectable rise in EMG above the steady state (Allum & Pfaltz, 1985; Crenna et al., 1987; Inglis et al., 1994; Woollacott et al., 1988) while others used the point where the signal first deviates more than 1 or 1.5 Standard Deviation (SD) from the steady state level (Nashner et al., 1983; Nashner & Forssberg, 1986). A more detailed summary of the different methods used in the literature was reported by Hodges and Bui (Hodges & Bui, 1996) can be found in Appendix C. The onset of muscle activation can also be visually determined by experienced experimenters, this has been considered to be more accurate than the computer-based methods especially with noisy backgrounds (Brown & Frank, 1987; Horak & Nashner, 1986) It was suggested that combinations of the parameter could be used together for accurate determinations.

Table 3. 2: Muscle functions during cycling.

	Muscle	Bi- or mono-articular	Action
Anterior leg muscles			
Quadriceps	Rectus femoris	Bi-	Hip flexion and knee extension
	Vastus lateralis Vastus intermedialis Vastus medialis	Mono-	Knee extension
Posterior leg muscles			
Gluteals	Gluteus maximus	Mono-	Extend and outwardly rotate hip, extend trunk *Proximal part*: slight abduction *Distal part*: Slight adduction
	Gluteus medius Gluteus minimus	Mono-	*Anterior*: Flex and inwardly rotate hip *Posterior*: Extend and outwardly rotate hip
Hamstrings	Biceps femoris	Bi-	Knee flexion and outward rotation when flexed, and hip extension
	Semimembranosus Semitendinosus	Bi-	Knee flexion and inward rotation when flexed, and hip extension

Jorge and Hull (Jorge & Hull, 1986) went on to show that even for the same experiment set up and protocols, the muscle activation range could still be different for individual subjects (see Appendix C). An averaged results of their experiments of six professional cyclists is shown in Figure 3. 14. The onsets of activity for all muscles in the quadriceps group (②③④) occur well before Top Dead Centre (TDC: here defined as when the right leg is closest to the chest). The

onset of activity for the RF ② is close to the middle of the recovery phase (200 º to TDC) and terminates at about 120-130 º. VM ③ and VL ④ have slightly later onsets of activation compared to RF. Termination of the quadriceps muscles happen at roughly the same angle 135 º. The hip extensor muscles (6, 7, 8), being antagonistic to the quadriceps, are active from just after the TDC, to almost the start of the quadriceps activations. Their work provided guidance for the generation of our own muscle activation range in a later experiment (see 4.5).

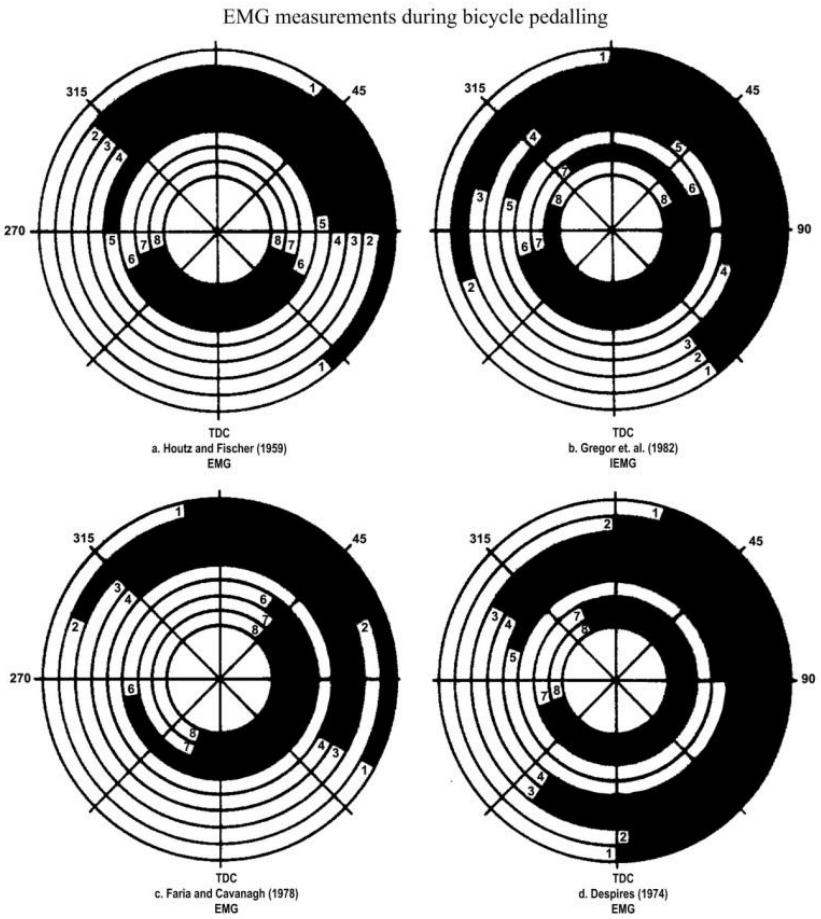

Figure 3. 13: Comparison of EMG activity regions reported by previous studies (Jorge & Hull, 1986). 1-Gluteus maximus (GM); 2-rectus femoris (RF); 3-vastus medialis (VM); 4-vastus lateralis (VL); 5-tibialis anterior (TA); 6-gastrocnemius (G); 7-biceps femoris (BF); 8-semimembranosus (S).

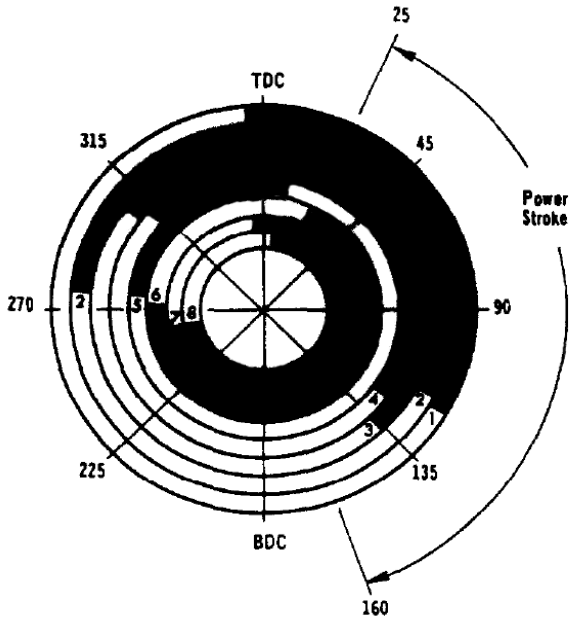

Figure 3. 14: Average muscle activation range for six subjects, reproduced from (Jorge & Hull, 1986). 1-Gluteus maximus (GM); 2-rectus femoris (RF); 3-vastus medialis (VM); 4-vastus lateralis (VL); 5-tibialis anterior (TA); 6-gastrocnemius (G); 7-biceps femoris (BF); 8-semimembranosus (S).

3.12 State of Art - Discussion on the commercial FES cycling systems

There is a lot of research going on FES cycling, but only few of the output actually make it to the market. After reviewing 4 models from companies worldwide: REGYS (Therapeutic Alliances Inc.) (USA); RT300 (Restorative therapies website, 2011) (USA), BerkelBike BV (BerkelBike, 2011) (Netherlands), RehaBike (Anatomical Concepts (UK) Ltd), the following conclusions were drawn:

- Timing: All four models share the same method to produce the stimulation pulses at the right timings. A sensor in the cranks continuously informs the computers about the position of the cyclist's legs. The time at which each muscle needs to be stimulated is then calculated and the stimulation pulses are sent to provide a fluent pedalling movement.
- Mobility: Most of the models are designed for home use.
- Control strategy: Most of the systems are passive stimulation with motor assistant. Two models (REGYS-2 and RehaBike) mentioned closed-loop with speed as the feedback. None of them used EMG feedback.

Almost all these systems claim to have positive effects both on physical and mental health, including relaxation of muscle spasms, improved circulation, increased muscle mass, improvement in cardiopulmonary function, a reduction in the frequency of pressure sores, improvements in bowel and bladder function, increased range of motion (Website, 2011). The users also said how much they enjoy cycling and that it makes them feel much better, they

general have an improved self-esteem as a result of training (Therapeutic Alliances Inc website, 2011). None of them mentioned the possibility of recovering the lost functions.

3.13 Motivation for developing a closed-loop FES cycling system

For patients with incomplete spinal cord injury, it is possible to detect the electrical activity in muscles which result from their own voluntary attempts to use these muscles. This could be used as a signal to control a stimulator. Could it be arranged that stimulation only occurs when the patient tries to pedal voluntarily, hence ensuring the coincidence of the antidromic APs with the natural APs of the anterior horn cell?

Thus far we have seen that the difficulty of analysing EMG signal from the muscle being stimulated. This is due to the presence of large stimulus artefact and various reflexes in the EMG. The stimulus artefact, being an entirely physical phenomenon, is only dependent on the stimulation. Both the stimulus artefact and the M wave are independent of the voluntary drive of the subject where the reflexes (H reflex and the F wave) are much more complicated. If they are present at all, they may affect the EMG signal in a way we can't easily predict.

The muscle fatigue model (3.9) means that the EMG is likely to change with time during cycling. Even for a constant voluntary drive, the EMG may vary in amplitude or spectrum. Another complication that might be brought by the muscle fatigue is the change of cycling mode. The subjects may be able to use muscles differently (e.g. he may still be using the same muscle group, but in a different proportion) without even notice the change. These may also affect the EMG recordings.

Here we propose to design a FES cycling system for SCI patients with residual voluntary effort. Such a system will use the patient's voluntary drive as a control signal to the stimulator. There are only a few EMG-controlled stimulation systems at present (3.10) and these systems differ from ours in the following points:

- Complexity of the exercise. These systems focus on finger movements or knee extension, unlike a dynamic movement like cycling.

- The stimulation intensity is not controlled by the EMG, it is only the ON/OFF of stimulation that is controlled. The cycling process is more complicated than the finger movement or foot twitch as there are more muscles involved and more sophisticated control algorithm will be required.

Our research questions are:

Can we find a signal to represent the patient's voluntary drive during FES cycling? Can this signal be used as a control signal to modulate the stimulation of FES cycling?

The first step to answer the research question is the development of a FES cycling system that enables us to do experiments. For this reason, chapter 4 is dedicated to discussing the design

and development of the various pieces of electronic equipment. Even with the appropriate apparatus, the recording of useful EMG signals under stimulation has proved to be complicated. Therefore two ways of estimating the voluntary drive via the EMG signal recorded during FES cycling are experimented in both time domain (chapter 5 where we use RMS EMG amplitudes) and frequency domain (chapter 6 and 7 where we study the spectrum of the EMG signals). As stated by the research question, not only we aim to find a signal as an estimation of the voluntary drive but also need to evaluate it as a control signal of our FES cycling system. This was performed in the end of chapter 5 and chapter 7.

Should such a FES cycling system be designed, there is a potential market for our system since it has all the benefits of the existing systems described in 3.12 but also with improved mobility and targets functional recovery.

CHAPTER 4: THE APPARATUS AND THREE PRELIMINARY EXPERIMENTS

4.1 Introduction

This chapter introduced the essential apparatus used for the project. Some apparatus was adopted from other projects, like the tricycle, the shaft encoder, the EMG amplifier with current conveyor (CC EMG amplifier) and the biphasic stimulator; some equipment or devices were bought, like the ergotrainer and Data Acquisition module (DAQ); and some apparatus was constructed or designed specifically for the project, like the commutator, the isolation amplifier boxes, the stimulator, the differential EMG amplifier, the fast recovery EMG amplifier and the blankable EMG amplifier.

Table 4. 1: The list of apparatus.

Name of the apparatus	Designed, modified, or adopted	How many were made/used?
Tricycle	Adopted	1
Shaft encoder	Adopted	1
Commutator	Designed and constructed	1
Stimulator	Designed and constructed	1
Instrumentation EMG amplifier	Constructed	1
Fast recovery EMG amplifier	Constructed	1
Blankable EMG amplifier	Constructed	4
CC EMG amplifier	Adopted and modified	1
Isolation box	Designed and constructed	4
Biphasic stimulator	Adopted and modified	1
Tacx ergotrainer	Adopted	1
Laptop and DAQ	Purchased	1 each

One major difficulty of our project was to record EMG from a muscle during stimulation with the presence of stimulus artefact (see 3.5). Therefore it was important to choose the right EMG amplifier. Four were introduced (see 4.3) and tested to compare their ability of recovery quickly after stimulation through experiments (see 4.4). All experiments were performed on able-bodied subjects with approval of the UCL Research Ethics Committee. For each experiment, there is a brief introduction followed by a description of the experiment setups and procedures, an

analysis of the results and a discussion. Among the four amplifiers, three of them (the instrumentation, the fast recovery and the blankable EMG amplifier) were constructed in the early stage of the project. Therefore they were compared first with the stimulator. The blankable EMG amplifier was found to have the fastest recovery time and was used in the experiments in chapters 6 & 7. The CC EMG amplifier (tested with the biphasic stimulator) was only available in a much later stage of the project: tests were described in 4.4.3. The results were satisfactory as it provided reduced recovery time than that of the blankable EMG amplifier. It was adapted in the experiments in chapter 5.

Following the test of apparatus, some of them were used in a preliminary experiment looking into the activation range of the leg muscles during cycling. There was a large discrepancy in the reviewed articles (see 3.11) as many factors could affect the results. Therefore it was necessary for us to generate our own muscle activation range for the particular setup we had. This range will help us to decide the stimulation pattern in the future experiments as we would like to have the stimulation pulses delivered to the muscles during the muscles' natural activation range.

4.2 Apparatus

The EMG-controlled FES cycling system provides EMG signal recording and processing as well as control of the stimulator as proposed in 3.13. These functions are executed by different apparatus. Figure 4. 1 is a block diagram of a closed-loop FES cycling system, which also gives a list of apparatus required to perform the experiment. These apparatus were designed and constructed following the International Electrotechnical Commission (IEC) standards for the safety and effectiveness of medical electrical equipment BS60601. These are introduced accordingly in the following sections.

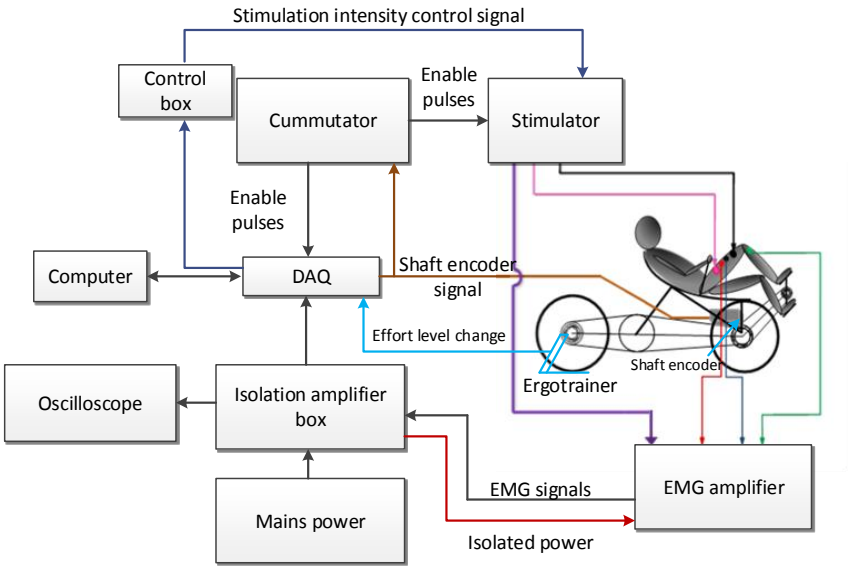

Figure 4. 1: Block diagram of a closed-loop FES cycling system.

4.2.1 *TRICYCLE AND SHAFT ENCODER*

A commercially available recumbent tricycle (Trice Classic) modified by Mr Tim Perkins (Perkins et al., 2001) was adapted for this project. As the trike will be used by SCI patients in the future and very likely outdoors, this particular model was chosen for its inherent stability and custom designed comfortable seating. A 7-bit shaft encoder was mounted to it, driven by a short chain attached to the crank shaft. The shaft encoder generates a ramp signal ranging from 0V to 5V (which corresponds to the crank angle 0° to 360°), serving as a voltage representation of the cyclist's foot position, which was used for data analysis and control. The Top Dead Centre (TDC) is defined as the pedal position when the left hip is most flexed, left knee closest to the chest.

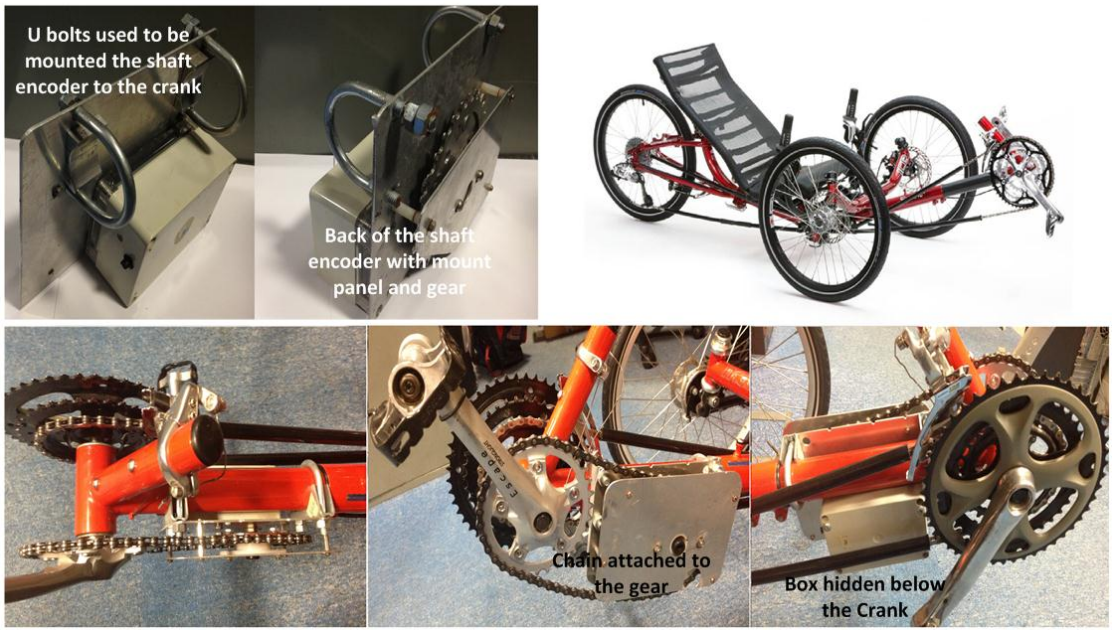

Figure 4. 2: The shaft encoder before and after mounting to the trike, the sprockets on the shaft encoder and the crank shaft are the same size.

4.2.2 *THE ERGOTRAINER*

An ergotrainer *Tacx Cycle Force Excel* is used to set the resistance applied to the back wheel of the trike which controls the effort exerted by the cyclist. It comes with a cycling computer which enables changing of the effort levels as well as monitoring the averaged power output. In the cycling computer control panel, this effort level is called "slope" as if the cyclist were going uphill (circled and underlined Figure 4. 3). The slope ranges from 0-9. The ergotrainer changes the slope by applying different amount of resistance to the back tyre of the trike, thereby changing the effort the user needs to make if a constant cadence is maintained. The power output of the frequently used slopes was measured using the cycling computer at 60rpm. The output power of

the effort levels ranging from 3-9 (Level 3— Level 9) were 160-220 watts in steps of 10 watts. From now on, the effort levels are used in the thesis as a reference to the different power outputs. One reason for this is that we could evaluate the EMG output of the subjects at constant power output. Another reason is because the ergotrainer used was an old model and there was no software support for it. Therefore it was not possible to record the instantaneous output power from the ergotrainer without taking it part.

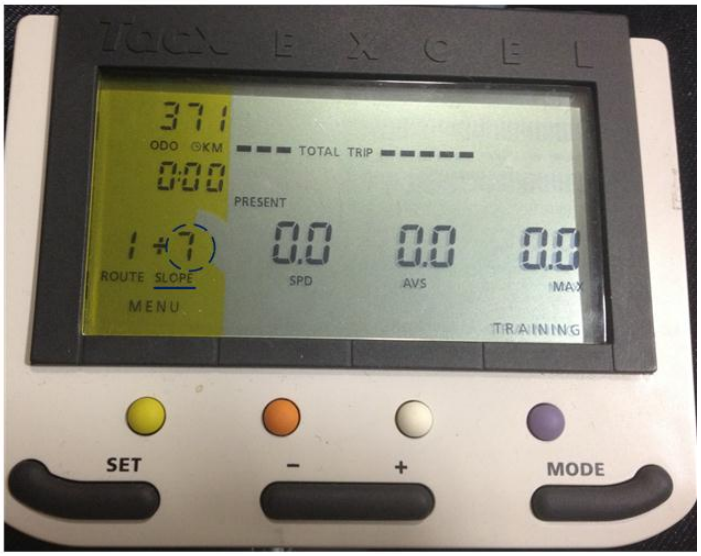

Figure 4. 3: The cycling computer to control the resistance applied to the back tyre of the trike, the slope (effort level) was circled.

Figure 4. 4: Left: The Tacx ergotrainer mounted to the back wheel of the trike. Right: Tyre rested on roller which has electrically controlled brake.

4.2.3 THE COMMUTATOR

For this project, the FES cycling system only stimulates the subject while the corresponding muscles would naturally be contracted. To achieve this, a device called the *commutator* was

designed and constructed to control the stimulation. The term commutator is an analogy to the 'commutator' used in motors which directs currents through different coils. In this case, the commutator directs "enable pulses" to the stimulator. The idea behind the commutator is that it takes the angle signal from the shaft encoder (voltage values between 0-5V) and produces enable pulses at desired crank angles set by the operator. By comparing the voltages on potentiometers on the front panel to the shaft encoder voltage (position of the leg), a monostable is used to produce a pulse of 1ms duration when a comparator output goes high. The commutator has 16 channels with individual fitted ON/OFF switches, the monostables from the ON channels are passed through an OR gate to produce the enable pulse to trigger the stimulation.

- The design specifications of the commutator is as follows:

It allows three modes, being continuous mode, single pulse mode and the doublet mode. In each mode the trigger signal, which is called the enable pulse, is set to be at amplitude = 5V and duration 1ms.

- Continuous mode: The enable pulse is controlled by a starting and stopping angle set by the potentiometers in the front panel (see Figure 4. 5), during the enable pulse the stimulation is continuous.
- Single pulse mode: Each potentiometer on the front panel sets a single enable pulse which triggers a single stimulation pulse.
- Doublet mode: Two enable pulses close to each other (doublet) are set by one potentiometer on the front panel, therefore giving extra muscle contraction when needed.

Figure 4. 5: Front panel of the commutator.

The commutator was built in a 19'' aluminium box with detachable front panel. From left, there are three LEDs as power indicators and the LEDs to the top right corners of the potentiometers flashes when the channel is enabled. The black buttons below the diodes, when pressed down,

produce a reading displayed in the LCD monitor to the right. The reading shows the current potentiometer wiper voltage of the selected channel. One toggle switch is fitted to each channel for ON/OFF.

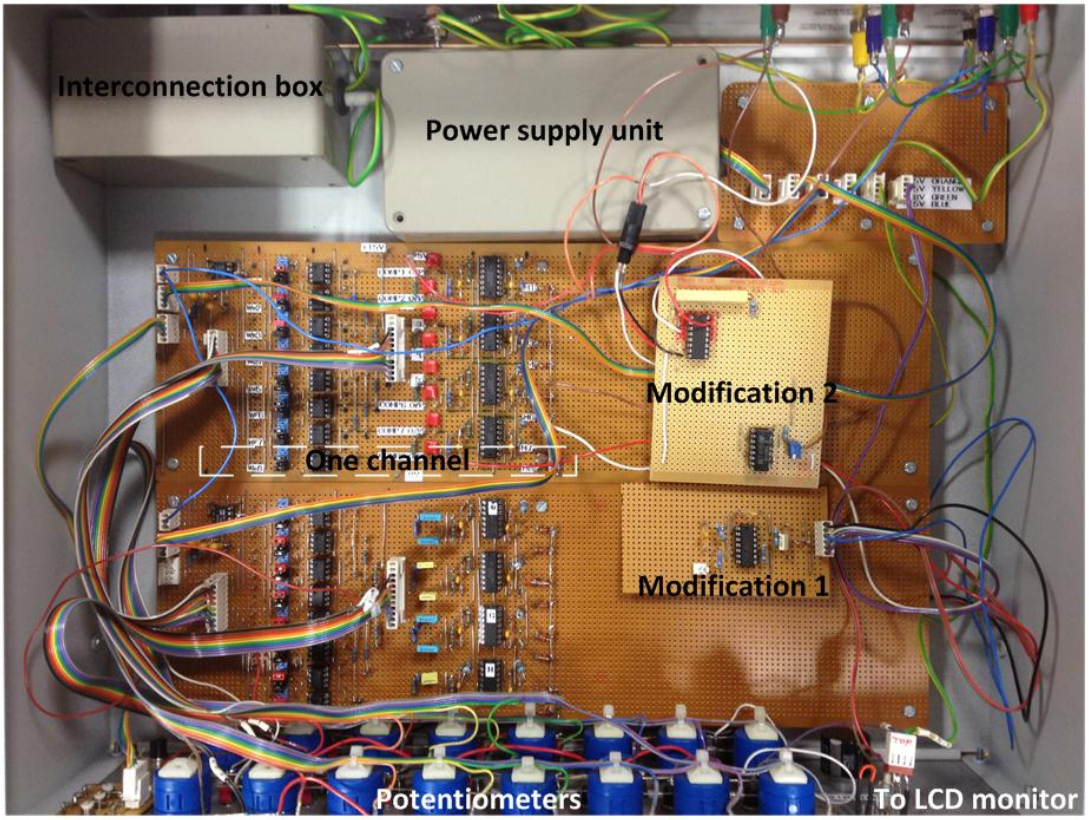

Figure 4. 6: The inside of the commutator, showing the interconnection box, the power supply unit, the 16 channels and two further modifications on separate vero boards, the 16 potentiometers connected to the front panel, the LCD monitor.

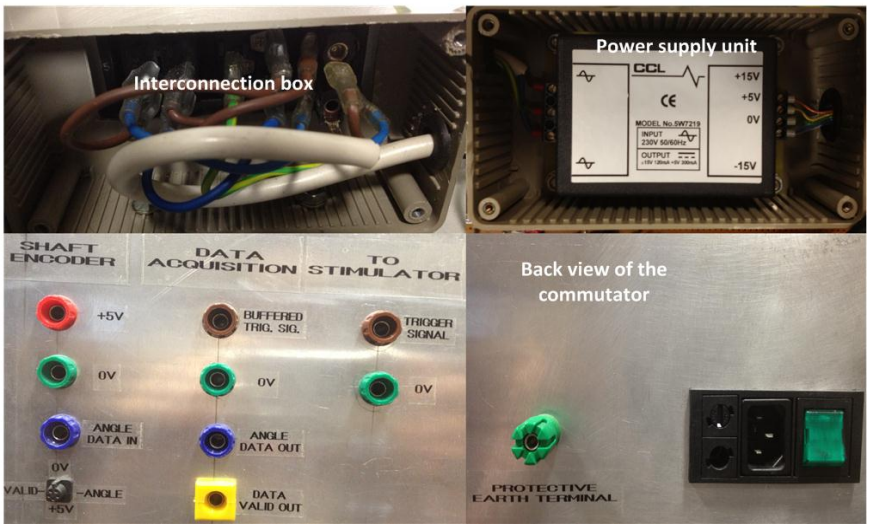

Figure 4. 7: Details of the commutator.

The interconnection box facilitates connection of the mains power supply to the power supply unit of the commutator. Both the interconnection box and the power supply unit are encapsulated in plastic boxes for safety. The back of the commutator supports all the necessary sockets to receive or send signals from other devices (shaft encoder, stimulator, DAQ). There is also an earth terminal and power switch on the back panel.

4.2.3.1 Circuit design

The comparators compare the voltages (corresponding to start and stop angles set by the potentiometers) to the shaft encoder voltage (corresponding to position of the leg). The output of the comparator becomes low when the set angle voltage matches the shaft encoder voltage. The falling edges of the comparators' output trigger monostables which act as the set and reset pulses for the JK flip-flop. The output of the JK flip-flop remains high until a stop pulse appears on the reset terminal.

Figure 4. 9 shows the enable pulse corresponds to the starting and stopping angles. The output from the stimulator in continuous mode during cycling is shown in the bottom trace, where the stimulator generates continuous pulses of at 20Hz for the preset crank angle positions.

4.2.3.2 Continuous mode

Traditionally, bursts of continuous stimulation are used during FES cycling. The commutator is built with a "*Continuous Mode"* where the 16 comparators are grouped in pairs so that one potentiometer sets the starting angle of stimulation and the other sets the stopping angle as shown in Figure 4. 8. In the range between the two angles, the stimulation will always be on. The stimulation frequency in this mode must be set by the stimulator (see 4.2.5 free running mode of stimulator).

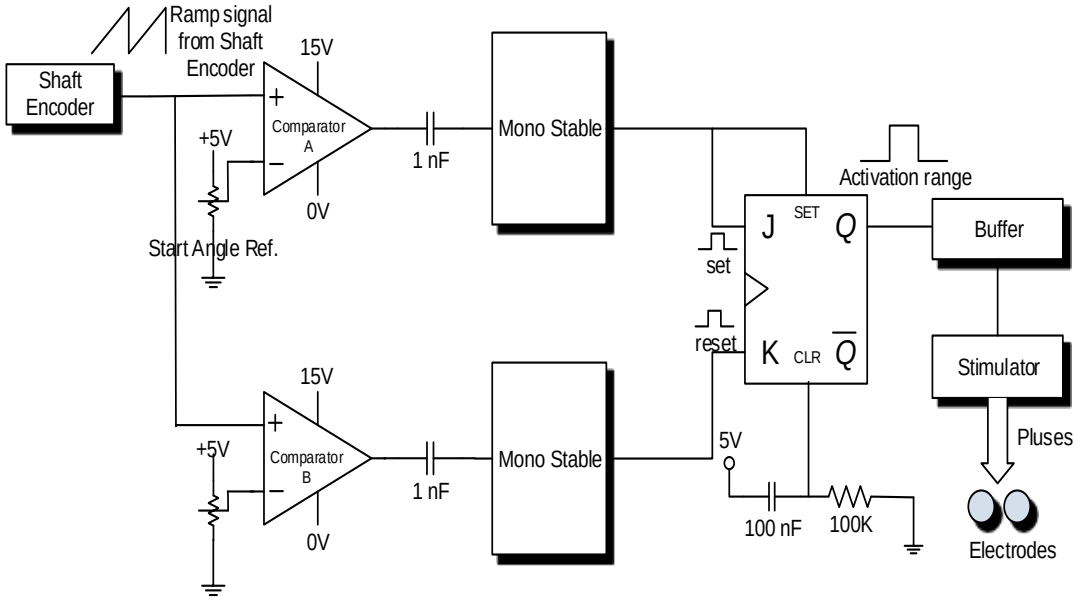

Figure 4. 8: Layout for the commutator modification for the continuous mode.

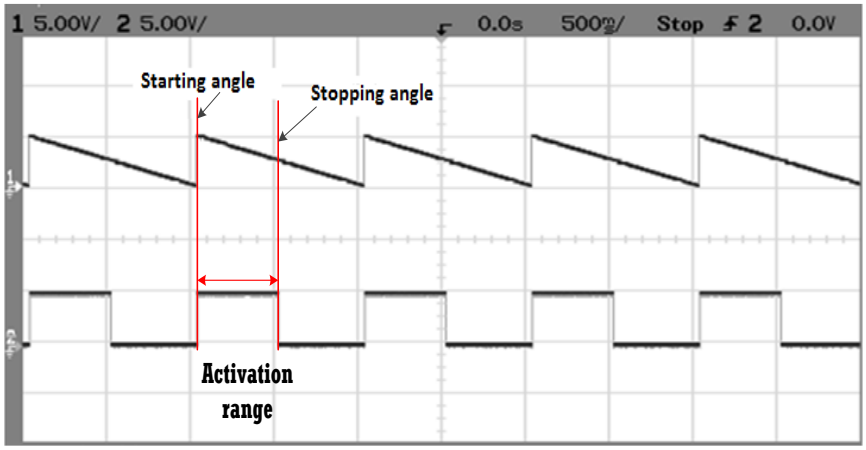

Figure 4. 9: Upper trace: shaft encoder signal showing the starting and stopping angles; lower trace: the enable output from commutator for stimulator.

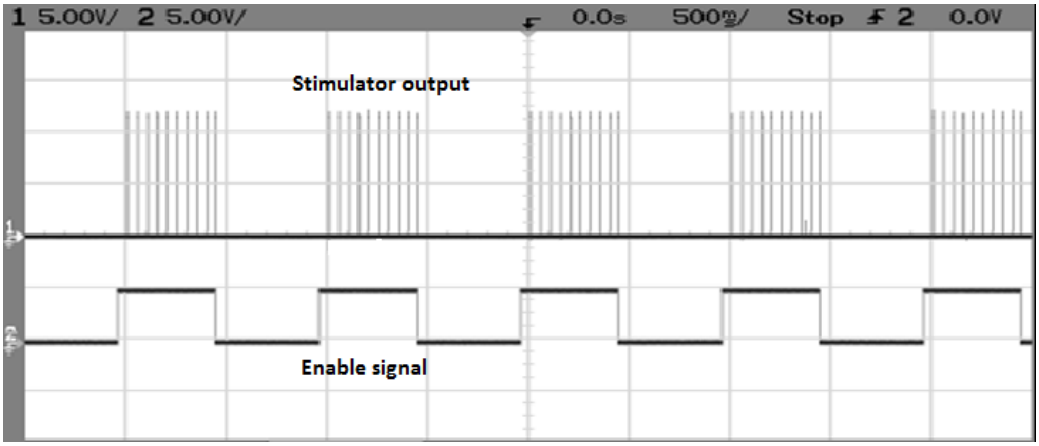

Figure 4. 10: Stimulator output triggered by enable pulse.

4.2.3.3 Single pulse mode

In this mode, the sixteen rotary switches each generate an enable pulse to control the timing of the stimulation. Each channel triggers the stimulator at the set angle (shaft encoder voltage) to generate a single stimulation pulse. Therefore up to 16 pulses with variable frequencies can be produced. Different combinations of the pulses can be arranged in this mode. Figure 4. 11 shows up to 16 enable pulses generated by the commutator which is also the maximum number of output pulses in one revolution in single pulse mode. The potentiometers on the front panel set the trigger levels. Note here the shaft encoder signal was simulated by a signal generator therefore having a constant gradient from 0V to 5V. When the trigger levels were equally spaced, 0.25V here, the pulse frequency will be constant if the cadence is constant. In a real cycling experiment, the shaft encoder signal may not have a constant gradient as the subject cannot maintain perfectly constant cadence, therefore the trigger levels, even when equally spaced in

voltage, may have different time delays between them. This concept was important as it was adapted in the design of angle trigger stimulation in the coherence experiments in 6.5.2. The pulses can also be grouped together freely to meet other purpose as shown in the right graph. The 16 pulses were grouped into two groups of 8 pulses closer together and leaving a larger time window between the two groups.

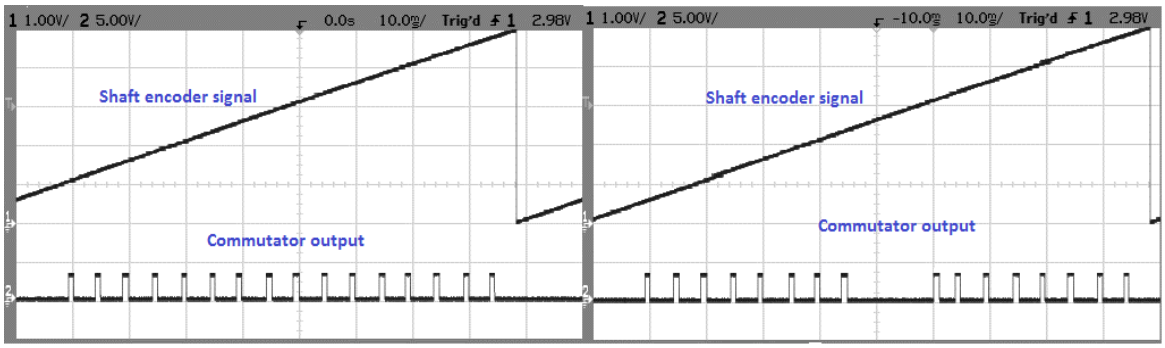

Figure 4. 11: Left: The commutator output showing 16 enable pulses with equal spacing; Right: The 16 enable pulses were divided into two groups.

4.2.3.4 Doublet mode

As discussed in 3.9, FES stimulated muscles exhibited premature muscle fatigue. A possible approach to this problem is using patterned stimulation, which is stimulation with non-uniform stimulation frequency. A doublet consists of two closely spaced pulses emitted at a regular frequency often preferred in a non-uniform stimulation pattern. Stimulation with initial doublets more closely mimics how the central nervous system (CNS) activates muscles under voluntary control (Karu et al., 1995). Routh & Durfee also reported that for a given amount of work for FES stimulated muscle, the fatigue was reduced if patterned stimulation was used (Routh & Durfee, 2003). Before deciding the stimulation pattern, it is necessary to revisit our project aims at this stage. We wanted to acquire a signal from the EMG recorded during electrical stimulation to represent the voluntary drive of the subject. However, due to the presence of the stimulus artefact it is difficult to analyse the EMG signal immediately after a stimulation pulse. The time available for the analysis of the EMG signal is also limited by the interpulse interval between the consecutive stimuli, which is 50ms at 20Hz stimulation frequency. As only one estimation of the voluntary drive is needed per cycling revolution, a reasonable approach is to leave a longer window between the two stimulation pulses while keep the number of stimulation pulses the same to ensure enough power output. The longer window is achieved by using one channel to initiate a doublet at a desired angle followed by a larger delay then the other potentiometers are set as for single pulse mode.

The commutator was modified further to generate the doublet (modification 1). Two 556 timers each containing two monostables were used. In Figure 4. 12, monostable A and B are used to produce two stimulation pulses with fixed pulse widths of 1ms and monostable C is used to control the delay between the pulses. This delay is determined by the values of capacitor C (1µF), the fixed resistor R (4.7KΩ) and a potentiometer (10KΩ) on the front panel of the commutator.

The minimum delay occurs when the potentiometer is set to zero. The factor of 1.1 is inherent to the monostable.

$T_{min} = 1.1\{1\mu F \times (4.7K\Omega + 0\Omega)\} = 5.2ms$

$T_{max} = 1.1\{1\mu F \times (4.7K\Omega + 10K\Omega)\} = 15.2ms$

The operation of the modified circuitry is illustrated by the timing diagram shown in Figure 4. 13. On the falling edge of the output of the comparator, the monostables A and C are triggered. The output of monostable C is adjustable and triggers monostable B.

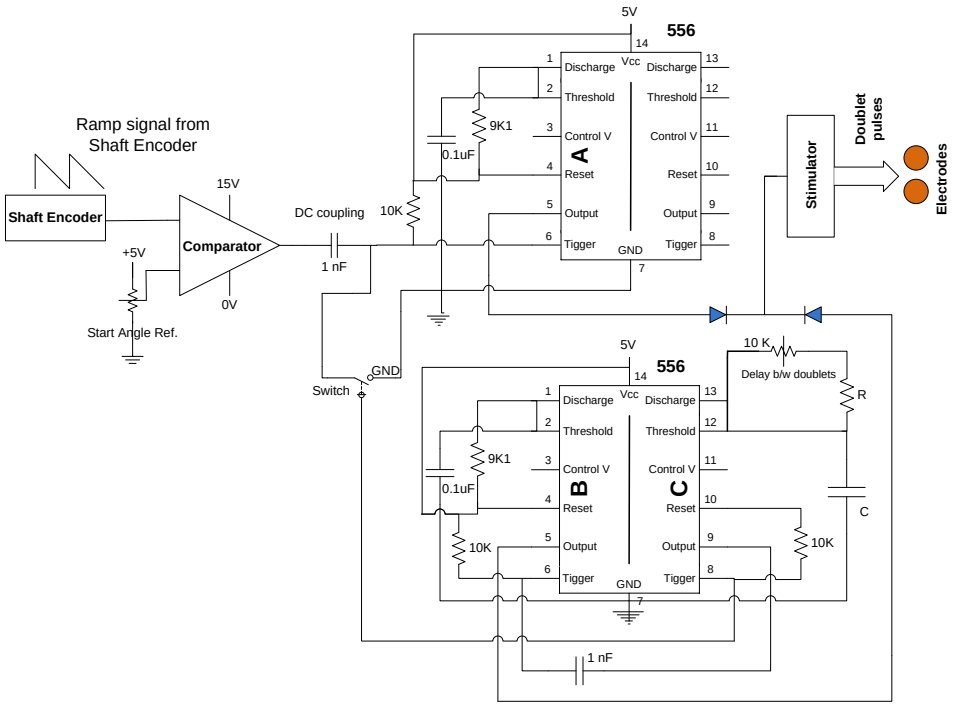

Figure 4. 12: Circuit Diagram for Doublets using 556 timer ICs.

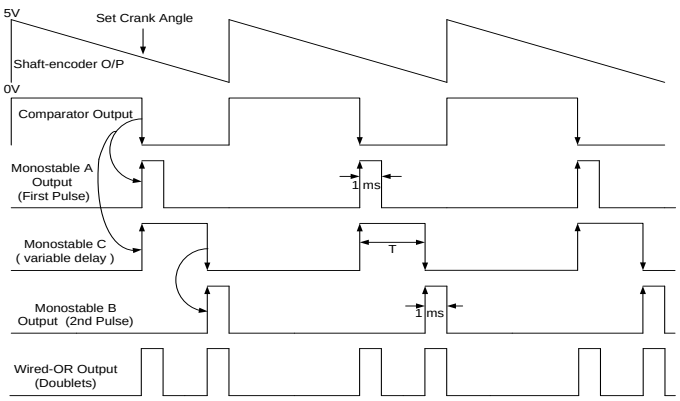

Figure 4. 13: Timing diagram for doublet circuit.

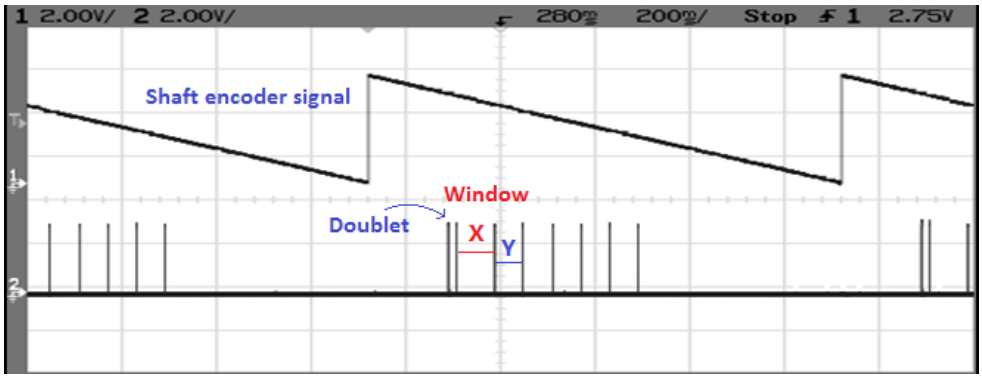

Figure 4. 14: A Stimulation pattern initiating with Doublets, the gap between the doublet and the next stimulation pulse (the X window) is longer than the delay between single stimulation pulses (the Y window).

4.2.4 *THE ISOLATION BOX*

The isolation box was designed not only to protect the subjects from mains power supply but also to provide isolated power supplies to the EMG amplifiers. Four were constructed to isolate the front end of the EMG amplifiers from the DAQ system as well as providing isolated power to the EMG amplifiers. They also feature additional gain stages which provide the variable gains from 1× to 120× by a rotary switch.

As illustrated in Figure 4. 15, the isolation amplifier is powered by mains through a DC-DC converter (PWS726A) and the stimulation pulses are sent from the stimulator to the blankable EMG amplifier as a control signal through an opto-isolator (HP6N139). The EMG signal is recorded through an isolation amplifier (ISO121). In this way, the subject is completely isolated from mains to ensure their safety.

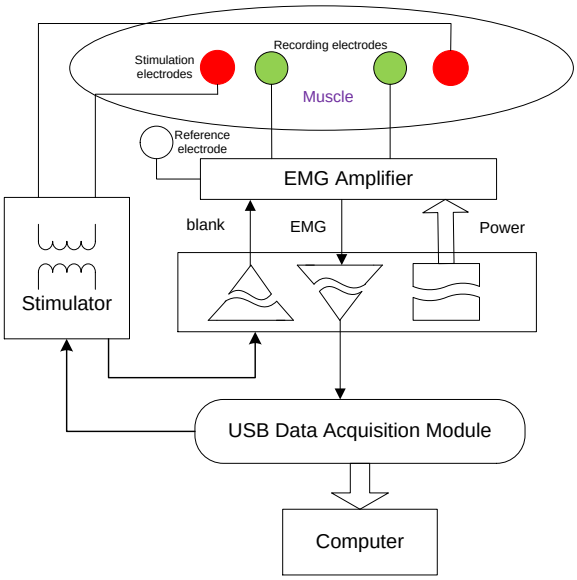

Figure 4. 15: The function of the isolation amplifier in the system.

The socket, in the bottom left corner of the front panel, connects to the EMG amplifier. Above this socket, a BNC connector can be seen on the left, from which the EMG output is measured.

The BNC connector on the right receives the blanking timing information from the stimulator. The rotary switch in the centre controls an extra gain stage to the EMG amplifier. The LEDs below indicate that the amplifier is powered up. The mini jack sockets were used during development for testing purposes only.

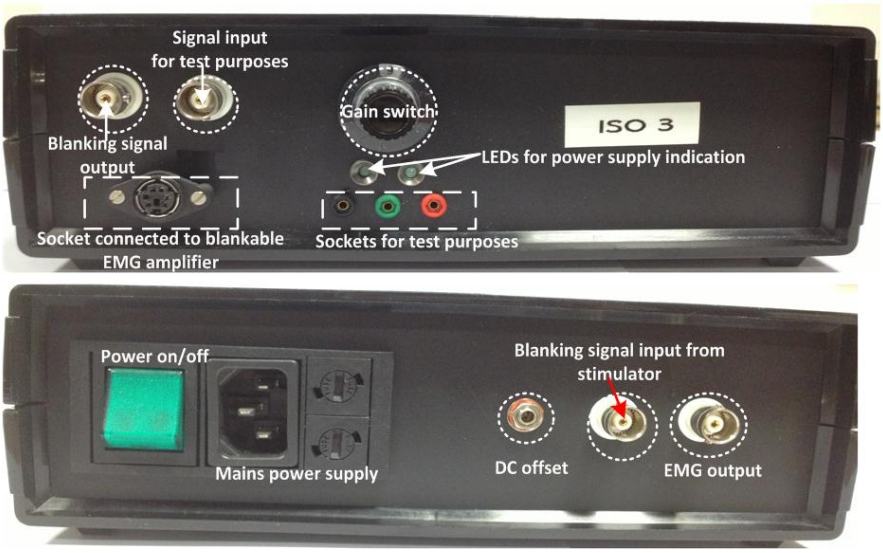

Figure 4. 16: The isolation amplifier box front panel (above) and back panel (below).

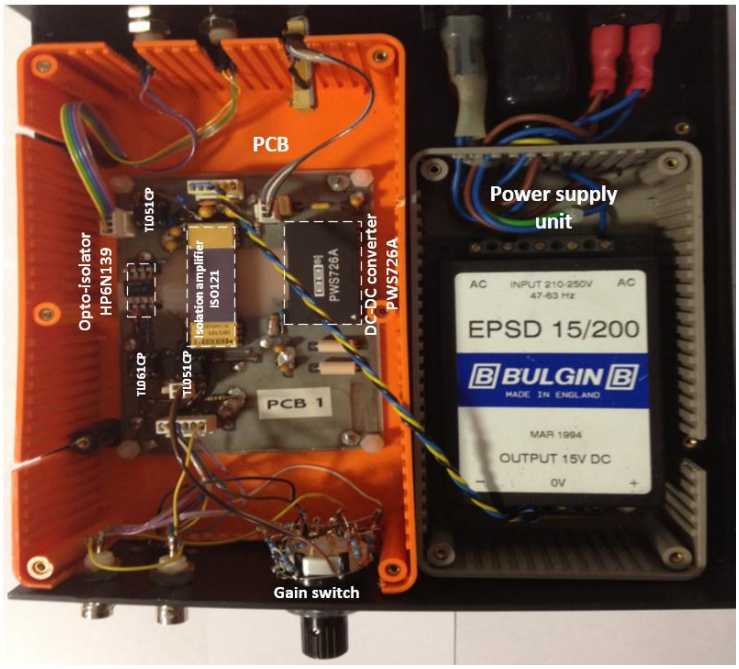

Figure 4. 17: The inside of the isolation amplifier, left half is a PCB containing all the ICs and the right side is the battery. Both the PCB and the power supply unit are fixed in plastic boxes.

4.2.5 THE STIMULATOR

The stimulator generates stimulation pulses with adjustable frequency, voltage amplitude and pulse width. The stimulator works in conjunction with the commutator and the blankable EMG amplifier.

4.2.5.1 Circuit design

As shown in Figure 4. 18 the stimulator has two modes, one is the Trigger mode to be driven by the commutator's single pulse mode and doublet mode; the other is the free running mode when the stimulator is driven internally by an oscillator with variable frequency, this mode is to be used with the commutator's continuous stimulation mode. In trigger mode the stimulator generates a stimulation pulse when there is an enable pulse coming from the commutator. While in free running mode, the stimulator generates continuous stimulation pulses at the chosen frequency for the duration of the enable pulse if provided by the commutator. Therefore the stimulator triggers on the falling edge of the commutator's enable signal, which is 5V, 1ms. The stimulator has only one stimulation output channel. The output voltage range is decided to be from 20V to 130V, with a frequency range from 1Hz-50Hz and pulse width from 50-500µs. These parameters were decided according to the most popular range of stimulators for muscle stimulation. However, the final design of the stimulator has a stimulation pulse width ranging from 54 to 880µs and stimulation frequency ranging from 1.42 to 63.6Hz. The blanking signal can be varied in a time window from 1.16ms to 40ms with a pre-blanking pulse from 0.5ms to 5ms. The resultant specifications are not exactly matching the design expectations due to the limitations of the available components, but it covers the most essential range. These parameters can be adjusted by potentiometers on the front panel of the stimulator.

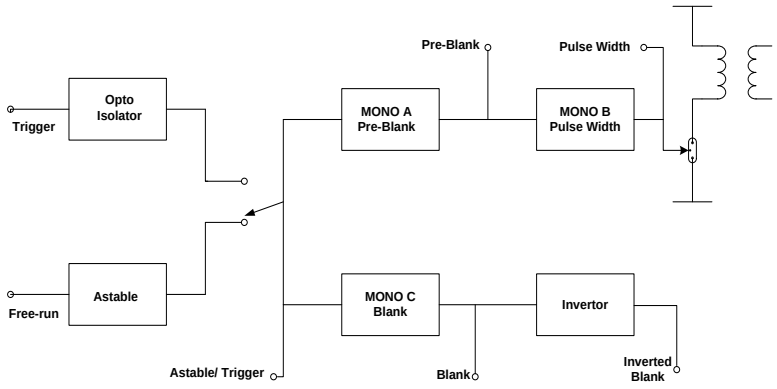

Figure 4. 18: Block diagram of the stimulator.

The timing diagram of the stimulator is shown in Figure 4. 19. The falling edge of the astable output (in free running mode) or the enable pulse (in trigger mode) simultaneously triggers two monostables: pre-blank (A) and blank (C). The width of the pre-blank monostabe is a delay introduced to make sure the blanking (turning off) of the EMG amplifier occurs before the initiation of the stimulation pulse. The Stimulation pulse is produced by monostable B on the

falling edge of the pre-blank pulse. The output of monostable C determines the total blanking time i.e. how long the EMG amplifier is powered off.

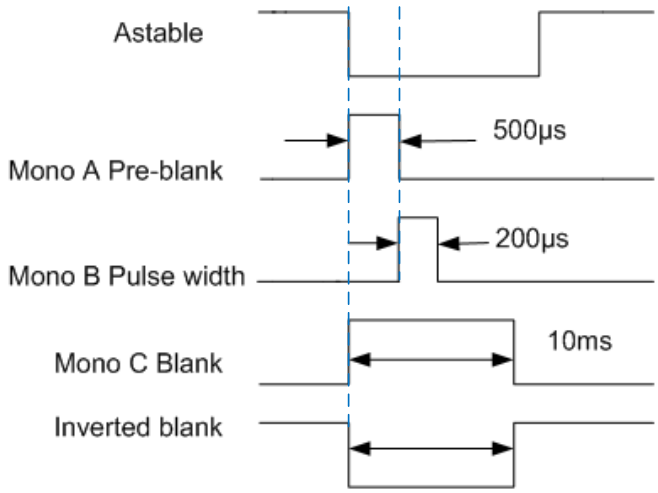

Figure 4. 19: The timing diagram for stimulator.

4.2.5.2 Construction of the stimulator

The stimulator is housed within a black ABS case (231x212x67mm) with removable front and back panels (see Figure 4. 20). The two modes of the stimulator can be switched by a toggle switch on the front panel. The socket labelled “remote”, when plugged in with a push button at the end of a long cable, allows the experimenter to remotely switch on/off the stimulator when sitting at some distance away. The five BNC sockets in turn carry the output of stimulation frequency (by square pulses at the output frequency), pre-blanking pulse width, the stimulation pulse width, blanking pulse width and the inverse blanking pulse width. These values can be adjusted by using a screw driver to adjust potentiometer settings, the access point for which can be seen in the figure above each BNC connector. The rotary switch to the top right corner turns the device on as well as controls the amplitude of the stimulation pulses (stimulation intensity). The LED beside it gives a visual indication when the device is on. The stimulation output is delivered by the socket in the bottom right corner when connected with a customised cable.

Figure 4. 20: The stimulator front and back panels.

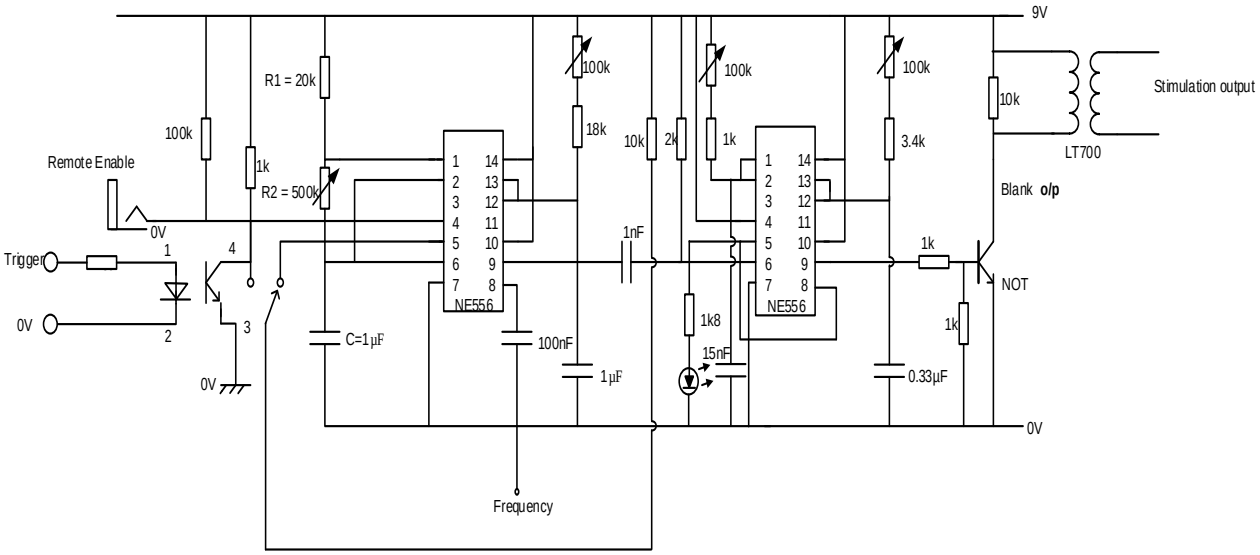

Figure 4. 21: Circuit diagram of the stimulator.

Equation 1 was used in the free running mode to determine the stimulation frequency.

$$\boldsymbol{Frequency} = \frac{\mathbf{1.44}}{(\boldsymbol{R_1} + \mathbf{2}\boldsymbol{R_2})\boldsymbol{C}}\boldsymbol{Hz}$$

Equation 1: The frequency calculation of the free running mode

And the components used to generate the three monostables (Mono A, B & C) are calculated from Equation 2. All the values are as labelled in Figure 4. 21.

$$\boldsymbol{T = 1.1RC}$$

Equation 2: The monostable duration calculation.

Figure 4. 22: The stimulator – inside view.

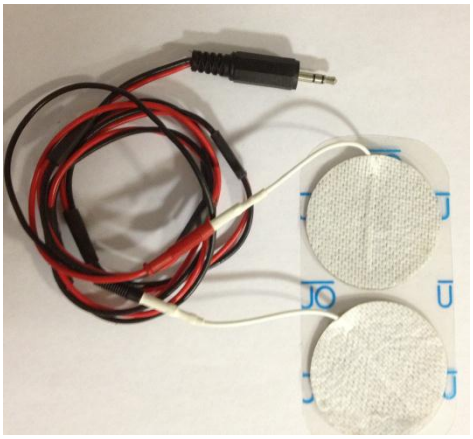

Figure 4. 23: Output cable of the stimulator with 4mm jack plug to the stimulator and two 2mm mini jack plugs connected to two 50mm diameter electrodes from Nidd Valley.

4.2.6 THE DATA ACQUISITION CARD AND THE COMPUTER

A 14-bit National Instrument DAQ USB-6009 was selected to record analog/digital inputs and send digital control signals. It samples the analog input signals (EMG, shaft encoder signal and stimulation pulses) and convert these to digital data that can be recorded and processed by a computer. It has 8 analog inputs with 14 bit resolution and 48k samples/s bandwidth. It also has 12 bi-directional digital inputs/outputs which will be useful in the future for the control logic of the system (see 7.4). The DAQ connects to a Dell laptop with Windows XP operating system that runs both MATLAB and LABVIEW as the control platform. To achieve real time control of the stimulation during FES cycling, the CPU of the laptop we used needed to be fast enough. Two laptops were used throughout the project; the first one was the Dell D830 with Intel Core 2 Duo. With the increasing demand of faster data processing speed towards the later stage of the project, when high CPU-demanding software and real time signal processing was used, a Dell LATITUDE E5420 with Intel Core i7 was purchased.

4.3 Introduction to the EMG amplifiers

4.3.1 General introduction

The amplifier is a critical apparatus in EMG recording since it provides the first recording of the EMG signal. There are a few aspects that need to be considered when choosing the amplifier. EMG amplifiers saturate when there is a large input signal, and they need time (typically 10s of ms) to return to their normal working. Often a stimulation pulse is sufficient to cause this. When stimulating the nerve at 20Hz, there is 50ms less the width of the stimulation pulse (which is normally in 100s of μs) between two consecutive stimuli. It is important to extract the voluntary drive from the signal during such an interpulse interval with the presence of the stimulation artefact, the M wave, silent period and other reflex phenomena. This makes the ability of the amplifier to recover quickly from saturation a key issue when selecting the EMG amplifiers. As described in 3.5.3, there are many different ways to compensate for the presence of stimulus artefacts and extract the M-wave, in this thesis we focus on the modification of EMG amplifiers. There are four different EMG amplifiers to consider:

1. An instrumentation EMG amplifier;
2. A fast-recovery amplifier that uses control loops to negate the need for the blanking signal (Thorsen 2002).
3. A blankable EMG amplifier that uses electronics capable of blanking the amplifier during the stimulation pulse (FESTIVAL Project (Bristol University), 1995)
4. EMG amplifier with current conveyor.

These EMG amplifiers are discussed next and their abilities in handling stimulus artefacts compared.

All four EMG amplifiers should meet the design specifications of a standard surface EMG amplifier, which means they should have a gain of roughly 120 and frequency range 0-500Hz. On top of that, the need of fast recovery also limits the recovery time to roughly 10ms.

4.3.2 The instrumentation EMG amplifier

A design of a two-stage differential EMG amplifier is shown in Figure 4. 24. The first stage is usually an instrumentation amplifier having no more than a 20x gain. This output is then AC coupled to block any DC signal thereby preventing saturation of the second stage of amplification. Only AC signals (EMG) are allowed to pass. A second stage with higher gain is used to provide further amplification of the signal. The high pass filter was there to remove offsets from the electrodes.

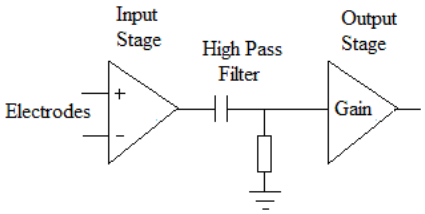

Figure 4. 24: Two stage EMG amplifier with AC coupling.

The ICs used in Figure 4. 25 are the OP200 dual precision (IC1a and IC1b) and the OP07 (IC2) ultra-low offset voltage operational amplifiers.

Table 4. 2: Gain stages of the simple differential EMG amplifier and the cut-offer frequency for the high pass filter

First stage gain	Second stage gain	Total gain	Cut-off frequency
10.4	31.3	326 or 50dB	15Hz

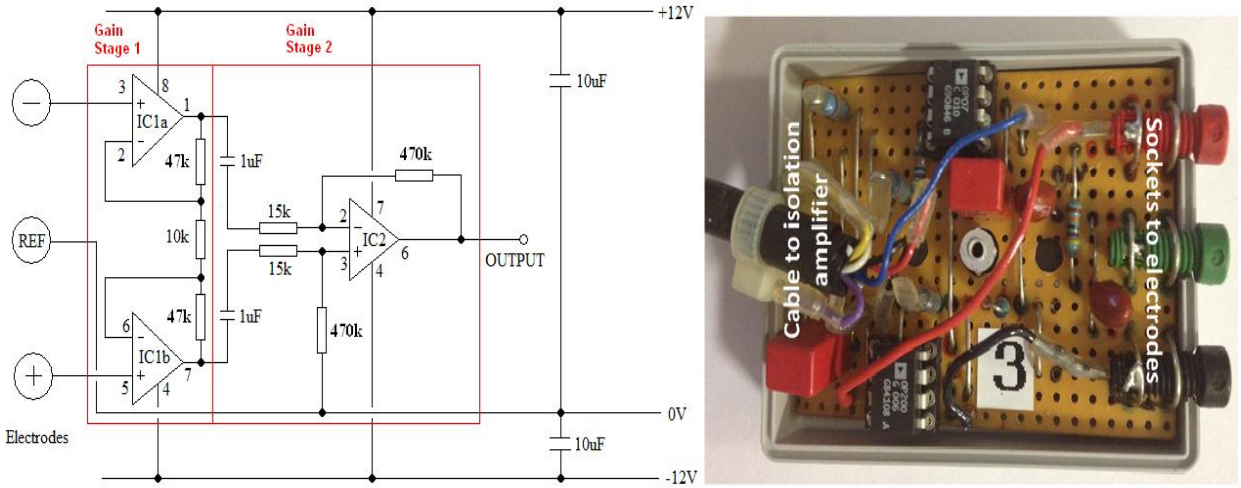

Figure 4. 25: Left: The circuit design of the differential EMG amplifier. Right: Photograph of a constructed differential EMG amplifier.

When EMG signals are to be recorded from muscles being stimulated by electrodes placed next to the recording electrodes, this simple EMG amplifier becomes saturated due to the very large stimulation pulses. There is a recovery period which follows saturation before the amplifier can adequately measure the EMG signal due to the time taken to discharge the capacitor. The simple EMG amplifier sets a baseline for the comparison for with amplifiers designed to use with stimulation. This gives us an upper limit of how long an amplifier needs to recover. Although they were inappropriate for EMG controlled FES systems, they were used later in the experiment without stimulation to find the muscles' activation range during tricycling in 4.5. Four of these amplifiers were built so that EMG could be simultaneously measured in four muscles (RF, VL, VM and Hamstring).

4.3.3 The Fast-Recovery Myoelectric Amplifier

This amplifier was designed by Thorsen to have the ability to prevent amplifier saturation giving rise to stimulus artefacts and motion artefacts (Thorsen 2002)by utilising fast recovery. A special feature of this amplifier is that high-pass filtering is achieved using a non-linear feedback loop.

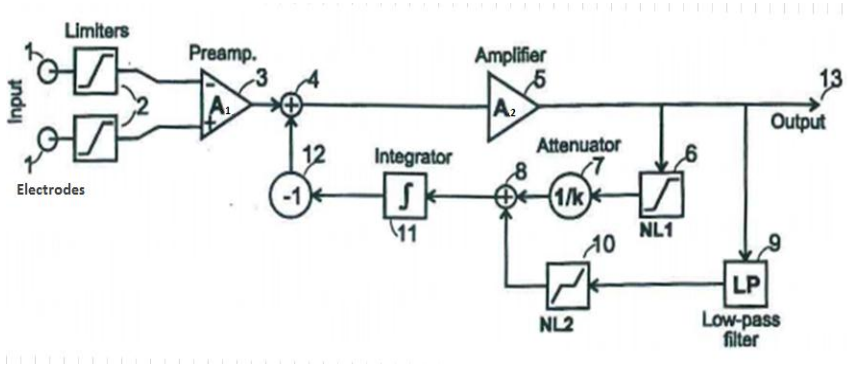

Figure 4. 26: Principles of the fast recovery amplifier (Rune Thorsen, 1997).

The input signals are picked up by the electrodes ① and limited by ② to reduce stimulus artefacts and to protect the pre-amplification circuit ③. The pre-amplifier 3 has a differential gain of A1 and its output ③ is added ④ with the negative output ⑫ from the feedback network which provides an estimate of the DC-offset at the pre amplifier output ③. The offset regulated signal from the addition ④ is fed to a post-amplifier ⑤ with again A2. The feedback network is divided into two parallel paths to accommodate different behaviour to small signal as well as to large signal offsets.

<u>High pass filter</u>

Small signal feedback (⑥-⑦-⑧-⑪-⑫-④) realises the high pass filtering of the small signals. The output from the post-amplifier ⑤ is limited by a non-linear function NL1⑥. NL1 has the input output relation illustrated in Figure 4. 27. Clipping the signal in NL1 reduces the influence of impulses in the subsequent circuit. After clipping ⑥ the signal is attenuated ⑦ by a factor k where k is determined by the amplification A2 and the desired overall high-pass cut off frequency. Hence the signal is integrated ⑪ and phase shifted π ⑫. The integrator ⑪ is a linear element and the processing of the signals from the added ⑧ outputs form the

attenuation ⑦ and the non-linear function NL2 ⑩ does not influence on each other. This part of the signal path provides linear high-pass filtering of small signals.

DC-offset compensation

Large signal feedback (⑨-⑩-⑧-⑪-⑫-④) provides offset compensation. The output from the post amplifier ⑤ is low-pass filtered ⑨. The cut off frequency of the filter ⑨ determines the overall recovery time for the fast recovery amplifier. The filtered signal is fed to a non-linear function NL2 ⑩. NL2 has the I-O relation illustrated in Figure 4. 27. Only if the absolute value of the input of NL2 exceeds a threshold value, will the output of NL2 be non-zero, after which the signal goes through the adder ⑧, to the integrator ⑪, thus establishing the offset compensation. It is this part of the circuit that provides the fast recovery time of the entire circuit.

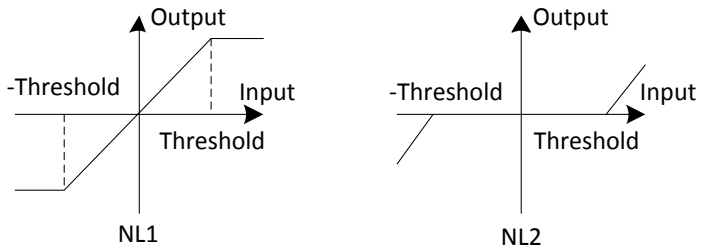

Figure 4. 27: Non-linear functions (re-plotted according to (Rune Thorsen, 1997))

The circuit diagram used to realise Thorsen's fast recovery amplifier is shown in Figure 4. 28. One such amplifier was constructed and tested.

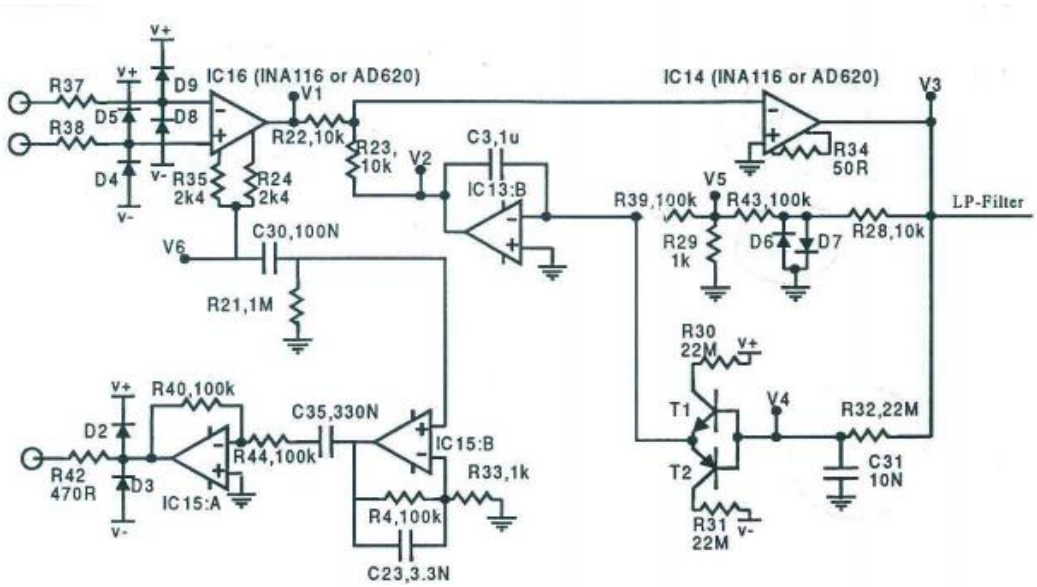

Figure 4. 28: Simplified schematic of the Fast-Recovery Myoelectric Amplifier (R. Thorsen, 2002) .

Figure 4. 29: The front and back of the fast recovery EMG amplifier.

4.3.4 The Blankable EMG pre-amplifier (Festival project, 1995)

The blankable EMG pre-amplifier provides blanking of the stimulus artefact. Providing the recovery time is fast enough, the blankable amplifier might be a good choice. The circuit design for this pre-amplifier was replotted from the FESTIVAL Project 1995 (FESTIVAL Project, 1995).

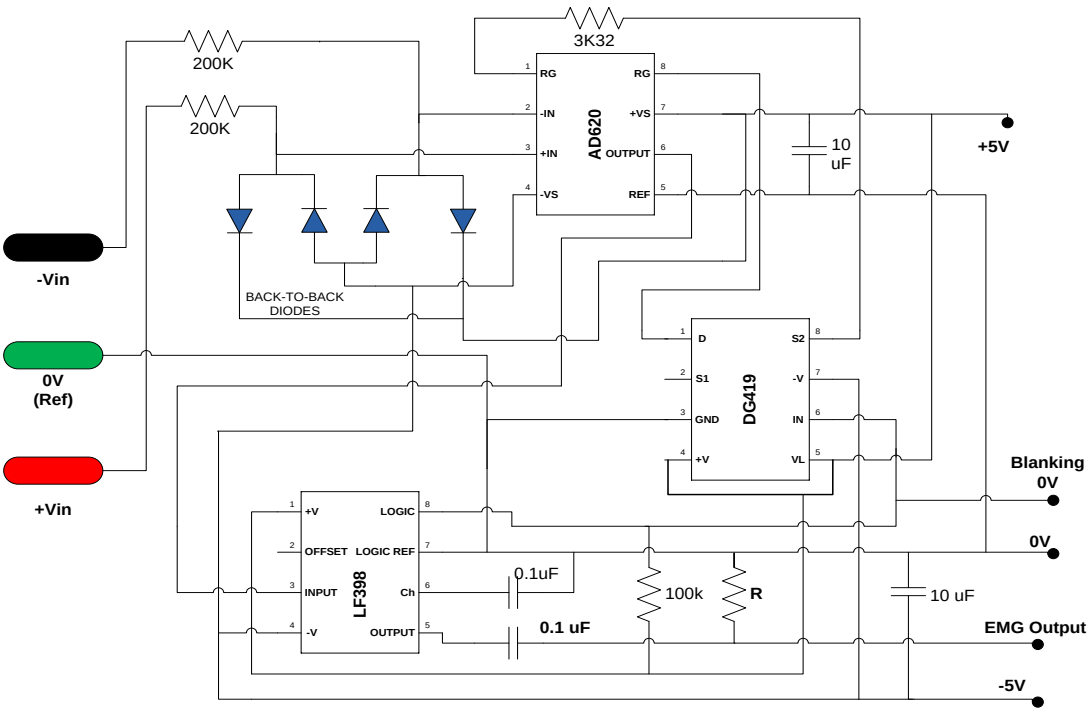

Figure 4. 30: Blankable Pre-Amplifier circuit diagram.

The input end of the circuit contains a pair of 200kΩ resistors on the positive and negative inputs in order to protect the patient from possible high currents, should there be a fault in the AD620 op-amp. The 3.32kΩ resistor is used to set the gain of the pre-amplifier circuit to approximately 15.8x (or 24dB) using Equation 3 below (Analog Devices Inc. 2009):

$$GAIN = 1 + (49.4k\Omega/3.32k\Omega) = 15.88$$

Equation 3: Gain of the pre-amplifier circuit

The gain is small as this circuit only acts as the first stage of amplification in a two stage design. The 0.1uF capacitor is used as the hold capacitor for the LF398 sample and hold circuit. It sets the droop rate of the LF398 to 200uV/s (Analog Devices Inc., 2009). The droop rate is the rate of change of the output voltage when the input signal is in the hold state. The circuit can only hold the signal for so long as a squared wave before the voltage begins to "droop" down due to leakage currents. In other words, once the blanking signal is applied to the circuit, the LF398 will hold the previous signal constant as long as the blanking signal is shorter than its droop rate. In the experiments discussed in later chapters (4.4.2), the blanking signal used ranges from 1.5ms-15ms to blank out the stimulus artefact and M-wave. These time interval were too short to see any droop in the held signal.

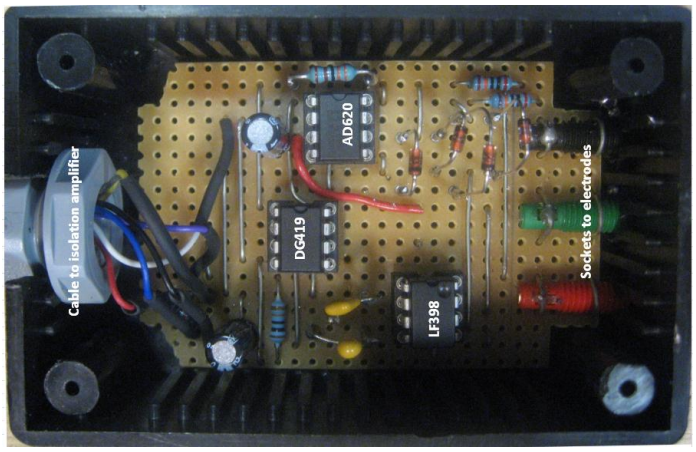

Figure 4. 31: Inside of the blankable EMG amplifier.

4.3.5 The EMG amplifier with current conveyor (CC EMG amplifier)

This piece of apparatus was used in the Time domain experiments in Chapter 5. It uses current conveyors which prevented EMG amplifier from saturating. A current conveyor is a three terminal device that was firstly introduced by Sedra and Smith in 1968 with a concept that "current is conveyed between two ports at different impedance levels". Bruun and Haxthausen (Bruun & Haxthausen, 1991)were the first to use a current conveyor in an EMG amplifier application to address the problem with the stimulus artefact. The current conveyor effectively shuts down the EMG amplifier during stimulation. The amplifier circuit uses two second generation positive current conveyors at the input stage. This EMG amplifier is able to prevent itself from saturation to return to a working state directly after the stimulation pulse.

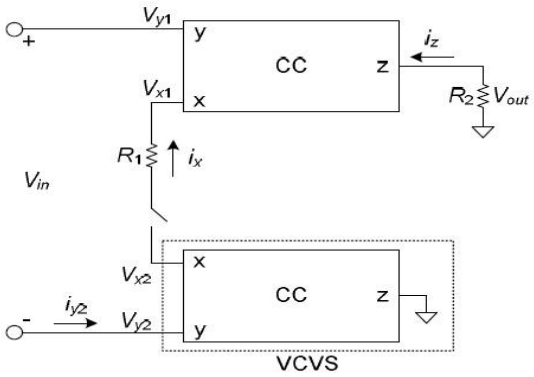

Figure 4. 32: Schematic diagram of the current conveyor at the input stage of the EMG amplifier (Bruun and Haxthausen, 1991).

With reference to Figure 4. 32, for each current conveyor, input terminal y is a high impedance node, while input terminal x is a low impedance node. The voltages at these two nodes are held constant, $V_x = V_y$, while the current in i_x is reflected at the output, i_z. In the figure the lower current conveyor is connected as a voltage controlled voltage source (VCVS) (Sedra & Smith, 1997) that ensures $V_{y2} = V_{x2}$ while $i_{y2} = 0$.

$$\begin{bmatrix} i_y \\ v_x \\ i_z \end{bmatrix} = \begin{bmatrix} 0 & 0 & 0 \\ 1 & 0 & 0 \\ 0 & 1 & 0 \end{bmatrix} \begin{bmatrix} v_y \\ i_x \\ v_z \end{bmatrix}$$

Equation 4: The terminal voltages and currents of the current conveyor.

The CC EMG amplifier described here is based on this design of Bruun and Haxthausen (Bruun & Haxthausen, 1991). It is shut down by opening the switch between the low impedance nodes. By switching on the low impedance nodes, as opposed to a high impedance node, the switching spikes are kept small and thus prevented from saturating the amplifier. The EMG signals normally bear a bandwidth 20—500Hz, so an EMG amplifier with a cut-off frequency of 1kHz is more than sufficient. The gain range of the amplifier is 56.5dB to 96.5dB. There are three output channels which enable recording from three muscles simultaneously.

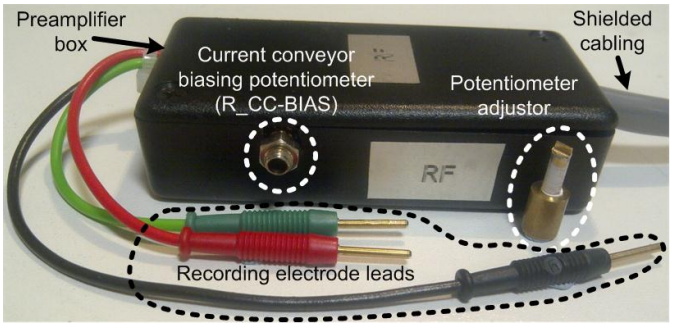

Figure 4. 33: The preamplifier for the EMG amplifier with current conveyor.

Figure 4. 34: The front and back panel of the EMG amplifier with current conveyor.

The amplifier can be used on its own to record voluntary EMG, or, or in combination with the biphasic stimulator discussed in 4.4.3 as a blanking EMG amplifier.

4.3.6 The Electrode selection

In this project, surface electrodes are used to detect EMG and to apply stimulation to the muscles. For this purpose, there are some requirements that the electrodes need to meet:

- Good electrical contact to the skin.
- Low impedance.
- Bio-compatibility (low chance of skin irritations).
- Easy to use.
- Economical

Two types of electrodes were used. The first were the ACUPAD Electrodes from Nidd Valley Medical that were used with the stimulators as well as the conventional EMG amplifier, the fast recovery EMG amplifier and the blankable EMG amplifier. The second set of electrodes were the Neuroline 720 from Ambu, which were used with the CC EMG amplifier.

The conductive surfaces of the ACUPAD electrodes are made from woven stainless steel fibres. This was backed with ultra-thin polyurethane film on one side and patented multistick adhesive gel on the other. The adhesive gel was suitable for cycling and remains tacky for approximately 45 applications (Nidd Valley Medical website, accessed 2009). These electrodes are reasonably priced; therefore it was possible for each subject to have their own set of electrodes.

Figure 4. 35: ACUPAD electrodes, round, 50mm diameter.

The Neuroline 720 electrodes were chosen for their strong adhesion which ensured that the electrode stays in place for the entire cycling trial examination, even when the patient sweated. These electrodes were compatible with the design of the current conveyor EMG amplifier (see 4.3.3) and were used later in the time domain experiments (See 5.3).

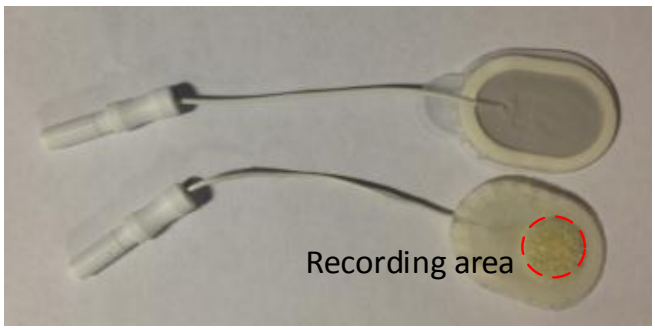

Figure 4. 36: The Neuroline 720 electrodes from Ambu. The bottom one had its plastic cover peeled off to show the actual recording area (circled in red).

4.4 Test of the EMG amplifiers

The main objective of the tests is to compare the performance of the four EMG amplifiers by investigating their ability to prevent the EMG signal being distorted by the presence of stimulus artefact. Using the results from these tests we can choose which amplifier is appropriate to use in future experiments.

4.4.1 Differential EMG amplifier VS Fast recovery EMG amplifier

These two EMG amplifiers were the first to be compared. The experimental setup is shown in Figure 4. 37. The same setup was used to compare all of the EMG amplifiers. The recording electrodes were placed over TA. The amplified EMG signal was firstly passed through the isolation amplifier box before being collected by the DAQ and displayed on the oscilloscope. The stimulator generates a constant voltage stimulation pulse (0V-240V no load, 0V-75V with 1kΩ load).

Skin preparation

Properly prepared skin can improve the electrode-skin contact and movement artefacts. It can also enhance the quality of the EMG signal as it reduces the chance of an imbalance existing between the electrodes as well as reducing 50Hz noise (SENIAM, 2010). SENIAM suggested that hair should be removed first by shaving followed by skin scrubs or sandpaper to reduce the skin impedance and also variations of the impedance. The last step of skin preparation normally consists of cleaning the skin with alcohol and allowing it to dry before applying the electrodes (SENIAM, 2010).

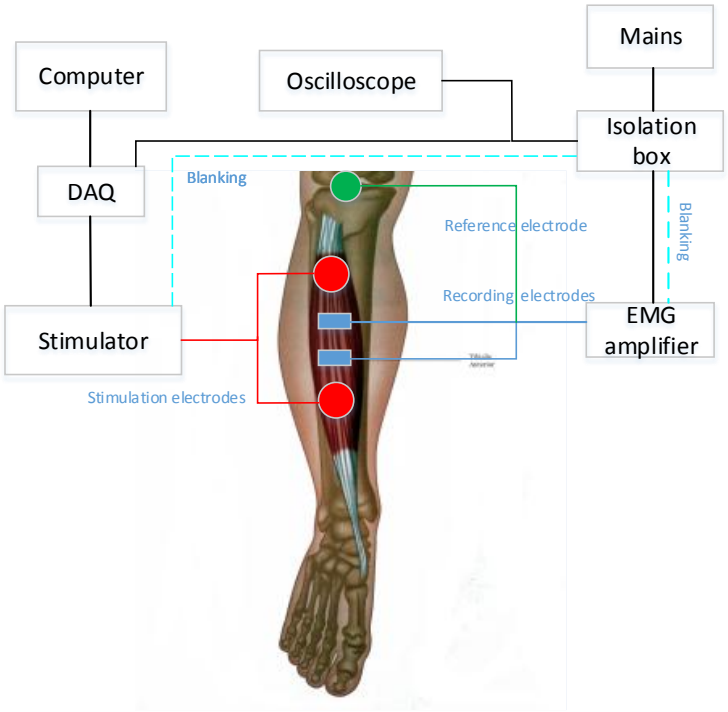

Figure 4. 37: The experiment setup used to test the EMG amplifiers. For the testing of blankable EMG amplifier (see 4.4.2), a cable (dotted line) from the stimulator with the blanking signal was sent to the EMG amplifier via isolation box.

Figure 4. 38: A subject showing skin preparation of a muscle (here the RF was used): shaving of the hair, removal of the dead skin and cleaning with a cotton ball.

Electrode placement

The electrode placement of this project follows the European recommendations for sensors, and, sensor placement procedures, as developed by the SENIAM project (SENIAM, 2010). The procedures always involve positioning the subject in the starting posture, and then the recommended position of the electrodes can be measured and marked. The starting posture and the measurement method vary depending on which muscle EMG is to be recorded from. Details on the major four muscles used in this project, and the SENIAM guidelines for each, can be found in Appendix D.

Procedures

For both amplifiers, three data sets were recorded.

- Part 1: The subject was asked to voluntarily contract the TA muscle, no stimulation was applied.
- Part 2: The subject was asked to consciously relax his muscle during continuous stimulation. A recording time of 5s was used during the recording time the continuous stimulation was always on (20Hz and 150µs pulse width).
- Part 3: The subject was asked to voluntarily contract the TA muscle during stimulation. (The same stimulation parameters were used as in Part 2).

Results

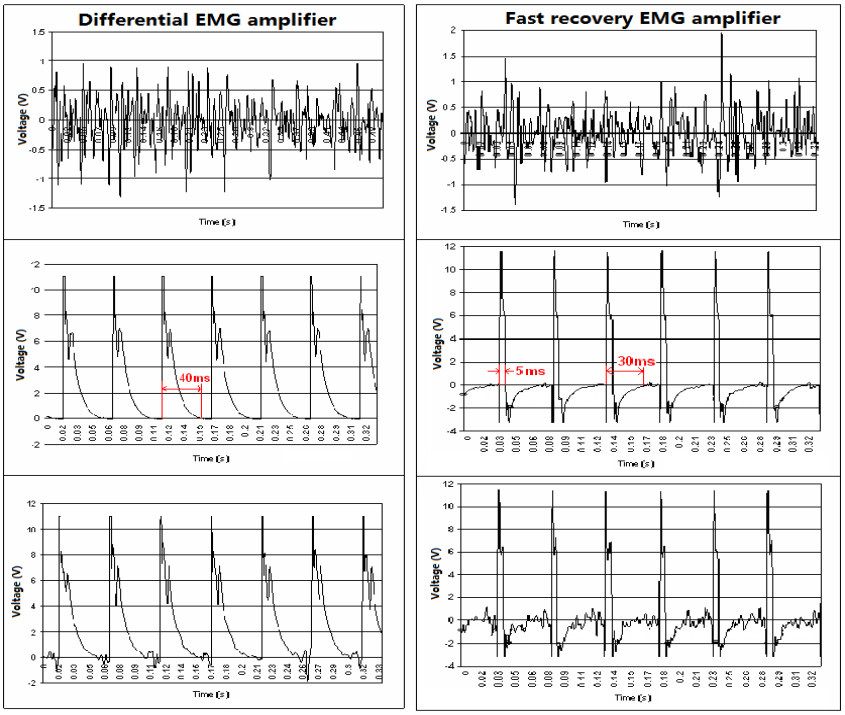

Figure 4. 39: Results of the two amplifiers.

The top traces show the results recorded during part I (voluntary contraction only). Both amplifiers functioned well and produced good quality EMG results. The second part of the experiment evaluates the ability of the amplifiers to recover to their working state. It took the differential EMG amplifier 40ms to recover as seen in the second trace. At a stimulation frequency of 20Hz this left 10ms in each 50ms window, during which an EMG signal could be recorded. For the fast recovery EMG amplifier, the recovery time was around 5ms. However the EMG signal showed a settling time of around 30ms before the signal had returned to the baseline value it was at just prior to the stimulation pulse. This meant that during the 25ms after the stimulation pulse, the EMG signal was still affected by the stimulation. Therefore in a 50ms window, only 20ms yielded a useful EMG signal from which the voluntary drive could be extracted for use as a control signal.

4.4.2 Testing of the blankable EMG amplifier with the stimulator blanking function

As described in 4.2.5, the stimulator was designed with a TTL output that served as a trigger signal for the blankable EMG amplifier. The objective of this experiment was to test the recovery time of the blankable EMG amplifier as well as the blanking performance.

Experiment setups

The experimental setup was similar to that used in the previous section, except for the addition of the connection of the blanking signal, taken from the stimulator through the isolation amplifier box, to the blankable EMG amplifier. The data acquisition module recorded the 3

signals: the stimulation signal, the blanking signal, and the EMG signal. The stimulator was set on free running mode (stimulation frequency 20Hz, stimulation intensity 40V, and pulse width 200µs). An oscilloscope was used to monitor the signal in real time so that the blanking signal width could be adjusted as necessary.

Procedures

The subject was asked to consciously contract the TA muscle when continuous stimulation at 20Hz was applied. With the EMG signal displayed on the oscilloscope, it was possible to adjust the blanking signal width to blank different lengths of the EMG signal. Each recording lasted for 3 seconds.

Results

The stimulator can generate a proper control signal to blank the inputs of the blankable EMG amplifier for different times. At first, the blanking pulse width was adjusted to be equal to the length of the stimulus artefact. Half a second of the complete data is shown in Figure 4. 40; the stimulus artefact is completely removed when using a blanking pulse of 5.33ms. This leaves the M wave and the voluntary signal undisturbed.

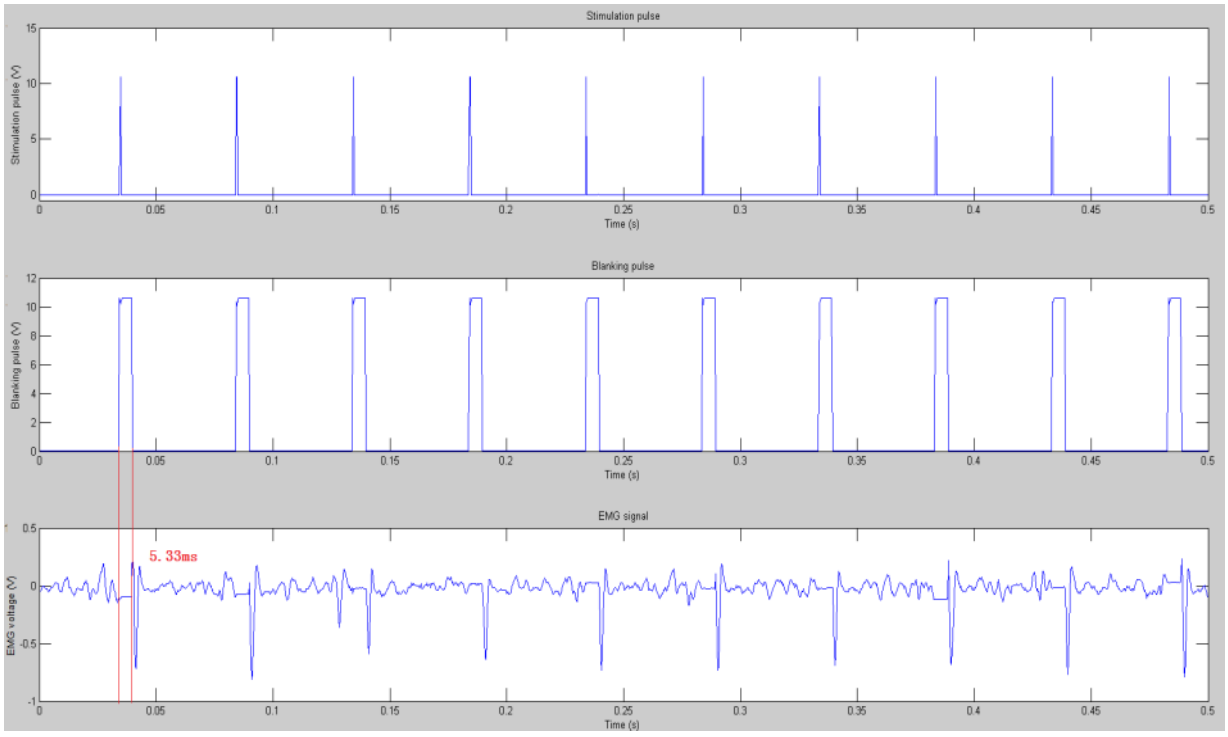

Figure 4. 40: Blanking the stimulus artefact only: blanking pulse width 5.33ms.

By further increasing the blanking pulse, we were able to blank the M wave as well. With a 10ms blanking pulse, both the stimulus artefact and the M wave were removed, leaving only an undisturbed voluntary EMG signal between blanking pulses, as in Figure 4. 41. With a 50ms window, 40ms of EMG signal could be used as a measure of the voluntary drive.

Discussion

The blankable EMG amplifier functions well with the stimulator control. It has the shortest recovery time of the three EMG amplifiers. For this reason it was used in the coherence experiments (chapter 6 and 7) until the current conveyor EMG amplifier became available in the later stage of the project. The latter was also tested, as discussed in the next section.

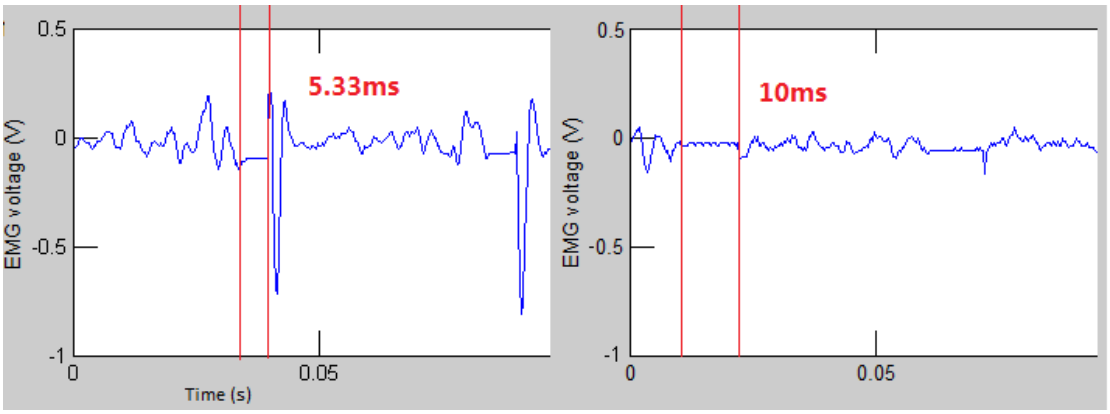

Figure 4. 41: Zoomed two stages of blanking. LEFT: stimulus artefact blanking. Right: stimulus artefact and M wave blanking.

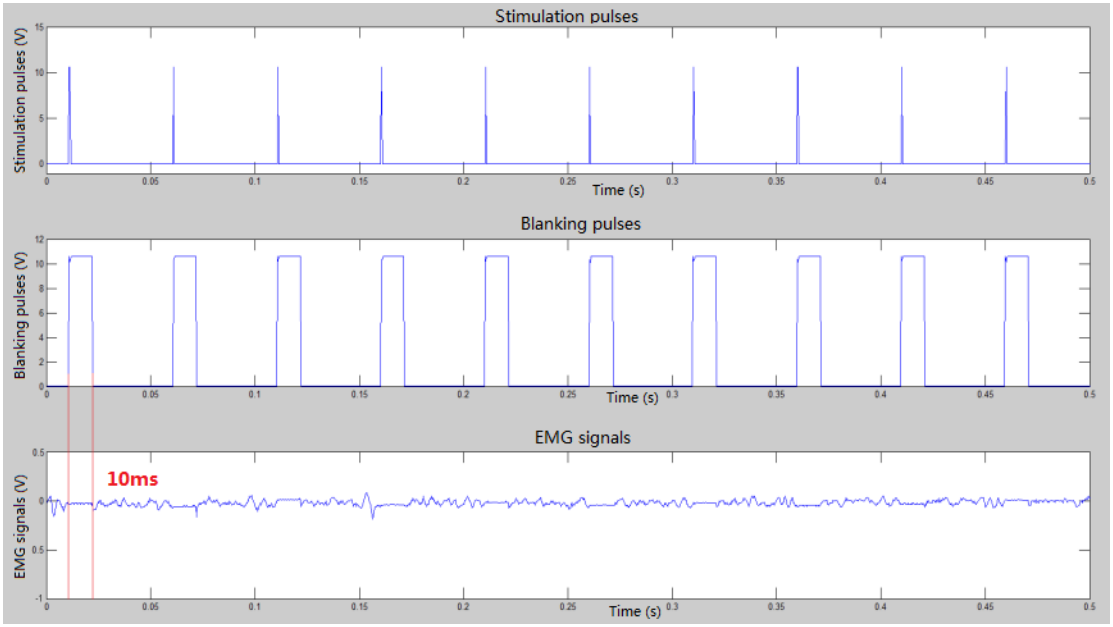

Figure 4. 42: Blanking the stimulus artefact and the M-wave: blanking pulse width 10ms.

4.4.3 Test of the CC EMG amplifier with a biphasic stimulator

The CC EMG amplifier was designed to work with a biphasic current stimulator. The biphasic stimulator sends a trigger signal to the EMG amplifier to tell it when to shut down. This stimulator features a continuous mode and a recruitment curve mode (which were not used in this project). For use in this project, modifications were needed. An external trigger mode was

added to the stimulator so that it could be triggered by the commutator. Further modifications were made to both the stimulator and the commutator.

Modifications of the commutator

The original output of the commutator consisted of a 1ms rising pulse at 5V. However, the microcontroller which is used to control the biphasic stimulator operates on a 3.3V rail. Furthermore, the stimulator triggers on a falling edge. Therefore, at the output of the commutator, a circuit as shown in Figure 4. 43, was added. It features a HEF4528B dual re-triggerable-resettable monostable multivibrator as the core of the circuit. Only one of the two available monostables of the HEF4528B was used. The circuit was used to generate a falling edge pulse (as required by the stimulator) from the rising edge pulse generated from the commutator (see Figure 4. 44). The output was then passed through a potential divider to reduce the amplitude to 3.2V.

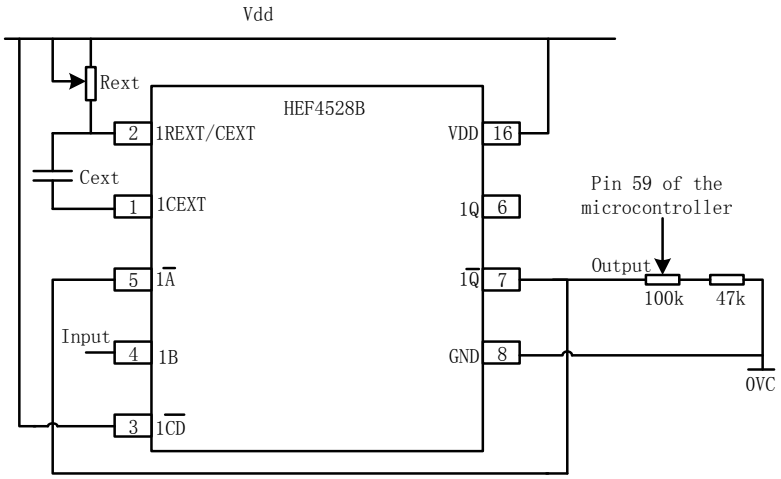

Figure 4. 43: The circuit used to adjust the output of the commutator.

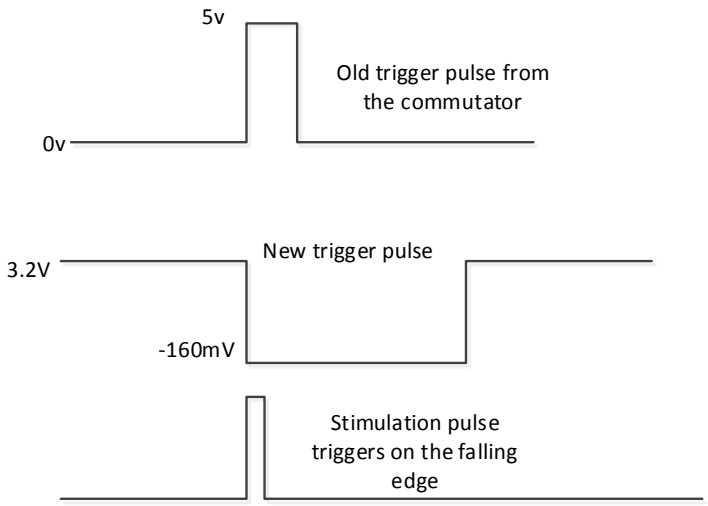

Figure 4. 44: New timing diagram of the commutator output

Limitations of the biphasic stimulator

When testing the trigger function of the stimulator, there is one limitation of the original design that we noticed. The stimulator uses a microcontroller produced by Texas Instruments MSP430F149 to display the user interface menus on the LCD for parameter selection and generate various control signals according to the user-selected parameters. The microcontroller was programmed using the C-compiler found in the MSP430 IAR *Embedded Workbench*®, which is an Integrated Development Environment software package. The processing speed of the microcontroller limits its ability to program the trigger function without delay. The minimum delay it could accept was 1ms, anything less than this caused the code controlling the LCD display to hang and become non-responsive to user inputs. Therefore the maximum sweep rate for detecting a trigger pulse is 1sweep/ms, an interruption signal is sent to sweep signal when a trigger pulse is found and this resumes when the stimulation finishes (see Figure 4. 46 for the logic flow of the trigger mode). This limitation was tested and the results were shown in Figure 4. 45. The top left figure shows three stimulation pulses being triggered by three commutator channels. The rest of the figures illustrated the zoomed version of the three stimulation pulses, with clear indications of the different delays.

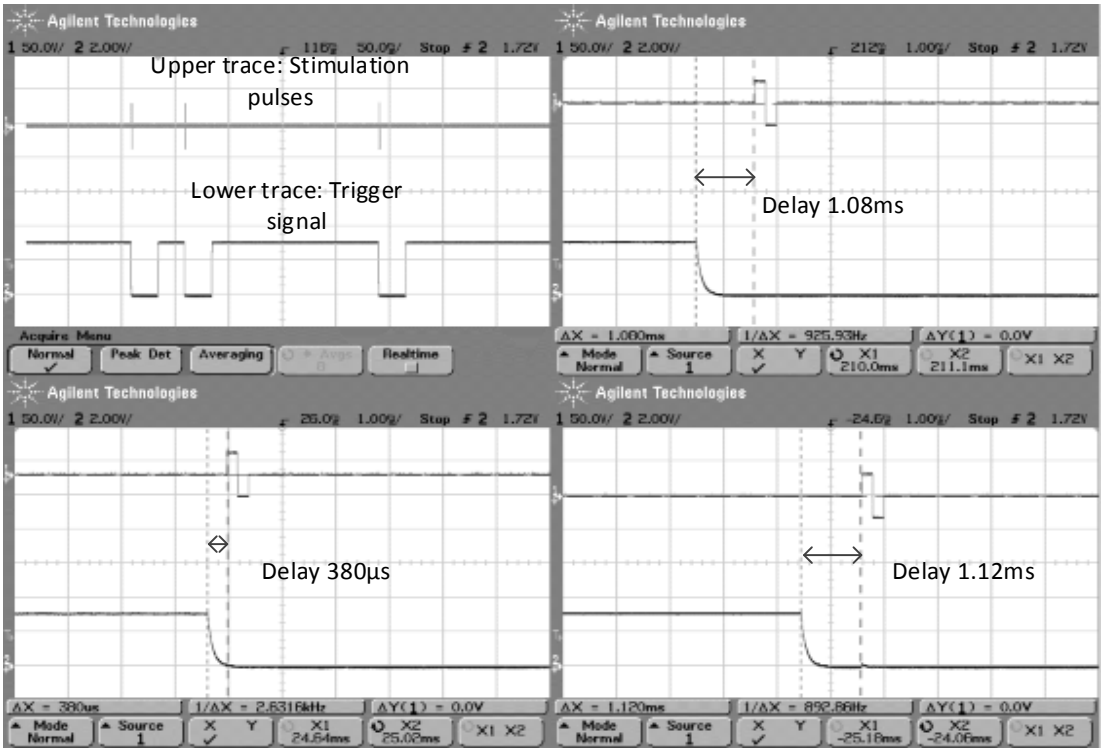

Figure 4. 45: The delay from the trigger signal to the stimulation pulses. For a delay of 380µs, the LCD display of the stimulator had become unresponsive; therefore the stimulator had stopped functioning correctly as the user was unable to stop the stimulation. This was however not the case for a delay of 1.08ms or 1.12ms.

There are basically two logic loops of the stimulator. One is the main routine shown in Figure 4. 46, and the other is the interrupt routine show in Figure 4. 47. The interrupt routine only executed every 1ms (as set by the user) if it has been activated by the main routine.

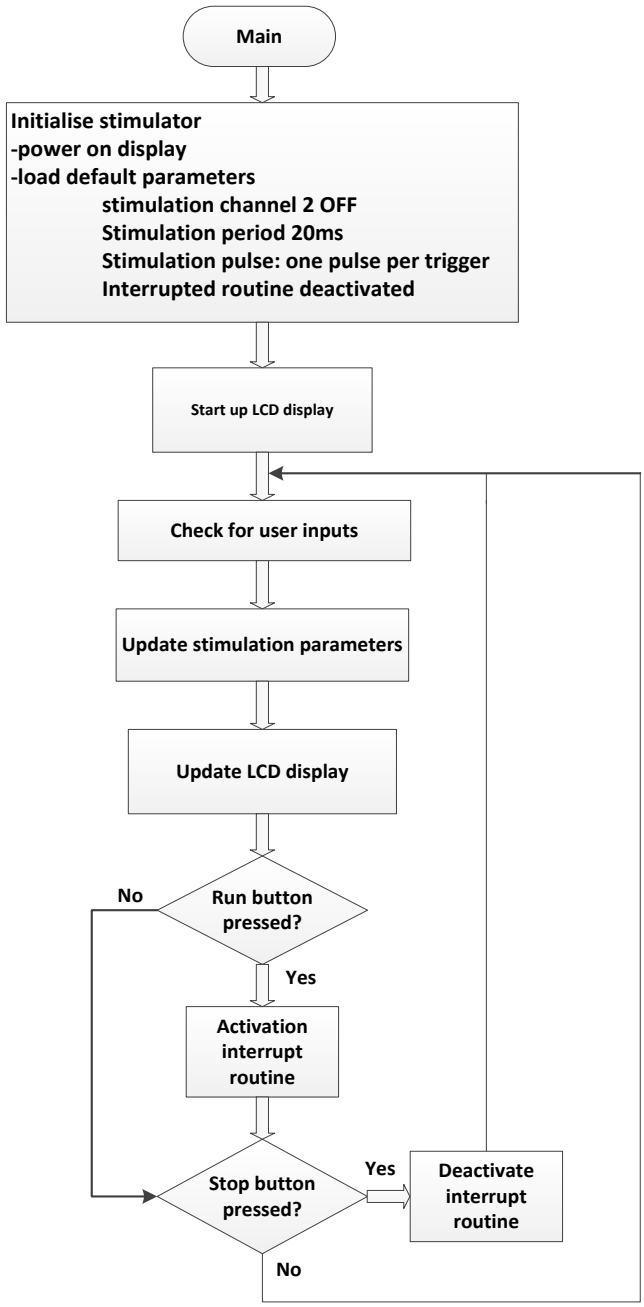

Figure 4. 46: The logic flow of the biphasic stimulator main routine in the external trigger mode.

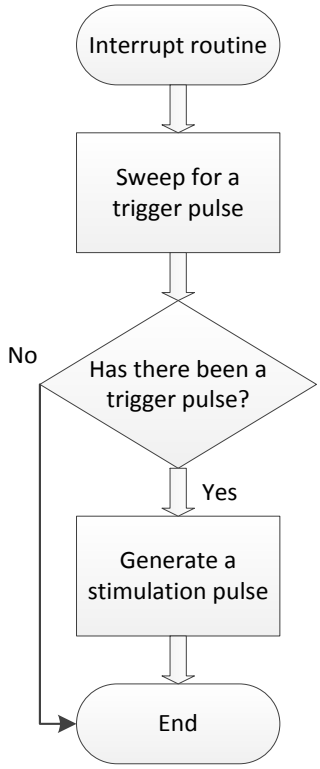

Figure 4. 47: The interrupt routine of the biphasic stimulator of the external trigger mode.

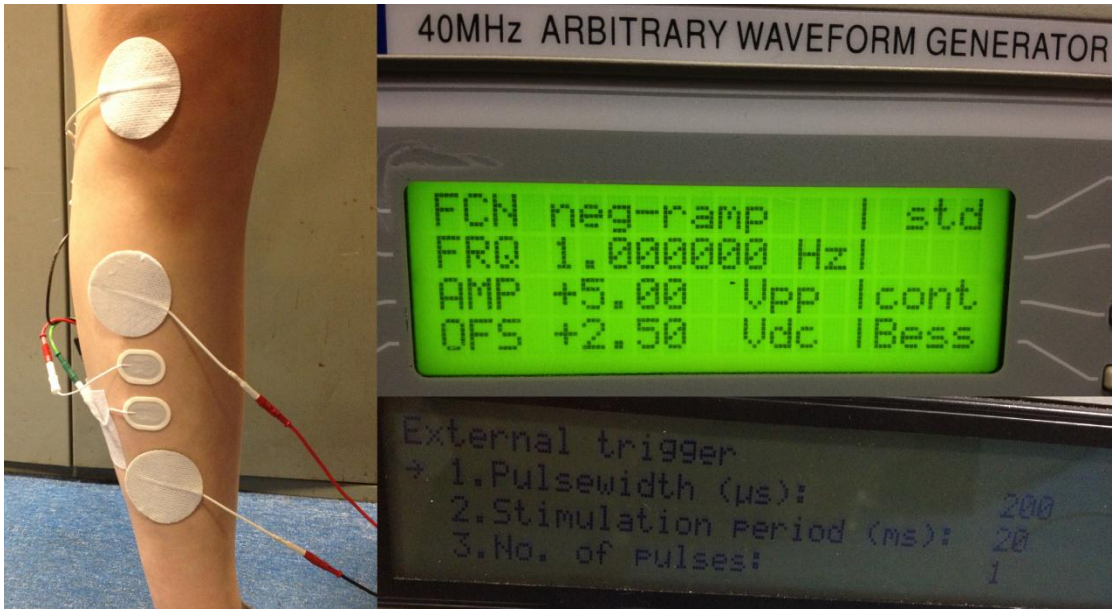

Figure 4. 48: Experimental setup, showing the electrode positions, the signal generator and the stimulator setups.

Figure 4. 48 shows the two different types of electrodes that were used (refer to 4.3.6). Both the electrodes and the cables connected to them were taped in place during the experiment to minimise motion artefact. The CC EMG amplifier and the biphasic stimulator were tested

together with a signal generator. A 1Hz negative ramp signal was generated to mimic the shaft encoder signal as if a subject was cycling at 60rpm. The setup of the signal generator can be found in the top right corner of Figure 4. 48 with the setup for the biphasic stimulator shown below. Two enable pulses were generated by the commutator as external trigger pulses to the stimulator. These two enable pules were arranged so that when triggered by the signal generator output at 1Hz, the separation between them was 50ms.

The experiment followed the same procedure as that outline in 4.4.1, and the results are shown in Figure 4. 49. The top trace shows the EMG recorded during voluntary contraction only. The second trace showed the EMG amplifier output with stimulation, the subject was asked to relax his muscle. Judging by eye and with the aid of the cursor function found on the oscilloscope, the amplifier took about 4.5ms to return to its normal working state. The ripples seen on the trace were measured to be 50Hz main interference. This was further dealt with using a Notch filter in software in future experiments described in Chapter 5, 6 and 7. From the bottom trace (stimulation with voluntary muscle contraction), it is easy to see that the EMG amplifier with current conveyor recovered quickly enough for us to have 45.5ms of sufficient EMG signal, between two consecutive stimulation pulses, 50ms apart (as seen when using a stimulation frequency of 20Hz). However, it is noticed that the period after the blanking pulse (red circled) show some high variations which could be result from a combination of the residual stimulus artefact and the M wave. The influence of these variations are further discussed in 5.6.4.

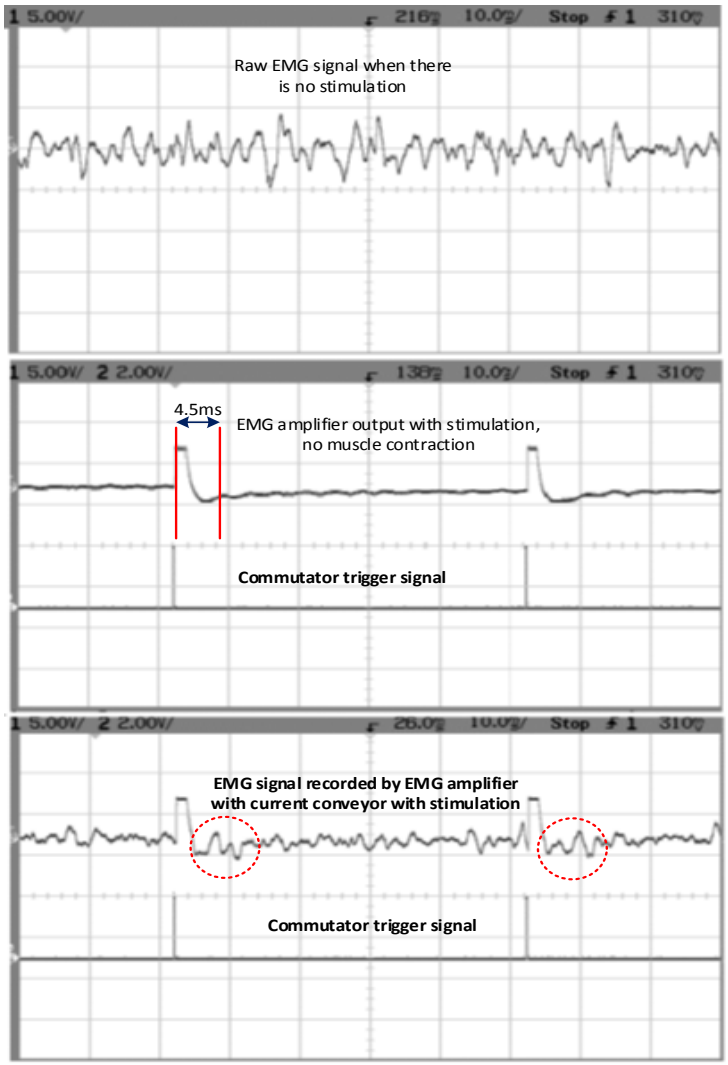

Figure 4. 49: Test results of the EMG amplifier with biphasic stimulator.

Discussion

It is difficult to acquire EMG signal under continuous stimulation as the time between the consecutive stimuli is limited (at 20Hz, it is 50ms). The window size where the EMG signal is collected has been decided to be 40ms (see 5.2.1). Therefore the EMG amplifiers must have the ability to recover fast from the stimulation. Four EMG amplifiers were constructed and tested for this purpose. The instrumentation EMG amplifier and the fast recovery EMG amplifier did not meet the requirement.

Both the CC and the blankable EMG amplifiers have met our requirement as they have fast recovery time (around 5ms for stimulus artefact blanking). The CC EMG amplifier was designed originally to capture the M wave. As for the application in the project, M wave is considered as an artefact (see 3.5.1). Further experiments also show that the EMG signal collected soon after the simulation is still contaminated by the residual artefacts (see 5.4.5). When blanking both the stimulation artefact and the M wave together, both EMG amplifiers need around 10ms. The two

types of EMG amplifiers were used at different stages of the project and both worked very well for this purpose.

4.5 Muscle activation range during recumbent cycling

4.5.1 Aims

As described in the review (3.11), there are large differences in the reported range of normal muscle activation, yet all four references performed their experiments on conventional upright bicycles, different from the semi-recumbent tricycle we used. Therefore it was necessary to measure the muscle activation for our setup. This experiment helps us to understand how the muscle activity is coordinated during tri-cycling and hence decide the appropriate timing of the stimulation for the different muscles. For our application there are 4 muscles of interest, namely, RF, VM, VL and BF. For each of these muscles a "muscle activation range" plot is generated.

4.5.2 Experiment setups

To measure EMG from the right leg muscle, two recording electrodes were placed on each of the muscle of interest and one reference electrode on the knee. Four blankable EMG amplifiers (worked as normal EMG amplifiers without stimulation) together with isolation amplifiers with additional gain stages were used. The data was acquired using a MATLAB program via DAQ. The experiment was performed on five AB male and female participants.

4.5.3 Procedures

Electrodes were stuck over the four muscles of the right leg. The subjects were then asked to cycle according to a metronome which beats once per second, in this way the cycling cadence is kept roughly constant at 60rpm. EMG was recorded from each participant during cycling for 36s for 3 trials.

4.5.4 Methods

The first step of the experiment is to find out the corresponding offset voltage which is the shaft encoder voltage when the subject is at the TDC. These voltages are added to the MATLAB program for automatic calculation of the crank angle (see Table 4. 4). Full wave rectification was performed on the data, and the rectified EMG of each muscle was plotted against the corresponding crank angle. There were two criteria to be met when determining the onset of muscle activation: 1. It is when the EMG firstly exceeded 1SD from the steady state (where the subject exerts constant effort with a chosen muscle); 2. The EMG had to maintain this level or above for more than 50ms. The steady state of the EMG signal is measured for each muscle first and saved as thresholds to the program.

4.5.5 Results

The results for the two of the subjects are shown in here (Figure 4. 50 and Figure 4. 51). The results for the other subjects can be found in Table 4. 4. The red lines in the graphs represent the steady states of these EMG plots.

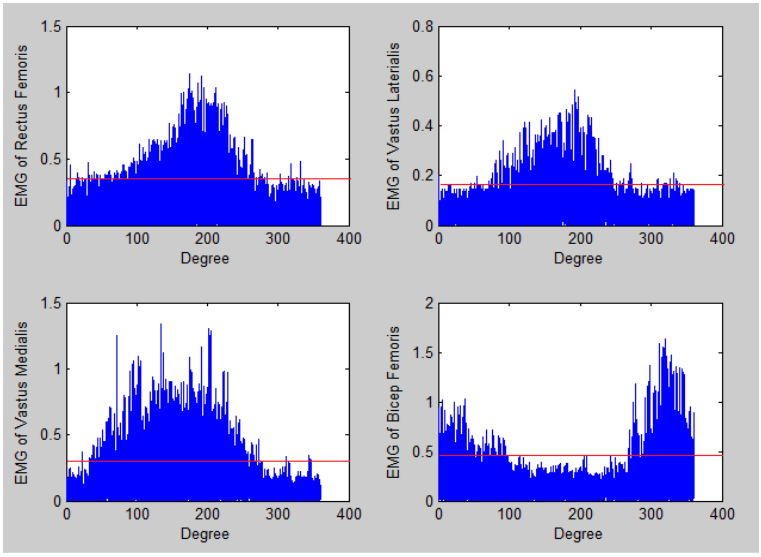

Figure 4. 50: Abs EMG voltage (V) VS crank angle (degree) averaged over 36s – for a male subject for 1 trial. Angle measured relative to left TDC.

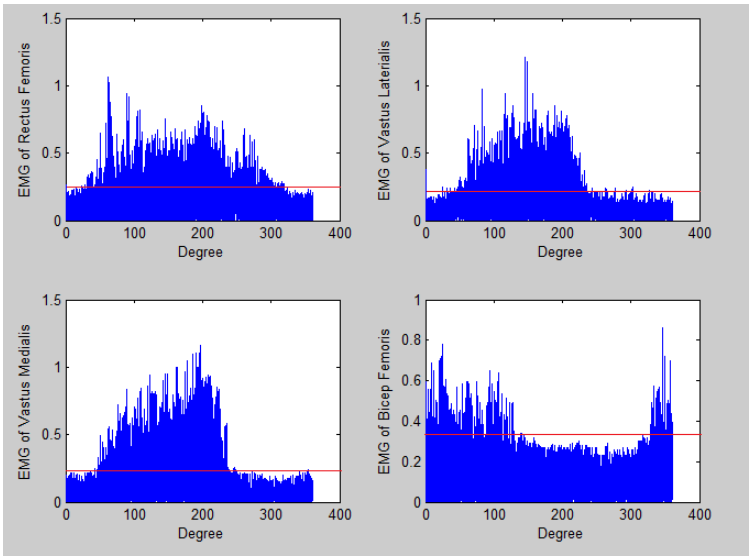

Figure 4. 51: Abs EMG voltage (V) VS crank angle (degree) averaged over 36s – for a female subject for 1 trial.

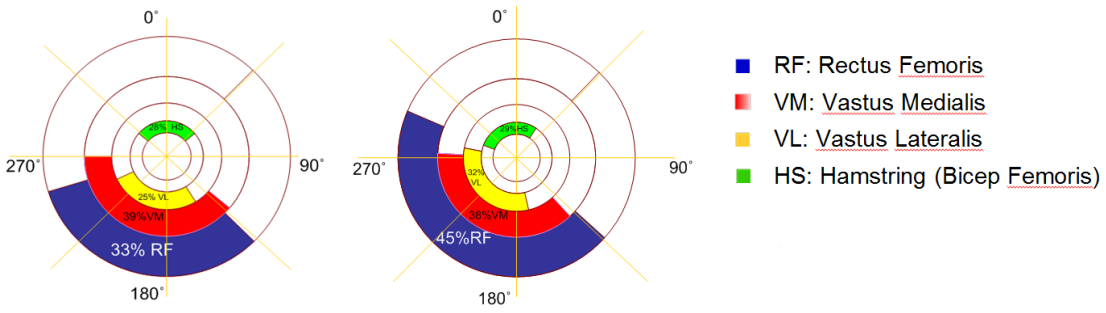

Figure 4. 52: The muscle activity in polar form- for a male subject (Left) and a female subject (Right).

The coloured areas are the regions of muscle activity in polar form with each bar representing a different muscle (as labelled). The experiment was repeated on 5 AB subjects and the results are shown in Table 4. 4. Table 4. 3 presents the mean start and stop angles of the fours muscles.

Table 4. 3: Mean start and stop angles, SD of the four muscles summarised from Table 4. 4.

	RF (mean start angle ± SD)	RF (mean stop angle ± SD)	VM (mean start angle ± SD)	VM (mean stop angle ± SD)	VL (mean start angle ± SD)	VL (mean stop angle ± SD)	BF (mean start angle ± SD)	BF (mean stop angle ± SD)
Male	105 ± 5	233 ± 9	89 ± 1	217 ± 10	130 ± 7	223 ± 12	309 ± 8	44 ± 10
Female	60 ± 7	229 ± 2	82 ± 9	231 ± 11	79 ± 4	198 ± 2	335 ± 3	76 ± 4

Table 4. 4: The crank angle region for 5 AB subjects, mean, and offset values.

Subjects	Offsets (V)	Rectus Femoris		Vastus Medialas		Vastus Lateralis		Bicep Femoris	
		Starting angle	*Stopping angle*	*Starting angle*	*Stopping angle*	*Starting angle*	*Stopping angle*	*Starting angle*	*Stopping angle*
Male Subject 1	2.3	106	223	89	229	122	211	312	54
Male Subject 2	2.2	100	235	89	210	133	235	300	35
Male Subject 3	2.3	110	241	91	213	135	225	315	45
Female Subject 1	2.1	65	228	88	223	82	197	333	74
Female Subject 2	2	55	231	76	239	77	200	337	79

4.6 Discussions and Conclusions

4.6.1 General conclusions on the apparatus

The chapter firstly introduced the essential apparatus designed for future experiments. They were designed, constructed and tested, their performance evaluated and then compared so as to identify the best choice of apparatus. The four EMG amplifiers were compared on their abilities of handling stimulus artefacts.

The blankable EMG amplifier with extra gain stage (4.2.3) was initially found to be the best choice of EMG amplifier and was therefore chosen for the coherence experiments described in chapter 6&7. At a later stage of the project, the CC EMG amplifier (4.3.5) had become available for use. This amplifier showed the fastest recovery time, even faster than the blankable EMG amplifier. Consequently, this amplifier was chosen for use in the time domain experiment (Chapter 5).

A stimulator (4.2.5) was designed to work with the blankable EMG amplifier (4.3.4). They were tested together to check their performance on blanking any unwanted signals (stimulus artefacts and other reflexes) without distorting the EMG left between the stimuli (4.4.2). The results were satisfactory. With 20Hz stimulation, there was about 40ms of EMG remaining between any successive stimuli after the blanking.

The biphasic stimulator (4.4.3) was adapted for use in conjunction with the EMG amplifier with current conveyor. It was further modified to be triggered by the commutator and digitally controlled by a computer through a DAQ. It was used in the time domain experiments discussed in Chapter 5.

The chosen apparatus were then put together to perform a preliminary experiment on exploring the muscle activation patterns for 4 leg muscles during tricycling. The results from this experiment gave a reference to the experiments with stimulation and helped us to decide the stimulation pattern since we wanted the stimulation pulses to be timed with the muscle's natural activation region. A data base was constructed in MATLAB to store the information on regions of muscle activity for each subject. A stimulation pattern tailored to each individual subject might be considered in further experiments.

4.6.2 Calculation of muscle activation range

In chapter 3, we have reviewed muscle activation range during cycling generated by different authors (see 3.11). There were various ways of determining the thresholds of the muscle activation. Some people argue that computer-based methods can be influenced by the presence of background noise and movement artefacts in the EMG signal, therefore they chose to use visual inspection by experienced experimenters (Brown & Frank, 1987; Horak & Nashner, 1986). However, visual inspection was useful when the number of data sets is small and when only post-processing of the signal was needed. Here the range was detected by a program written in MATLAB as we would be dealing with realtime signals in future experiments. The results were as expected as BF acts antagonistically to the three quadriceps muscles as seen in Figure 4. 52. Take male Subject 1 for example, during the flexion part of the revolution (312º – 54º, when the leg is fully extended and beginning to flex), it is natural for the BF muscle to activate in order to bring the leg around until the quadriceps muscles take over in order to push through the extension

part of the revolution (122º – 211.58º, when the leg is fully flexed and beginning to extend). Similar results were obtained for the female participant.

From Table 4. 4, we could say that there was significant difference in the RF (start angle), VL (start angle) and BF (stop angle) between the male and female subjects. Here we defined the significant difference as being more than 15% difference from each other. As we can see from Table 4. 3 and Figure 4. 52, the female EMG graphs are more evenly distributed, for example, the activation region of female RF muscle covering 163 degree, while the activation region of the male RF muscle covering 117 degree, which could be resultant from different cycling style or gender. The male participant shows a narrower region of muscle activity for RF, VM, VL muscles, and the result for BF were very close for both male and female. They have overlapping regions with some non-overlapping parts that could be due to different cycling habits or muscle characteristics of different subjects. The rest of the start and stop angles were fairly similar (no more than 10% difference) cross the male and female groups. At this stage we did not have enough subjects to say that the trend we found between male and female subjects was conclusive.
It was noticed by the experimenter that 1 of the subjects (male Subject 3) preferred to cycle with his heel on the pedal while the other four subjects used their forefoot. We have learnt from 3.11 that the habit of cycling can alter the EMG plot of muscle activation range. It is difficult to estimate how much the cycling habit of male Subject 2 would influence his muscle activation range at this stage. It was not surprising to see differences between the subjects. Because of these differences, we decided not to use a generalised muscle activation range for all the subjects, instead, a personalised profile was built for each subject. The profiles were saved in a database which was then used in the experiments in the later chapters.

4.6.3 How different is our activation range different from the literature?

The four muscles we were interested in are the numbers 2,3,4,7 in Figure 3. 12 in chapter 3. If we compare our results with the results from Jorge and Hull (Jorge & Hull, 1986), we could conclude that:

1. In all cases there were some overlap in muscle activation range and different start and stop angles were found in comparison to Hakansson and Hull's study.
2. No evidence support that muscle coordination between Recumbent and Upright cycles are different.

This agrees with the results presented in Hakansson and Hull's work (Hakansson & Hull, 2005), that the activation patterns and ranges of the leg muscles were similar for both the recumbent and upright pedalling positions. The leg muscles function similarly in the recumbent and upright positions. Therefore the difference could be results of different setups and cycling habit of different subjects. The important thing for us is to have accurate timing of the muscle activation so that we could provide stimulation accurately. Therefore the difference between the subjects and the difference between our work and the literature is acceptable as we will use individual's muscle activation range as a guidance for future experiments.

CHAPTER 5: ESTIMATION OF THE VOLUNTARY DRIVE IN THE TIME DOMAIN

5.1 Introduction

An important feature of the myoelectrically controlled stimulator system for FES cycling is that it stimulates with an intensity related to the subject's voluntary drive (not necessary proportional), which serves as an indication of the effort the subject is making to pedal. With such a system, the subject is free to cycle at different speeds, thereby changing the effort he is making, causing the system to adjust its stimulation intensity. The focus of this chapter is to investigate three important questions:

1) Can a control signal be extracted from the EMG to represent the voluntary drive?
2) How is the extracted signal related to the effort the subject is making?
3) Can we show that the control signal we find is a good estimation of the voluntary drive?

The importance of these questions are considered first, after which a series of planned experiments are discussed in an attempt to answer each of the questions.

5.2 Understanding the three questions

5.2.1 Can a control signal be extracted from the EMG to represent the voluntary drive?

For the myoelectrially controlled FES cycling system to work, we must be able to estimate the voluntary drive using the EMG signal measured from the stimulated muscle. This is not easy because of the presence of the stimulus artefact and other reasons. The period over which these events occur is relatively long compared to the typical inter-pulse interval that is required to produce strong, smooth muscle contractions. Carefully selected EMG amplifiers can recover quickly at around 5ms after the stimulation. How can the voluntary effort during cycling be estimated from the EMG while the muscle is being stimulated at such frequencies? Signal processing techniques and statistical methods are required to make a reliable reading of the EMG signal after the stimulation with minimum influence from any persisting artefacts.

The EMG during voluntary muscle contraction is a random signal. The variance of the signal increases as the muscle contracts more strongly. Root Mean Square (RMS) EMG is defined here as the RMS value of the raw EMG calculated during a window of some period (see 3.3). A single number will therefore represent the EMG amplitude measured from one window and this is what will be called "the RMS EMG amplitude" from now on. If a random signal is stationary and we measure its amplitude in this way, longer windows will give better estimates of the true amplitude. Bendat & Piersol (Bendat & Piersol, 2011) state that (for continuous signals) the estimation error can be calculated from Equation 5, where B is the bandwidth of the signal and ε is the ratio of the error to the true value. The error is the RMS value of the differences between calculated values and the true value, for a large number of estimates. The true value is the amplitude calculated with a very long window.

$$\varepsilon \approx \frac{1}{2\sqrt{BT}}$$

Equation 5: Estimation error for continuous signals.

In practice, the window length was decided to be 40ms during which the RMS EMG amplitude will be calculated. It was adapted from previous work done by our group in 2004 (Norton et. al, 2004) where EMG was recorded from 10 normal subjects while they were producing a steady isometric contractions. The EMG records were then cut into segments of various lengths and their RMS values computed. Correlation coefficients were then calculated between successive measurements. With 40ms windows, the correlation coefficient between pairs was >0.7 for all subjects. If we use B = 480Hz (EMG 20-500Hz), T = 40ms, the estimation error ε = 11% which is acceptable.

In a practical FES cycling trial, continuous stimulation during a leg muscle's activation range is required to generate enough pedaling force (see Figure 5. 1). We could certainly calculate the RMS EMG amplitudes from the windows between successive pulses but then it is difficult prove that these amplitudes are good estimations of the voluntary drive. What is needed is something to compare the results against. To solve this problem, the situation was simplified by applying only one stimulation pulse during the muscle's activation range per revolution. In doing so we can then introduce the idea of a pre-stimulus window and a post-stimulus window (see Figure 5. 3).

It is possible to calculate the RMS of the EMG signal in these windows, to find the *pre-stimulus amplitude* and *post-stimulus amplitude* respectively. The pre-stimulus amplitude happens before the stimulation, therefore is undisturbed by the stimulus artefact. If we use the pre-stimulus amplitude as a representation of the subject's voluntary drive, then by comparing it with the post-stimulus amplitude, it is possible to tell how closely they are related to each other. Ideally, the measured post-stimulus amplitude will vary with the voluntary drive. It is not required that the post-stimulus amplitude equals the pre-stimulus amplitude, nor that they are linearly related, only that they are related. Therefore we can say how good the post-stimulus amplitude is as an estimation of the voluntary drive. As illustrated in Figure 5. 2, both pre- and post-stimulus windows are selected on the EMG data for all revolutions (showing 3 revolutions here); the calculated EMG amplitudes can then be averaged to find a mean value.

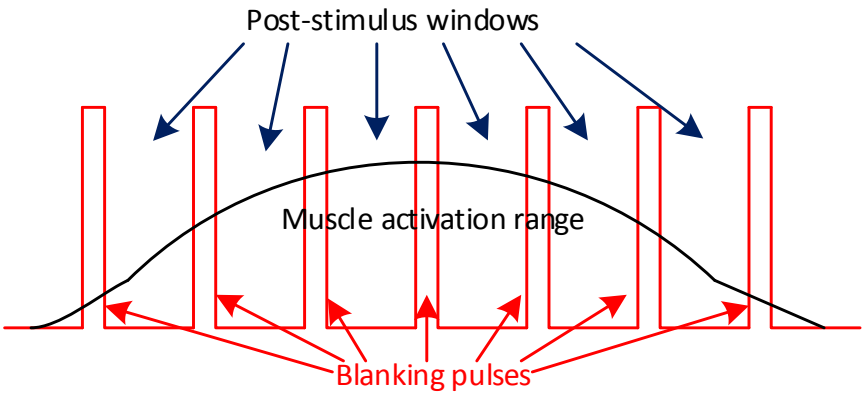

Figure 5. 1: Mimic the continuous stimulation case, with black curve as the muscle activation range, red square pulses as the blanking pulses, the gaps left between the blanking pulses as the post-stimulus windows.

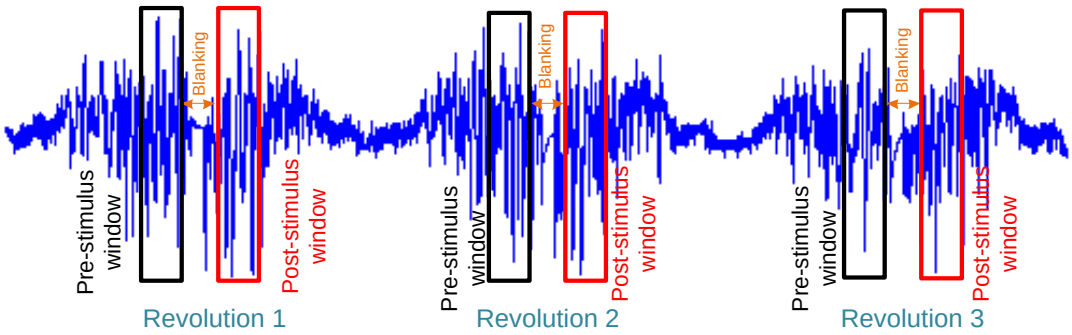

Figure 5. 2: Raw EMG signal from Rectus Femoris during cycling, showing 3 revolutions with labelled pre-stimulus window (black blcok), post-stimulus window (red block) and the blanking period (orange arrow).

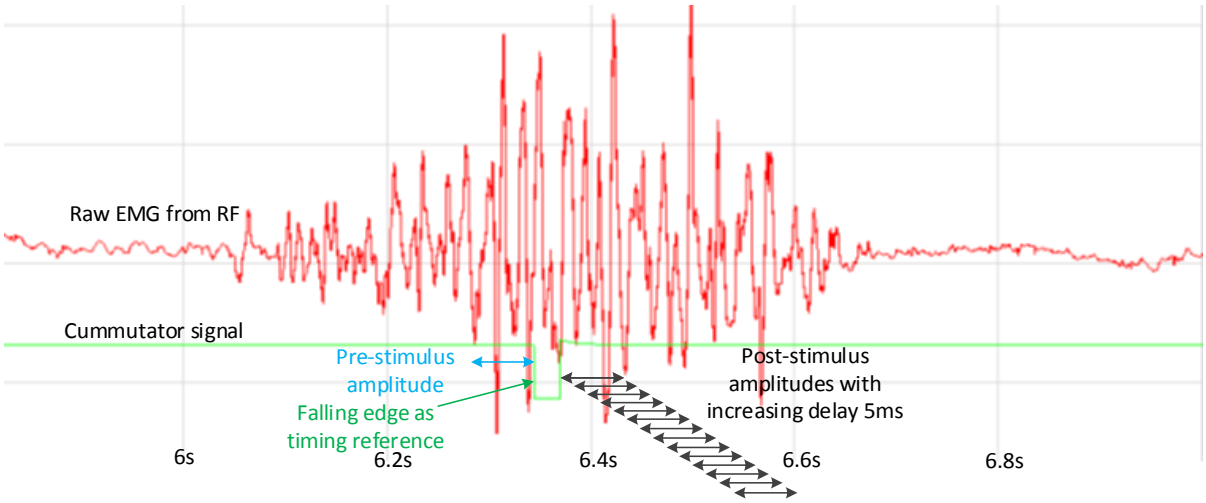

Figure 5. 3: Post-stimulus window selection, with the raw EMG in red and commutator signal in green. The pre-stimulus window range is marked in cyan and the post-stimulus windows in black.

Moving post-stimulus windows

The question that we want to answer is: what interval between the stimulus pulse and the window allows a good estimation of the voluntary drive to the muscle? When there is stimulation the window immediately after the blanking pulse may not provide the best correlation with the pre-stimulus amplitude, as the results might be influenced by the stimulus artefact. By moving the post window along the EMG signal (away from the stimulation pulse), better or worse correlation between the post-and pre-stimulus amplitudes may be calculated. Figure 5. 3 shows a possible method of selecting post-stimulus windows. A suitable delay after the blanking pulse to the start of the post-stimulus windows is introduced. The exact delay can only be decided after experimentally comparing the possible combinations. The blanking time is set visually to be 5ms by displaying the EMG signal with stimulation on an oscilloscope and inspected the length of the stimulus artefact (See 4.4.2). It is important to choose the post-stimulus window correctly in order to give a good estimation of the voluntary drive of the subject. Since there is only one stimulation pulse per revolution, therefore the moving post window delay is rather flexible. To increase the number of observations the windows were

overlapped and the starting time range extended from 0ms to 70ms (towards the end of the muscle activation range) with a 5ms increment. In this case, the windows overlapped the adjacent windows by 35ms and 15 post windows in total. A demonstration of the overlapping window selection is shown in Figure 5. 3 with the data in the pre-stimulus window highlighted with a cyan arrow and the post-stimulus windows marked with black arrows. The arrows illustrated how the delay and the window were defined.

5.2.2 How is the RMS EMG related to the effort the subject is making?

The second question is crucial for us because it will validate our intension of using the RMS EMG amplitudes as a control signal as well as enabling us to setup the thresholds for the control loop. In other words, we need to understand the amplitudes of the extracted signal from the short time windows, how are they related to the subject's effort? But how do we know how much effort the subject is making during cycling? This is achieved by forcing the subject to cycle at manageable effort levels. As described 4.2.2, it is possible to set the resistance applied to the back wheel of the trike (effort levels). When producing a given power during cycling, the subjects work against the resistance from the pedal and try to maintain a constant cadence, i.e. the effort generated by the subject stays roughly constant. When the resistance level is altered, the effort of the subject would also change accordingly to maintain the same cadence. The change in the effort of the subject is then compared against the EMG signal. In so doing it is hoped to predict the effort level in future experiments, by looking at the EMG. It should be noted that the relationship between effort and EMG does not necessarily need to be linear, as long as they are related in a predictable manner.

5.2.3 Can we show that the control signal we find is a good estimation of the voluntary drive?

Question 3 demands a verification that the control signal we find is a good estimation of the voluntary drive with the presence of continuous stimulation during cycling. Here another new idea is introduced, referred to as "interrupted stimulation". During a cycling session, the stimulation protocol is designed such that the stimulation pulses will be absent for a few revolutions (not consecutive but occasional). This is achieved by controlling the stimulation intensity by using software and randomly setting the intensity to zero during a cycling trial. The EMG recorded in the interrupted revolution is free from any contamination of the stimulation, and can be used to represent the voluntary drive. By comparing the RMS EMG signal from our selected windows in the stimulated revolutions to the ones selected under the same condition in the interrupted revolutions, we can then evaluate the methods we used in Question 1&2 for estimating the voluntary drive in FES cycling.

There are five experiments planned in this chapter. Experiment 1, 3, 4 and 5 did not have stimulation, Experiment 2 used stimulation; Experiment 1, 2 and 3 did not use orthoses, Experiment 4 and 5 used orthoses.

5.3 Experiment 1: Understanding the relationship between pre and post-stimulus amplitude without stimulation

5.3.1 Aims

Experiment 1 was designed to build the essential foundation that would allow us to carry on further experiments: How are the post-and pre-stimulus amplitudes related? Can we use the post-stimulus amplitude to estimate the pre-stimulus amplitude? To simplify the problem, there was no stimulation used in Experiment1. The major point being explored was: in the ideal case when in fact there is no stimulation, how well do the post-stimulus amplitudes predict the pre-stimulus amplitudes. The data was analysed as if there was stimulation (only the stimulation intensity was zero). To mimic the case with stimulation, a single commutator trigger signal timed near the centre of the subject's RF muscle activation range was generated every revolution.

5.3.2 Experiment setup

Figure 5. 4 is the block diagram for the experiment setup. EMG was recorded from the right RF muscle using the EMG amplifier with current conveyor (see 4.3.5). The two recording electrodes were positioned along the muscle and the reference electrode on the knee. The positions of the recording electrodes were noted for repetition of the experiment on different days so that they could be repositioned with minimum change. The commutator was set to send a trigger pulse at a pre-set angle during RF's activation range in each revolution, only this time there was no stimulation used. The commutator signal here served as a timing reference for data analysis.

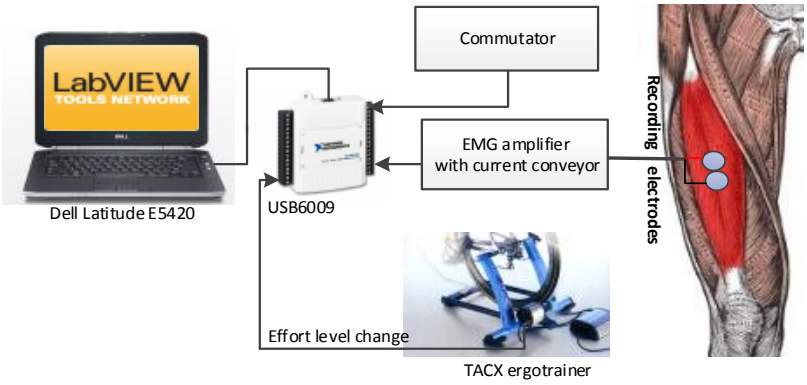

Figure 5. 4: Experiment setup for experiment 1.

5.3.3 The five subjects

Five AB subjects participated in all five experiments described in this chapter. The gender and the fitness of the subjects could affect the experiment outcomes. Table 5. 1 shows the gender and exercise routine of the five subjects. The effects of the general fitness of the subjects could be seen later in the experiments.

Table 5. 1: Gender and exercise routine of the five subjects.

	Subject 1	Subject 2	Subject 3	Subject 4	Subject 5
Gender	Male	Female	Female	Male	Male
Exercise routine	Does not exercise regularly	Gym exercise regularly	Regular cyclist (twice weekly)	Gym exercise regularly	Regular cyclists (twice daily)

5.3.4 LABVIEW program design

Two LABVIEW programs were written for Experiment 1. The first one recorded three analogue inputs from DAQ: the EMG signal from RF, the commutator signal and the shaft encoder signal. This program then saved the recorded data into a TDMS file to a desired directory set by the experimenter. The analysis of the data was performed post-experiment by another program. The raw commutator data was firstly passed through a threshold detector to find the falling edge as the reference index and then the post and pre windows were selected accordingly. Both pre and post windows were set to be 40ms. There were 15 post windows chosen with the method illustrated in Figure 5. 3 and named by the delay it had from the rising edge of the commutator signal, 0 to 70ms. The corresponding linear regression lines were also calculated for each window named as Regression 1-15.

5.3.5 The use of statistical terms: r, r^2 and p

The linear regressions model the relationship between the post and pre-stimulus amplitudes by fitting linear equations to the recorded data. The strength of the linear association between two variables is quantified by the correlation coefficient (r). By calculating the correlation coefficients of these models, we could decide if there is a relationship between the post and pre-stimulus amplitudes and the strength of the relationship. The correlation coefficient always takes a value between -1 and 1, with 1 or -1 indicating perfect correlation (all points would lie along a straight line in this case). A positive correlation indicates a positive association between the variables (increasing values in one variable correspond to increasing values in the other variable), while a negative correlation indicates a negative association between the variables (increasing values is one variable correspond to decreasing values in the other variable). A correlation value close to 0 indicates no association between the variables.

In a linear regression model, *coefficient of determination or* r^2 (range 0-1), is the square of the correlation coefficient (r). It represents the percentage of the data that is close to the line of best fit. The closer the points to the line, the better the fit, i.e. it provides a measurement of the points spread along the regression line. It also can be interpreted as a percentage of how good a predictor Y is to X (see 5.8.2). For example, an r^2 value of 0 means no correlation and an R squared value of 1 means that X and Y are 100% correlated.

The p-value is the estimated probability of rejecting the null hypothesis of a study question when that hypothesis is true. One often "rejects the null hypothesis" when the p-value is less than the predetermined significance level, which is often 0.05 or 0.01, indicating that the observed result would be highly unlikely under the null hypothesis. For example in Experiment 1, the null hypothesis is: post-stimulus EMG amplitude is not related to the pre-stimulus EMG amplitude. Therefore if we get p values lower than 0.01, then we can say: we are 99% confidence to reject the null hypothesis and say the post-stimulus EMG amplitude is related to the pre-stimulus EMG amplitude. The degree of how well they are correlated depends on the r values. In the data analysis session, all three terms, r, r^2 and P are used to interpret the results.

5.3.6 Experiment procedures

The subjects were asked to cycle with a constant cadence at 60rpm in time with a metronome. EMG was recorded from the Rectus Femoris muscle for 2 minutes at Level 5.

5.3.7 Results and Data analysis

The front panel of the LABVIEW program for data analysis shows the raw EMG plot, shaft encoder signal and the commutator signal. It also allows experimenter to display the wanted

windows by check/uncheck the boxes in front of the window names (see Figure 5. 5). The correlation coefficient (r), the slope of the regression line, the coefficient of determination (r^2) and the corresponding p values for each window (15 moving windows in total) are displayed in the bottom of the front panel as arrays. The data point in the lower graph each represents the RMS EMG amplitudes from post and pre-stimulus windows from one revolution (a total of 120 revolutions).

Figure 5. 6 illustrated the three raw signals for six revolutions recorded by the recording program. As we could see from this picture, even for the same effort level, the amplitude of the raw EMG signal showed some variations. For example, EMG from the third and the fifth revolutions had noticeably higher amplitude than the other four and the EMG from Revolution 6 had longer duration than the others. We need to bear in mind that EMG signal is very complicated especially when recorded from a sophisticated exercise like cycling. We hope to find some predictable trends from these signals and help us to understand them better.

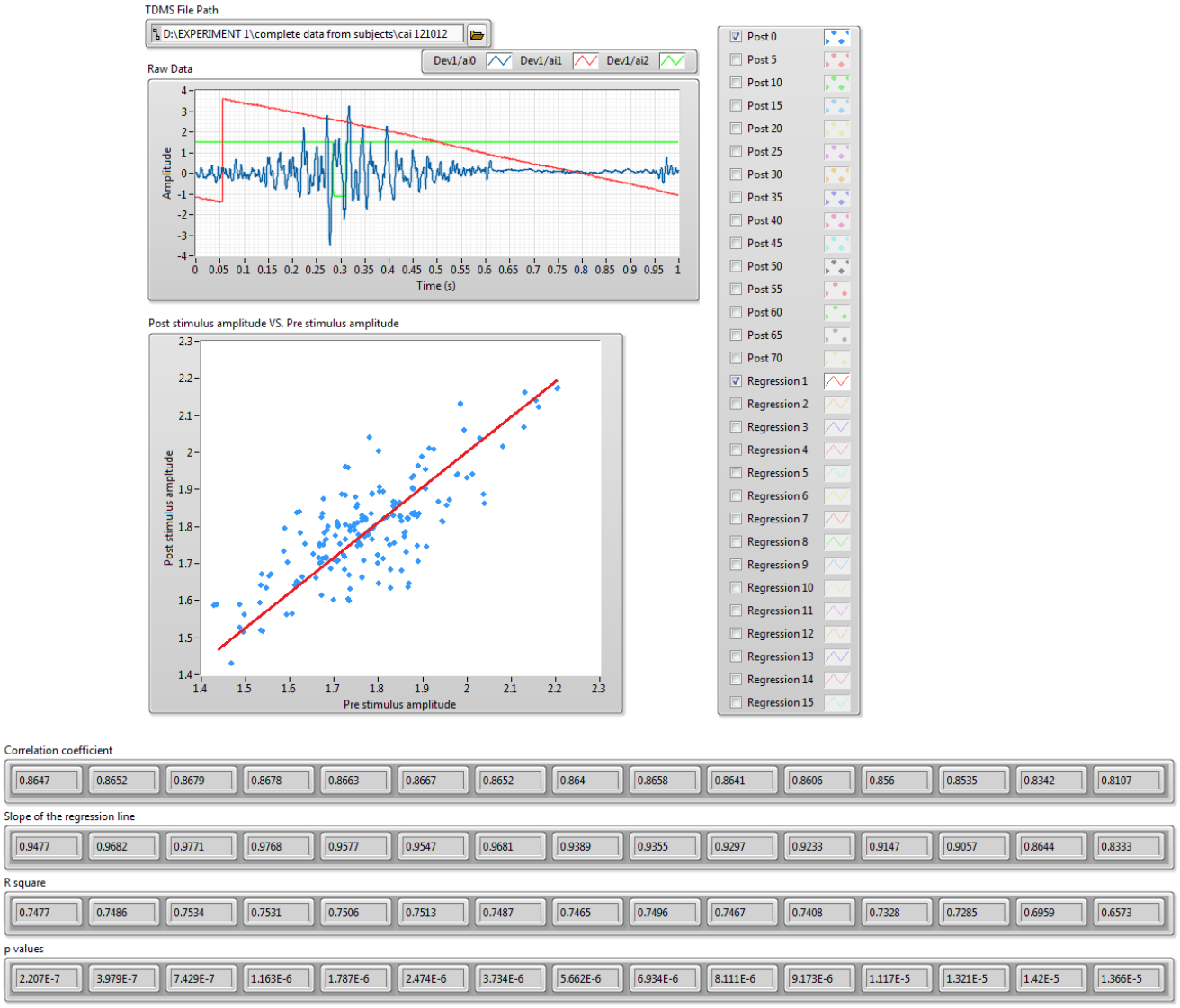

Figure 5. 5: the front panel of the data analysis program for experiment 1.

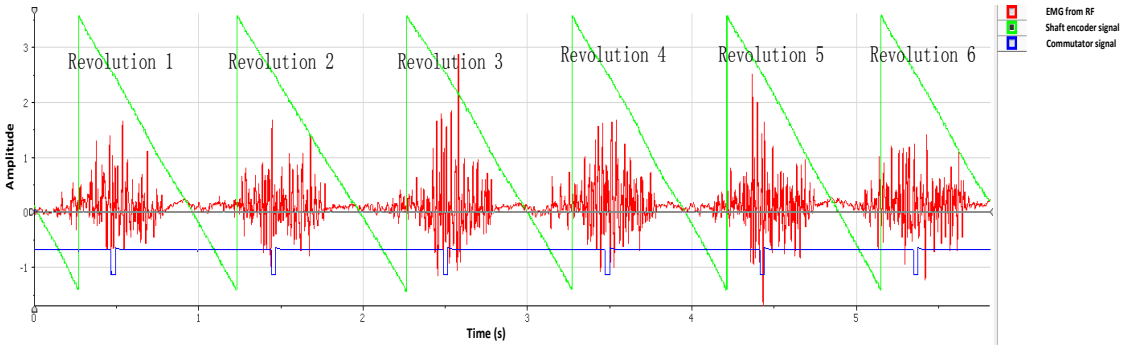

Figure 5. 6: Recorded data clip from experiment 1, showing 6 revolutions of cycling, red signal is the raw EMG recorded from Rectus Femoris, green is the shaft encoder signal, and blue is the commutator signal.

Figure 5. 7 shows the plot of the post stimulus amplitude versus pre stimulus amplitude for one subject. By comparing the pre- and post-stimulus EMG amplitudes from EMG signal obtained without stimulation, it is possible to get an idea how the two amplitudes related to each other in the ideal case, without stimulation. The pre-stimulus windows was chosen to be right before the stimulation pulse. The first post window, which is 0ms after the blanking pulse, was chosen here to demonstrate the relationship. The correlation coefficient was calculated to be 0.8647 with an r^2 value at 0.7477. The null hypothesis for correlation test was: the post-stimulus amplitude is not related to the pre-stimulus amplitude. The resultant p value was 2.207×10^{-7} which was way below the significance level 0.01. Therefore we could reject the null hypothesis and say the post stimulus amplitude was in fact related to the pre-stimulus amplitude.

Regression lines were then fitted to the post-pre stimulus plots. An example of such a plot was shown in Figure 5. 7. The regression line was plotted in solid red line. If the post stimulus amplitude perfectly estimated the pre stimulus amplitude, the regression line would have been the same as the 45º line (black dotted line) given the x and y axes were of the same dimension. The slope of the regression line was 0.9477 which was quite close to the ideal case which is 1. The difference is understandable as it is within the expected range of EMG amplitude fluctuations (see 3.2). This fluctuation is defined by Norton et al in 2004 where they record EMG from RF muscle during constant contraction. The EMG signal is then divided into 40ms windows and correlation between the RMS EMG from different windows are compared. It shows a correlation of 9.6 for adjacent windows which dropped to a minimum of 0.453 for windows 160ms apart. Which means that a variation of 0.123 is typical of EMG fluctuations. Therefore a correlation of 9.477 falls within this range and is reasonably high.

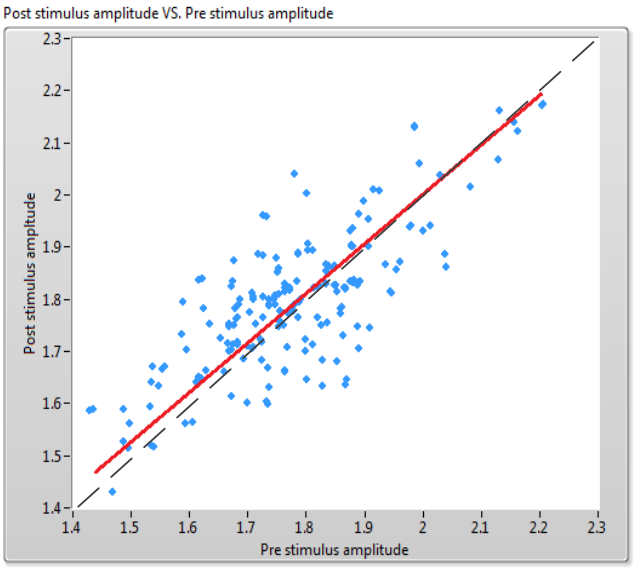

Red line: regression line
Black dotted line: 45 degree line

Figure 5. 7: Plot of post stimulus amplitude vs pre stimulus amplitude for subject 1 window 0 without stimulation.

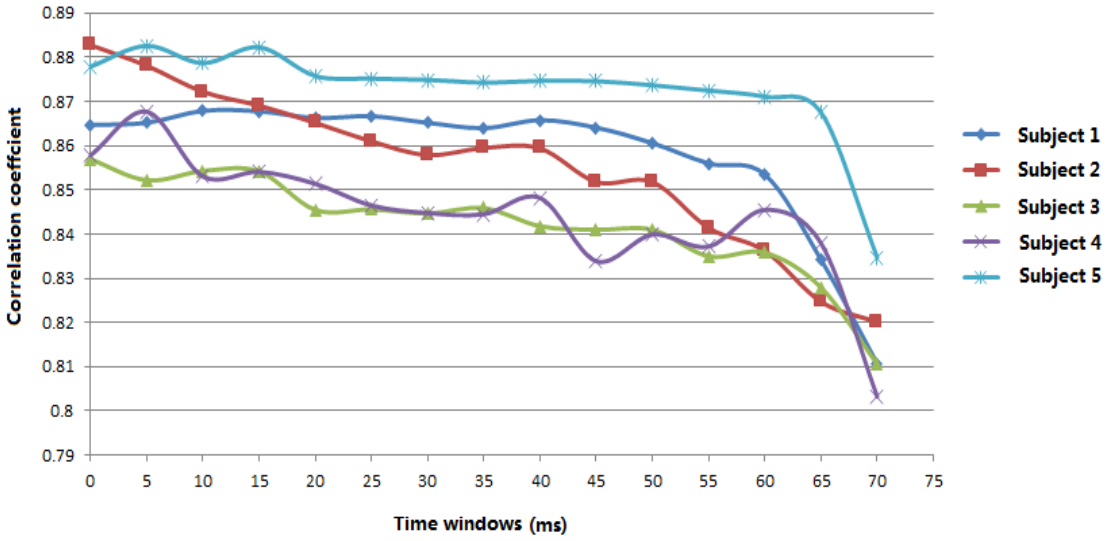

Figure 5. 8: Correlation coefficent change for different time windows for five subjects without stimulation.

Generally the subjects displayed a decreasing trend from window 0 to window 70 (with some occasional rises and falls). The starting correlation coefficients (r) for all subjects were above 0.85 which was considered to be high. The highest r was 0.8823 of subject 5 at window 15. All subjects showed a sharp decrease at window from window 60 to window 65, with the lowest r at 0.8016.

5.3.8 Discussions

The question we need to answer is: Can we use the post-stimulus amplitude from different windows to estimate the pre-stimulus amplitude when there is no stimulation? The high correlation obtained for all subjects from windows starting 0-55ms showed that the post and the pre-stimulus amplitudes were significantly related. The correlation was generally high in the

early time windows. It gradually reduced with a much steeper drop for the last few windows. The reason for this was found when inspecting the raw EMG carefully. Figure 5. 3 shows that for the post window starting from 70ms after the commutator trigger signal, there is not as much EMG activity as this window covers the end of the muscle activation range.

The overall correlation obtained for most of the time windows were satisfactory, with the highest correlation at 0.8826 and the lowest at 0.8032. The high correlation and the low p values support our conclusion that when there is no stimulation, the post-stimulus amplitude is highly correlated to the pre-stimulus amplitude. We have up to 70ms after the stimulation to obtain a reliable estimation. The results indicate that it may be possible to use the post-stimulus amplitude from selected windows to estimate the pre-stimulus amplitude. However, this conclusion is based on the experiment performed without stimulation, therefore further experiments with stimulation are needed to confirm this.

Table 5. 2: Correlation coefficient r, coefficient of determination r^2 and the corresponding p values for five subjects in experiment 1.

	Window														
	0ms	5ms	10ms	15ms	20ms	25ms	30ms	35ms	40ms	45ms	50ms	55ms	60ms	65ms	70ms
Subject 1	R^2=0.7477	R^2=0.7486	R^2=0.7534	R^2=0.7531	R^2=0.7506	R^2=0.7513	R^2=0.7487	R^2=0.7465	R^2=0.7496	R^2=0.7467	R^2=0.7408	R^2=0.7328	R^2=0.7285	R^2=0.6959	R^2=0.6573
	r=0.8647	r=0.8652	r=0.8679	r=0.8678	r=0.8663	r=0.8667	r=0.8652	r=0.8640	r=0.8658	r=0.8641	r=0.8606	r=0.8560	r=0.8535	r=0.8342	r=0.8107
	P <0.01	P <0.01	P <0.01	P <0.01	P <0.01	P <0.01	P <0.01	P <0.01	P <0.01	P <0.01	P <0.01	P <0.01	P <0.01	P <0.01	P <0.01
Subject 2	R^2=0.7795	R^2=0.7711	R^2=0.7608	R^2=0.7554	R^2=0.7486	R^2=0.7414	R^2=0.7360	R^2=0.7387	R^2=0.7385	R^2=0.7256	R^2=0.7152	R^2=0.7079	R^2=0.6993	R^2=0.6801	R^2=0.6726
	r=0.8828	r=0.8781	r=0.8722	r=0.8691	r=0.8652	r=0.8610	r=0.8579	r=0.8595	r=0.8594	r=0.8518	r=0.8518	r=0.8414	r=0.8362	r=0.8247	r=0.8201
	P <0.01	P <0.01	P <0.01	P <0.01	P <0.01	P <0.01	P <0.01	P <0.01	P <0.01	P <0.01	P <0.01	P <0.01	P <0.01	P <0.01	P <0.01
Subject 3	R^2=0.7345	R^2=0.7263	R^2=0.7298	R^2=0.7297	R^2=0.7149	R^2=0.7151	R^2=0.7136	R^2=0.7156	R^2=0.7087	R^2=0.7073	R^2=0.7074	R^2=0.6973	R^2=0.6985	R^2=0.6854	R^2=0.6571
	r=0.8570	r=0.8522	r=0.8543	r=0.8542	r=0.8455	r=0.8456	r=0.8447	r=0.8459	r=0.8418	r=0.8410	r=0.8410	r=0.8350	r=0.8358	r=0.8279	r=0.8106
	P <0.01	P <0.01	P <0.01	P <0.01	P <0.01	P <0.01	P <0.01	P <0.01	P <0.01	P <0.01	P <0.01	P <0.01	P <0.01	P <0.01	P <0.01
Subject 4	R^2=0.7359	R^2=0.7529	R^2=0.7277	R^2=0.7296	R^2=0.7249	R^2=0.7165	R^2=0.7137	R^2=0.7132	R^2=0.7195	R^2=0.7037	R^2=0.7055	R^2=0.7009	R^2=0.7149	R^2=0.7020	R^2=0.6451
	r=0.8578	r=0.8677	r=0.8531	r=0.8541	r=0.8514	r=0.8465	r=0.8448	r=0.8445	r=0.8482	r=0.8339	r=0.8399	r=0.8372	r=0.8455	r=0.8379	r=0.8032
	P <0.01	P <0.01	P <0.01	P <0.01	P <0.01	P <0.01	P <0.01	P <0.01	P <0.01	P <0.01	P <0.01	P <0.01	P <0.01	P <0.01	P <0.01
Subject 5	R^2=0.7707	R^2=0.7789	R^2=0.7722	R^2=0.7785	R^2=0.7671	R^2=0.7660	R^2=0.7655	R^2=0.7644	R^2=0.7651	R^2=0.7649	R^2=0.7635	R^2=0.7612	R^2=0.7589	R^2=0.7526	R^2=0.6968
	r=0.8779	r=0.8826	r=0.8787	r=0.8823	r=0.8758	r=0.8752	r=0.8749	r=0.8743	r=0.8747	r=0.8746	r=0.8737	r=0.8725	r=0.8711	r=0.8675	r=0.8347
	P <0.01	P <0.01	P <0.01	P <0.01	P <0.01	P <0.01	P <0.01	P <0.01	P <0.01	P <0.01	P <0.01	P <0.01	P <0.01	P <0.01	P <0.01

5.4 Experiment 2: Understanding the relationship between pre and post-stimulus amplitudes with stimulation

Experiment 2 saw the incorporation of stimulation by including a biphasic constant current stimulator, to the existing setup used for Experiment 1 (see 4.4.3). The LABVIEW recording program was modified to record an additional analogue signal: the stimulation pulses and the data analysis program were modified to use the stimulation pulse as the timing reference from which windows were selected.

5.4.1 Aims

In Experiment 1, we studied the correlation between pre- and post-stimulus amplitudes, calculated in different windows. The aim of Experiment 2 is to see if the results we found in Experiment 1 are still valid when stimulation is present. This is important to understand as there will be stimulation in the proposed FES cycling system.

5.4.2 Experiment setup

Figure 5. 9 shows the positions of the electrodes, as used during Experiment 2. After skin preparation, the two recording electrodes (blue dotted square in the figure) were placed on top of RF with an inter-electrode distance (measured from the centre of the electrodes) roughly equal to 1cm. The two stimulation electrodes (round electrodes shown in the figure) were placed on either end of the recording dipole. The reference electrode was placed on the knee cap. The pre-amplifier box was taped to the thigh of the subject while all of the cables were also taped in place. This was done to both secure the electrodes in place and to reduce movement artefact.

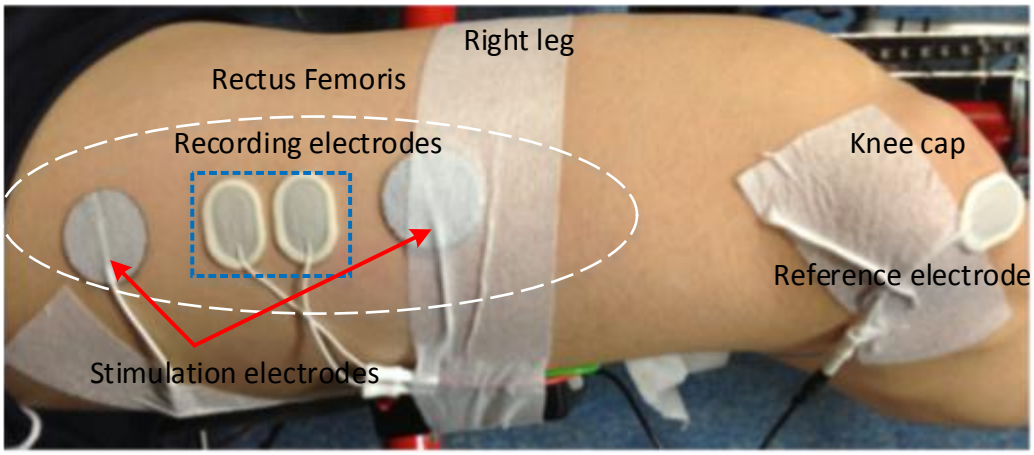

Figure 5. 9: The thigh, as viewed from above, showing the electrode configuration of experiment2. The electrodes were carefully aligned over the right RF.

Figure 5. 10: Parameter setup for the stimulator

The stimulator was set to external trigger mode (see 4.4.2 and Figure 5. 10) with a stimulation pulse width at 200µs after each commutator signal. The third setting shown on the display, 'No. of pulses', defines the number of stimulation pulses. It was set to 1 in this experiment for the

reason explained in 5.3.2. The pulse number could be set to a value greater than 1, in such a case the stimulation period 20ms (2nd setting in Figure 5. 10) determines the interval between consecutive pulses. However, when using a setting of 1 pulse, the stimulation period setting is irrelevant.

Stimulation intensity was set individually for each of the five subjects, based on the outcome of a short experiment. Each subject was tested with a continuous stimulation pulse (at 20Hz) from the stimulator (the stimulator was set to continuous mode), the stimulation intensity was increased from 0mA gradually until a contraction of the RF muscle was seen. During these experiments two factors were considered:

1. The stimulation intensity had to be high enough to activate the muscle?

   Ideally the stimulation intensity had to be high enough to fully activate the muscle. This was considered to be the case when a strong contraction in RF was visible during stimulation. If we consider the final product of the FES cycling system, the targeted group is incomplete SCI patients with paralysed limbs. Therefore, we will need the stimulation to be strong enough to activate the muscles so that the SCI patients can produce a cycling action.

2. Why not chose any intensity higher than that?

   For all the experiments presented here, AB subjects were used. It was therefore necessary to consider the pain threshold of the AB subjects. The stimulation intensity was held at a level that was sufficient to activate the muscle (Motor Threshold MT) while also being tolerable for AB subjects.

Table 5. 3: Stimulation intensities for the five subjects.

Subject 1	Subject 2	Subject 3	Subject 4	Subject 5
25mA	28mA	30mA	32mA	27mA

Before the formal experiment, the subjects were also put on the trike to experience the triggered stimulation, the pedal position that they should expect a stimulation pulse was explained to them. It is necessary that the subjects know what they should expect in the experiment to avoid anxiety. If there is a fault in the system that causes a stimulation pulse to be missed, the error could be detected in two ways. Firstly the experimenter could monitor this on the computer, and secondly, the subject would notice and could notify the experiment. Such an error would result in the experiment being stopped.

5.4.3 Results and Data analysis

Note here the windows were labelled as window 0 – 75 with the window number being the delay of the window from the blanking pulse. Figure 5. 11 is a plot of the post-stimulus amplitude against pre-stimulus amplitudes for Subject 1 and Window 0. Compared with the Experiment 1 (Figure 5. 7), the regression line differs from the 45º line by a significant amount, the slope was calculated to be 0.714. Note in 5.3.7, we have explained the experimental upper and lower limit for the variation in the correlation coefficient, with 9.6 for the 2 adjacent windows and 0.453 for windows 160ms apart. Here comparative with the case without stimulation, there is a reduction in the r^2 value from 0.7477 to 0.3852, and r from 0.8647 to 0.6206 with p values <0.01.

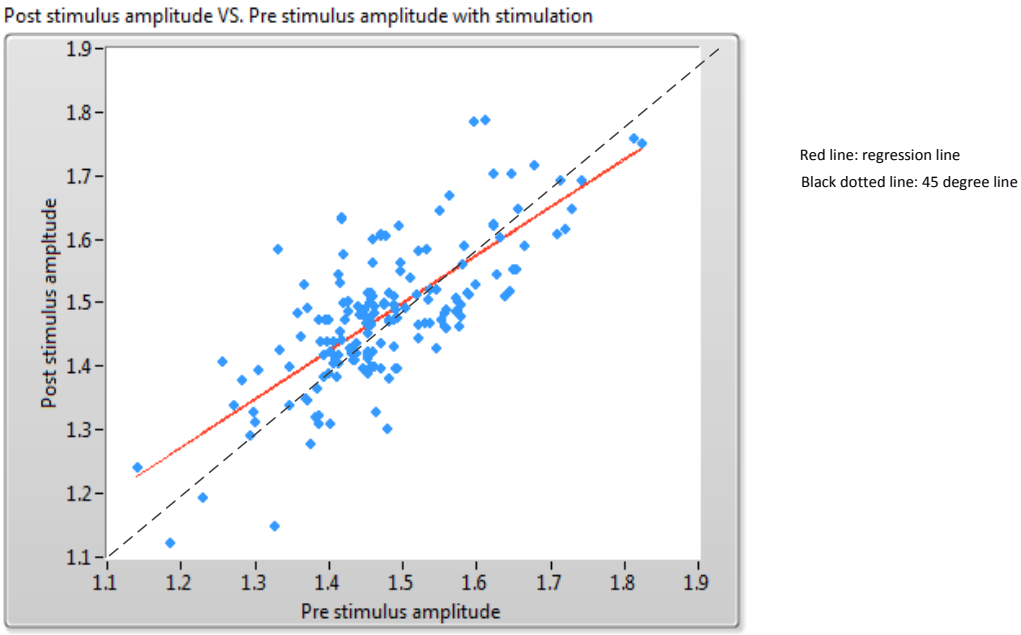

Figure 5. 11: Post stimulus amplitude vs. pre stimulus amplitude for subject 1 window 0 with stimulation.

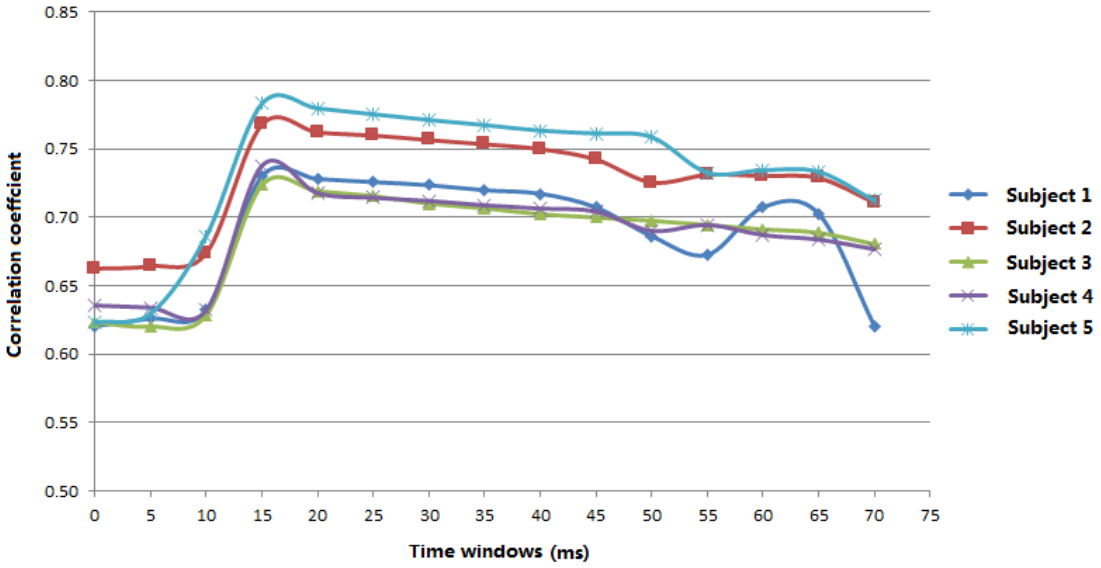

Figure 5. 12: Correlation coefficient change for different time windows for five subjects with stimulation (each window is 40ms long)

Figure 5. 12 shows that the correlation coefficient starts with much lower values in the first three time windows right after the blanking pulse. It rises after windows 15, sharply for all subjects. The correlation coefficients in window 15-50 bear a slow decreasing trend. After that, the trend diversifies for different subjects. Subject 2 and 4 have a small drop at around Window 50 follow by a small rise and slow decay. Subject 1 and 5 also show similar drops at Window 55 although the gradient of drop is much steeper. Compared to Subject 5, Subject 1 has a faster rising after the drop follows by a faster decay towards Window 70. Subject 3 gradually decreases from Window 15 to Window 70. The average correlation coefficient, for all 5 subjects, was found

at each window, as shown in Table 5. 4. The averaged r is also plotted against the windows in Figure 5. 13.

Table 5. 4: Averaged correlation coefficient for all subjects at each time window.

Window 0	Window 5	Window 10	Window 15	Window 20	Window 25	Window 30	Window 35
0.6331	0.6349	0.6507	0.7485	0.7413	0.7382	0.7347	0.7313
Window 40	Window 45	Window 50	Window 55	Window 60	Window 65	Window 70	
0.7279	0.723	0.7117	0.7051	0.7101	0.7074	0.6801	

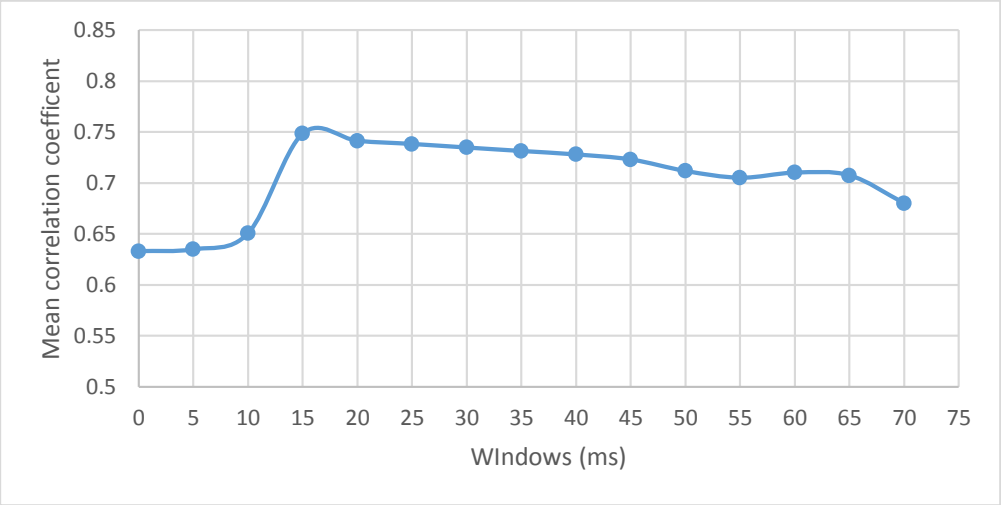

Figure 5. 13: Mean correlation coefficient at different windows.

5.4.4 Discussion

This experiment evolved from Experiment 1 with stimulation. In general, the correlation coefficient r was reduced by around 0.1 to 0.2. The r values started much lower at round 0.6 in the first three windows (0-15ms). This could be due to the M wave seen soon after the stimulation artefact. As the window number increases (i.e. the delay after the stimulation increases), and the correlation coefficient is seen to increase quickly to above 0.7 at Window 15. After this it gradually drops from Window 15-65. Following the decreasing trend from Windows 15-65, there were some fluctuations in 4 out of 5 subjects in Windows 50 or 55. This feature does not exist in Experiment 1, which lead us to think that the origin of this could be stimulation. In 3.6, we have discussed various physiological effects (reflexes) that might occur in the EMG signal with after stimulation. The two reflexes that were most likely to contribute to the results are the H and F reflexes which both happen around 40-55ms after the stimulation. The delay and the shape could vary from different subjects as a different population of the anterior horn cells are activated each time.

Table 5. 5: correlation coefficient r, coefficient of determination r^2 and the corresponding p values for five subjects in experiment 2.

	Window														
	0ms	5ms	10ms	15ms	20ms	25ms	30ms	35ms	40ms	45ms	50ms	55ms	60ms	65ms	70ms
Subject 1	r^2=0.3852	r^2=0.3920	r^2=0.3996	R^2=0.5330	R^2=0.5301	R^2=0.5268	R^2=0.5235	R^2=0.5183	R^2=0.5145	R^2=0.5002	R^2=0.4709	R^2=0.4525	R^2=0.5005	R^2=0.4935	R^2=0.3852
	r=0.6206	r=0.6261	r=0.6321	r=0.7301	r=0.7281	r=0.7258	r=0.7235	r=0.7199	r=0.7173	r=0.7072	r=0.6863	r=0.6727	r=0.7074	r=0.7025	r=0.6206
	P <0.01	P <0.01	P <0.01	P <0.01	P <0.01	P <0.01	P <0.01	P <0.01	P <0.01	P <0.01	P <0.01	P <0.01	P <0.01	P <0.01	P <0.01
Subject 2	r^2=0.4389	r^2=0.4413	r^2=0.4541	R^2=0.5894	R^2=0.5808	R^2=0.5773	R^2=0.5723	R^2=0.5676	R^2=0.5624	R^2=0.5510	R^2=0.5264	R^2=0.5345	R^2=0.5332	R^2=0.5311	R^2=0.5052
	r=0.6625	r=0.6643	r=0.6739	r=0.7677	r=0.7621	r=0.7598	r=0.7565	r=0.7534	r=0.7499	r=0.7423	r=0.7255	r=0.7311	r=0.7302	r=0.7288	r=0.7108
	P <0.01	P <0.01	P <0.01	P <0.01	P <0.01	P <0.01	P <0.01	P <0.01	P <0.01	P <0.01	P <0.01	P <0.01	P <0.01	P <0.01	P <0.01
Subject 3	r^2=0.3885	r^2=0.3845	r^2=0.3953	R^2=0.5236	R^2=0.5171	R^2=0.5121	R^2=0.5042	R^2=0.4993	R^2=0.4934	R^2=0.4889	R^2=0.4866	R^2=0.4823	R^2=0.4778	R^2=0.4743	R^2=0.4629
	r=0.6223	r=0.6201	r=0.6287	r=0.7236	r=0.7191	r=0.7156	r=0.7101	r=0.7066	r=0.7024	r=0.6999	r=0.6976	r=0.6945	r=0.6912	r=0.6887	r=0.6804
	P <0.01	P <0.01	P <0.01	P <0.01	P <0.01	P <0.01	P <0.01	P <0.01	P <0.01	P <0.01	P <0.01	P <0.01	P <0.01	P <0.01	P <0.01
Subject 4	r^2=0.4040	r^2=0.4021	r^2=0.3997	R^2=0.5443	R^2=0.5151	R^2=0.5102	R^2=0.5071	R^2=0.5025	R^2=0.4991	R^2=0.4960	R^2=0.4764	R^2=0.4823	R^2=0.4721	R^2=0.4676	R^2=0.4579
	r=0.6356	r=0.6341	r=0.6322	r=0.7378	r=0.7177	r=0.7143	r=0.7121	r=0.7089	r=0.7065	r=0.7043	r=0.6902	r=0.6945	r=0.6871	r=0.6838	r=0.6767
	P <0.01	P <0.01	P <0.01	P <0.01	P <0.01	P <0.01	P <0.01	P <0.01	P <0.01	P <0.01	P <0.01	P <0.01	P <0.01	P <0.01	P <0.01
Subject 5	r^2=0.3886	r^2=0.3966	r^2=0.4713	R^2=0.6132	R^2=0.6079	R^2=0.6012	R^2=0.5947	R^2=0.5891	R^2=0.5828	R^2=0.5796	R^2=0.5756	R^2=0.5368	R^2=0.5395	R^2=0.5377	R^2=0.5072
	r=0.6234	r=0.6298	r=0.6865	r=0.7831	r=0.7797	r=0.7754	r=0.7712	r=0.7675	r=0.7634	r=0.7613	r=0.7587	r=0.7327	r=0.7345	r=0.7333	r=0.7122
	P <0.01	P <0.01	P <0.01	P <0.01	P <0.01	P <0.01	P <0.01	P <0.01	P <0.01	P <0.01	P <0.01	P <0.01	P <0.01	P <0.01	P <0.01

5.4.5 Checking for other effects

Stimulation can give rise to physiological effects such as a reflex response in the muscle. The presence of such responses would alter the recorded EMG signal during the cycling experiments. This would in turn alter the correlation for the time windows they belong to. The presence of such reflexes was investigated by averaging the raw EMG data, before and after the stimulation, over a number of revolutions. A voluntary EMG signal on its own is a random signal, consequently, when the average is calculated the positive and negative parts of the wavelets add up and cancel each other out. Therefore the averaged value should be close to zero. Any reflexes that are common to the EMG signal would appear as a non-zero average value.

It was difficult to average the data over time, as the time taken for the subjects to complete a revolution differed. It was therefore decided to align the EMG data using the commutator signal as a reference. Roughly 340 data points before the stimulation and 460 data points after the stimulation were selected for each revolution. At 5k/s sample rate, 340 samples = 68ms; 460 samples = 92ms. These data points were selected as they covered the time where the fluctuations occur, as shown in Figure 5. 12. The data points before the stimulation were chosen to represented EMG data without stimulation. The aligned EMG data was then averaged over the number of revolutions as shown in Figure 5.14.

For simplicity, the blanking period is not shown in the figure and the averaged EMG signal before and after the stimulation are plotted consecutively. The data was averaged over 5, 10, 20 and 50 revolutions. As we increase the number of revolutions averaged, the mean EMG becomes smoother and tends to be centred around 0. During the period immediately following the stimulation pulse, large variations can be seen from roughly 1050-1150 (corresponding to 0-15ms). There seems to be some variations at between 1350-1450 (roughly 45ms-55ms) when averaged over 20 revolutions (circled) which could be due to the reflexes. Further analysis was carried out to check this. The mean and SD of the same data set was calculated over every 20 revolutions (0-20, 20-40, 40-60, 60-80, 80-100) in the same manner and the results are shown in Figure 5.15.

Discussion on the presence of other effects

The period immediately after the blanking time (0-15ms) shows high variations, which indicates the presence of some effects. This could be residuals of the M wave and stimulation artefact. This explains the low r found in these windows in 5.4.3.

There are some variations between 1350-1450 (roughly 45ms-55ms) in Figure 5.14 which are still visible after averaging over 20 revolutions and become less visible after averaged over 50 revolutions. This feature, occurring at 45-55ms, was further investigated by using a moving window of 20 revolutions, to determine if the variations in the mean EMG after the stimulation were consistently there. It was found that although there tended to be more variations around 45-55ms, they were not always present. For example the variations were not evident in the

20-40 and 60-80 revolutions. Furthermore, when the variations did occur, as in the 40-60 and 80-100 revolutions, the shape of the signals was not the same, unlike the shape of the variations seen in the 0-15ms interval which were attributed to M-waves and stimulation artefact. These variations cannot be simply removed by subtracting a mean value from the raw data. The variations themselves do not appear to show more variance than is typically seen in the fluctuations found in the 1150-1350 data point interval. Therefore at this stage, we cannot conclude that these variations are due to reflexes.

From the analysis of the experiment results, we can conclude that post-stimulus windows starting at 15-45ms give best correlation to the pre-stimulus windows with correlation coefficients higher than 0.7.

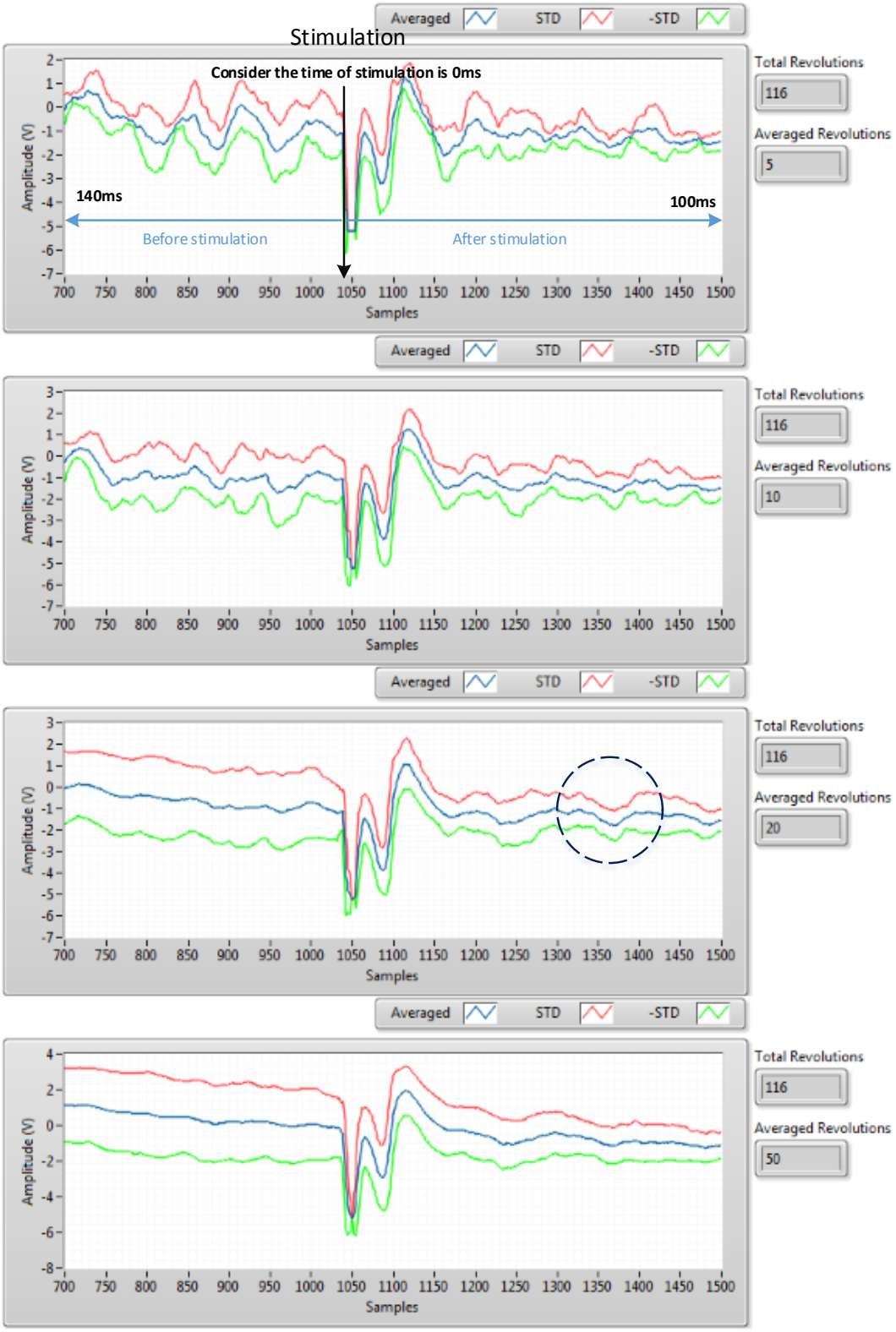

Figure 5. 14: The blue trace: the mean EMG signal over 10-50 revolutions; the red and green traces: mean EMG ±standard deviation

Figure 5. 15：Mean EMG signal before and after the stimulation averaged by a moving window of 20 revolutions, revolution numbers are at the top right corner of each graph.

5.5 Experiment 3: How does RMS EMG change with effort level?

5.5.1 Aims

The effort level was held constant in Experiments 1&2. To understand the relationship between RMS EMG amplitudes and the effort level (see 5.2.2), the latter was varied in Experiment 3. The RMS EMG amplitudes were calculated from EMG captured during a 40ms time window during cycling. The aim was to find out how these amplitudes vary with the effort levels.

5.5.2 Methods

The LABVIEW program

Figure 5. 16 shows a picture of the front panel used in Experiment 3. (The same program was also used in Experiments 4 and 5 but with recording from different muscles.) Experiment 3 focused on only right RF muscle while later experiments targeted other muscles.

The display of the LABVIEW program, which is shown in Figure 5. 16, is divided into two parts. On the left hand is the control panel where the experimenter can control the settings of the experiment. From the top of the control panel is a *stop* button which is used to stop the program during the experiment. Before starting the program, the experimenter will need to select the destination folder that the data will be saved to using the *file save path*. The duration in seconds sets the total running time of the experiment. The experimenter needs to manually input the subject's name and the generated random sequence for the effort level. The effort level sequence is randomly generated using a free online random sequence generator ("RANDOM.ORG - Sequence Generator," first accesed June 2010). The *threshold* (-1 in the diagram) indicates that the selection of the window starts at the falling edge of the commutator signal. Both the "time elapsed" and the progress bar in the centre of the diagram serve the same purpose, namely monitoring the progress of the experiment. The RMS array in the left panel is saved separately for used in future analysis. The EMG sampling period, i.e. the muscle activation range of each subject was determined by the experiment results obtain in 4.5.

On the right hand side is the indication panel. The indication panel contains both the raw input signals and the processed RMS values. When used in Experiment 1, the program reads three analogue inputs (the EMG signal, the commutator signal and the shaft encoder signal) and one digital input signal (the effort level change). The analogue inputs share a same wave graph to the top left of the indication panel and the digital input of the effort level sits below it. The processed RMS EMG data is shown on the right side of the indication panel.

The experiment design

There are a few parameters that needed to be decided before starting the experiment. The total recording time of the experiment was set to be 150s with 30s for each effort level. Effort levels 3-7 were chosen to be applied in the experiments. These effort levels were chosen as they were found to be within for the capability of all of the recruited subjects. Effort levels 0-2

did not show much muscle activity in the EMG measurements, while levels 8-9 were found to be too tiring for the female subjects, especially during the longer cycling sessions. The cadence was set to be 60rpm, which was regulated by means of a metronome that was set to beep twice every second.

5.5.3 Experiment procedures

Five AB subjects were recruited for the experiment. They were asked to cycle at 60rpm, against 5 different effort levels. The effort levels were changed every 30s by the TACX ergotrainer as described in 4.2.2; the sequence was randomised. The subject was not told what the sequence of the effort levels would be.

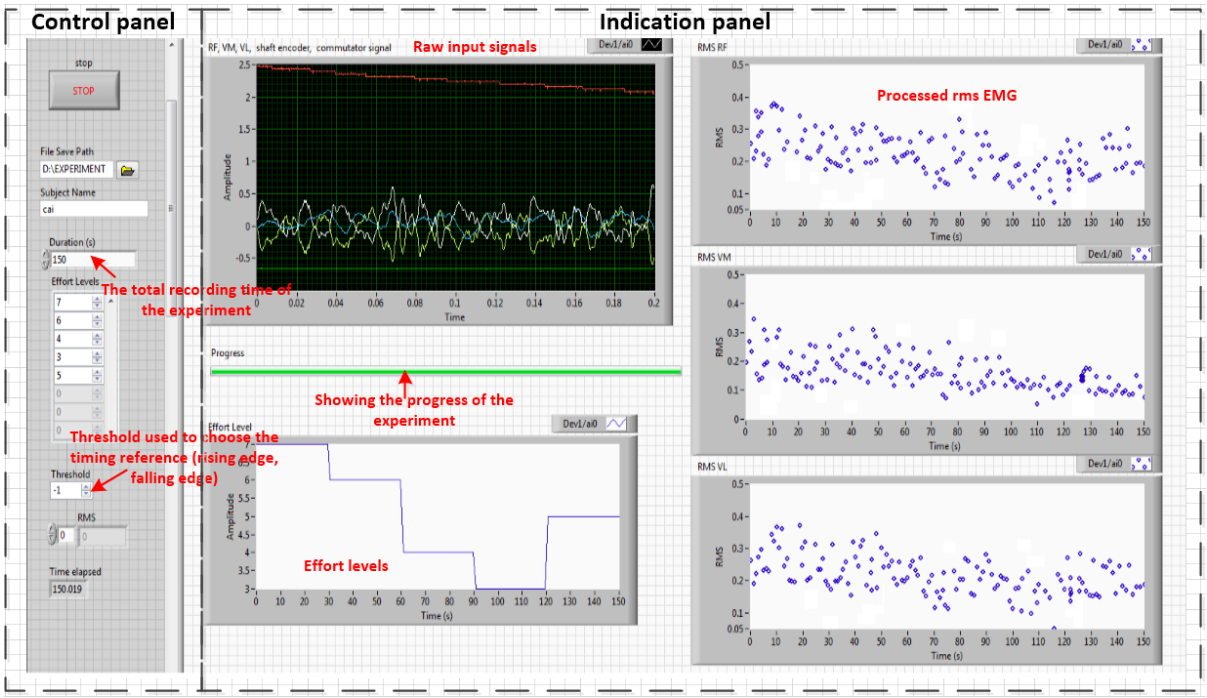

Figure 5. 16: Front panel of the real time recoding and processing software.

5.5.4 Results and Data analysis

In general, a clear trend exists between the RMS EMG amplitude and changes with the effort level, as seen in Figure 5. 18. However, a few irregularities were noted for subject 1 and 2, during the last 30s. The two subjects found it difficult in maintaining the cadence towards the end of the experiments due to fatigue. As mentioned before in 4.2.1, the shaft encoder produces a voltage signal from +5V to 0V during each revolution. The duration of the signal to decrease from 5V to 0V was dependent on the pedalling speed of the subject, the faster the speed, the shorter the duration. An example of the raw shaft encoder signal at different cadence is shown in Figure 5. 17. Therefore by plotting the instantaneous gradient (three times per second) of the shaft encoder signal, we could monitor the cadence. When the subject is cycling at 60rpm, the slope of the shaft encoder should be around -5. Figure 5. 19 shows the

gradient plot of the shaft encoder signals for all five subjects. A slow cadence will result in a higher amplitude in Figure 5. 19. The plots clearly show that Subject 1 and 2 began to lose speed around 75s and the condition became worse after 120s. The inconsistency in cycling cadence would affect the EMG output and also RMS EMG amplitudes.

To see the trend clearly, the mean RMS EMG amplitudes were plotted against effort levels with SD bars. These mean RMS EMG amplitudes were averaged over roughly 30 revolutions. The mean RMS EMG were plotted against effort level 3-7 regardless of their original effort level sequences. As the effort levels were selected randomly for each subject, the mean values for the last two effort level in the sequence, where cadence of the subjects are mostly to be affected, are circled (4^{th} in blue, 5^{th} in red).

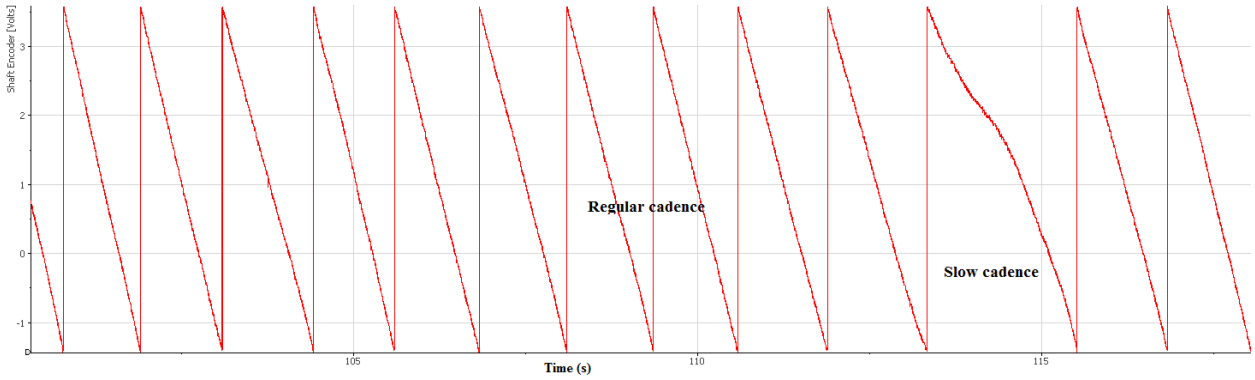

Figure 5. 17：The raw shaft encoder signal showing the slow cadence.

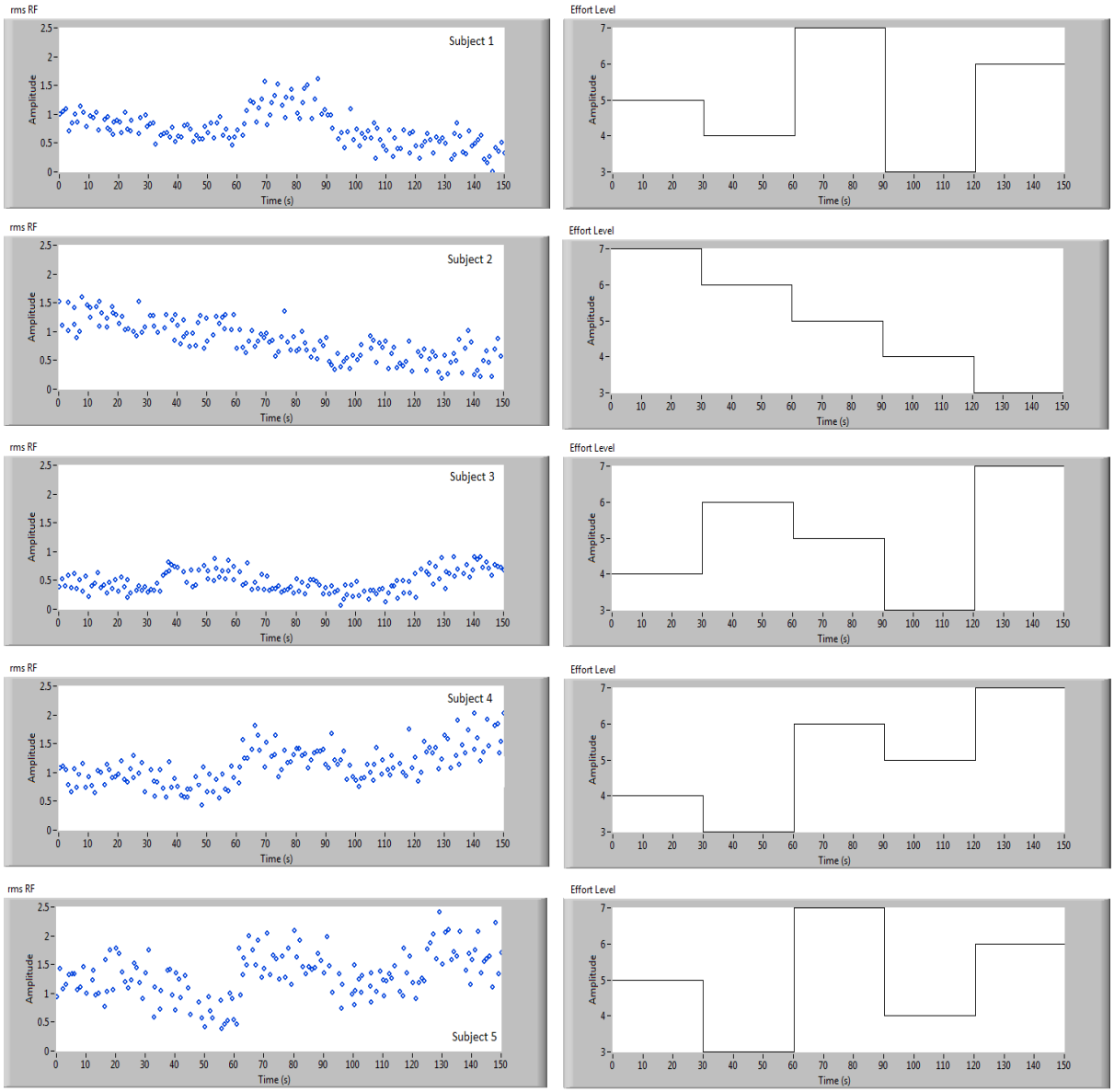

Figure 5. 18： RMS EMG amplitudes change with effort level during a 2.5mins cycling trial, from FIVE subjects.

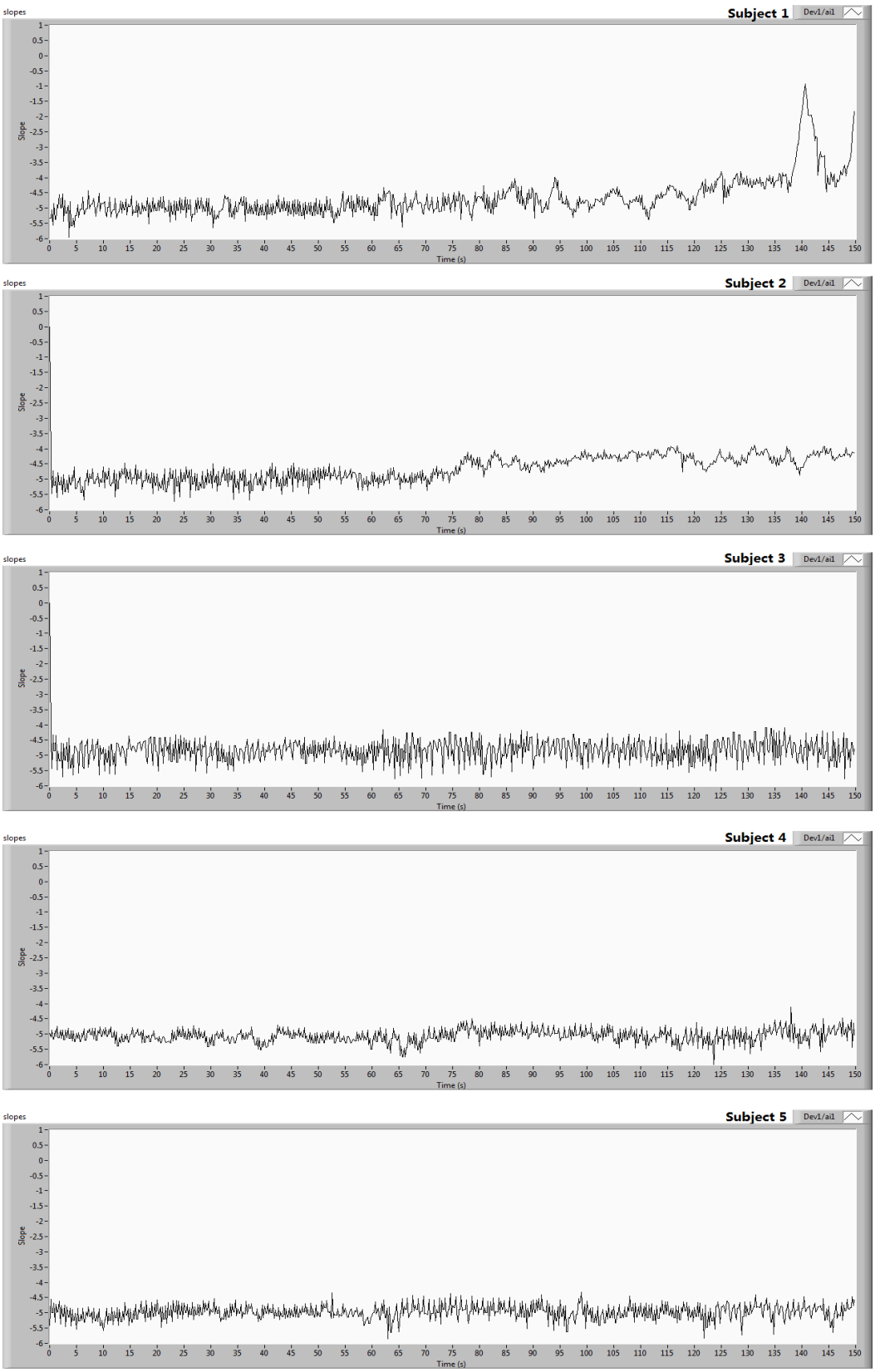

Figure 5. 19: Gradient of shaft encoder during Experiment 2 for five subjects.

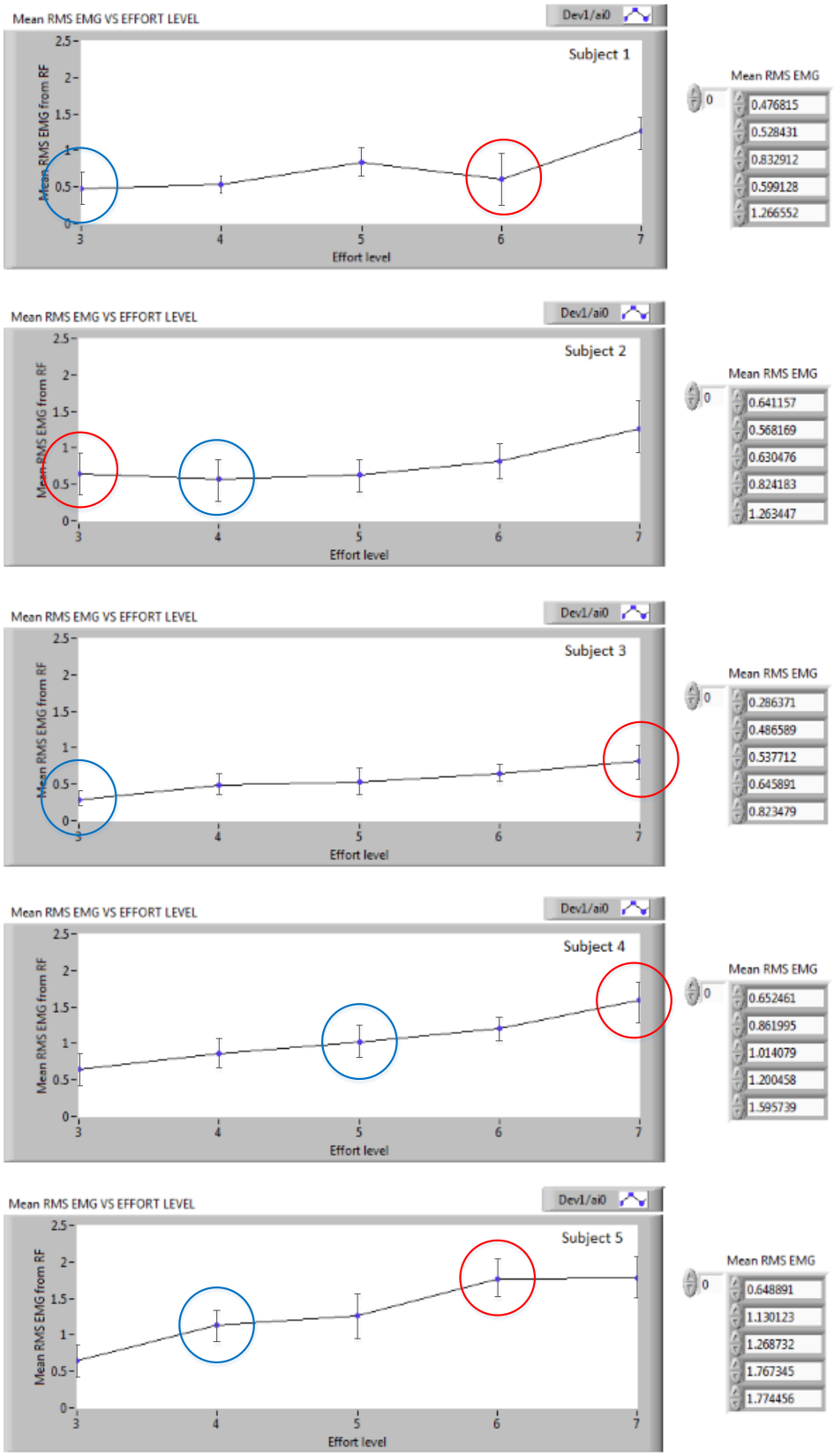

Figure 5. 20: Mean RMS EMG amplitudes at five effort levels for 5 subjects. The error bars are the standard deviations.

5.5.5 Discussions

Experiment 3 explored the relationship between RMS EMG amplitude and effort levels. As shown in Figure 5. 20, the general trend of the RMS EMG amplitudes increases with the effort level. Subject 1 and 2 struggled to keep a constant cadence for the last 75s, therefore their RMS EMG may not represent the true values of corresponding effort levels (red circled (and blue?) in Figure 5. 20).

The changes in mean RMS EMG for different effort levels were small. Looking at the original plot in Figure 5. 18, the RMS EMG amplitudes form a cluster at each effort level. For every given effort level, the RMS EMG amplitude shows a lot of variation, so much that the data points for different efforts overlap. Subject 5 appeared to have the most distinct values for different effort levels, this could be related to him being a regular cyclist. The spread of points in each cluster would represent two effects:

- the variance due to the finite window length;
- unsteadiness in the subject's voluntary drive to RF;

The two effects would both contribute to the overall scatter of the plot. Among the five subjects, Subject 3 had the minimum spread of the data points (lowest SD) while Subject 5 had the highest (highest SD). Subject 5 also bore the highest amplitude and Subject 3 the lowest. It is not surprising that Subject 5, being the fittest and slimmest of all, had the highest amplitude. But Subject 3 also cycles regularly, so what could be the reason of the low RMS EMG amplitude? Subject 3 is a female and has higher subcutaneous fat in the thigh (compared to all the other subjects by a pinch test). The low RMS EMG amplitude was explained in the experiment performed by Kuiken (Kuiken et al., 2003), the fat layer could reduce the EMG amplitude significantly (3mm fat layer can reduce the RMS EMG by 31%).

The results from Experiment 3 show us that it is not always reliable to use EMG from a single muscle to estimate the effort level as it is difficult to judge the intensity correctly, even though a trend is seen in the RMS EMG in which the amplitude increases with effort level. Variability of the RMS EMG is large compared to the slope, assessing this for a certain effort level needs averaging over a large number of revolutions. Forming an estimate of voluntary drive from one muscle is difficult as the time needed to do this is too long. The results were therefore not satisfactory.

What could possibly be the reason of such variation and spread in the RMS EMG data? Is it because the subjects began to use other muscles more when they felt the need of more power to maintain the cadence? According to the cycling mode change we discussed in 3.11, the subjects may change the way they use the muscles during cycling very freely without being aware of it. Does it mean we should gather our control signal from multiple muscles rather than one? In Experiment 4, we examine this by recording from multiple thigh muscles at the same time as well as using orthoses to constrain the ankle joints.

5.6 Experiment 4: Using orthoses to restrict muscle activation

5.6.1 Aims

From 3.9.2, fatigue can change the muscle recruitment pattern and muscle coordination during cycling. There are a number of possible muscles that the subjects may begin to use differently apart from RF, for example the calf muscles, the hamstrings and the Vastii. It is possible to reduce the number of possibilities by using orthoses. An orthosis is a rigid or semi-rigid device that supports a weak or deformed body part. It is also used to restrict or eliminate motion in a diseased or injured part of the body (Edelstein & Bruckner, 2002). Experiment 4 use ankle-foot orthoses (AFO) which cover the foot and a portion of the lower leg. The AFOs here constrain the ankles of the subjects thereby preventing the subject from using the calf muscles during cycling (Hsu et al., 2008).

The other possibilities being the hamstrings and the Vastii. Here the Vastii are chosen because of the possible compensation effect with RF as suggested by Hautier (Hautier et al., 2000) (see 3.9.2). Therefore the variations of RF amplitudes in Experiment 3 could possibility be explained by analysing VM and VL together.

5.6.2 Experiment setup

The ankle orthoses used were ROM Walker from *Technology in Motion Ltd*. These orthoses came with 4 Velcro strips that firmly locked the ankles and feet in place with minimum degree of freedom. Holes were drilled on the foot soles to fix the boots to the pedals according to a template made on a piece of stainless steel board (see Figure 5. 21 Right). There are 10 holes drilled on each foot sole but only 6 are needed to secure the orthoses, the range of holes can provide different fitting for different subjects' preferences.

5.6.3 Experiment procedures

The same procedure was followed as that used in experiment 3 (Levels 3-7; 30s cycling interval at each effort level; effort level sequence randomly selected and not made known to subjects).

5.6.4 Results and Data analysis

From Figure 5. 23, the raw EMG signals of quadriceps shared a similar activation range, this was previously discussed in 4.5. From Figure 5. 23 and Figure 5. 24, we could again see that the activation ranges of the three quadriceps muscles were very similar, therefore the RMS windows were chosen to be at the same timing and duration for all three muscles. The commutator signal's falling edge was used as the timing reference of the window selection.

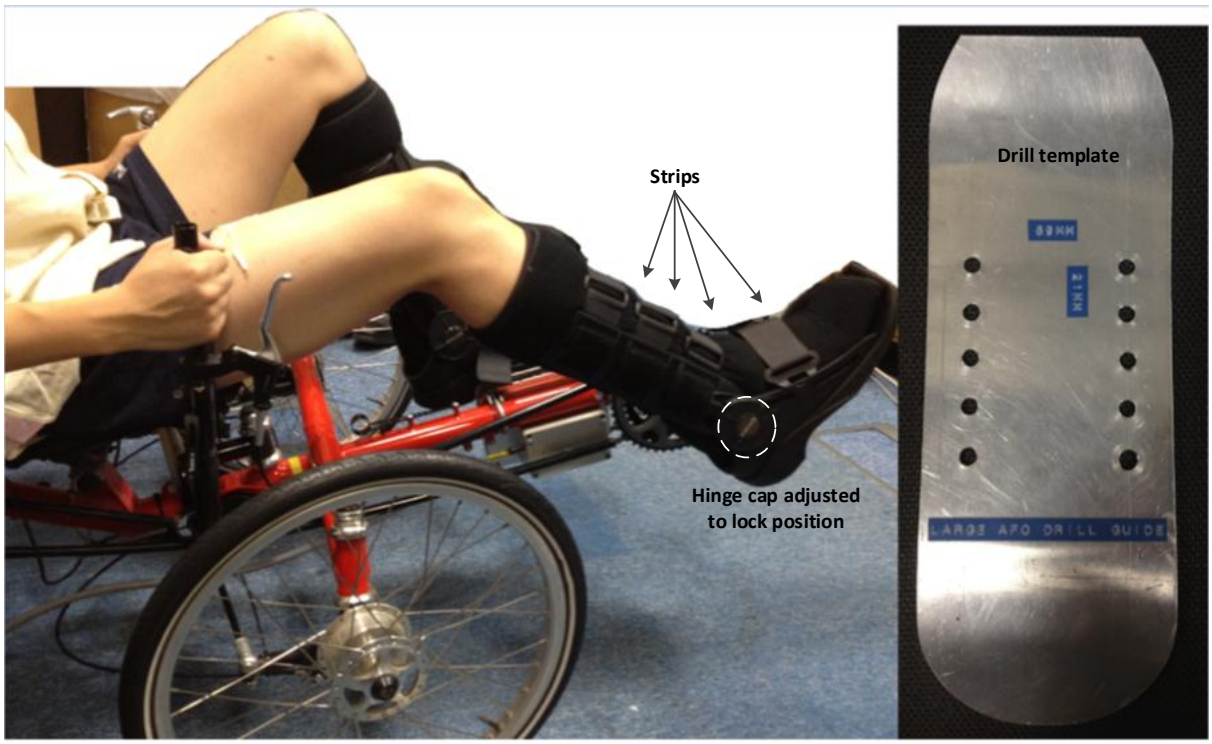

Figure 5. 21: Left: A subject sits in the trike with the ankle orthoses; Right: drill template made for drilling holes through the soles.

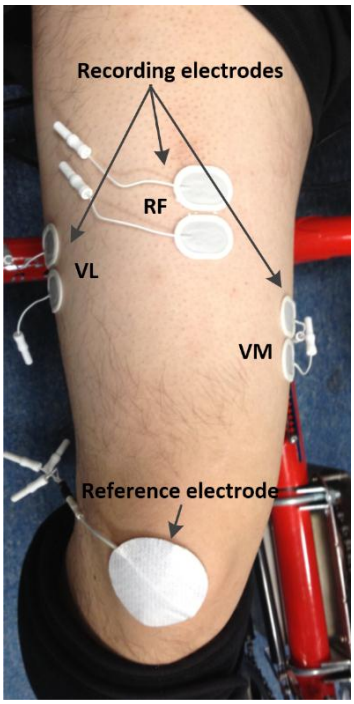

Figure 5. 22: Electrode position for three muscles with common reference electrode on the knee cap.

The RMS EMG of the three muscles are plotted against effort level in Figure 5. 25: RMS EMG changes with effort levels for subject 1 and 2. Figure 5. 25—Figure 5. 27 and the corresponding shaft encoder slope is shown in Figure 5. 28. The RMS EMG amplitudes are shown separately at each effort level sequence, to explore two things:

- How similar are the RMS EMG patterns of the three muscles?
- How does this relationship change when the subjects began to fatigue?

Figure 5. 28 shows that for Subject 1 & 2, the cadence was not stable from roughly 90s onwards, which coincides with the last two effort levels tested. The slope changed from that seen during the first two minutes, by up to 57%. Subject 3 also showed some variations starting from around 112s, which coincided with effort level 7, during this subject's cycling sequence. Subjects 4 and 5 showed a stable cadence throughout the experiment. An increment in the slope in this case means the subject takes longer to complete a revolution, as he is cycling at a slower cadence. An observation during the experiment shows that the subject often loses his breath and struggles to keep pedalling, which could indicate that he is fatigued.

The mean of each subject is plotted against different effort levels in Figure 5. 26—Figure 5. 30. The two mean values representing the last one minute of data are circled in blue (4th in the effort level sequence) and red (5th) respectively, as they are most likely to be influenced by fatigue. For Subject 1, there is a drop on all muscles at Level 5 and 7, which could be due to the reduced cadence, a possible indication of the subject beginning to fatigue. Subject 2 shows an abnormal increase in mean RMS EMG for two muscles at Level 5 where he had a reduced cadence. Subject 4 and 5 have fairly constant cadence even at the last 1 minute, yet there is a drop in RF and VM amplitudes for Subject 4 at Level 5.

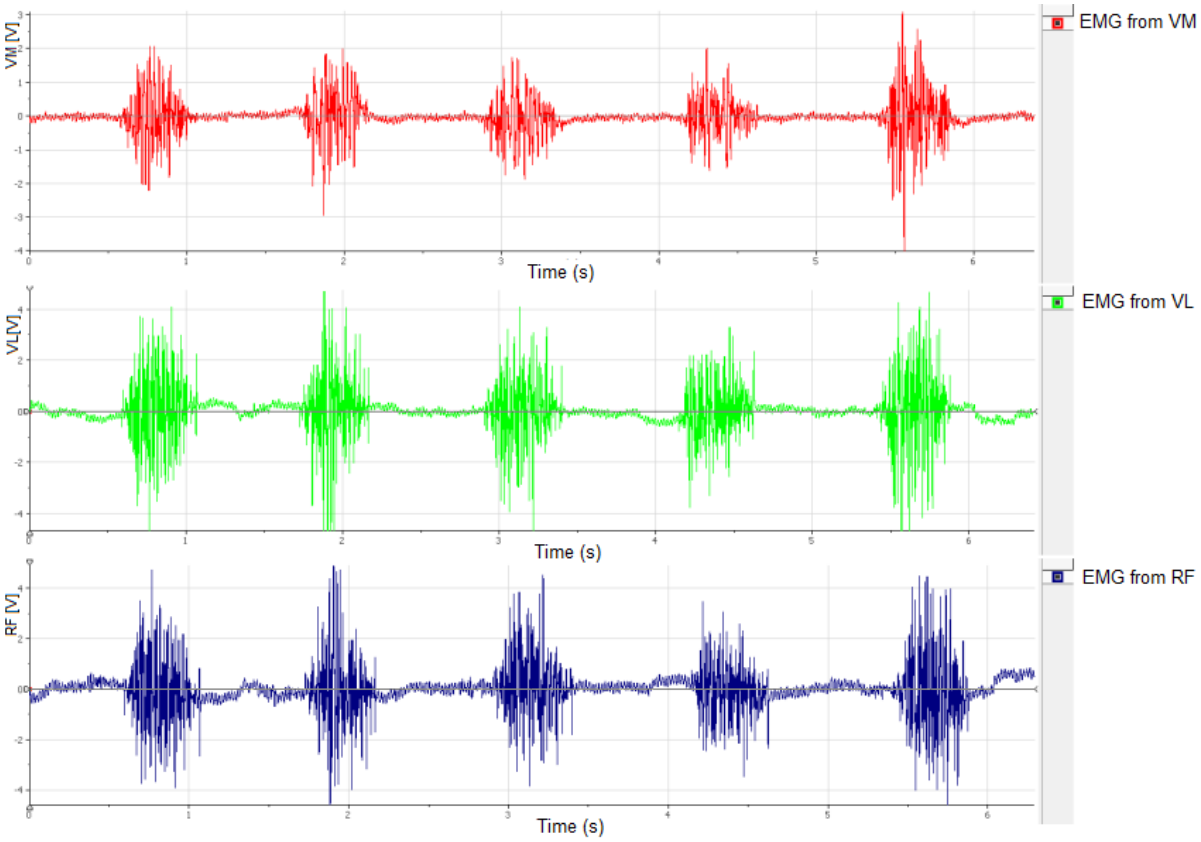

Figure 5. 23: Raw EMG signals from three muscles showing 5 revolutions.

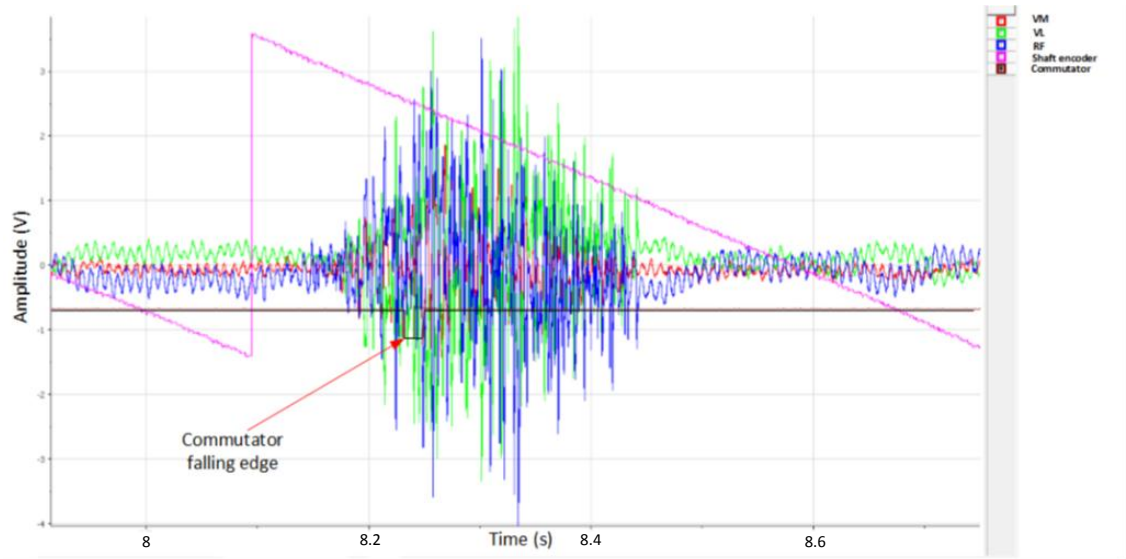

Figure 5. 24：Recorded EMG from three muscles, shaft encoder and commutator signals from one revolution.

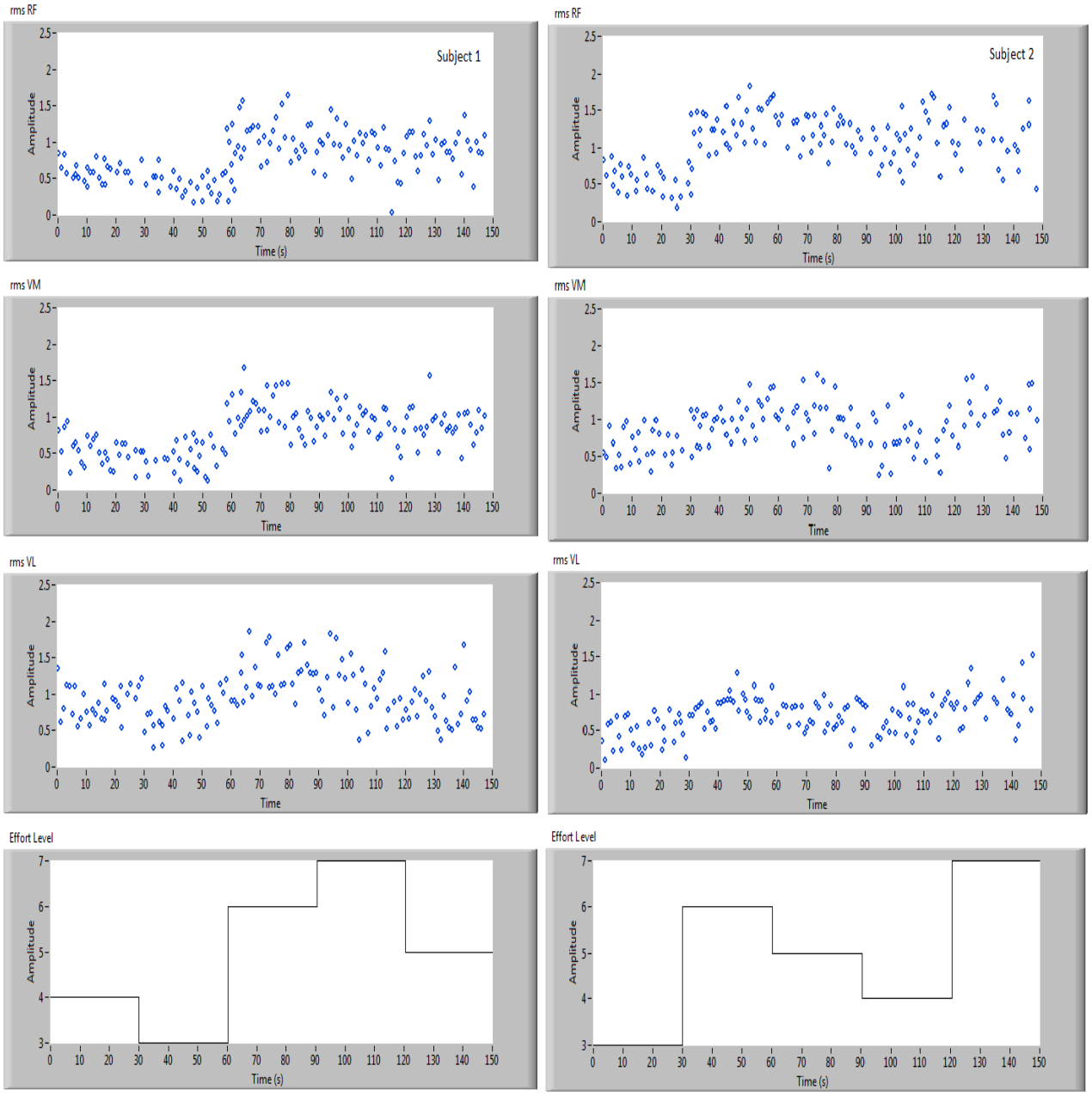

Figure 5. 25: RMS EMG changes with effort levels for subject 1 and 2.

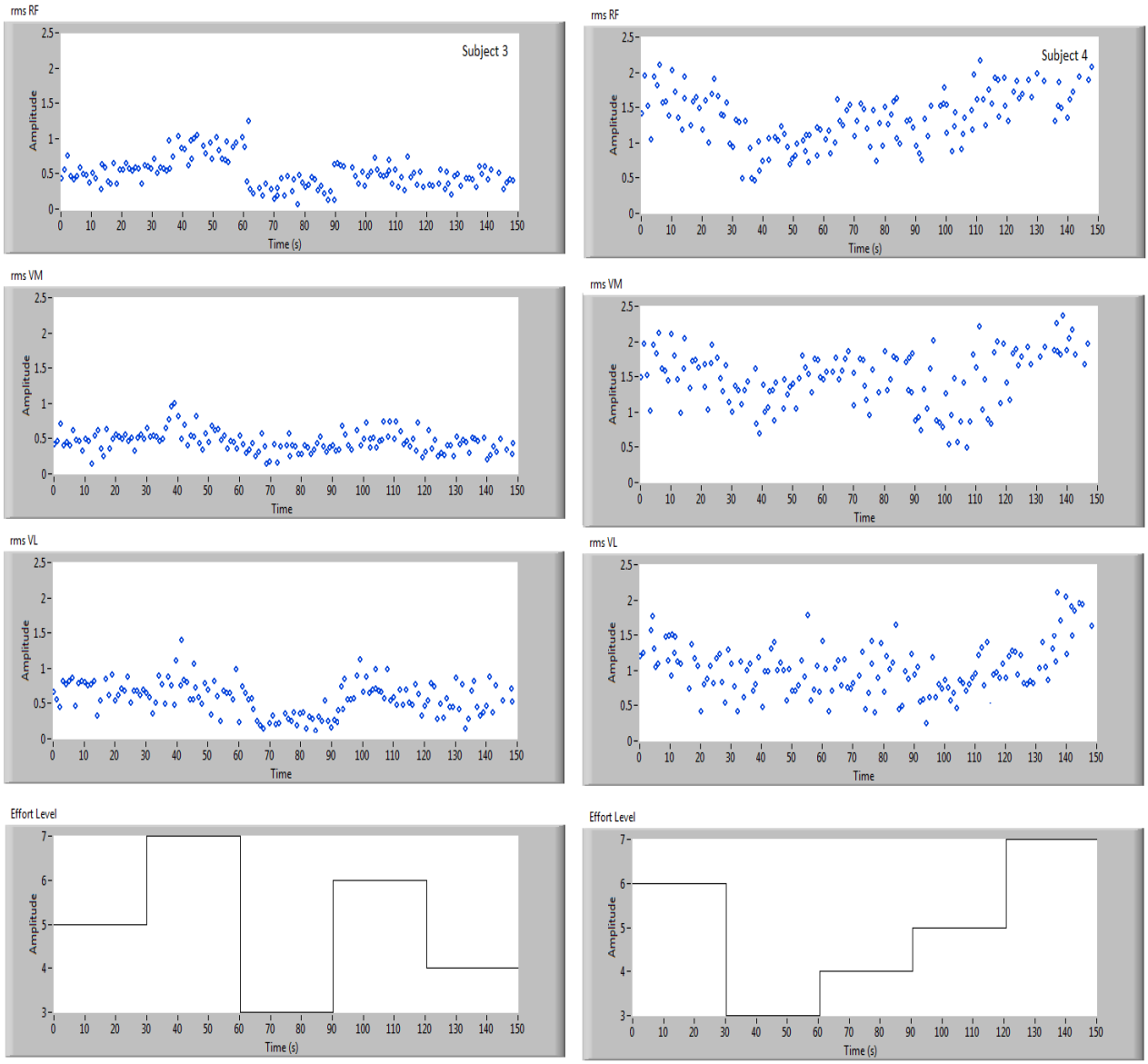

Figure 5. 26: RMS EMG changes with effort levels for subject 3 and 4.

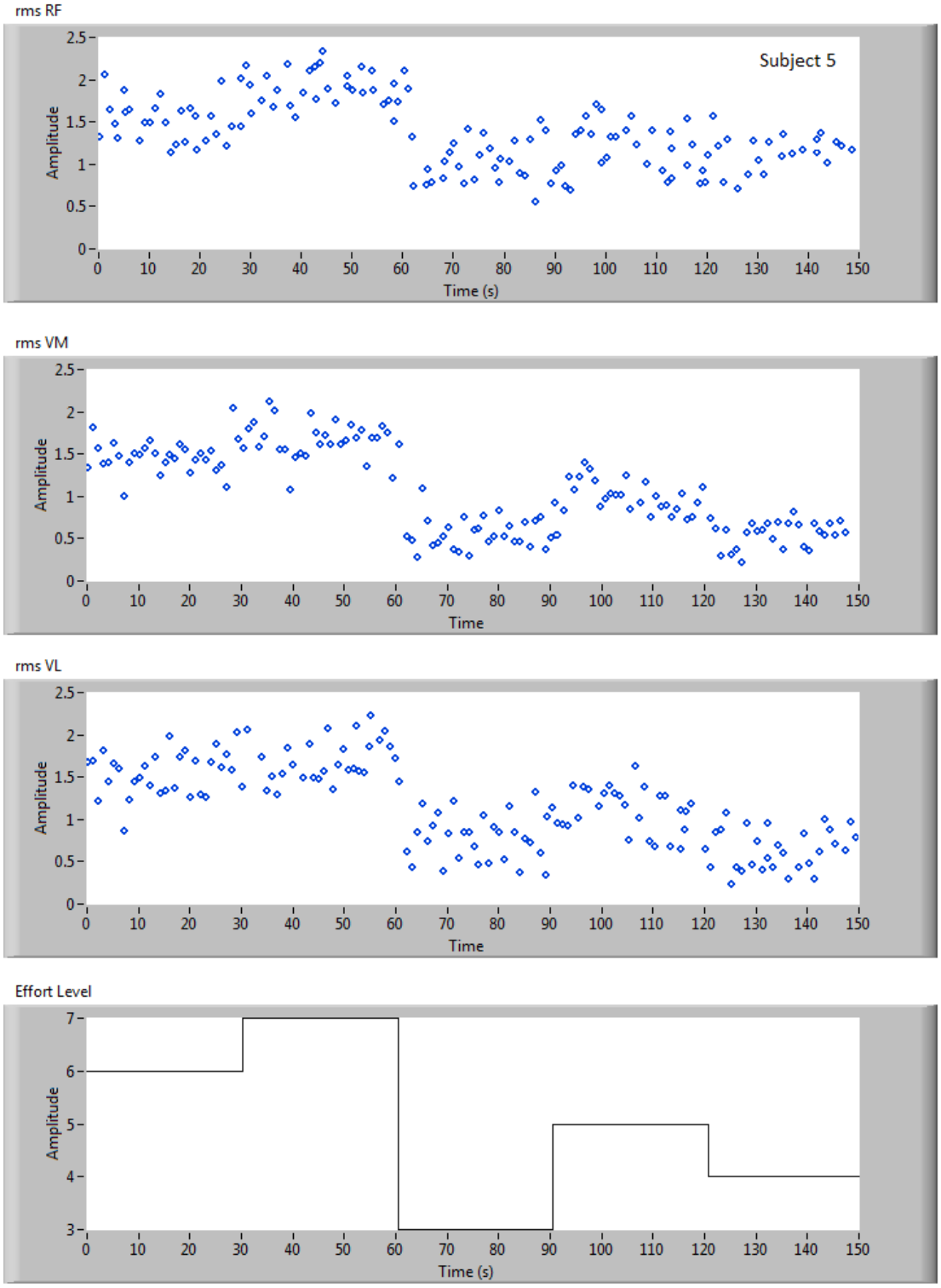

Figure 5. 27: RMS EMG changes with effort levels for subject 5.

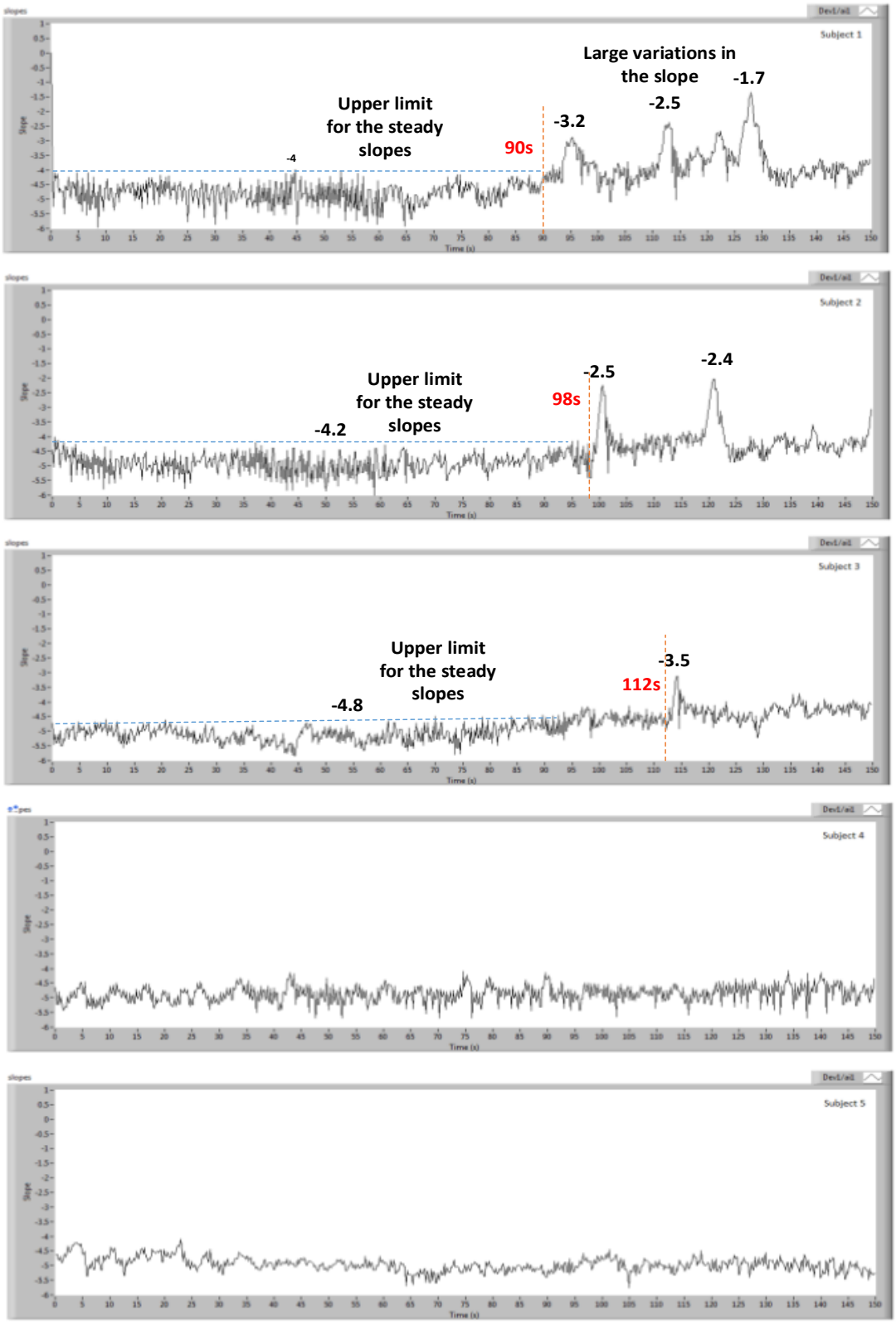

Figure 5. 28: The slope of the shaft encoder for all five subjects.

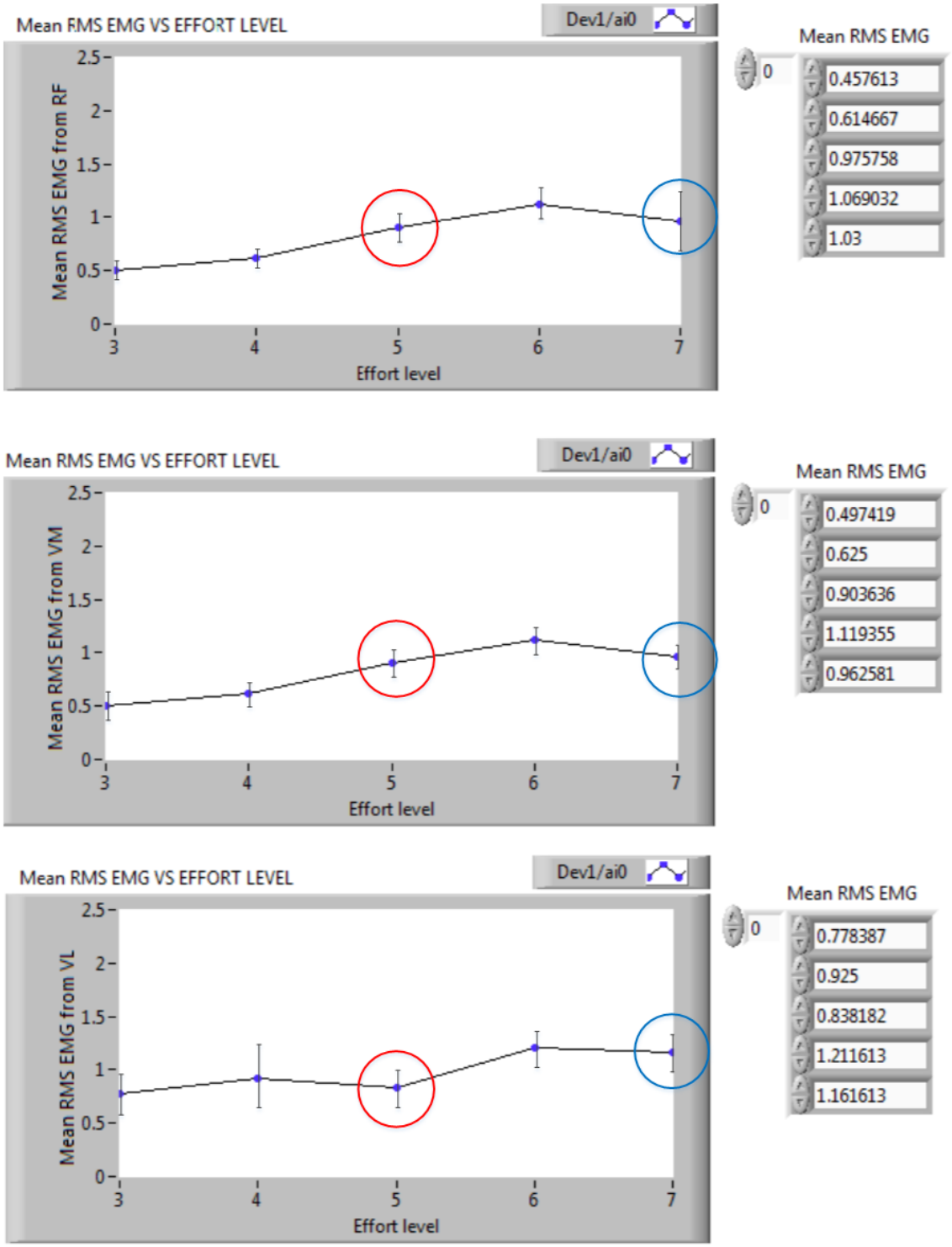

Figure 5. 29: Mean RMS EMG amplitudes of RF, VM, VL for Subjects 1 against effort levels.

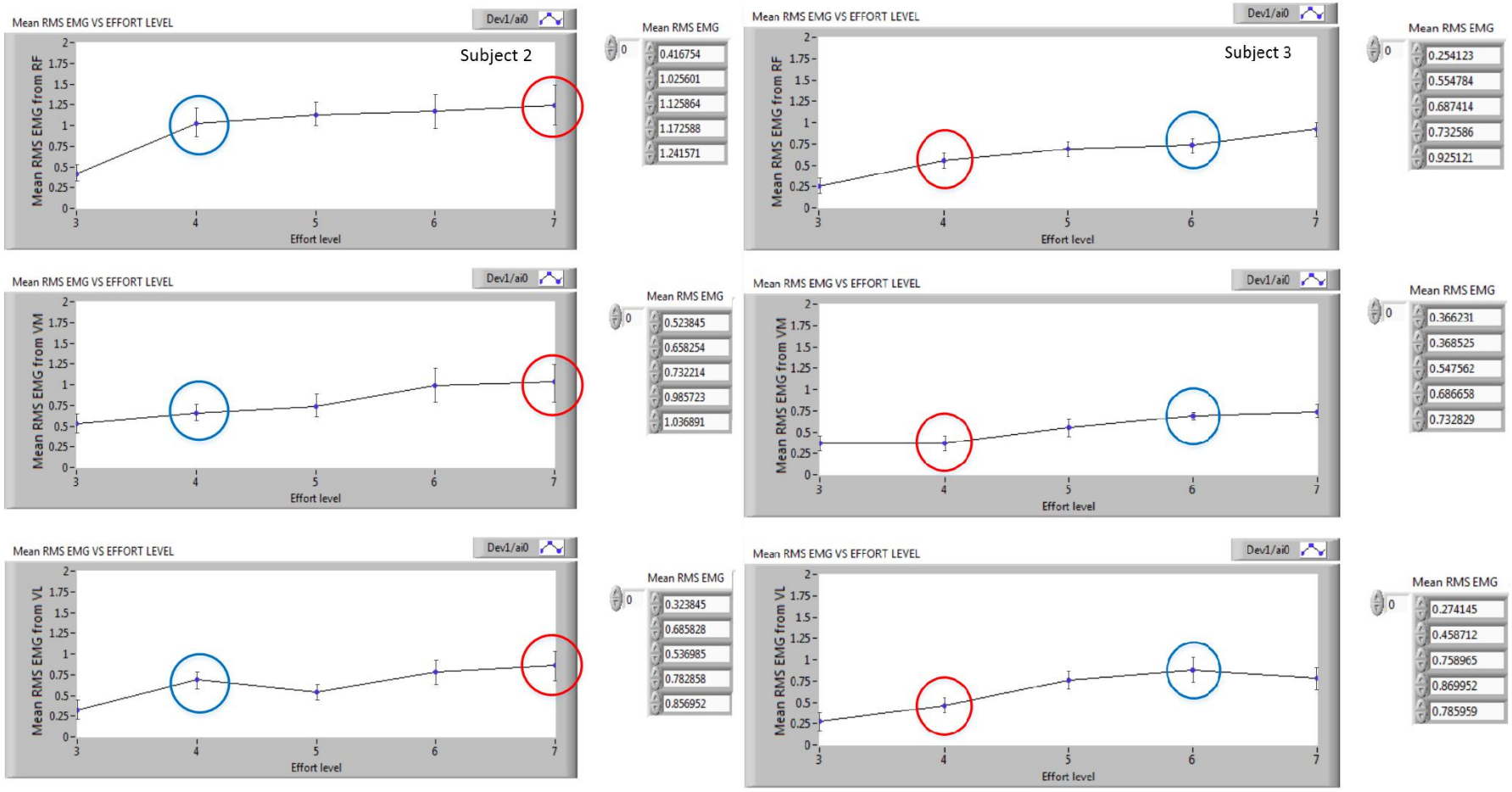

Figure 5. 30: Mean RMS EMG amplitudes of RF, VM, VL for Subjects 2 & 3 against effort levels.

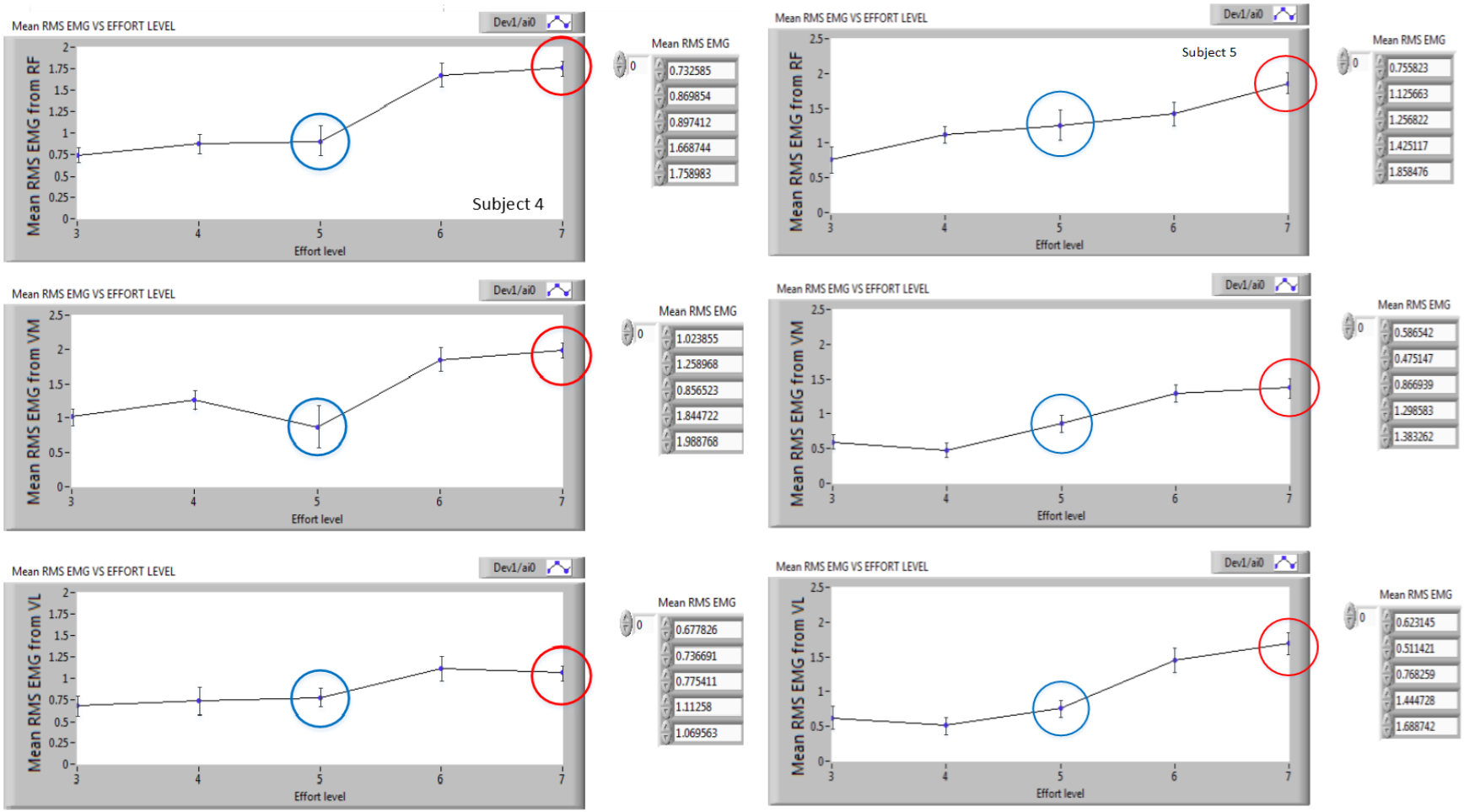

Figure 5. 31: Mean RMS EMG amplitudes of RF, VM, VL for Subjects 4 &5 against effort level

The correlation between the three muscles

Further analysis was performed to compare the correlation between the three muscles. Figure 5. 32—Figure 5. 37show the RMS EMG amplitudes plotted against each other for Subject 1. The effort level sequence is 4-3-6-7-5, therefore the two effort levels where fatigue is most likely to happen are Level 5 & 7. The data points in the figures are tagged by the corresponding effort levels and Level 5 & 7 are the blue crosses and orange dots respectively.

The correlation between the RF and VM pair is 0.754 which indicates a relatively strong positive correlation which indicates the two muscles are being used in the same manner. Inspection of the RF and VM pair show that the points are in overlapping clusters showing an increasing trend from Level 3 to 6. Level 7 requires the most effort from the subject to maintain the constant cadence. In this experiment, Level 7 happened at a rather late stage (when the subject is mostly likely to fatigue). The points for Level 7 show a large scatter, mostly overlapping with the range of Level 5 & 6 and a few in the low effort level range. Generally speaking, the data points spread around the regression line, with an r^2 at 0.568. Comparison between the regression line and 45º line shows that the amplitude of VM increases faster than that recorded for RF at low effort levels (3-4); this leading trend is not so visible at high effort levels. Regression lines are then fitted to each effort level for each muscle pair. The r and r^2 of each effort level for different muscle pairs are summarised in Table 5. 6. High effort levels seem to have a tendency of low r^2 as yellow highlighted, which indicates more spread at these effort levels. The two effect levels where the cadence are affected are marked in grey.

Table 5. 6: The r and r^2 for each effort level of the three muscle pairs for Subject 1.

Combinations	Effort Level 3	Effort Level 4	Effort Level 5	Effort Level 6	Effort Level 7
RF&VM r	0.619	0.601	0.474	0.276	0.456
RF&VM r^2	0.383	0.361	0.225	0.076	0.208
VM&VL r	0.457	0.356	0.642	0.351	0.207
VM&VL r^2	0.209	0.127	0.413	0.123	0.043
RF&VL r	0.519	0.403	0.495	0.225	0.482
RF&VL r^2	0.27	0.193	0.245	0.051	0.232

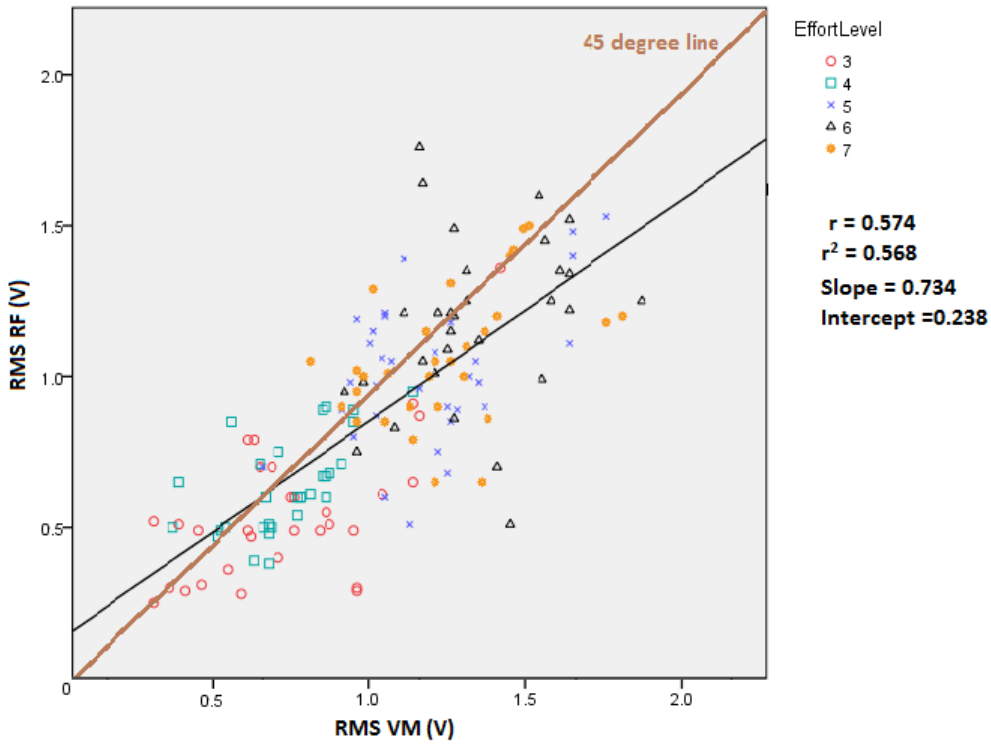

Figure 5. 32: RMS RF Vs. RMS VM for one subject at five effort levels. The black line is the linear regression line and the brown line is the 45º line. The slope and intercept of the regression line as well as the r and r^2 are also shown on the right of the graph.

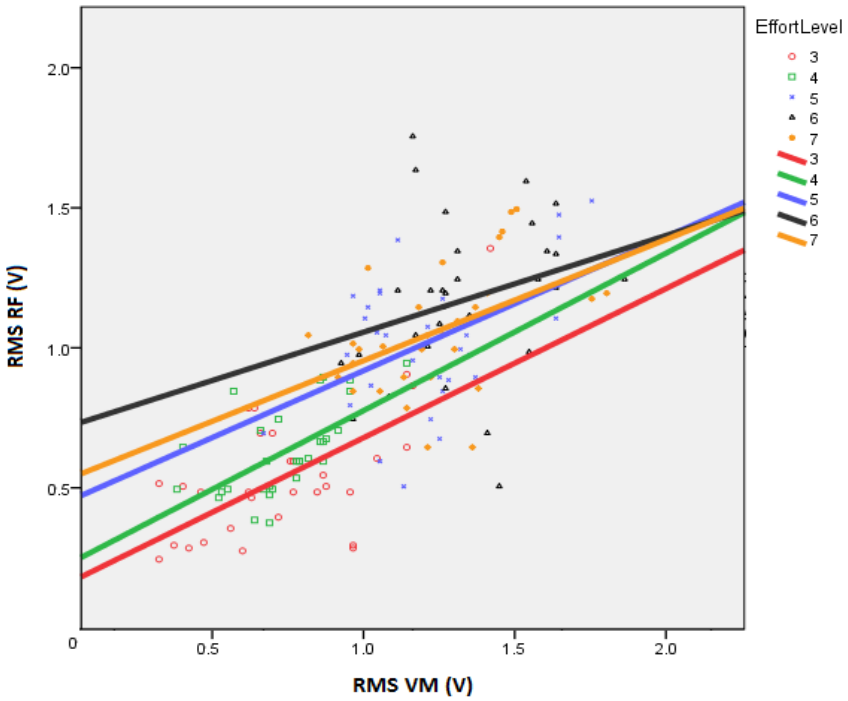

Figure 5. 33: RMS VM Vs. RMS VL for one subject at five effort levels with lines fitted at different effort levels.

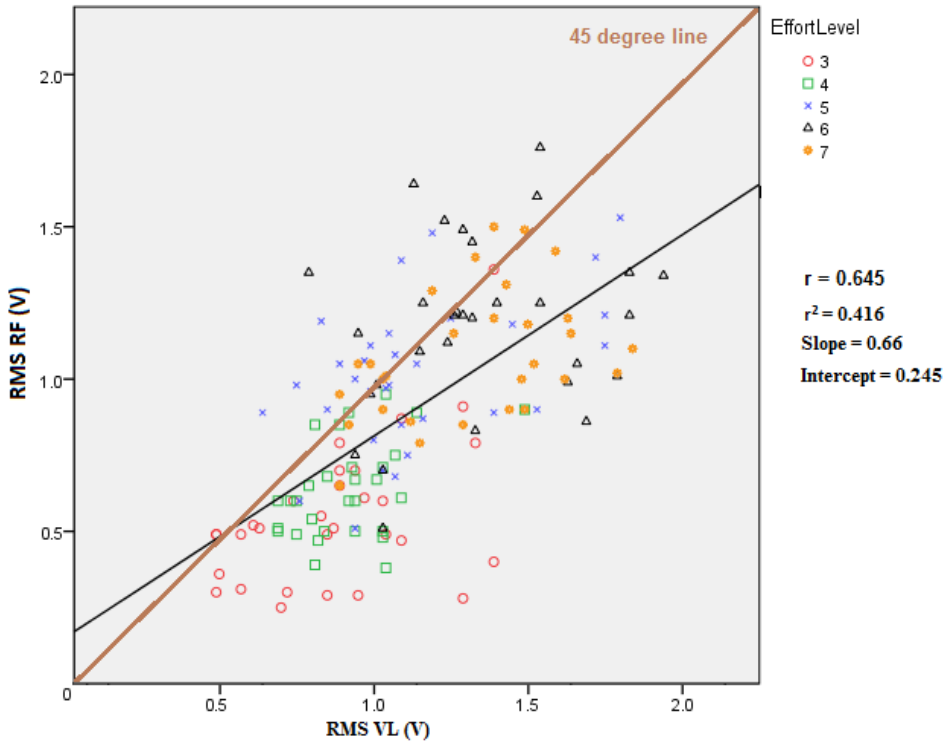

Figure 5. 34： RMS RF Vs. RMS VL for one subject at five effort levels, with overall regression line.

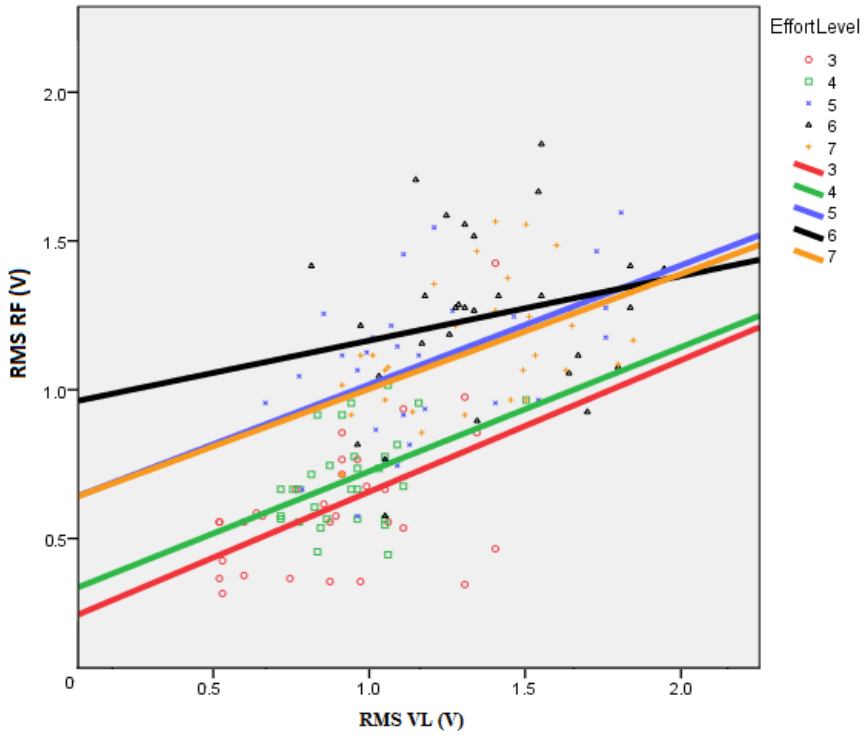

Figure 5. 35: RMS RF Vs. RMS VL for one subject at five effort levels with lines fitted at different effort levels.

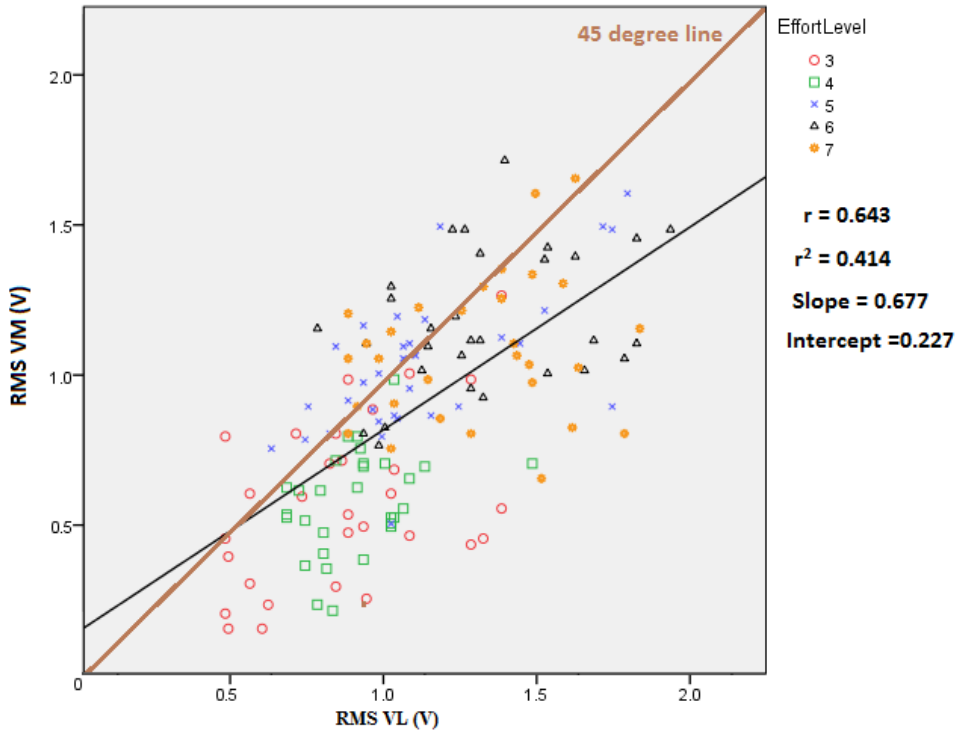

Figure 5. 36: RMS VM Vs. RMS VL for one subject at five effort levels, with overall regression line.

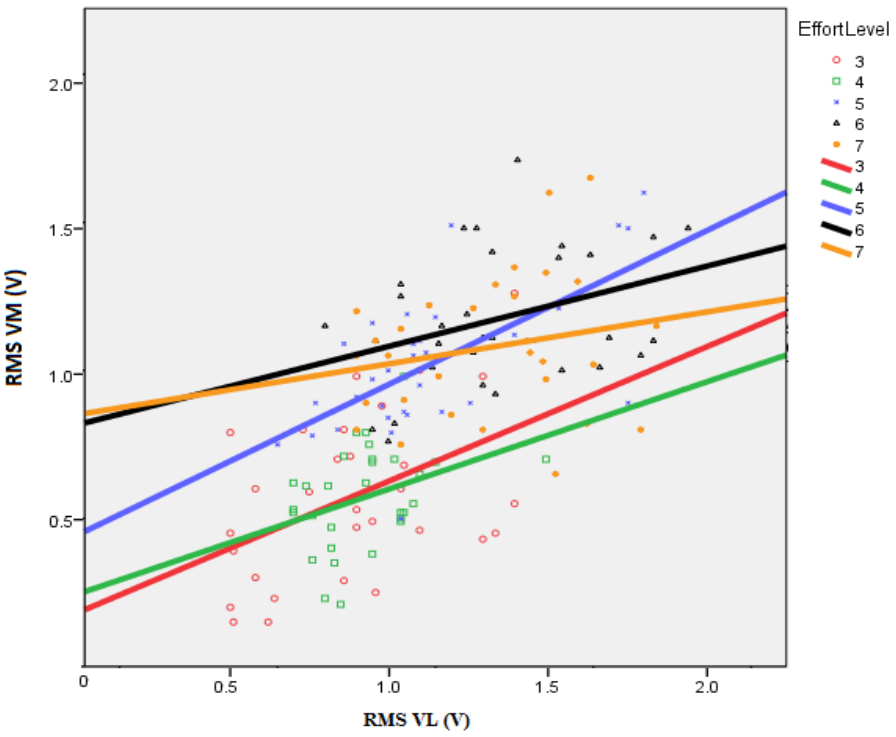

Figure 5. 37 RMS VM Vs. RMS VL for one subject at five effort levels with lines fitted at different effort levels.

Comparing the RMS EMG of three muscles with one muscle

An aim of this experiment was to find out if averaging the RMS EMG of all three quadriceps muscles would enhance the relationship of RMS EMG with effort levels. Figure 5. 38 shows the averaged RMS EMG at different effort levels and Figure 5. 39 shows the mean of the averaged RMS EMG against effort levels.

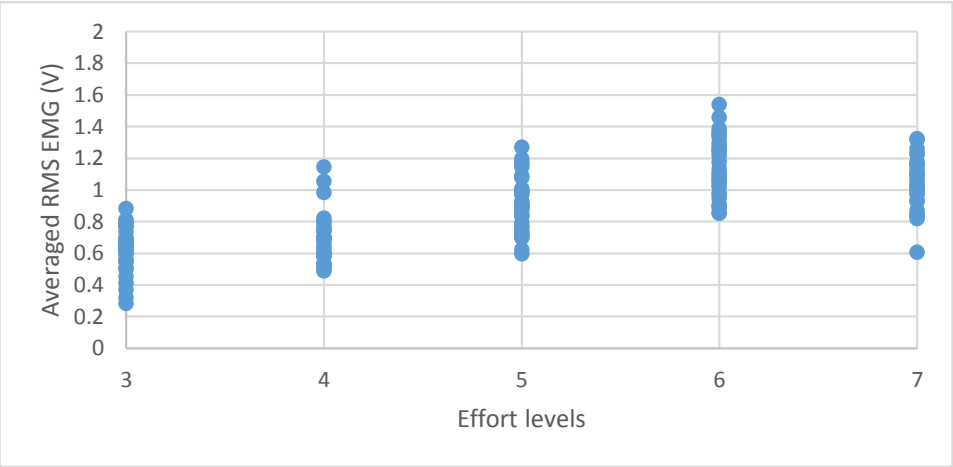

Figure 5. 38: Averaged RMS EMG against effort levels.

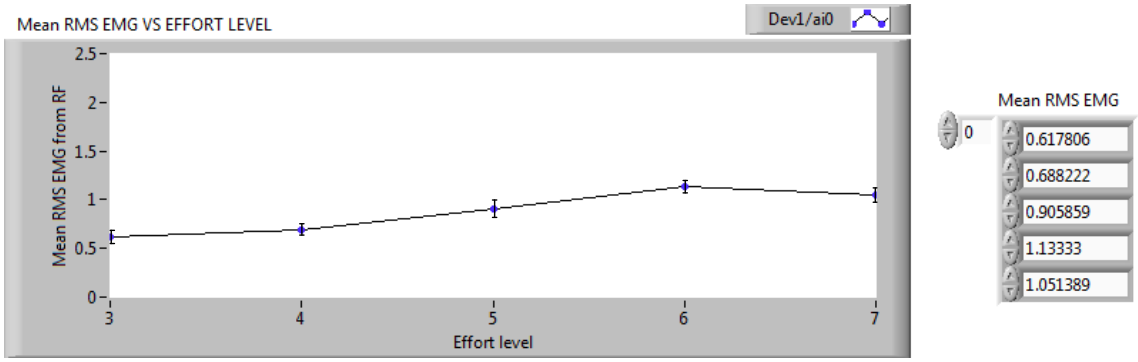

Figure 5. 39: The mean RMS EMG from three muscles against effort levels.

Table 5. 7 summarises the mean and SD of the muscles. A reduced SD is seen at the overall muscles. The coefficient of variation (CV), which is defined as the ratio of the standard deviation to the mean, is used here to describe the variation of the RMS EMG around its mean. CVs are calculated for the individual and the averaged muscles as shown in Table 5. 7.

Table 5. 7: The mean, SD and CV for each muscle and for the averaged three muscles

		Effort level				
		3	4	5	6	7
RF	mean	0.49	0.61	0.98	1.07	1.03
	SD	0.17	0.15	0.23	0.38	0.26
	CV	0.35	0.24	0.24	0.35	0.25
VM	mean	0.59	0.53	0.90	1.12	0.96
	SD	0.26	0.19	0.21	0.26	0.24
	CV	0.45	0.37	0.23	0.23	0.25
VL	mean	0.78	0.93	0.84	1.21	1.16
	SD	0.33	0.37	0.36	0.32	0.35
	CV	0.43	0.40	0.42	0.27	0.30
Averaged over three muscles	mean	0.62	0.69	0.91	1.13	1.05
	SD	0.16	0.15	0.20	0.17	0.18
	CV	0.26	0.21	0.22	0.15	0.17
Difference in CV % compare the averaged to invidual muscle	Min	25%	12.50%	8%	34%	8%
	Max	42%	47.50%	47.60%	57%	43%

5.6.5 Discussion

Experiment 4 attempted to answer the following questions:

How closely are the three muscles working together during cycling?

It is reasonable to think that the subjects may change their use of the muscles during cycling especially when they become tired. That was why orthoses were used in Experiment 4 to constrain the low leg muscles and the ankle movement of the subjects, thereby leaving us only a few possible muscles to investigate. Here the RMS EMG amplitudes of other quadriceps muscles, VM and VL were also plotted together with RF. The RMS EMG data (refer to Figure 5. 25 to Figure 5. 27) showed that, for the same subject, the RMS EMG from the three muscles mostly followed the changes in the effort levels, with some variations at the same effort level and overlap between different effort levels. This was even clearer if we plot the mean RMS EMG with SD bars as in Figure 5. 29 –Figure 5. 31. It is important to know how closely these muscles work together. This is achieved by calculating the r between each pair. Inspection of the three muscles show similar amplitudes for the three muscles with moderate r values around 0.7. When the subject loses his cadence, the amplitudes of the muscle pairs both reduced which suggests that they are affected in the same way. Table 5. 6 show that the data points are likely to be more spread at high effort levels. There is no sign of difference in the dispersion of the data points (SD) when the subject loses his cadence (marked in grey).

Can the unsteadiness and spread be reduced by combining the RMS EMG from multiple muscles?

The conclusion from Experiment 3 is that there is too much variation in RMS EMG of RF at the same effort level. We might need to consider using RMS EMG from multiple muscles instead. To investigate this two other quadriceps muscles, VM and VL, were selected. Despite the fact that these muscles are co-contracting, there is sometimes more variation in one muscle than

the others, which may indicate that they are not always used in the same proportion. However, the spread of the RMS EMG are quite different for the three muscles at the same effort level. This was seen across the results of all 5 subjects.

The averaged RMS EMG amplitudes still overlaps with each other at different effort levels as seen in Figure 5. 38. Although in general an increasing trend is shown in Figure 5. 39 (except Level 7 which could be affect by the loss of cadence and fatigue). There is still little variation between the amplitudes of the mean values at different effort levels, which is similar to the individual muscles. An 8% -57% reduction in CV is found when comparing the averaged RMS EMG to that of an individual muscle. This indicates that the randomness in the RMS EMG is reduced when averaged over three muscles. However, the overlap in the RMS EMG makes it difficult to estimate an effort level accurately. Therefore using RMS EMG from multiple muscles to help with the estimation of the effort level is not feasible.

5.7 Experiment 5: Investigation on the contralateral legs

5.7.1 Aims

We have shown, in the previous experiments, the characteristics of RMS EMG of quadriceps muscles of one leg changes with effort levels during cycling. Experiment 5 aims to investigate if there is any difference in the contralateral leg.

5.7.2 Experiment procedures

The subjects were asked to cycle at constant cadence at 60rpm for 2.5 minutes. EMG was recorded from contralateral RF of the subjects. A same effort level sequence 4-3-5-7-6 was used for all five subjects.

5.7.3 Results and Data analysis

The LABVIEW program used to analyse the data was modified from the program used in 5.3.4. Figure 5. 40 shows the RMS EMG amplitudes changes with effort level for all five subjects and the slope of the shaft encoder (hence the cadence) is shown in Figure 5. 41. A different approach is used to examine the similarity between the RMS EMG in contralateral legs. As EMG measured at successive times— a sampled EMG signal can be considered as a discrete time series (when the observations of data are taken at specific times, usually uniformly spaced), cross-correlation is used to compare the similarity of the two signals.

Cross correlation

The cross correlation function is a measure of the similarity between two data sets (Shaw & McEachern, 2013). One set is shifted relative to the other and the corresponding values of the two sets are multiplied together, before they are summed to give the value of the cross-correlation (see Equation 6).

$$\emptyset_{xy}(\tau) = \sum_k x_k y_{k+\tau}$$

Equation 6: The cross correlation formula.

The cross correlation is large when the two data set are nearly the same. When the data sets are unlike, some of the produces will be positive and some negative, and hence the sum will be small. Figure 5. 42 shows the cross-correlation of the RMS EMG measured from contralateral RF for one subjects. The cross-correlation is high (above 0.9) when there is 0.5s shift to the positive side. When the subject is cycling at 60rpm, time to complete a revolution is roughly 1s. Therefore it makes sense that the patterns of the RMS EMG from the two legs are most alike when they are 0.5s apart. The cross correlation for all five subjects are summarised in Table 5. 8.

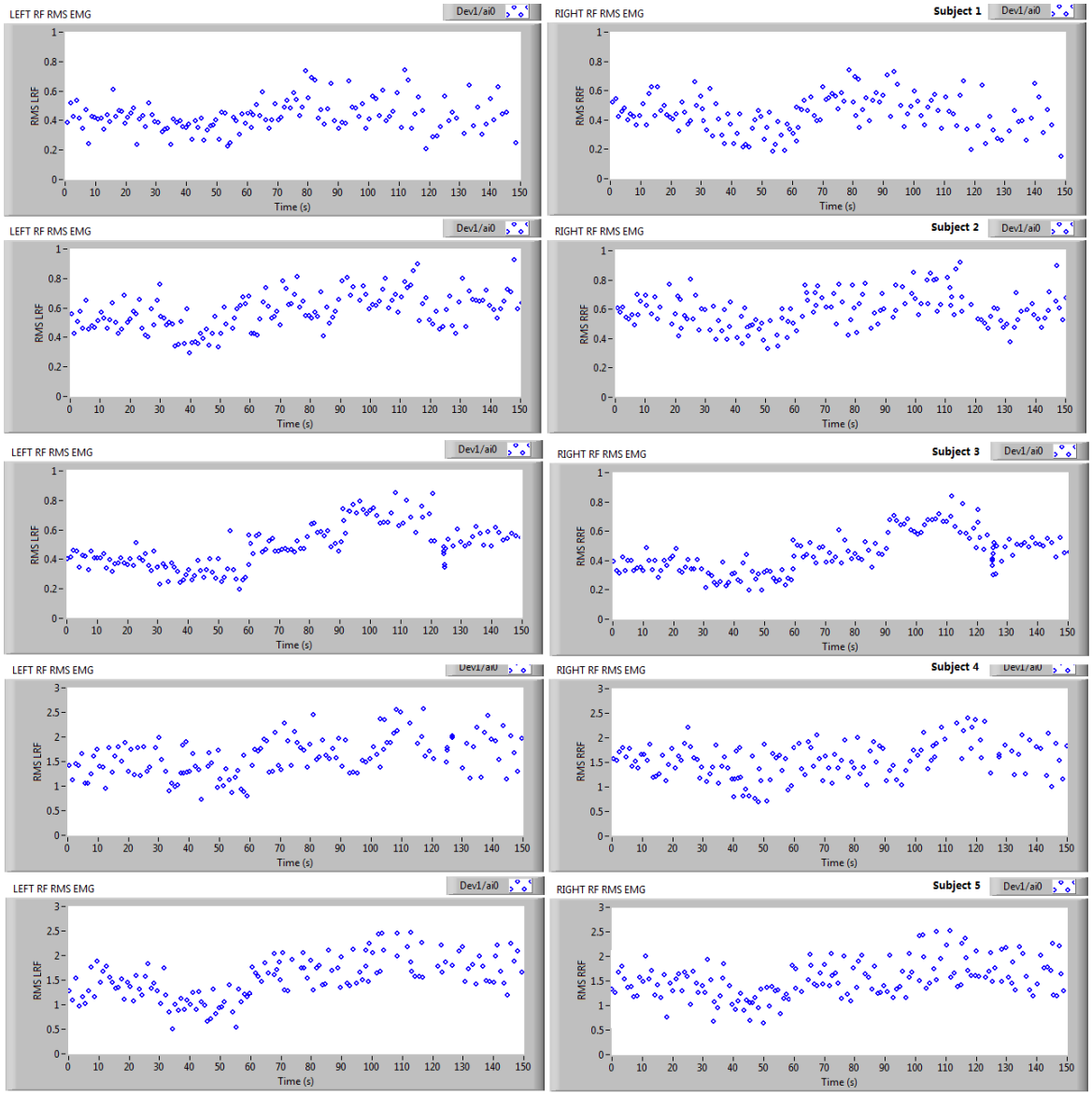

Figure 5. 40: RMS EMG from contralateral RF during 2.5mins of cycling for five subjects.

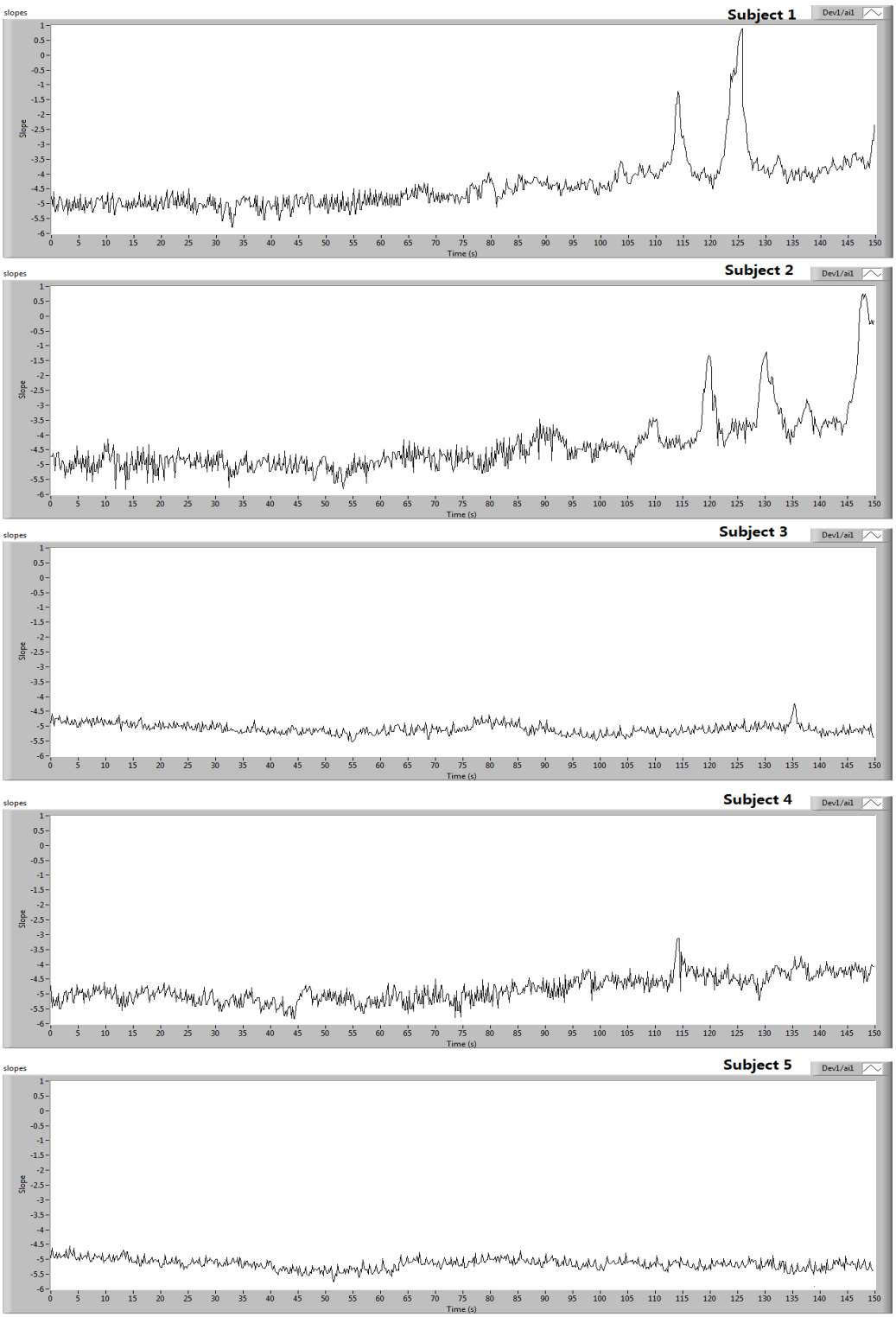

Figure 5. 41: Slope of shaft encoder signal for all five subjects.

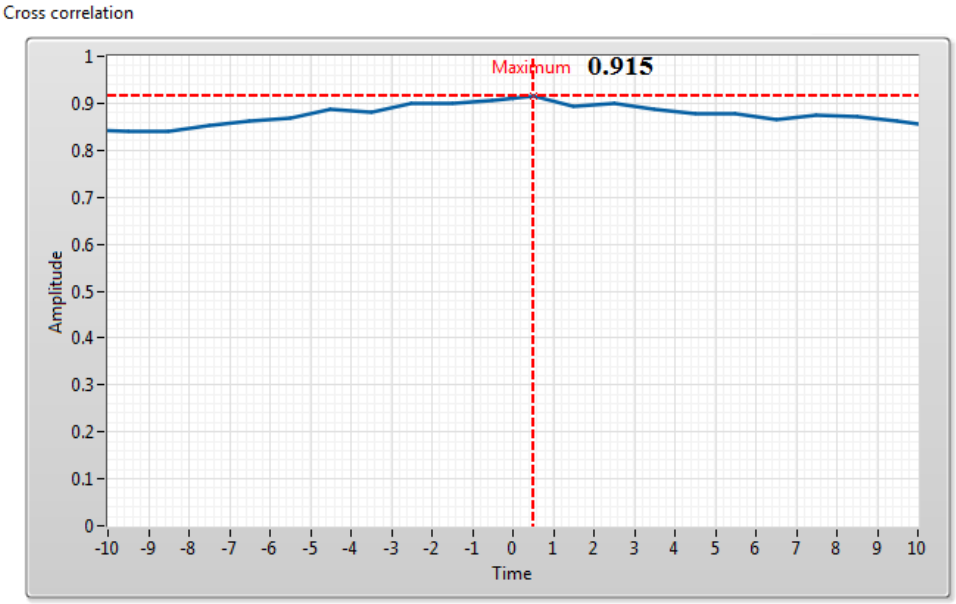

Figure 5. 42: cross correlation of RMS EMG of contralateral legs for one subject.

Table 5. 8: Cross correlation for the contralateral RF of five subjects.

	Subject 1	Subject 2	Subject 3	Subject 4	Subject 5
Cross correlation	0.915	0.928	0.979	0.961	0.977

5.7.1 Discussion

The cross-correlations in Table 5. 8 are all above 0.9. The high cross-correlations indicate that the RMS EMG from the contralateral legs are of very similar shapes for five subject, i.e. the subjects were using the muscles from both legs in a very same manner. Variations in slopes are seen in Figure 5. 41, especially in the last 1 minute for Subject 1 and 2. Because of their level of fitness, the two subjects tend to fatigue quickly than the others (see 5.5.4). The RMS EMG of the two legs were consistent both when the subject is cycling at the constant cadence and when they were fatigued. This could also be seen from the RMS EMG plots in Figure 5. 40. There is no evidence to support that the two legs are used differently when the subjects are fatigued. The results found in the all the experiments we did on one leg still hold for both legs.

5.8 Discussion

5.8.1 The three questions

In the beginning of this chapter, we asked ourselves three questions which would lead us to the conclusion whether or not we could use RMS EMG calculated from a short time window as an estimation of the voluntary drive.

1) Can a control signal be extracted from the EMG to represent the voluntary drive?

2) How is the extracted signal related to the effort the subject is making?

3) Can we show that the control signal we find is a good estimation of the voluntary drive?

The first two questions were tackled in this chapter through four experiments (Q1 experiment 1, 2; Q2 experiment 3, 4). We did not proceed with the last question which would lead to a further evaluation of the RMS EMG as a control signal, because of the unsatisfactory results obtained for Q2.

5.8.2 Experiment 1& Experiment 2

Experiment 1 and 2 aim to find the relationship between post and pre-stimulus EMG amplitudes without and with stimulation. The significance of the relationship could help us to determine whether the post-stimulus amplitude is a good estimation of the pre-stimulus amplitude. The RMS EMG amplitudes were calculated from 40ms windows during the muscle activation range. In both experiments, the pre-stimulus window was chosen to be just before the stimulus; and the post-stimulus windows were chosen to be ranging from 0ms-70ms after the stimulus. Correlation coefficient r, coefficient of determination r^2 and the p values were used to evaluate the significance of the relationship.

Without stimulation, the correlation coefficients are generally higher than those with stimulation. The correlation coefficients are high especially Window 0. This could be one of the reasons that the R square values of post-stimulus EMG amplitude to the pre-stimulus EMG amplitude in these windows are lower. The major differences occur in two window ranges: Windows 0-15 and Windows 45-65. Low r values are found in Windows 5-15 when there is stimulation. One possible assumption is that there are some minor persisting influences from the stimulation artefact and the M wave after the blanking period and the recorded EMG signal is therefore contaminated. In the literature, some researchers have assumed M wave to be a stationary and removed it by simply extending the blanking period or used a fixed comb filter (Crago et al., 1991; Peasgood et al., 2000). But the M-wave is clearly a non-stationary signal in a statistical sense, mainly due to the fact that its temporal variation depends on many factors, such as stimulation intensity, fatigue, the contraction level of the muscle, etc (Merletti et al., 1992). Thus, it is not appropriate to use the windows immediately after the stimulation for the estimation.

The differences in Windows 45-65 could originate from other physiological effects that happen after the stimulation (see 3.6). These muscle reflexes, namely H reflex and F reflex, result in decrement in 4 out of 5 subjects in these windows, while only Subject 4 is not affected. Among the five subjects, Subject 4 seems to behave differently from the other subjects in some windows, both with and without stimulation. However, we do not have enough information to answer the question why his results is different from the others. In summary, the stimulation reduces the correlation coefficient between the post and pre-stimulus amplitudes. To give the

most reliable estimate of the effort of the subject (pre-stimulus amplitude) from the post-stimulus amplitude, windows starting 20-40ms after the stimulation could be selected.

How reliable the estimations are?

We have proven that the post-stimulus amplitude is highly correlated with the pre-stimulus amplitude using r. r^2 were also obtained when comparing the post-stimulus amplitude with the pre-stimulus amplitude with various delays. In one way, it provides information on the spread of the data points along the regression line (see 5.3.5). Another interpretation of the r^2 (range 0-1) is that it gives the proportion of the fluctuation of one variable that is predictable from the other variable. Take one result from Experiment 1 for example, r^2 is 0.7477 for Subject 1 Window 0. We can make the following statement: when predicting the pre-stimulus amplitude with post-stimulus amplitude, 74.77% of the total variation in the pre-stimulus amplitude can be explained by the relationship between them, the remaining 25.23% is unexplained (Steel & Torrie, 1960). The question is then asked: "What's a good value for r^2?" Sometimes the claim is even made: "a model is not useful unless its r^2 is at least x", where x may be some fraction greater than 50%. In other cases, for example, the prediction of the next season sale an r^2 is less than 25%, but that is considered as a good estimation. The correct way of interpreting r^2 depends on the case itself. In our case, it is hard to define an r^2 as a standard.

The use of finite window

The choice of 40ms for the windows was arbitrary but is a compromise between the interpulse interval and the estimation error (see Equation 5). Increasing the window length reduces the error slowly, for example, had we doubled the length to 80ms, the theoretical error would only fall from 11 to 8%.

5.8.3 Experiment 3, 4, 5

To be an effective measure, the RMS EMG amplitudes should accurately reflect the effort of the subject. The slopes of the mean RMS EMG amplitudes are shallow compared to the effort level change from 3-7. (Note the mean RMS EMG Vs. effort levels graphs were not plotted in the most justified manner, as the x-axis considers effort levels as numbers 3-7, therefore the graphs appeared to be stretched).

Variations in the RMS EMG

The measured RMS EMG and force relationship suffers from variability as discussed in 3.8. The muscles we measured from are large leg muscles with agonist-antagonist muscle interaction during a complex exercise. SEMG is only recorded from the superficial muscles and is affected by the electrode size and the position, which in our case, the recording electrodes (see 4.3.6) used have a recording area of 0.75cm^2. Changes in the motor unit recruitment in the pick up area during the contraction could also contribute to the fluctuations in the EMG amplitude.

The random nature of EMG signal and the fact short time window is used. It has been proven theoretically that increasing the length of the window can moderately improve the accuracy

(5.2.1). However, this is restricted by the finite interpulse interval (50ms for 20Hz stimulation frequency). .

The RMS EMG is also influenced by a change in the cycling style. At higher effort levels, it is difficult for the subjects to continue cycling at the same cadence, the fact that the subjects tries very hard to maintain the cadence might cause him to use other muscles that are involved in the cycling motion but not used that much normally. This might be a problem with AB subjects as it is natural for them to coordinate the muscles without the need to think about it. However, this should not be a problem since the system is targeting the SCI patients who are unable to do this.

Recording from multiple muscles

In Experiment 4, we explore the possible change of muscle coordination during cycling especially when the subjects begin to fatigue. RMS EMG from three muscles RF, VM and VL were recorded and compared to 5 effort levels. At first, a compensation effect of the RMS EMG was expected (see 3.9.2), i.e. for a certain effort level, a decrease in the RMS EMG amplitude for one muscle might be compensated by an increase in that of the other two muscles. Especially when the subjects began to fatigue, as they may have changed involuntarily changed muscle activation. This characteristic was not obvious in the results of this experiment. There is not enough evidence to show that the quadriceps muscles which work together in the pushing phase of the cycling have any compensation effect on each other when the subjects are fatigued.

By recording from multiple muscles, we could effectively reduce the dispersion of the data points as shown in Table 5. 7. However, the averaged RMS EMG still overlaps at the different effort levels. It is difficult to tell the effort level correctly from the RMS EMGs. Therefore the idea of using RMS EMG from multiple muscles (at least the ones we selected) to provide an accurate estimation of the voluntary drive is not practical.

Evaluate it as the control signal

We have concluded that the RMS EMG amplitudes from short time windows are not appropriate as an estimation of the voluntary drive of the subjects during cycling. The poor steadiness and overlap of it change with effort level have stopped it from being a reliable control signal. Such a sampling method in the time domain therefore may not be suitable for this project.

5.8.4 Experiment limitations

The effort levels used as an indication of power output, throughout the thesis, were measured using the cycling computer connected to the ergotrainer. However, these effort levels, as set by the ergotrainer company, does not reflect the true power output of the subjects. As the subjects start to pedal, their instantaneous power output is constantly changing. It is also unnatural to force the subjects cycling at a fixed cadence. By doing so we may accelerate the fatigue process. The effort levels can be a useful representation of the situation at this stage，

however, the large variations seen in the RMS EMG for the same effort level in Experiment 3-5 could be due to the unstable power output. It would be more accurate and informative if we could measure the power output with a more suitable apparatus. It can improve the time domain method by replacing the effort levels with more accurate assessment of the power output. See 8.6.1 for more details.

5.8.5 Possible improvement to the experimental setup

The design parameters we could improve in future experiments contain both experimental setup and subject recruitment. To start with, the variable that was chosen to represent the power output, the effort level, should be reconsidered. The effort level is set by the GrandExcel cycling computer, which is a commercial product that is not made for experimental purposes. Its accuracy has not been experimentally tested. Therefore it is better to replace it by a proper power transducer that could measure the instantaneous output power instead. Furthermore, the experiment setup requires the subjects to cycling at a constant cadence, which is a rather unnatural way of cycling. It is set that way so that with constant cadence and resistance applied to the back tyre, the output power should stay relatively constant. Therefore we could evaluate the change in RMS EMG relative to a constant power output. The power output, with the irregular cadence obtained, was actually not constant, therefore the variations seen in the results of Experiment 3 and 4 could be due to the unstable cadence. The problem could also be solved by careful subject selection. A small number of subjects were used in this project. For most of the experiments, five subjects were used, and, in some occasions four. These subjects had no experience of constant cadence cycling prior to the experiments, therefore training was needed before the formal trials. However, most of them (4 out of 5) were found unable to complete the cycling trials with stable cadence. It is not only that unnatural way of cycling could induce early muscle fatigue (see 3.9), but also the subjects, being recruited randomly, bear different fitness levels. The unstable cadence might be the main reason of the variations seen in Figure 5.18 and Figure 5.25-27.

It is difficult to judge the success of the time domain method, as it might actually be working only require different experimental setup – otherwise we wouldn't be seeing the rend of mean RMS EMG amplitudes following the effort level change but with shallow slopes (Figure 5.20 and Figure 5.29-31). Either using a different experimental setup (free cadence cycling) or by recruiting only professional cyclists for experiments, we could then re-evaluate the relationship between RMS EMG amplitudes and power output.

CHAPTER 6: ESTIMATION OF VOLUNTARY DRIVE USING COHERENCE

6.1 Introduction

The term coherence has been used in the literature to refer to different topics (Marple & Marino, 2005). It was used in optics to describe how waves can interfere with one another (Drude, 1902). Two waves are said to be coherent with each other, either because they come from the same source or because they have the same or nearly the same frequency (Challis & Kitney, 1990). The phases of the two waves must either be exactly the same or with a constant difference for them to be coherent. Coherence was first used in signal processing around 60 years ago (Brazier & Casby, 1952). The power spectral density describes the power distribution of a signal at different frequencies, where coherence can be used to define the narrowband power spectral density ratio between two signals (Brazier & Casby, 1952). Since then, coherence has been widely used in the signal processing field as a statistical tool that examines the relation between two signals or data sets. From the early 1990s, coherence began to be used to study the origins of the rhythms found in brain signals by analysing the coherence found in biological signals including EEG-EMG (electroencephalographic–electromyographic, i.e. electrical measurement of the brain activity–muscle activity), MEG-EMG (magnetoencephalographic-electromyographic, i.e. magnetic measurement of brain activity-muscle activity), and EMG-EMG during specific tasks (Hamm and McCurdy 1995; Conway et al., 1995; Amjad et al. 1997; Baker, Olivier, and Lemon 1996; Kilner et al. 1999). There is an increasing interest in this area in the last 10 years trying to understand more about this phenomenon (Cordivari et al., 2002; Farmer et al., 2007; Grosse et al., 2002; Kilner et al., 2000; Norton & Gorassini, 2006; Norton et al., 2004; Norton et al., 2003).

In this chapter, a new myoelectric signal measuring technique using coherence is introduced. Coherence, which here measures the similarity between EMG signals recorded from two muscles in the frequency domain, can be used to infer information concerning the neural drive to a given pair of muscles (Nielsen, 2002). The frequencies at which coherence occur provide information about the source of drive to these synergistic muscles. Synergistic muscles are groups of muscles that work together to produce the same movement (Nigg et al., 2000). The frequencies of interest are the brain waves at frequency below 100Hz. These brain waves are often divided into three bands: the α band, the β band and the γ band (see Table 6. 1). Among the three bands, the β-band of the coherence spectrum is of particular interest for this project because it represents the cortical drive to the muscles (P. Brown, 2000). Direct confirmation of this came from studies of MEG-EMG and EEG-EMG coherence which show that the cortical signal recorded from over primary motor cortex is coherent with the muscle signal at around 20Hz (Conway et al., 1995). Therefore the coherence measured between co-contracting muscles during common motor tasks can be used as an estimation of the common voluntary drive to these muscles.

Table 6. 1: The frequency bands of brain signals below 100Hz, generated from (Başar, 1998)

Band name	Frequency range(Hz)	Origination	Characteristic
α	8-15	Occipital lobe	Can be detected during wakeful relaxation with closed eyes, the magnitude reduces with open eyes, drowsiness and sleep
β	15-35	Motor cortex	Can be detected during low to medium muscle contractions, very sensitive to movement changes
γ	35-100, with the lower frequency 30-60Hz as the Piper rhythm	Motor cortex	Can be detected during maximum voluntary contractions of muscles

The hypotheses

We propose to use EMG-EMG coherence between synergistic muscles as a possible input to the controller of our FES cycling system. Two hypotheses were made:

No stimulation: we hypothesise that coherence between two synergistically activated muscles during cycling is related to the voluntary drive. Coherence can serve as a measure of voluntary drive when there is no stimulation in cycling.

With stimulation: The most challenging part of using the subject's voluntary drive to control the stimulation of FES cycling is how to remove the influence of the stimulation artefacts in the EMG measurement. So the second hypothesis is: The EMG-EMG coherence can be extracted as a control signal during FES cycling without the influence of the stimulation artefact. The first hypothesis must still hold when there is stimulation.

Motivations

There was a lot of interesting research using EMG-EMG coherence in the early 2000s. Kilner investigated the coherence between hand muscles during holding phase of precision grip, and found the coherence peaks between 18.5-25Hz for this task (Kilner et al. 2003). Norton looked into the coherence between leg muscles during stance phase of treadmill walking sessions for SCI patients to find signs of recovery related to an increase of the coherence (Norton & Gorassini 2006). However, there has not been a research on EMG-EMG coherence for FES cycling. In this chapter, coherence in different muscle combinations during cycling is studied without and with stimulation.

6.2 Coherence

6.2.1 The basics

Coherence can be used to examine the relation between two time series in the frequency domain. The coherence analysis can identify variations in the data which have similar spectral properties, e.g. high power in the same spectral frequency bands. The coherence C_{xy} between two signals x and y is defined as follows:

$$C_{xy} = \frac{|G_{xy}|^2}{G_{xx}G_{yy}}$$

Equation 7: The coherence calculation

Where G_{xy} is the cross-spectral power density between x and y, and G_{xx} and G_{yy} are the power spectral density of x and y respectively (Amjad et. al 1997). The cross-spectral power density is the Fourier transform of the cross-correlation function of x and y. In signal processing, cross-correlation (see 5.7.3) is a measure of the similarity of two signals x and y as a function of time lag applied to one of them.

To calculate the cross-spectral power density and the power spectral densities, Bartlett's method is used. It is a way of estimating power spectra in the following steps:

1. The data clip contains N data points is split into L data segments each length T

2. Compute the discrete Fourier transform of each segment, then computing the squared magnitude of the result and dividing this by T.

3. The results are then averaged for the L data segments.

The power densities G_{xx} and G_{yy} describe how the power of the time series is distributed in frequency domain. They are the Fourier transform of the autocorrelation function. The autocorrelation is the cross-correlation of a signal with itself with a delay. Given a signal f(t), its cross-correlation with a delay of τ is

$$\boldsymbol{R(\tau) = \left(f(t) * \overline{f(-t)}\right)(\tau) = \int_{-\infty}^{\infty} f(t+\tau)\bar{f}\,(t)dt = \int_{-\infty}^{\infty} f(t)\bar{f}\,(t-\tau)dt}$$

Equation 8: The cross correlation equation

where $\bar{f}$ represents the complex conjugate and * represents convolution.

Coherence values vary between 0 and 1. Unity indicates that x and y have a constant phase difference at that frequency, and a 0 shows that x and y are completely unrelated. Any value between 0 and 1 indicates that y is not entirely related to x, instead y will have some relationship to the presence of other variables or noise in the system.

Coherence should only be used for stationary data due to the nature of the Fourier transform involved in the analysis. Therefore data collected at the starting and stopping sector of muscle contraction, in which the data changes rapidly, should not be included. Coherence is strongest during a steady state contraction, hence in the initial recording, we are just aiming for a steady state contraction rather than one in which the contraction level changes.

6.2.2 Pooled coherence

As mentioned before, coherence analysis works better with the "hold" phase of the movement and it is difficult to perform it on short segments of data. For fast-changing movements like walking or cycling, there are not enough quasi-stationary EMG data within one revolution and the region of muscle co-activation is very short. One solution is to combine the EMG data from many revolutions which then will give us enough data to generate meaningful coherence. This method is called "pooled coherence" (Amjad et., al, 1997; Halliday & Rosenberg, 2000).

Pooled coherence was firstly proposed by Amjad in his study of motor units and physiological tremor (Amjad et al., 1997) followed by a paper by Halliday (Halliday et al., 1999). It was originally used to combine calculation of coherence from multiple experiments. The technique selects partial data from each experiment and then divides it into several sections each of the same length before joining them together. The new problem is that when combining the EMG data from many revolutions, there are discontinuities at the boundaries of the data. To solve this problem, the data is passed through a window first and then concatenated. Note that here the term "window" is a signal processing technique, not the same as the windows (time intervals) used in Chapter 5.

6.2.3 The use of window functions in coherence

Windows are used in signal processing to supress glitches in the spectrum caused by passing the signal through a Fourier Transform. The frequency response of a window function constitutes a main lobe and some side lobes. Figure 6. 1 shows the typical frequency response of a window function. The width of the main lobe, which is defined as the measure of the main lobe width at -3dB or -6dB below main lobe peak, determines its frequency resolution, i.e. the ability of selecting finest frequency components. Side Lobe Level is the height of the side lobe with the maximum peak. It is measured in decibels relative to the peak of the main lobe. In general, lower side lobes reduce the leakage in the measured FFT but increase the bandwidth of the major lobe. The side lobe roll-off rate is the asymptotic decay rate in decibels per decade of frequency of the peaks of the side lobes (Cerna & Harvey, 2000).

The lobes are a result of spectral leakage which occurs when performing a frequency analysis on a finite-length signal (Lyon, 2009). Each frequency component of the signal should contribute only to one single frequency of the Fourier Transform, but spectral leakage causes some energy to spread and leak out of the original signal into other frequencies. To minimise the effect of spectral leakage, three features are essential to a window function:

1) Main lobe width is small.

2) Side Lobe level is low.

3) Side Lobes fall-offs rapidly

Three typical window functions that fit the requirements are shown in Table 6. 2.

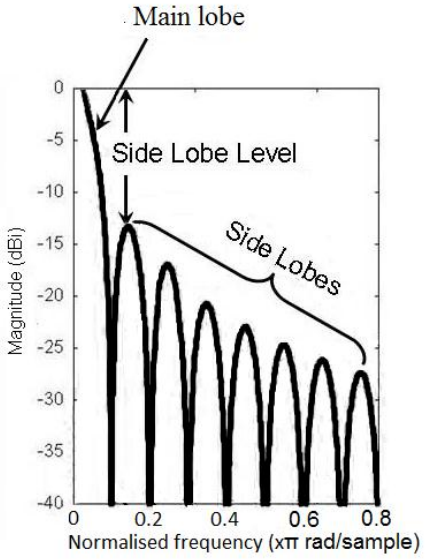

Figure 6. 1: A typical frequency response of a window function (a rectangular window was used as an example).

Table 6. 2: Features of three typical window functions.

Window	Main lobe bandwidth (3dB)	Side lobe level (dB)	Side lobe fall-off (dB/oct)
Rectangular	0.896	-13	-6
Hanning	1.472	-32	-60
Tukey (Default α =0.5)	1.344	-14	-18

The three windows

The rectangular window is the simplest window, equivalent to replacing all but *N* values of a data sequence by zeros, making it appear as though the waveform suddenly turns on and off. The Hanning window (or Hann window) is defined as

$$w(n) = 0.5\ \left(1 - \cos\left(\frac{2\pi n}{N-1}\right)\right)$$

Equation 9: The Hanning window function.

N represents the width, in samples, of a discrete-time, symmetrical window function *w*(*n*). *n* is an integer, with values $0 \leq n \leq N-1$. The ends of the cosine just touch zero, so the side-lobes roll off at about 18 dB per octave.

The Tukey window is also known as the tapered cosine window. It can be regarded as a cosine lobe of width $\frac{\alpha N}{2}$ that is convolved with a rectangle window of width $\left(1 - {}^{\alpha}/_{2}\right)N$, where α is the ratio of taper to constant sections and is between 0 and 1. At α = 1 it becomes a Hanning window and at α=0 it becomes a Rectangular window; the default value is *α*=0.5 (Harris, 1978).

Using the window design and analysis tool in MATLAB, the three windows were plotted in both time domain and frequency domain. It is easy to see the cut off of these windows.

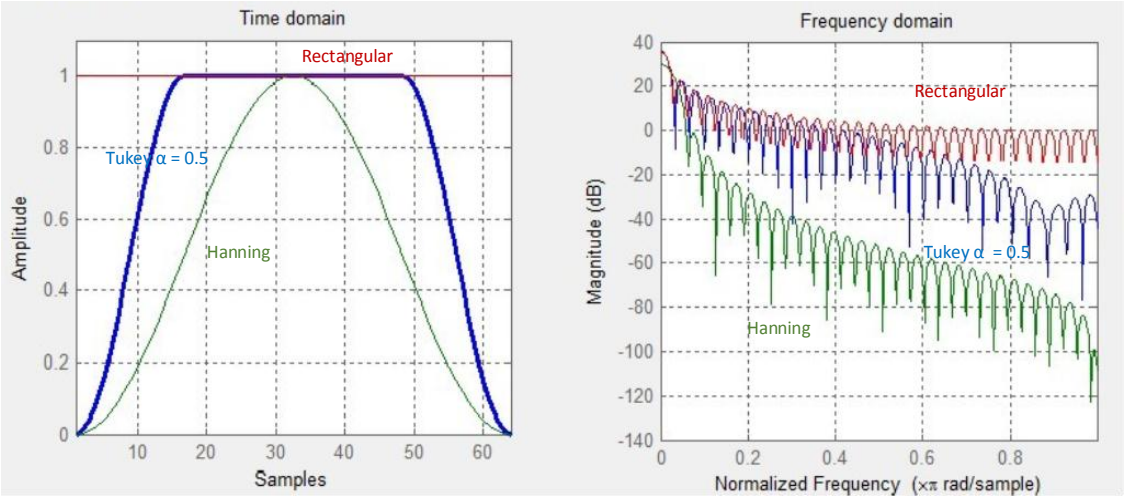

Figure 6. 2: The window function and frequency response of the three selected windows.

These windows were chosen because they have fairly low side lobe values and relatively fast side lobe fall-off rates. However, these are not the only features we were looking for. The windowed data would be used for further analysis, and for this experiment, since we were only selecting a short segment of data from every revolution and we were in need of rapid accumulation of data to get an early coherence calculation. Therefore we would want to preserve as much useful data as possible within the window. The rectangular window is the best in this manner, but it does not provide enough smoothing at the boundaries of the windows. When joining the data segments together, the discontinuities at the boundaries of the data segments are spaced equally in the data set (same segment length). Therefore these discontinuities, when performing the pooled coherence analysis, will result unwanted peaks in the frequency domain. This leaves us with the Tukey and Hanning windows. To compare the two windows, the original EMG plot selected from one cycling revolution was passed through different windows as plotted in Figure 6. 3. The Tukey window with α = 0.1 and Hanning window give very similar result; they both retained most of the EMG data yet smoothed the boundaries of the plot. The other two Tukey windows (α = 0.3, α = 0.5) cost too much unnecessary data loss compared to the Hanning and Tukey (α = 0.1) windows. The decision between the two windows can be arbitrary as Norton used the Hanning window for his work with EMG data during walking sessions (Norton and Gorassini 2006) but the Tukey window (α =0.1) was used when we worked together in May 2010. It was decided to use Tukey window (α =0.1) for the experiments in this project.

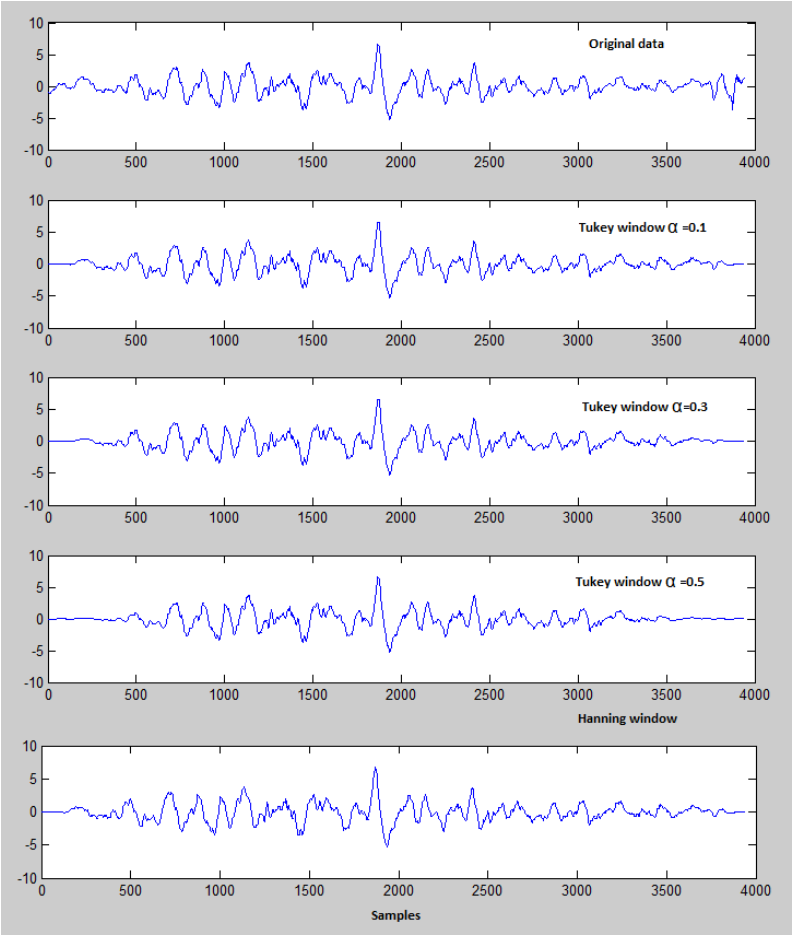

Figure 6. 3: Plot of EMG data through the Tukey windows of different coefficient and the Hanning window.

6.2.4 The MATLAB program for coherence calculation

The MATLAB program used to calculate coherence is a modified version of Neurospec 2.0 developed by David Halliday (Halliday, 2008). The block diagram below shows the flow of the software when used in a cycling experiment.

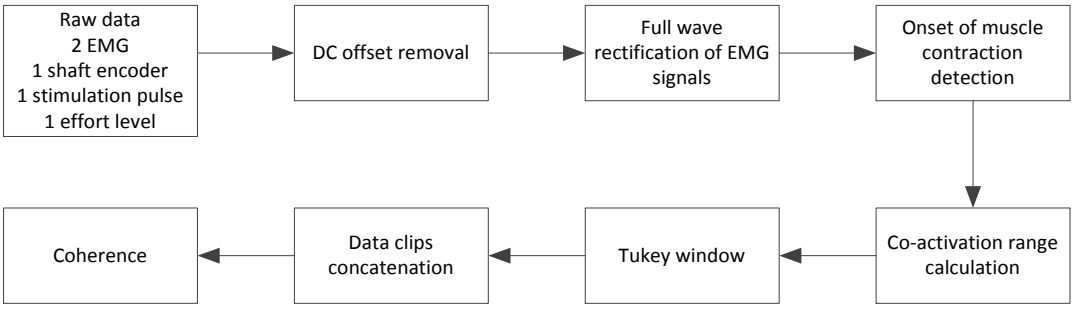

Figure 6. 4: Block diagram of the MATLAB program used for coherence calculation.

This MATLAB program does not run in real time, it reads the data stored in the hard drive and processes it. Prior to carrying out the coherence calculation, some pre-processing is necessary.

Firstly, DC offsets are removed and then the EMG signals are rectified. The raw surface EMG signal with both positive and negative going components contains information about the shapes of the many individual muscle action potentials (Halliday et al. 1995). For the coherence analysis in the frequency domain, full wave rectification can enhance the effect of the timing of the action potentials (Myers, 2003) and no time constant or smoothing techniques should be used to preserve the accuracy of the timing information. There are however, different opinions about performing rectification in the coherence analysis which is discussed in 6.7. Next the co-activation range of the two muscles is calculated based on an individual subject's profile and the selected data from each revolution. (A subject's profile consists of information specific to the subject, namely the coactivation range of the muscles and the thresholds for the control signal) This information is then passed through a Tukey window to smooth the boundaries. The windowed data from each revolution is concatenated to form the input data for the coherence analysis. However, please bear in mind that this window function (the Tukey window in this case) was only used because we were performing "pooled coherence" as mentioned in 6.2.2. When analysing a complete data set, NeuroSpec considers it is not necessary to use the window functions (as in the preliminary experiment in 6.3).

The NeuroSpec 2.0 program follows Bartlett's method (see 6.2) which divides a single stretch of data into L non-overlapping segments each containing T data points (as shown in Figure 6. 5), the total number of data points is N=LT. Only complete segments are analysed, data points at the end of the record that do not make a complete segment are not included in the analysis. Estimates of auto spectra are obtained using the discrete Fourier transform on individual segments and then averaged across segments.

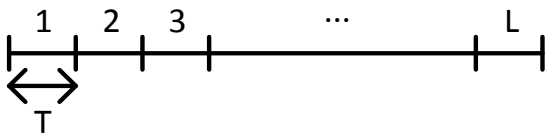

Figure 6. 5: Illustration of analysis in NeuroSpec 2.0

The output from the NeuroSpec program consists of 5 plots, as in Figure 6. 7, including two auto spectra, coherence and phase in the frequency domain, and the cumulant density in the time domain. The coherence plot also comes with a dashed line representing the upper 95% confidence limit. The cumulant density function is defined as the inverse Fourier transform of the cross-spectrum between the two inputs.

Both the phase and cumulant density plots provide timing information between the two muscles, either in phase or in time lag. A non-zero linear phase/time lag at the frequency of coherence peak shows that there is a consistent time difference between the muscles and the

activity does not result from electrical crosstalk (Halliday et al. 1995) as crosstalk would result as zero phase difference between the muscles at all frequencies (Norton et al. 2004).

6.3 A preliminary experiment

6.3.1 Aims

The first experiment was designed to understand the Neurospec software better as well as to find coherence in a simple scenario: during steady holding phase of two muscles' co-contraction. For simplicity, EMG signals from two hand muscle—abductor pollicis brevis (AbPB) and first dorsal interosseous (1DI) were recorded. They work synergistically when performing a certain task and have known high coherence between them (Kilner et al., 1999). This experiment does not involve any stimulation therefore two instrumentation EMG amplifiers were used.

6.3.2 Hardware specifications

Table 6. 3: Hardware specification of the hand muscle experiment.

Amplifier	Customised (no blanking)	DAC	USB 6009
Amplifier type	Differential	Input type	Analogue
Amplifier gain	326	Sample rate (samples/second)	5000
Passband	10-500Hz	Number of channels	2

6.3.3 Procedures

The subject was asked to grip a FSR (Force Sensitive Resistor) between the thumb and index finger of the right hand. The recording started when the subjected was asked to press against the resistor pad and try to maintain a constant grip force for 30s. The gripping force was monitored by a multimeter connected to the FSR. The experiment was repeated three times with short breaks (3 minutes) between sessions.

6.3.4 Results and analysis

The raw EMG is shown in Figure 6. 6, starting with muscles at rest (barely any EMG activity), and then the subject started to squeeze the FSR (at about 4s) and the plot shows a burst of EMG activity. The subject then tries to maintain a constant force on the FSR and the EMG appears relatively steady (holding phase) between 14.4s and 24.2s.

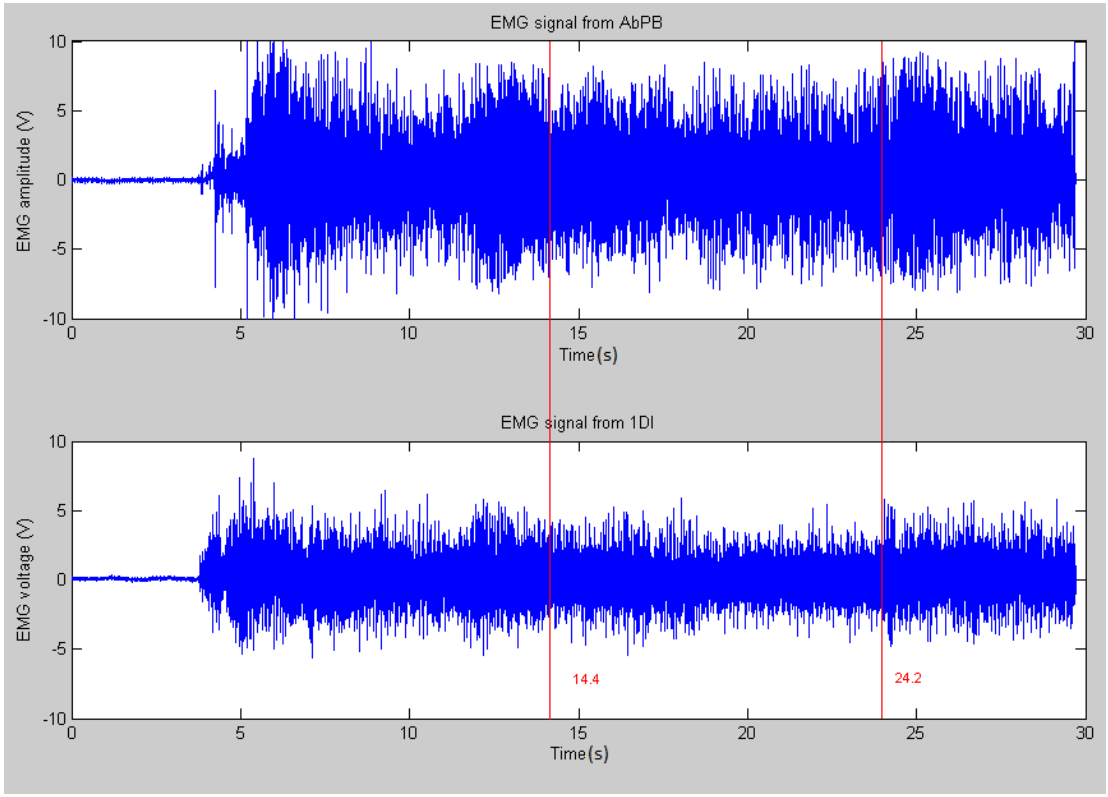

Figure 6. 6: Raw EMG plot from AbPB and 1DI muscles, red lines indicating the range of relatively steady co-contraction of the two muscles, i.e. the holding phase.

Data apart from the 14.4 to 24.2 were not used for the analysis because there was visible change in the amplitude of the EMG signals during those periods. The chosen EMG data was divided into 31 segments (L=31) and each segment length was 0.3144s. No window was used as we were not joining data segments together to perform pooled coherence. The result is plotted in Figure 6. 7.

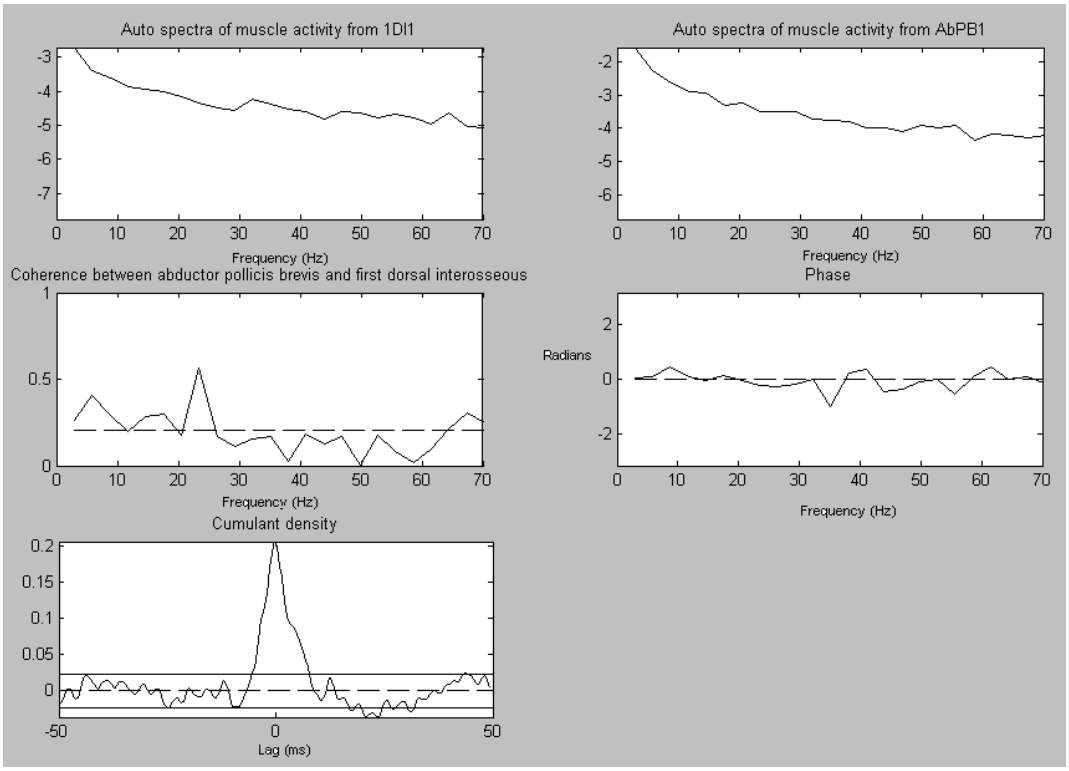

Figure 6. 7: Coherence plot of the hand muscle experiment using NeuroSpec2.0. The top two plots are the autospectra of abductor pollicis brevis and first dorsal interosseous. The middle left is the coherence plot between the two muscles. The dashed line in the coherence plot is the upper 95% confidence limit that allows us to assess the significance of coherence at different frequencies.

In the coherence plot, there is a clear peak dominating between 20.5-26.1Hz with the maximum value at 23.4Hz. This indicates the presence of common frequency components in the two EMG records. The phase plot show the relative timing of the two muscles at different frequencies. The phase should stay fairly constant in the regions when there is significant coherence (Halliday and Rosenberg 1999), which is the case in Figure 6. 7.

The coherence analysis interpreted together with phase and cumulant density could help us to understand the relationship between the synergistic muscles. The peak in the cumulant density in Figure 6. 7 at time 0 indicating the common neural drive to the two muscles arrive roughly at the same time, which means that the two muscles may be of same distance to the neural axis.

6.4 Coherence between synergistic muscles during cycling

6.4.1 Aim

In 6.3, the coherence was calculated from two pieces of continuous EMG data during the "holding phase" of muscle contraction. Now we move on to perform "pooled coherence" (see 6.2.2) during a fast-changing activity – cycling. The aim of the experiment is to study the coherence between different muscle pairs that work synergistically during cycling. VM, VL and

RF were chosen for their overlapping activation range (see 4.5). Different muscle combinations were tested for coherence. The consistency of coherence between the same muscle pairs of the contralateral legs was also evaluated.

6.4.2 Hardware specifications

Table 6. 4: Hardware specification of the cycling experiment with different muscle combinations.

Amplifier	Customised (no blanking)	DAC	USB 6009
Amplifier type	Differential	Input type	Analogue
Amplifier gain	326	Sample rate (samples/second)	5000
Passband	10-500Hz	Number of channels	4

6.4.3 Experiment procedures

- Part 1: Four AB subjects were recruited. The subject was asked to cycle at 60rpm at a constant resistance level, in time with a metronome. EMG signals were recorded for 3 minutes from three muscles of the left quadriceps: VM, VL and RF.

- Part 2: Under the same condition, EMG from the same muscles on the right leg was recorded for 3 minutes.

- Ten minutes of break was given to the subjects between the sessions, during which the subject was asked to remain seated in the trike.

6.4.4 Analysis of the results

The coherence plot for each muscle pair (VM and VL, RF and VM, RF and VL) are shown in this section for the four subjects (Figure 6. 8 & Figure 6. 9). The dotted lines in the figures are 95% confidence limit of the coherence. Therefore we consider any data above the dotted lines as significant. For the VM and VL pair of Subject A in Figure 6. 8, there is a single peak around 20Hz, while there is a wide range of frequencies with significant coherence for the RF and VM pair. Gentle slopes of the significant coherence in the frequency range between 12-25Hz are seen in the RF and VL pair for both legs. Comparisons of coherence spectra from all 4 subjects show: 1) Similarity between the same pairs of muscles in opposite legs; 2) Different shapes for different muscle pairs; 3) Different shapes for a given pair of muscles between subjects; 4) Different peak frequencies between subjects.

Subject A *Subject B*

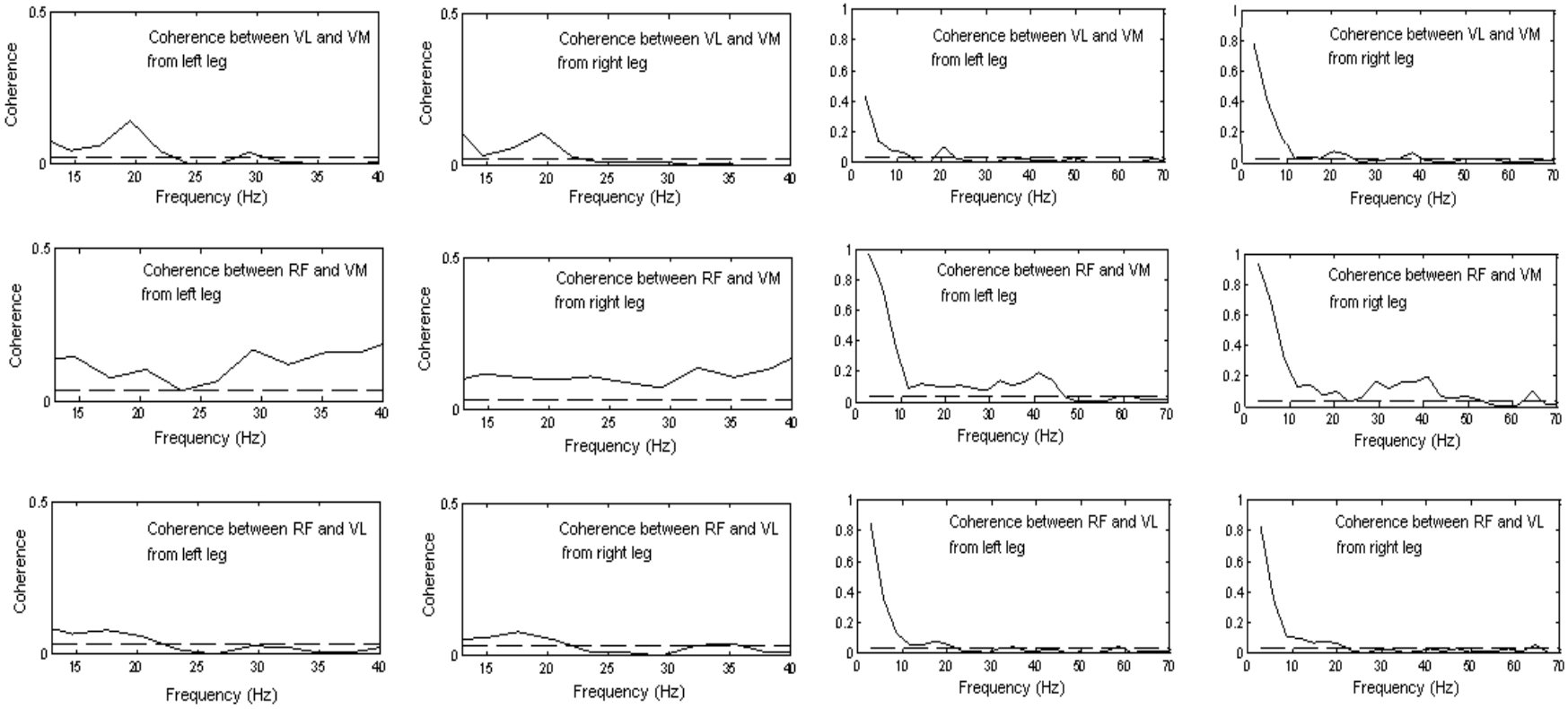

Figure 6. 8: Coherence plot between different muscle pairs for both legs for Subject A and Subject B.

Subject C *Subject D*

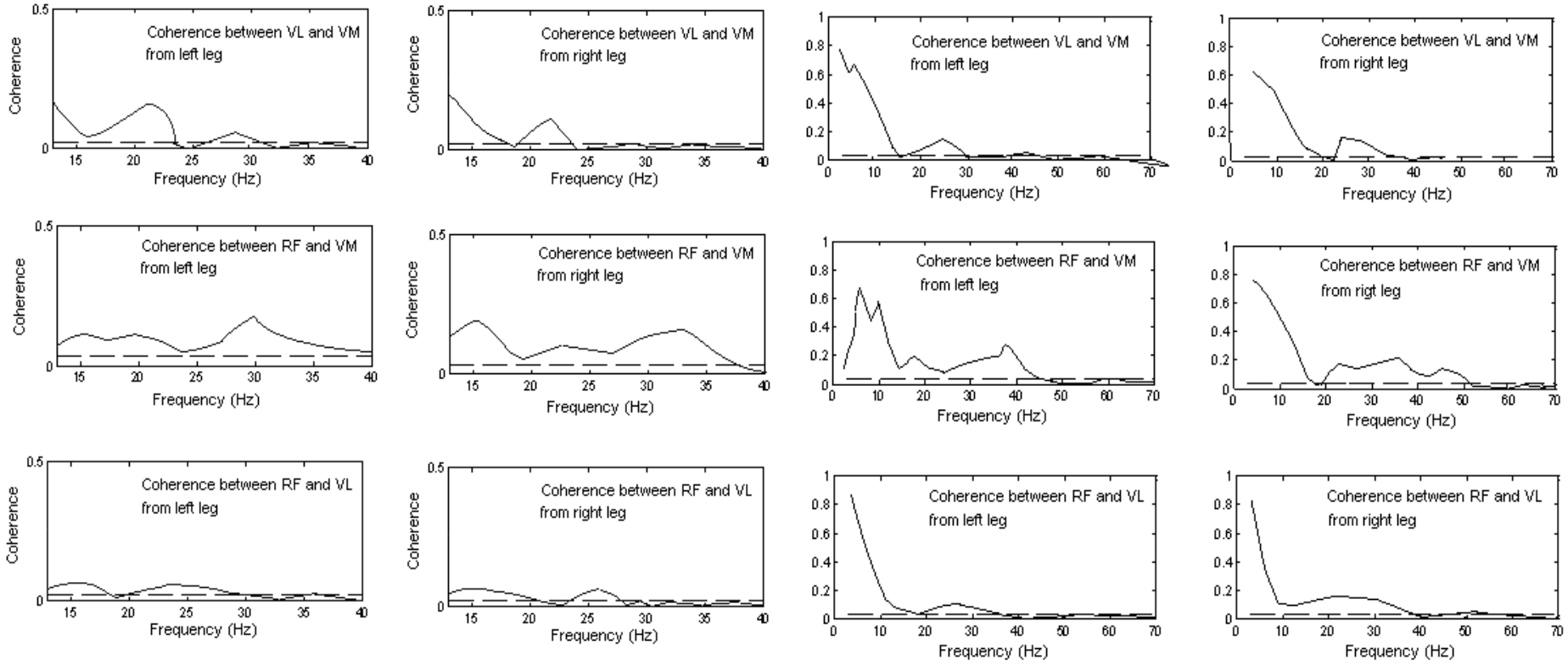

Figure 6. 9: Coherence plot between different muscle pairs for both legs for Subject C and Subject D.

6.4.5 The motion artefact

The high coherence found below 15Hz is considered to be motion artefact (movement of the cables during cycling). Experiments were performed to verify this. No electrodes were used in the experiment, but the cables to the electrodes were taped to the legs with resistors in between to replace the human-electrode interface. The experiment procedures were exactly the same as before, except the EMG amplifiers were not actually recording from the muscles. This was tested with two subjects and each repeated twice. Coherence was calculated and the results are shown in Figure 6. 10.

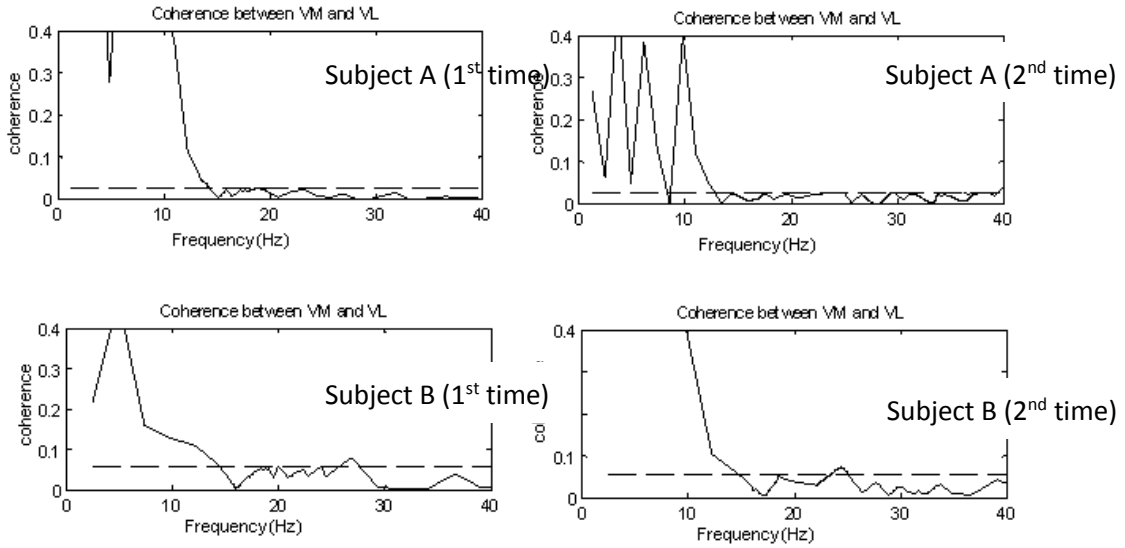

Figure 6. 10: Coherence calculated based on signals acquired during cycling experiment for 2 subjects, repeated twice, with resistor taped over the muscles to measure the motion artefact.

6.4.6 Discussion

Significant coherence in the β band between the quadriceps muscles was found during their co-contraction phase in cycling for all four subjects. We need a way to quantify the significant coherence. Two possibilities were considered here to represent the coherence between two muscles: a) the peak amplitude of significant coherence; b) the area under the coherence curve in the β band above the 95% confidence line (A_{sub} refer to Figure 6. 11 for an illustration. Another area called A_{β} is also shown in the figure which will be used later in 7.2).

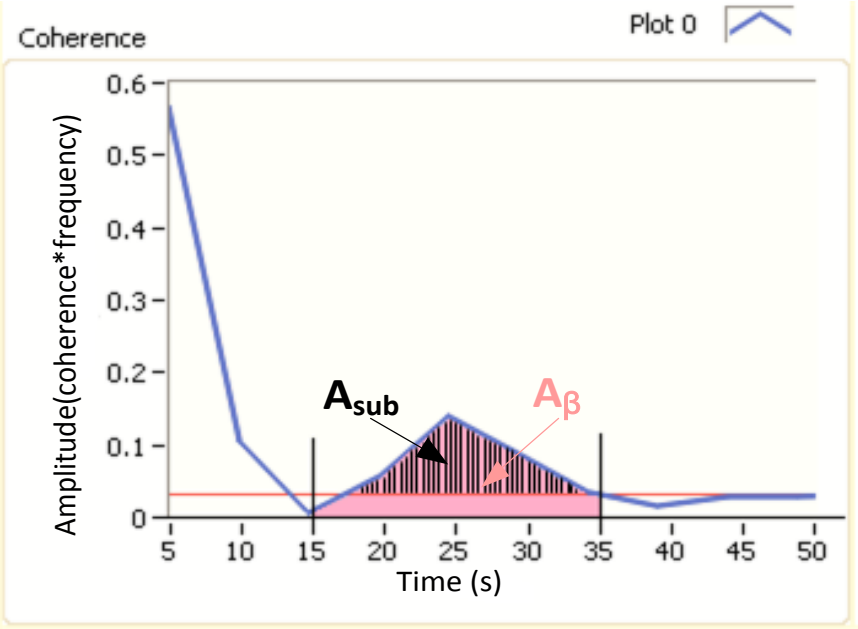

Figure 6. 11: Illustration of A_{β} and A_{sub}

Both the area and the peak amplitude have been used in the literature by different researchers. A_{sub} has been used in the literature previous by Norton et al. (Norton et al., 2006) to assess the improvements in locomotor skills of ISCI patients. Kilner et al. examined the peak coherence in the β band for different subjects during a hold task to study the task dependency of coherence (Kilner et al., 2003). For our experiments, the area is better than the peak amplitude as this method is widely applicable for different muscle pairs even when there is no distinct peak. A_{sub} of different muscle pairs for the four subjects are shown in Table 6. 5. Note here different effort levels were used for the subjects. The effort levels were chosen for each subject so that they were confident to maintain throughout the experiment. Subject A and C used Level 5, Subject B used Level 3 and Subject D used Level 7. This explains the wide range of A_{sub} seen across the subjects. The area was found to be similar between the same muscle pair of the contralateral legs of the same subject. This area was adapted in later experiments to quantify the change of a subject's voluntary drive during cycling against effort levels (see 6.6).

Table 6. 5: A_{sub} between different muscle pairs for 4 subjects

Subjects	VL & VM		RF & VM		RF & VL	
	Left Leg	Right Leg	Left Leg	Right Leg	Left Leg	Right Leg
A	1.23	1.14	1.92	2.13	1.12	1.26
B	0.51	0.64	1.19	1.27	0.27	0.21
C	1.56	1.28	2.05	2.12	0.74	0.68
D	1.77	1.65	2.45	2.53	0.9	1.13

In the experiments described in 6.4.3, note that we recorded the EMG from RF, VM, VL muscles from the left leg first, then repeated the same procedures to record from the right. The reason why we did not record from all six muscles together was due to the limitation of the apparatus.

There were four EMG amplifiers available and three of them were used in both parts of the experiments. The influence of recording the EMG from two legs in two separate experiments was minimized by keeping the subjects on the trike while changing the recording site from the left leg to the right leg during the 10 minutes of break between the sessions.

The motion artefact plays a role in the large coherence amplitudes measured below 15 Hz. However, this was less pronounced for Subject A and C, for which the cables were carefully taped along the leg and secured to the trike frame. Careful setup of the experiment can then reduce this artefact. As introduced in 6.2.1, the frequency band we are interested in is the β band, therefore the coherence of interest is not influenced by the motion artefact.

6.5 The influence of stimulus artefact on coherence

As explained in 3.5, one major difficulty of achieving EMG modulated FES cycling system is the presence of the stimulation artefact. It is important to understand whether the coherence is influenced by the stimulation artefact. This was investigated by applying constant frequency stimulation to the muscles. During the muscle's activation range the stimulation frequency is held constant, and the inter-pulse intervals stay the same. Would this constant frequency stimulation leave peaks in the coherence spectrum?

6.5.1 Simulation using LABVIEW

The situation was firstly simulated using LABVIEW. The input signals to the coherence function were set to mimic the EMG signal with stimulation. Here we used random noise (as EMG signal) combined with 20Hz square wave (as stimulation pulses). The coherence plot is as shown in Figure 6. 12. There are peaks at 20Hz, 40Hz and 60Hz in the coherence spectrum, if we extend the x-axis further, we could see that the peaks occur at the stimulation frequency 20Hz and its harmonics. The peak at 0Hz is a result of DC levels of the square pulses at both inputs of the coherence function.

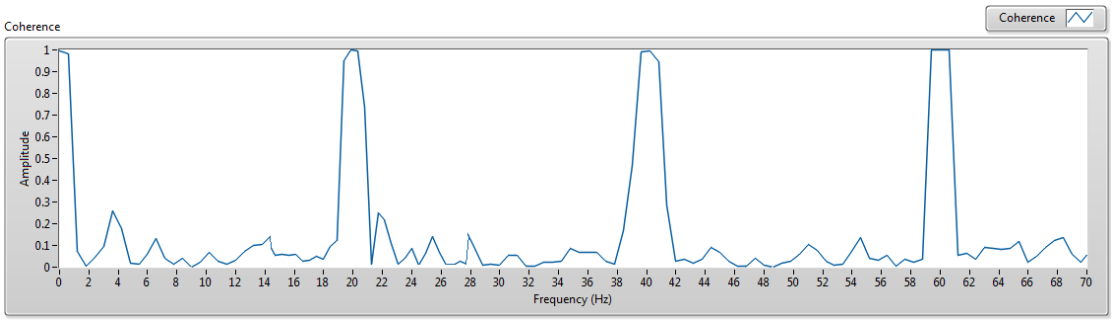

Figure 6. 12: The simulated coherence plot with constant frequency square wave.

The peaks at 20Hz and 40Hz fall into the frequency band of interest (β band) therefore they must be removed while keeping the number of stimulation pulses the same. There are about 6 stimulation pulses in a revolution when applying 20Hz stimulation to RF's activation range (the activation range lasts about 300ms) during cycling. From the understanding of the coherence

calculation, common frequency component in the two data sets will cause peaks in the coherence spectrum. Therefore the problem could be solved by adding a random number to each stimulation frequency pulse, for example, a random number a $(0 < a \leq 1)$ in order of 0.1. The random number was added in a While loop, so every stimulation pulse was altered slightly from the other. In this way we could still keep the number of stimulation pulses the same during the muscle's activation range. Figure 6. 13 shows the results simulated in LABVIEW with the modified stimulation pulses. The peaks at the stimulation frequency and its harmonics have disappeared after adding this random number to it.

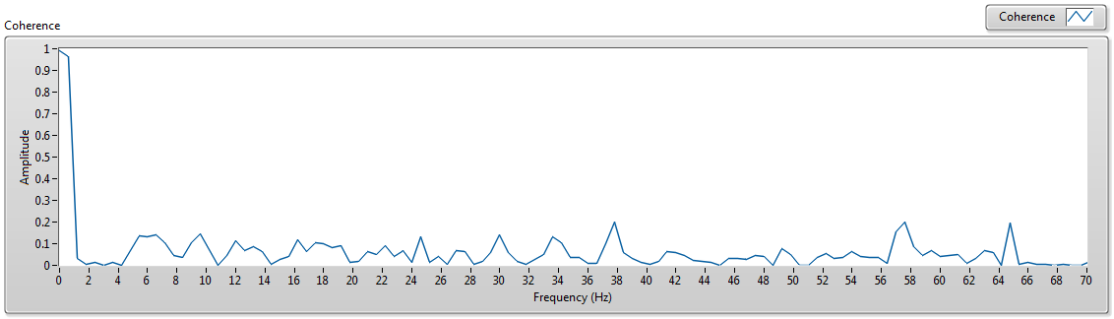

Figure 6. 13: The simulated coherence plot with altered stimulation frequency.

What does this random number added to the stimulation frequency mean?

This random number between 0-1 effectively changes the inter-pulse interval of the stimulation pulse. For a constant stimulation frequency f = 20Hz, there is 50ms between consecutive pulses. When the random number a is at its maximum value a=1 the stimulation frequency f = 21Hz, the interpulse interval between this stimulaion pulse and the next is 47.6ms. When the random number a is at its minimum a = 0.1, f = 20.1Hz the interpulse interval = 49.7ms. Therefore by adding this random number to the stimulation frequency, we are effectively creating an irregular interpulse interval stimulation.

6.5.2 Testing the stimulation patterns

In this experiment, both stimulation patterns described in 6.5.1 are tested in experiments. The first part of the experiment will be testing the coherence with constant stimulation frequency at 15Hz. To realise the irregular interpulse interval stimulation, a stimulation pattern named angle-triggered stimulation is proposed. The stimulation pulses are triggered when the pedal position passes certain angles during the muscle activation range. This makes the stimulation frequency dependent on the cycling speed, thus having irregular inter-pulse interval. Although the subject is trying to maintain a constant speed, this will never be exactly constant, therefore making the stimulation frequency vary in a small range.

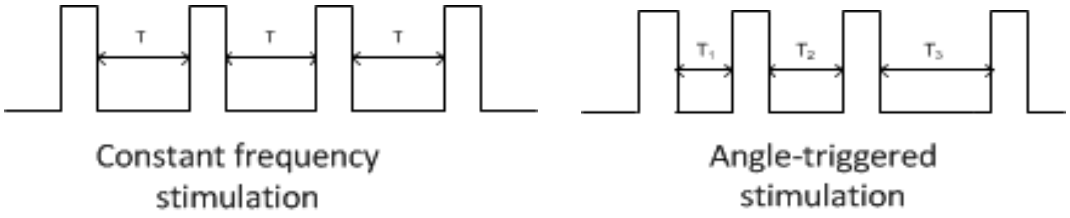

Figure 6. 14: Illustration of two stimulation patterns.

How can we ensure that the subject's cadence is not steady enough for the angle trigger stimulation to become constant frequency?

From our simulation in 6.5.1, the minimum value of a =0.1 which means the interpulse interval was altered from 50ms to 49.7ms. If we translate this to the cadence of the subject, which was set to be 60rpm, hence 1 revolution/s.

1 revolution/s ×0.3 ms = 0.3×10^{-3} revolution which is roughly 0.1 º.

So as long as the subject's cadence has changed by 0.1º between the stimulation pulses, the angle-triggered stimulation should not generate any false peaks in the coherence plot.

6.5.3 Hardware specifications

Table 6. 6: Hardware specification of the cycling experiment with stimulation.

Amplifier	Blanking amplifier Differential	DAC	USB 6009
Amplifier gain	15.5 with external variable gain stage	Sample rate(samples/second)	5000
Passband	10-500Hz	Number of channels	3

Setting the stimulation frequency for the angle-triggered stimulation

There were 6 pulses to be sent during RF's activation range. This is to match the number of stimulation pules if constant frequency stimulation was used. On the commutator, the trigger pulses need to be arranged so that when the subject's cycling at 60rpm, the stimulation frequency is 15Hz. From 4.2.3, we know that the commutator generates trigger pulses according to the set potentiometers on the front panel, which ranges from 0 to 5V. These voltage values correspond to crank angles of the shaft encoder. A 0.33V difference was used in setting the potentiometers on commutator front panel. With this setup, when the subject was cycling at 60rpm, the stimulator would produce a stimulation frequency at 15Hz.

6.5.4 Experiment Procedures

- Constant frequency at 15Hz stimulation was used at first, where the stimulator was set to work at continuous mode (see 4.2.3)
- Blankable EMG amplifiers were used
- For VL and VM, apply stimulation to both during their activation range while recording from them; at 60rpm for 1.5mins.
- The subject was given 10mins break before proceeding to the angle-triggered stimulation. The same procedures were followed for both stimulation patterns.

6.5.5 Results and analysis

Figure 6. 15 shows the results from the coherence analysis of the constant 15 Hz stimulation. Multiple peaks are seen in the power spectrum of the two muscles (top two graphs) at the stimulation frequency (15Hz) as well as its harmonics, as shown in the coherence plot. These peaks are resultant from the stimulation pulses dominating the spectra and make it impossible to interpret the coherence between the muscles.

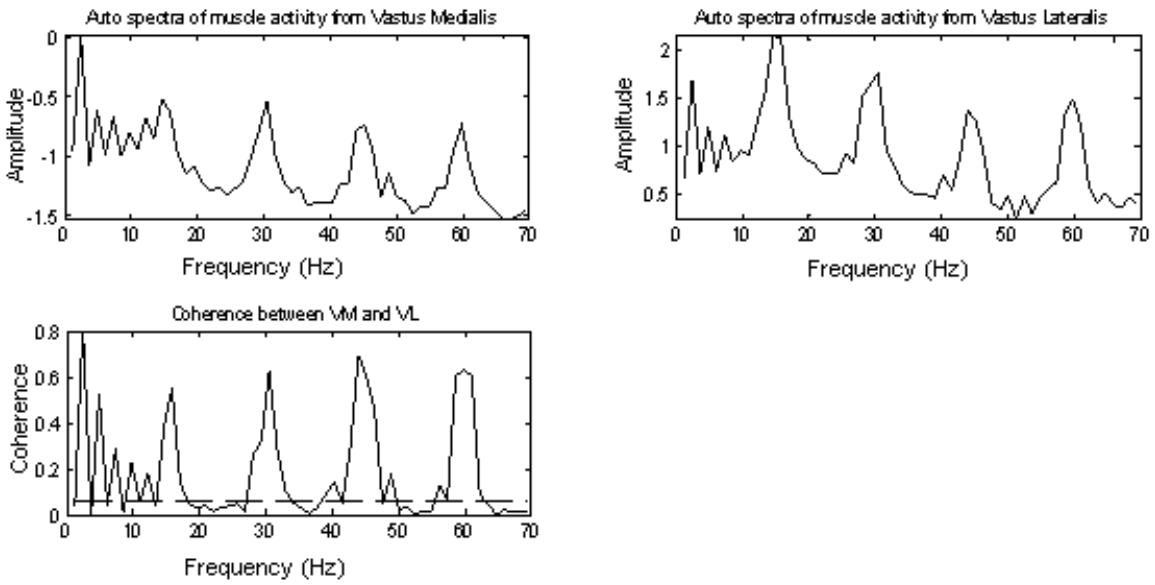

Figure 6. 15: Coherence plot with continuous stimulation at 15Hz.

For the angle-triggered stimulation, the stimulation frequency will be very close to 15Hz but not always equal to it. This provided similar output power as the constant frequency stimulation, but the peaks were absent from the spectra as shown in Figure 6. 16 as expected. The effects of different stimulation frequencies were also tested on the same subject; frequencies of 15Hz, 20Hz and 30Hz were chosen. These frequencies are often used in electrical stimulation and they fall in to the β band of the frequency spectrum. Therefore it is important to see if different stimulation frequency is going to influence the results. From Figure 6. 17, the coherence plots of the subject still peaks around 20Hz regardless of the stimulation frequency change.

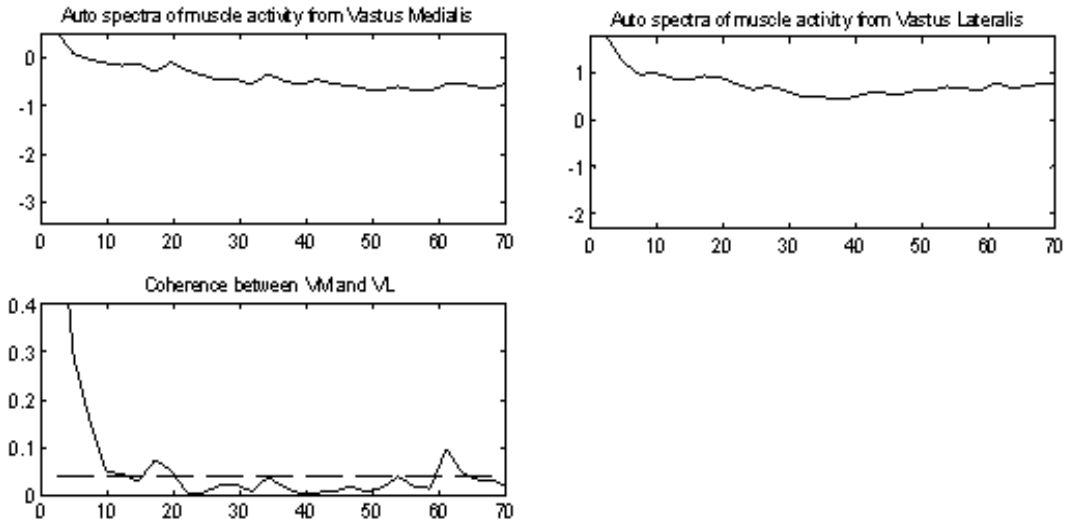

Figure 6. 16: Coherence plot with angle-triggered stimulation.

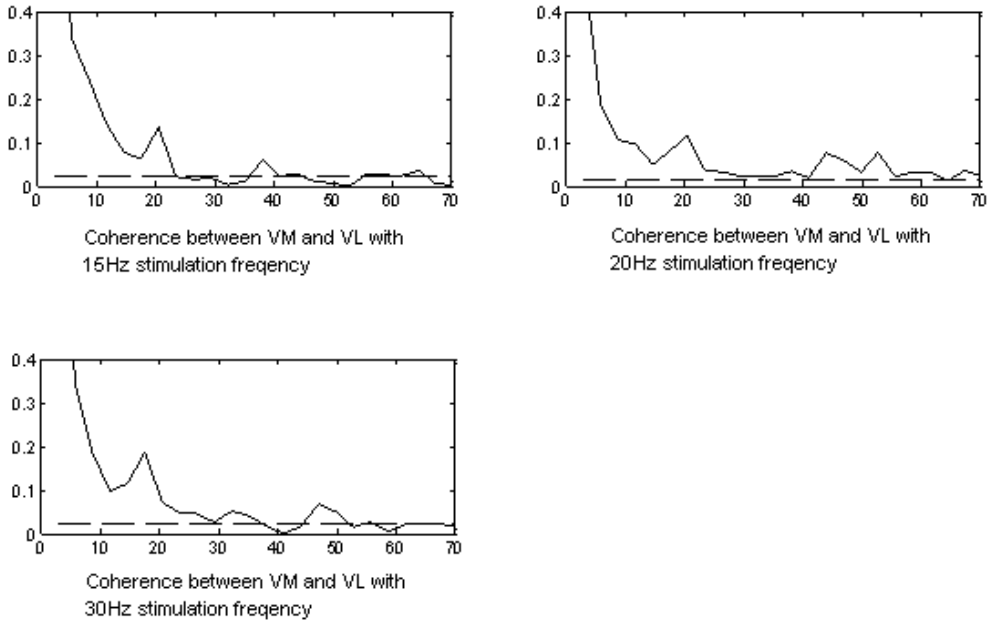

Figure 6. 17: Coherence plot with angle triggered stimulation at different stimulation frequencies.

6.5.6 Changing the recording time

The three-minute recording time is very long considering that it is ideal to have a control signal generated in real time. A further analysis of the data recorded from the previous experiment is shown in Figure 6. 18 where the 3-minute EMG data is divided into halves (1.5min) and quarters (45s). The results of the 1.5min data have similar pattern to the full 3 minute data with correlation coefficients at 0.99 and 0.95 respectively. More visible changes are seen on the 0.75min data. A_{sub} was used to evaluate the changes. A_{sub} calculated from 3min data is 0.635,

and reduces to 0.603 and 0.645 when the data length is halved. This is further reduced to 0.327 and 0.09 when the data length becomes 45s. The recording data length was decided to be 1.5mins for the following experiments described in this session as A_{sub} did not differ from the 3min data by more than 10%. This was further reduced to 1 minute (with a difference of less than 15% from the 3 minute data) when used in real-time later in Chapter 7 with further testing.

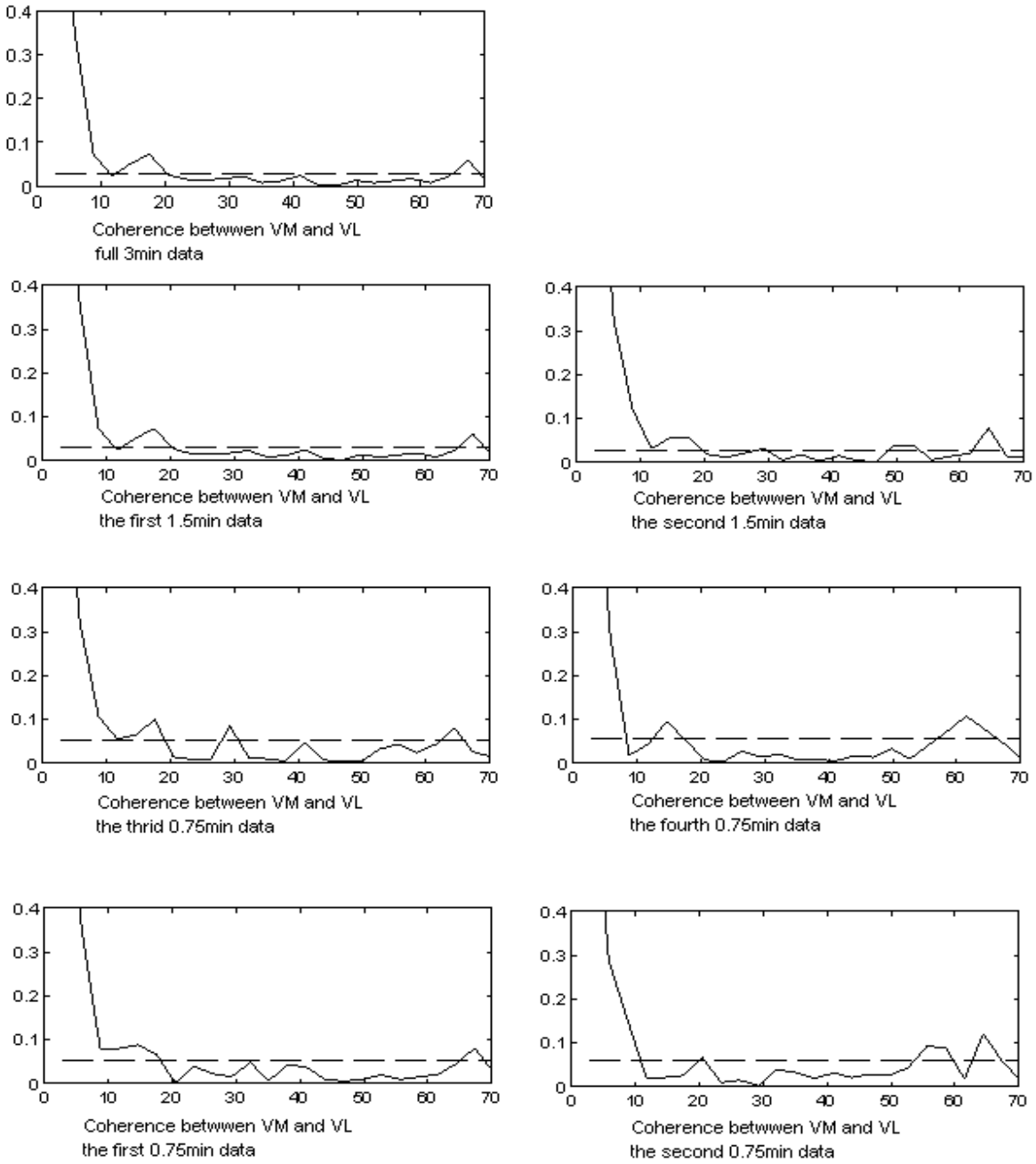

Figure 6. 18: The effect of data length on coherence calculation for a subject.

6.5.7 Discussion

The influence of the stimulation pulses was shown both in simulation and by experiments in this section. The constant frequency stimulation should not be used as it leaves peaks in the frequency band of interest, therefore making it difficult to analyse the coherence graph. The proposed angle-triggered stimulation is used in the following experiments as it leaves no peak in the coherence spectrum. Change in stimulation frequency seems to result in a tendency to increase in the peak coherence as shown in Figure 6. 17. However, there is not enough evidence for us to make such a conclusion. The recording time required to make a useful coherence calculation is chosen to be 1.5mins.

6.6 The effect of effort levels

As in the time domain method, the coherence method also was tested with different effort levels. Thus the coherence can be evaluated as a control signal and a control algorithm for the feedback control loop can be designed accordingly. This will be tested without and with stimulation.

6.6.1 Without stimulation

6.6.1.1 Aim

The experiment begins without stimulation to study how the coherence changes with effort levels naturally.

6.6.1.2 Hardware specifications

Table 6. 7: Hardware specification of the cycling experiment without stimulation.

Amplifier	Customised (no blanking)	DAC	USB 6009
Amplifier type	Differential	Input type	Analogue
Amplifier gain	326	Sample rate(samples/second)	5000
Passband	10-500Hz	Number of channels	3

6.6.1.3 Experiment procedures

Five able-bodied subjects were recruited for this experiment. Each subject was asked to do 5 trials of cycling exercises at 5 randomised effort levels. Each trial is 1.5 minutes with a minimum 5 minutes break in between.

The DAC was set to record 3 channels: two EMG signals through differential EMG amplifiers for the two muscles, VM and VL; and the third channel was for the shaft encoder. Only A_{sub} between VM and VL pair (not RF-VM and RF-VL) is compared to the effort levels due to the time limitation.

6.6.1.4 Results and analysis

Figure 6. 19 shows an example of coherence between VM and VL for a male subject at 5 effort levels from 5-9. Higher effort level range (5-9) was used as this subject felt that (3-7) was too low to get significant muscle activation. The red dotted lines in the graphs indicate the 95% confidence limits. Figure 6. 20 shows A_{sub} versus different effort levels without stimulation for the five subjects, with r^2 values ranging from 0.678 to 0.884. It clearly shows that A_{sub} has an increasing trend with the effort levels for the VM and VL pair.

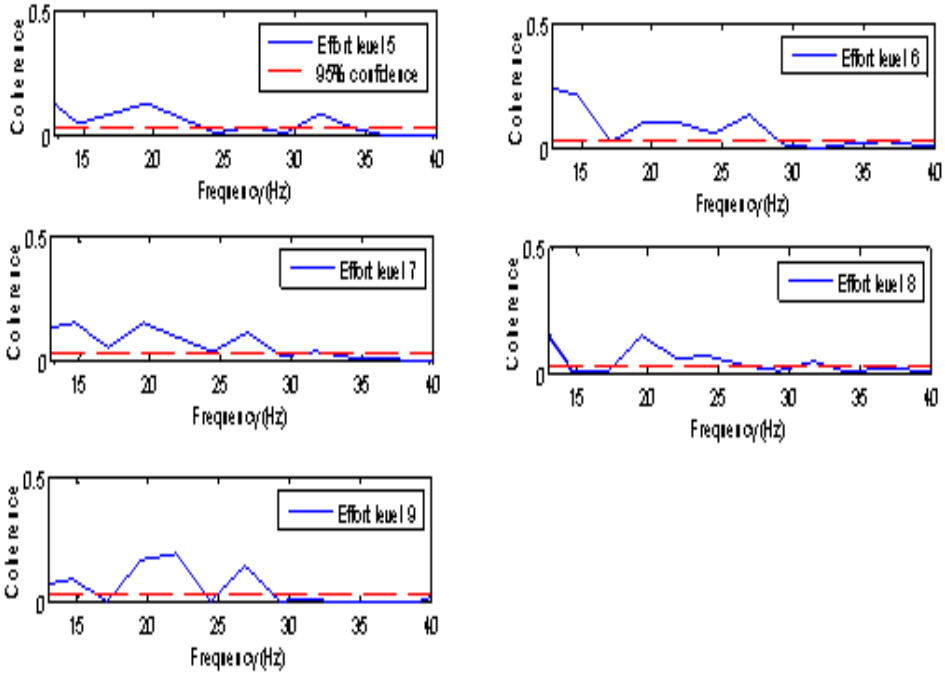

Figure 6. 19: Coherence between VM and VL for 5 effort levels during cycling without stimulation.

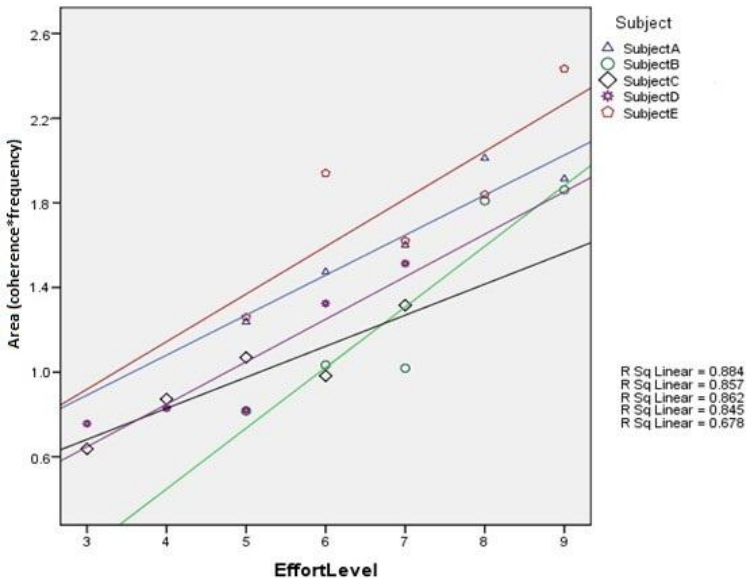

Figure 6. 20: A_{sub} (no stimulation) at different effort levels for 5 subjects, with regression lines.

6.6.2 With stimulation

6.6.2.1 Aim

The angle-triggered stimulation method was used in this experiment to study the influence of stimulation on the relationship between coherence and effort level.

6.6.2.2 *Hardware specifications*

Table 5. 9: Hardware specification of the cycling experiment with stimulation.

Amplifier	Blanking amplifier Differential	DAC	USB 6009
Amplifier gain	15.5 with external variable gain stage	Sample rate(samples/second)	5000
Passband	10-500Hz	Number of channels	3

6.6.2.3 *Experiment procedures*

The experiment follows the same procedures as the experiment without stimulation.

6.6.2.4 *Results and data analysis*

The coherence with stimulation was plotted against different effort levels in Figure 6. 21. Figure 6. 21 (with stimulation) is very similar to Figure 6. 19 (no stimulation). The coherence spectra were not dominated by peaks at the stimulation frequency thanks to the constantly changing inter-pulse intervals. Figure 6. 22 shows that the area is also increasing with increasing effort levels with stimulation for the five subjects.

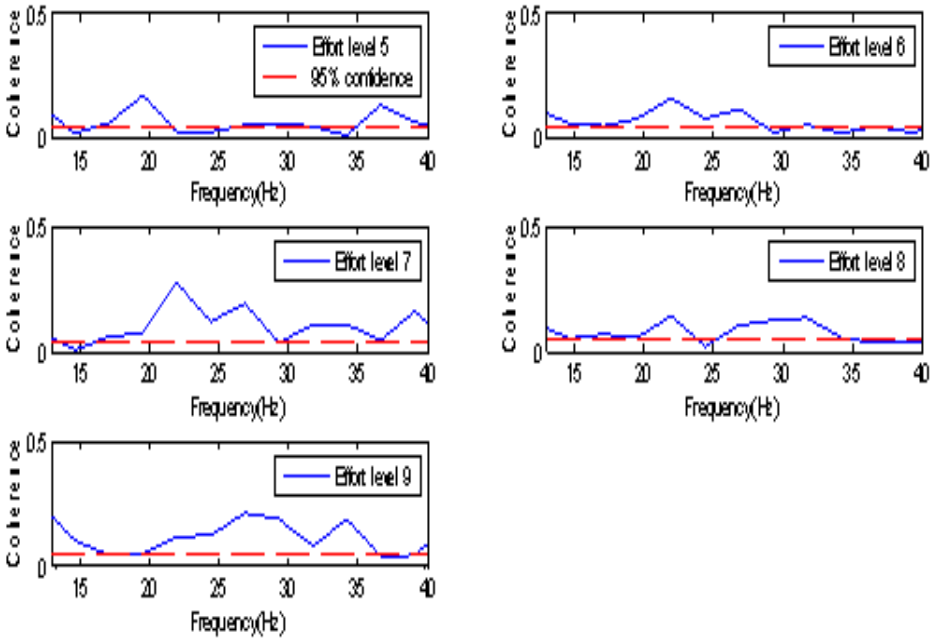

Figure 6. 21: Coherence plot between VM and VL with 2MT triggered stimulation for one subject.

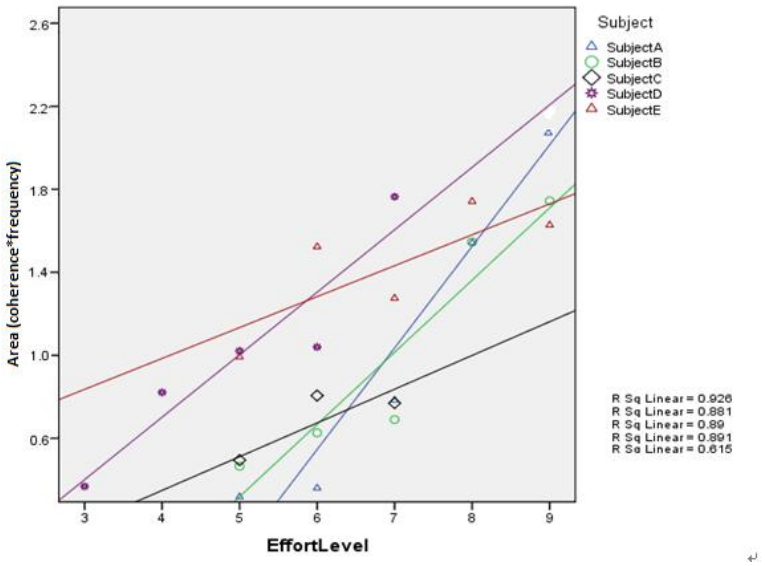

Figure 6. 22: A_{sub} (with stimulation) at different effort levels for 5 subjects, with regression lines.

Table 6. 8: The r^2 for the experiments with and without stimulation and the difference between them.

	Subject A	Subject B	Subject C	Subject D	Subject E
r^2 no stimulation	0.884	0.875	0.862	0.845	0.678
r^2 with stimulation	0.926	0.881	0.89	0.891	0.615
Difference in percentage	4%	0.60%	3%	5%	9%

6.6.3 Discussion

In 6.6, we investigated how A_{sub} changes with effort levels. The relation was tested with and without stimulation. In both cases, A_{sub} was found to be increasing with the increasing effort levels. The r^2 values of the two experiments are shown in Table 6. 8. There is not much difference between the r^2 values (less than 10% difference) therefore the relation between A_{sub} and the effort levels is not affected by the stimulation.

Another important finding is that although A_{sub} increases with the increasing effort levels, the intrasubject variability of it is huge, i.e. it is not reliable to infer the effort level from a given A_{sub}. It is only the change of the effort level that A_{sub} is showing. Therefore when using A_{sub} as a representation of the effort level, a base line of the subject (thresholds) must be known.

6.7 Discussion & Conclusions

Coherence was used in this chapter as an attempt to represent the voluntary effort between muscles that work synergistically. We began the process by calculating the coherence between two muscles that were known to have high coherence between them, the abductor pollicis

brevis (AbPB) and first dorsal interosseous (1DI). Significant coherence was found between the two muscles during the holding phase. This experiment ensures all the apparatus and the method were working properly. Then we moved on to test the coherence during cycling, which involved using the method "pooled coherence". In both cases, rectification of the EMG signal was used before performing the calculation. The reason for the rectification is based on the assumption that full-wave rectification of EMG demodulates the neural activation signal to the muscle (Mima and Hallett, 1999; Myers et al., 2003; Yao et al., 2007). Demodulation refers to the enhancement of underlying low-frequency components of the signal, which may not be easily observed due to the greater power of higher-frequency components of the signal. For the EMG signal, it is assumed that the carrying frequencies occur in β band and may represent common oscillatory inputs from the motor cortex (Brown, 2000; Myers et al., 2003). The evidence that rectification enhances the existing low-frequency component in the interference EMG signal comes from a study by Myers et al. (Myers et al., 2003), which is the reason rectification was used as the first step of the data analysis.

By the end of 6.4, we concluded that significant coherence can be found between muscles that work synergistically during cycling. Comparing the results from four subjects showed that the coherence between different muscle pairs varies in pattern and shape. We do not always get a single peak frequency, instead a range of significant coherence may be found. It was then decided to use the area under the coherence curve in the β band A_{sub} as a measure of the subject's voluntary drive rather than using the peak frequency of the coherence. This method was further evaluated in 6.6 with respect to different effort levels.

In 6.5, the influence of stimulation on the coherence spectrum was firstly simulated in LABVIEW, then tested in experiments. Constant-frequency stimulation should not be used in these experiments because it would yield false peaks in the coherence spectra. Angle-triggered stimulation is suitable for this application as it does not contaminate the coherence spectrum. We should note that the time taken to get a significant estimation of the coherence is rather long. The shortest period used to gather data in the experiment performed in this chapter was 1.5 minutes. This is due to the pattern of the muscle co- activation during cycling and only a small fraction of the recorded EMG can be selected in each revolution. In the FES-assisted standing experiment performed by Norton et al. in 2003 (Norton et al., 2003), the average time for each stand is typically 5 minutes. This is rather long as we expect a control signal can be extracted every few revolutions or ultimately every revolution. The timing would not be an issue if the data is only analysed for coherence after the experiment; but in our case, the data is required to be analysed in real time to extract a control signal. Therefore, the time needed to prepare for the first control signal is critical. Possibilities like using the save data from previous experiment for the same subject as a standard control signal for the first minute would be considered.

For all five able-bodied subjects, A_{sub} was found to increase with the effort levels (either effort level 3-7 or 5-9) with and without stimulation in 6.6. However, A_{sub} varies a lot for the same

effort level for different subjects which means it cannot be used to infer the effort level directly. One possible solution is to build a database for the subjects with thresholds of A_{sub} at different effort levels. Therefore the key finding of this chapter is that A_{sub} can be used to infer a change in the effort level, hence a change in the voluntary drive of the subject during FES cycling. The validity of using A_{sub} as a control signal will be tested further in the next chapter.

CHAPTER 7 TESTING THE COHERENCE AS A CONTROL SIGNAL

7.1 Introduction

The possibility of estimating the voluntary drive using an area (A_{sub}) related to coherence was discussed in Chapter 6. This chapter focuses on testing the area as a control signal in a real-time environment. The development of the real-time feedback control loop required both hardware design and software programming. An illustration of the theoretical closed-loop is shown in Figure 7. 1. On the hardware side, a control box was designed to enable the control of the stimulator with a digital signal from the computer. Consequent modification to the stimulator was also made for this purpose. In the software part, a real-time data processing-control program was developed in LABVIEW. Two experiments were conducted to observe the characteristic of area changes with effort levels. Experiment 1 involved an effort level change during the recording while experiment 2 focussed on the variability of the area at a fixed effort level during a longer period.

7.2 The Areas

A new term A_β is introduced in this chapter to be tested together with A_{sub}. It is our motivation to compare the two areas in their ability of reflecting the change in effort levels. The two areas are defined as follows:

- Area below the significant coherence in the β band (A_β), the pink area in Figure 6. 11;
- A_β minus the area below the 95% confidence limit in the β band is A_{sub}, shaded area in Figure 6. 11.

The results from Chapter 6 show that A_{sub} can reflect a change in the effort level and the calculation of A_{sub} is based on 1 minute of EMG data. Therefore the time needed to get a useful estimation of the effort level is long compared to what we would like to have as a control signal (a few seconds). A_β is introduced to see if it could reflect the effort level change better.

7.3 The design of a control box and the modifications to the stimulator

The aim of the control box was to be able to control the output of the stimulator digitally by an enable signal from the computer. The first and the simplest idea will be adding an electronic switch to the output of the stimulator. Such a switch could have many channels, therefore providing smooth control of the output stimulation. However, electronic switches could not stand the high voltage on the output side of the stimulator. A second thought was to use transistors with diode network on the primary coil side of the stimulator.

The control box was designed and constructed to be connected to the primary coil side of the transformer (LT700) of stimulator (see 4.2.5). A socket was added to the back panel of the

stimulator so that it could be connected to the control box. The design of the control box is shown in Figure 7. 2 with channels at 5 stimulation levels by passing series diodes (showing 5 channels with 10 diodes divided into 5 groups here). Each channel effectively shorted out some of the diodes, thereby changing the driving voltage across the primary coil. The voltage of each channel steps in about 1.4V increments (2 diodes) with Channel 1 having the lowest voltage across the coil (8.4V) & channel 5 the highest (12V). The output voltage varies accordingly (49-178V). The switches are zvp3306a PMOS and zvn3306a NMOS transistors that could be driven by an enable signal sent from the control software via the digital output channels of the DAC (4.2.6). The same enable signal also control the LEDs on the front panel to give a visual indication of the level of stimulation. The control box was tested using the software described in 7.4 and it worked well with the program.

The actual control box has 5 channels which sets the stimulation intensity to 5 levels. It was designed to be used with the 5 effort levels normally used in the cycling experiments. Because each subject may tolerate different levels of stimulation intensity, the decision of the voltage levels was quite arbitrary. It was selected to fit the range that most of the subjects we recruited fell into. It would be better if the change of the stimulation voltage is continuous rather than discrete levels as it would provide smoother control of the stimulation intensity. However, this would have required the design and construction of a new stimulator and therefore was not considered for this project.

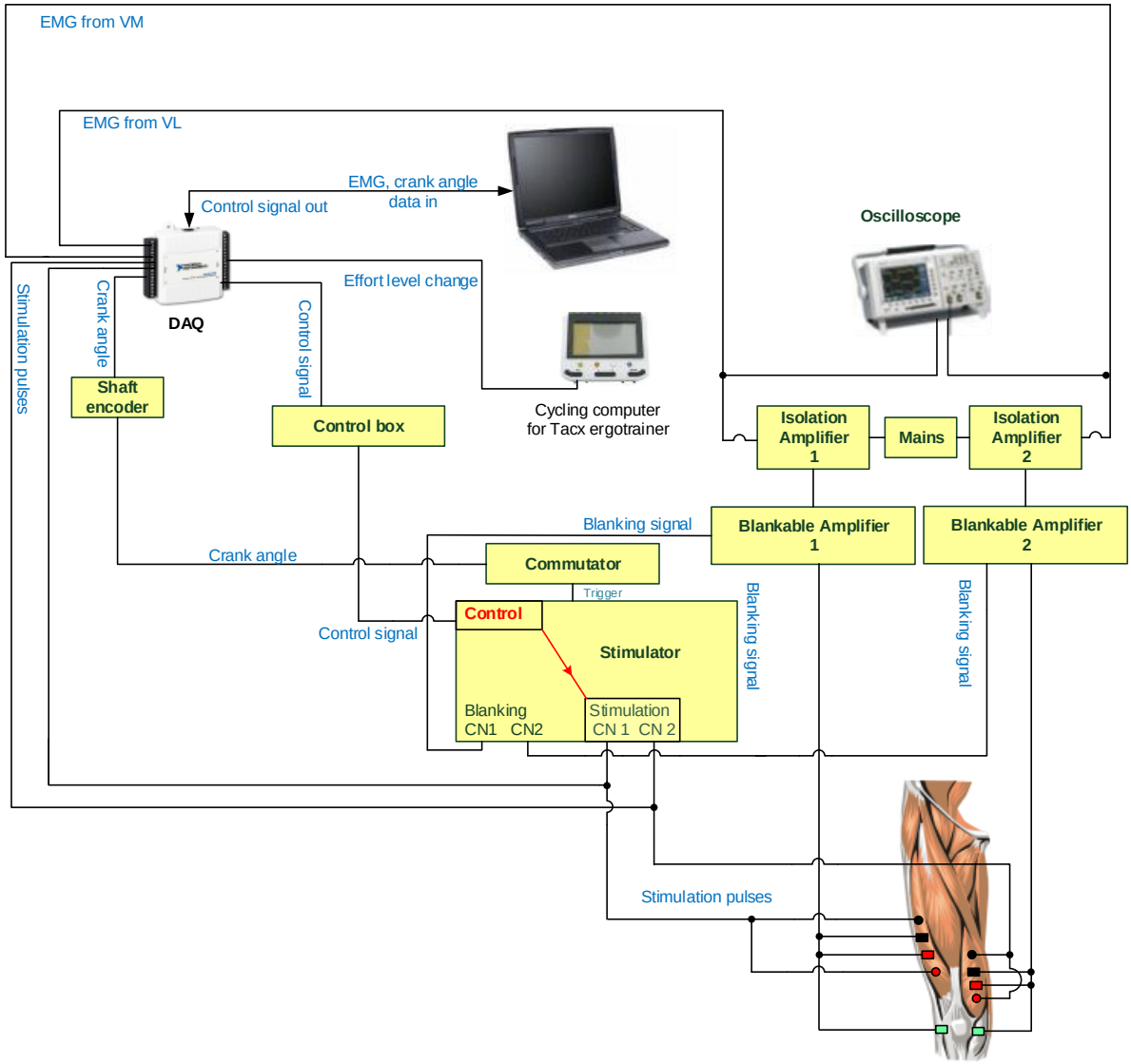

Figure 7. 1: Block diagram of the closed-loop feedback control cycling system.

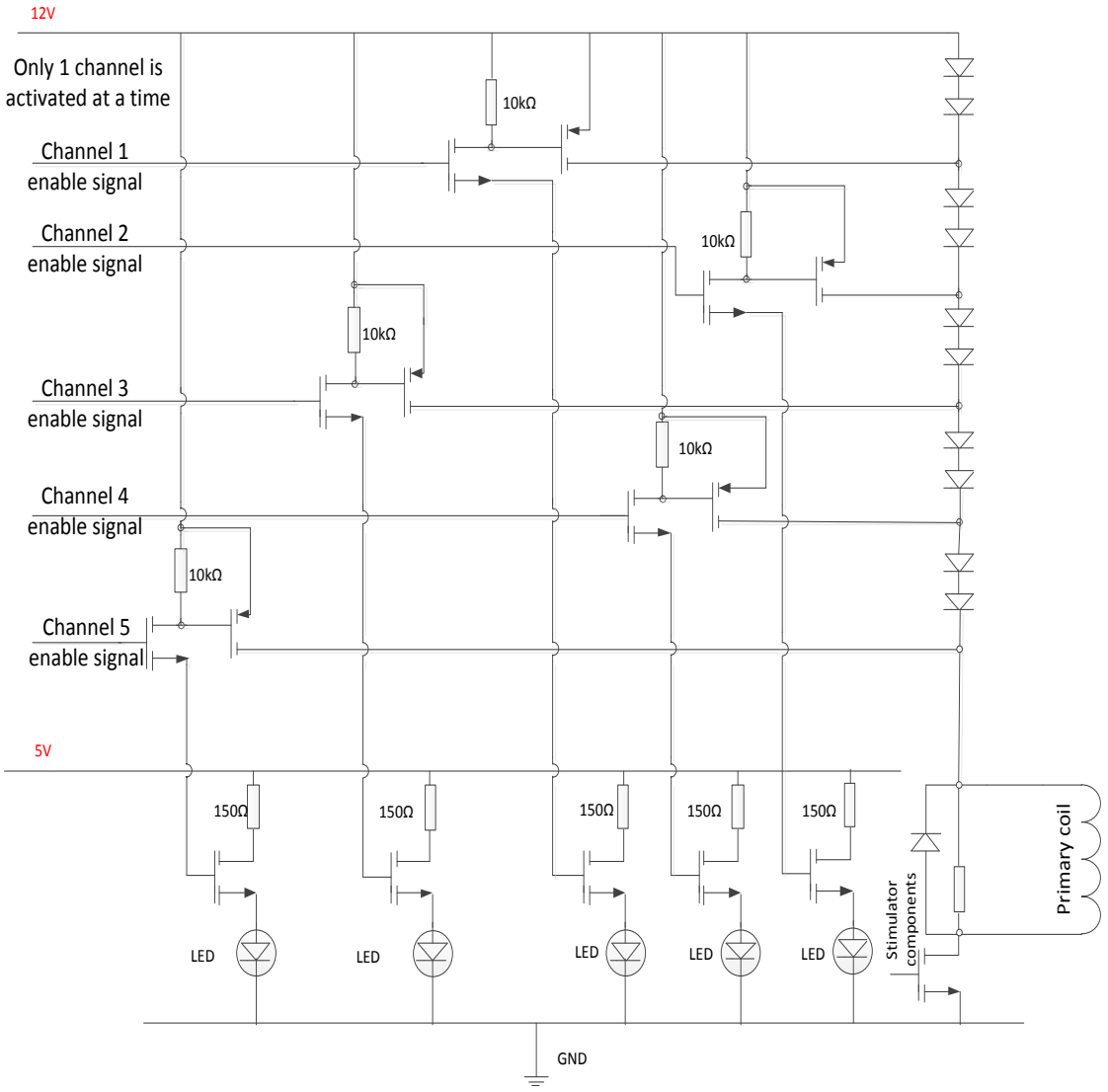

Figure 7. 2: The circuit diagram of control box and the modifications to the stimulator.

Figure 7. 3: A photo of the 5 channel control box sitting on top of the stimulator.

7.4 The real-time recording, processing and control software

7.4.1 Introduction

MATLAB was used to carry out the data recording, processing and analysis. The NeuroSpec 2.0 software that we adapted to analyse coherence was also written in MATLAB. It was expected that MATLAB would be used for the feedback control. One primary requirement for the feedback control software is that it should be processed in real time. However, obstacles were met when trying to program the control loop with MATLAB which is explained in the next section and a new method was explored.

7.4.2 The programming problem with MATLAB

The real-time feedback control loop requires real-time EMG signal recording, processing and control. Three possibilities were considered in MATLAB: 1) Built-in function—multithread; 2) The Parallel Computing Toolbox; 3) Compiled MATLAB code. Further research showed that the multithreaded computation for MATLAB only supports a number of functions which are automatically assigned and executed on multiple threads. The Parallel Computing Toolbox enables data-intensive tasks to be solved in parallel. For both cases, MATLAB improves the system's performance using the multi-core processor architecture, however, it is not possible to control which tasks are assigned to the threads. It is necessary for our application that EMG is recorded continuously while the coherence function is being calculated, at the same time when an enable signal is sent to the control box. Therefore the 3 tasks need to be executed at the same time, but the process must also be interruptible when needed. This means that we could not use MATLAB to calculate the coherence while continuing to record EMG data without any interruptions.

The final option was to compile the written MATLAB code. Even though the compile programs execute much faster than uncompiled code, they are still single-threaded; a standalone executable will only have as much multithreaded capability as the original non-compiled code which is not useful for us.

It was then decided that alternative software needs to be used instead of MATLAB, which meant that all the software programs (including the modified Neurospec 2.0) had to be converted. A high-level language, LABVIEW, was chosen as it is relatively simple to use and is compatible with the DAQ.

7.4.3 The software program in LABVIEW

After converting the existing software to a LABVIEW program, the code executed much faster than the MATLAB equivalent and the front panel was much more user-friendly.

The entire program was divided into three parts:

- Signal recording: analogue input signal recording and digital signal recording;
- Signal processing: signal conditioning and coherence-related calculation;
- Control: sending appropriate control signal to the stimulator.

The signal processing and the control parts are explained together in 7.3.3.2.

7.3.3.1 Signal recording section

The flow chart for the signal recording program is shown in Figure 7. 4. The computer reads data from the DAC through 3 analogue channels (two EMG signals and one shaft encoder signal) and 1 digital channel (effort level change signal) (The effort level change detection is explained in Appendix E). The run time is set by the operator on the front panel; the program continues to function for the duration of the run time setting.

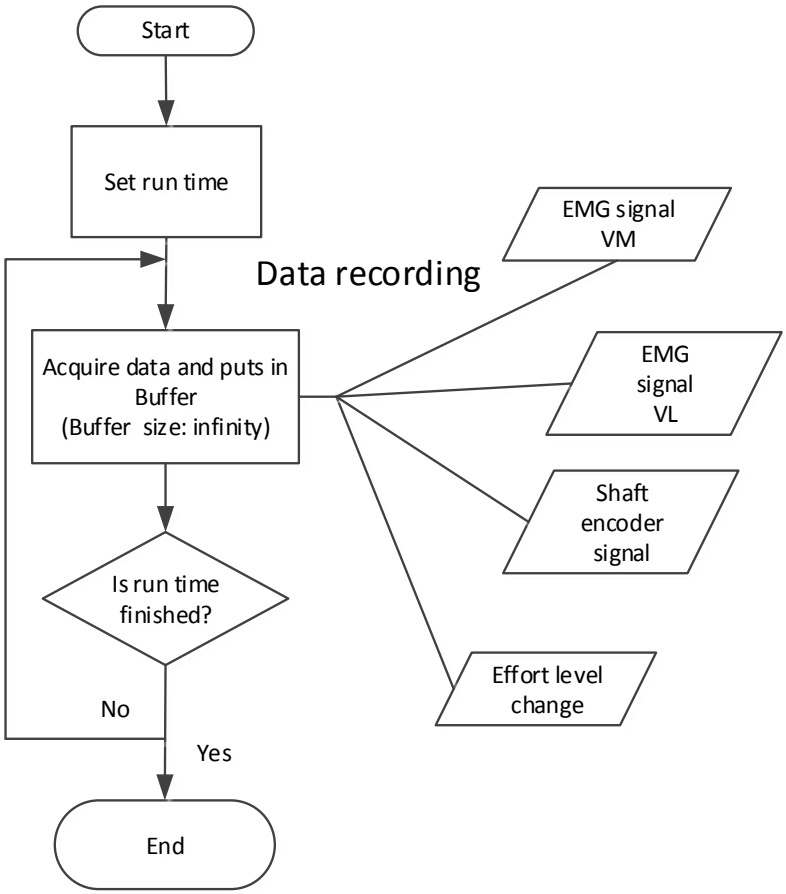

Figure 7. 4: Flow chart for the signal recording program.

7.3.3.2 Signal recording and control section

The flow chart for the signal processing and control section of the program is shown Figure 7. 5. As data begins to accumulate in the buffer, the program checks if there has been 1 minute of data recorded. The first coherence calculation happens when the data length in the buffer reaches 300k (given that the sample rate is 5k/s, 1 minute of data equates to 300k). This 1 minute of data block is then sent to the coherence & area calculation module where any DC offset is first removed. The program then loads the subject's profile, which contains the muscles' co-activation range. The selected co-activated EMG data segments from each revolution are then passed through a Tukey window to smooth out the boundaries and are then concatenated. Coherence is calculated based on the most recent 1 minute of data in the buffer every 0.5s (moving window). The area under the coherence curve with and without the subtraction of the 95% confidence limits area is calculated separately and displayed on the panel. This is running in parallel with the recording process which continuously acquires data as long for the length of the run time setting.

The control part of this program is simply a comparator block. The subject's profile contains all the thresholds. The comparator can then compare the calculated value to the thresholds to decide if there should be an effort level change.

7.3.3.3 The Graphical User Interface (GUI)

It is quite convenient to generate a GUI for the written LABVIEW program which gives real time display of the results and also helps to monitor the progress of the experiment. A snapshot of the GUI during an experiment is shown in Figure 7. 6. Before starting the experiment, the parameters on the left hand side needs to be set, including

1. Sample rate
2. Samples to display (which sets the window length for the real time EMG and shaft encoder signal display)
3. Total running time,
4. The time to calculate the first coherence,
5. How often coherence is calculated,
6. Segment power (which sets the resolution for the coherence plot).

The experimenter also needs to choose the subject's name from a drop down menu which will automatically fill the subject's saved muscle activation range and display it. Choosing the subject's name will also enable the program to save the resultant file with the subject's name and time and date when the experiment was performed. If the subject has a saved area value from previous experiments in his database, it will be shown below the activation range as a reference. This reference value can be considered as a threshold for the control signal, which is not applicable at this stage and will only be considered in the future experiments. In the bottom left corner is an expandable sequence showing the effort level change. Below the real time EMG/shaft encoder window to the left is the coherence display window which shows the real time coherence plot with 95% significant level. The third window is an area plot which contains two plots, A_{β} and A_{sub}. A progress bar is located below the area window to show the elapsed time. The green button in the bottom right corner flashes green when there is an effort level change. Below that is a window showing the delay caused by coherence calculation which refreshes every time when such a calculation is carried out. This delay is caused by the limited CPU processing ability of the computer performing all the tasks (recording, processing and write to hard disk) at the same time. The last window shows if there are elements queuing for the coherence calculation. These elements are EMG data clips selected from raw EMG signals. Any value below 100 should be satisfactory given the high sample rate at 5000 samples/s.

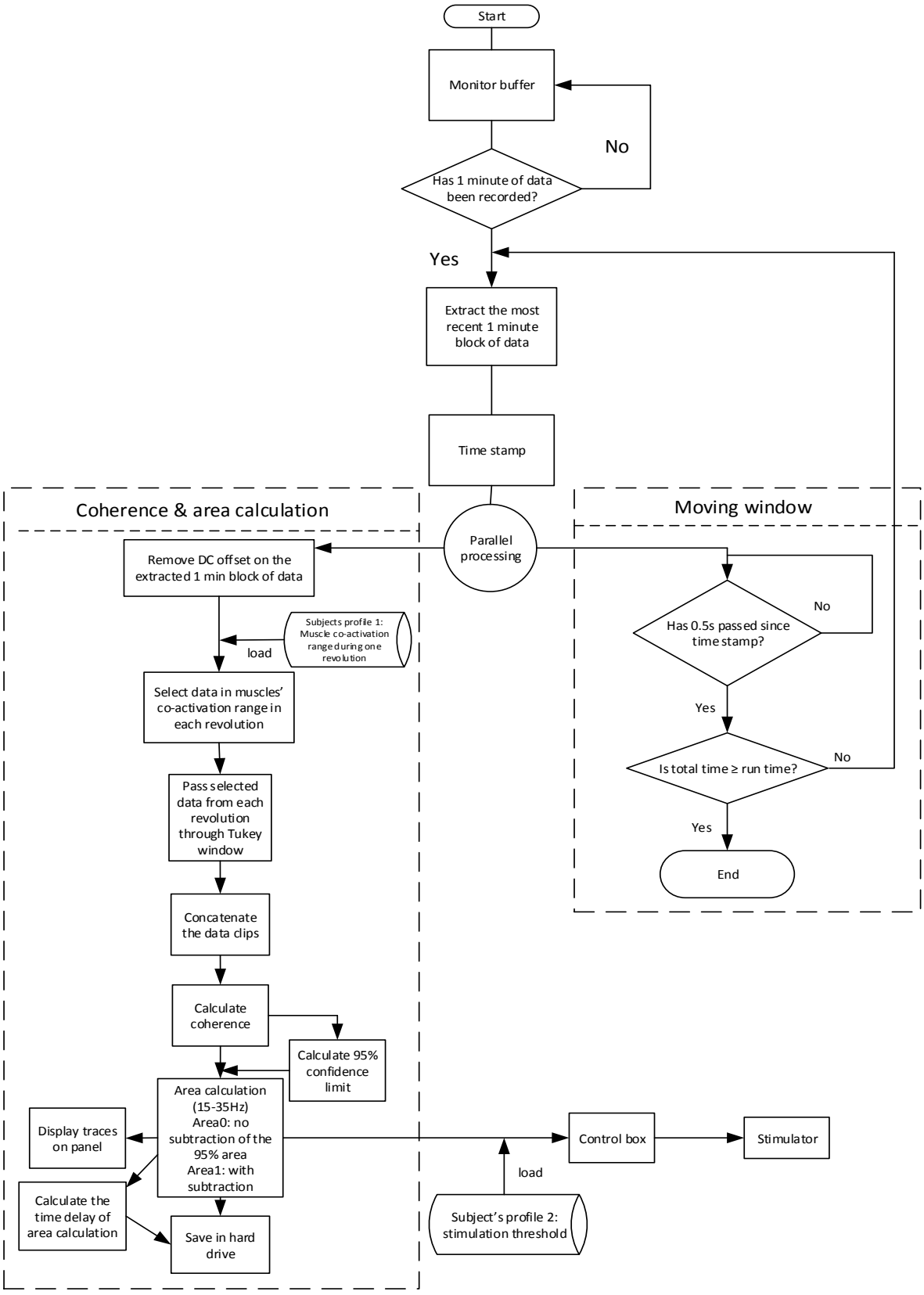

Figure 7. 5: The data processing and control parts of the LABVIEW program, showing the parallel processing.

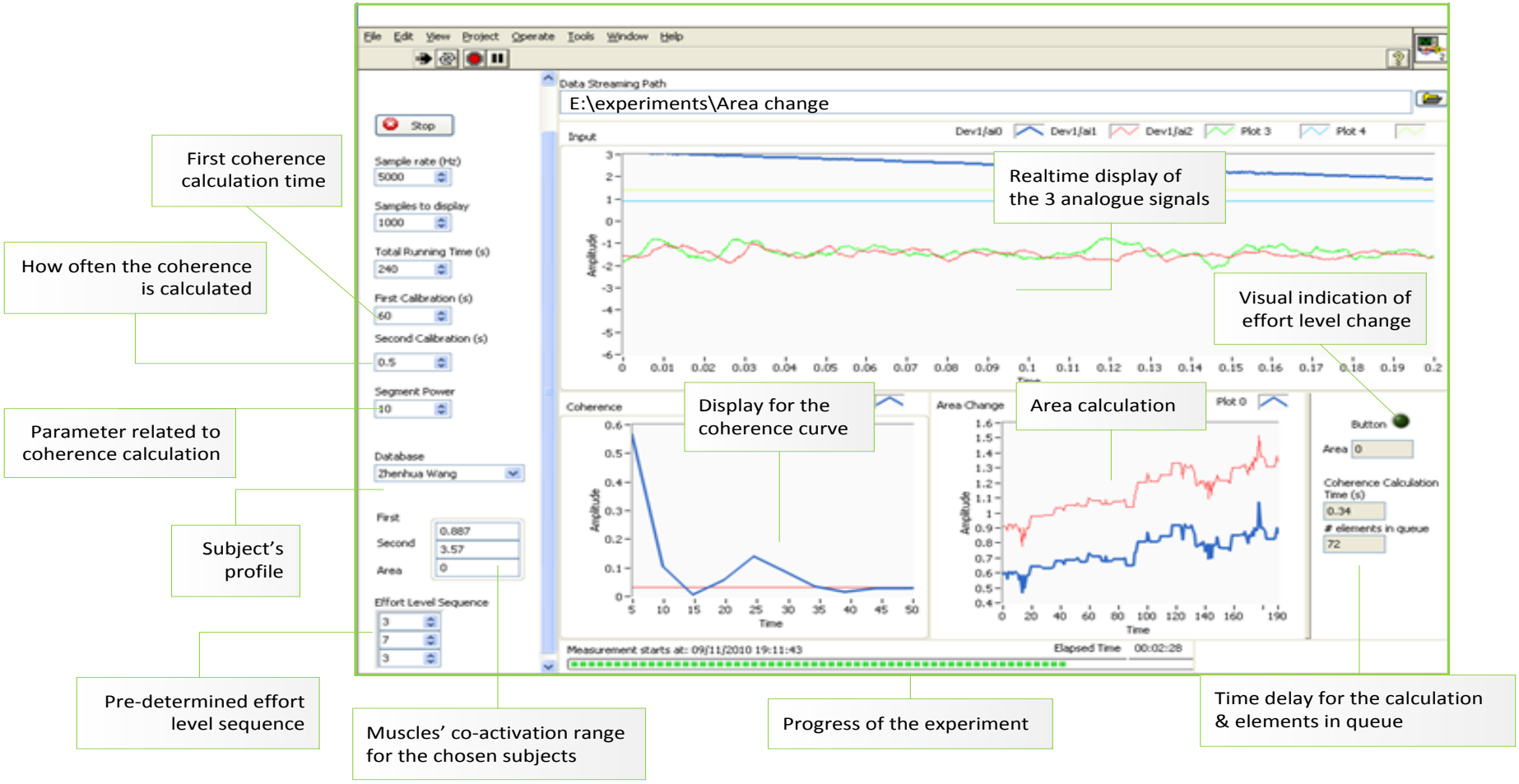

Figure 7. 6: A snapshot of the GUI during an experiment.

7.5 Experiment 1

7.5.1 Aims and initial considerations

This experiment was conducted to find out how the A_{β} and A_{sub} change with effort level changes in real time.

Figure 7. 7 shows what is expected based on our understanding of the matter. From the results of Chapter 6, we know that A_{β} changes with the effort levels in a predictable way. Here two effort levels (3 and 7) of with a large difference are chosen just to see how fast A_{sub} is following the change.

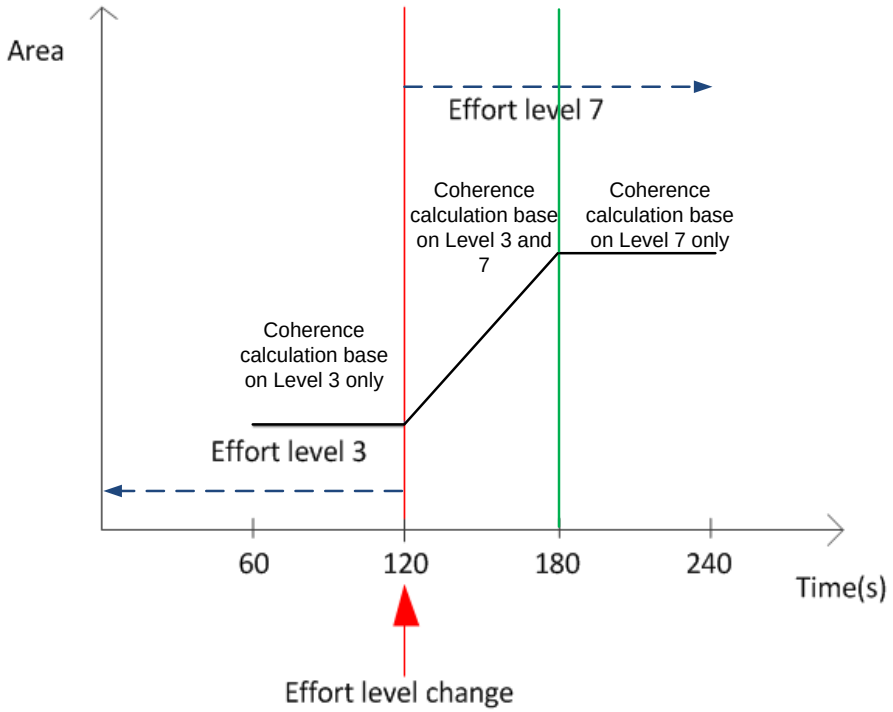

Figure 7. 7: Expected area change with effort level change.

The coherence calculation starts 1 minute after the experiment starts, and the window moves by 0.5s, which means the coherence (hence area) is refreshed every 0.5s. It is expected that for the second minute into the experiment, we shall see a rather straight line with some fluctuations, when the effort level changes at the end of the second minute, with the influence from the EMG at Level 7, a linear increase is expected. From the beginning of the third minute, when the coherence calculation is solely based on the previous minute of data at Level 7, again a horizontal line at a higher area level is expected similar to the pattern seen during the second minute.

7.5.2 Procedures

Five AB subjects were recruited for this experiment, among which Subjects A, B & D had attended the time domain experiments and therefore were familiar with the cycling experiment. Of the other 2 subjects, 1 had some experience (Subject E) and 1 was completely new to the experiment (Subject C).

Subjects were asked to cycle at a constant cadence (60rpm) for a total of four minutes, starting with Level 3 for two minutes. The coherence calculation starts at the end of the 1st minute. The effort level was changed to 7 at the end of the 2nd minute and held for 2 minutes.

7.5.3 Results

The results from the five subjects are plotted separately in Figure 7. 8—Figure 7. 12. The mean A_β from windows just before the effort level change (110-120s, 100-120s) and 1 minute after the effort level change (180-190s, 180-200s) were calculated, and the percentage of change which is defined here as $(Mean_{after} - Mean_{before})/Mean_{before}$ is shown in Table 7. 1.

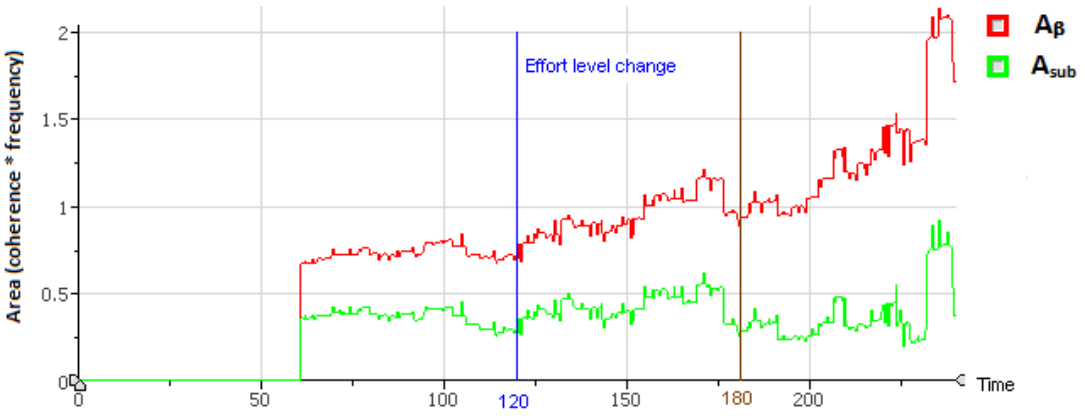

Figure 7. 8: Results from subject A, showing two plots of A_β and $A_{sub.}$ The blue vertical line at 120s indicates the instance of effort level change from 3 to 7. From the start of the coherence calculation to the blue vertical line, the coherence calculation is dependent on the EMG data recorded at Level 3. Between the blue and brown lines (120-180s), the coherence calculation, which is always dependent on the EMG data recorded of the previous minute, is dependent on EMG recorded from both effort levels. Coherence calculated beyond the brown line is solely dependent on EMG data from Level 7.

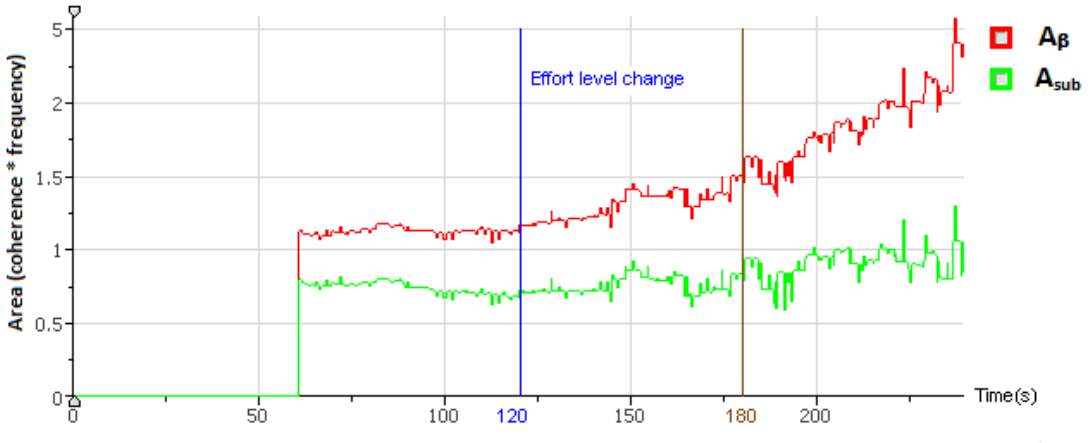

Figure 7. 9: Results from subject B under the same conditions.

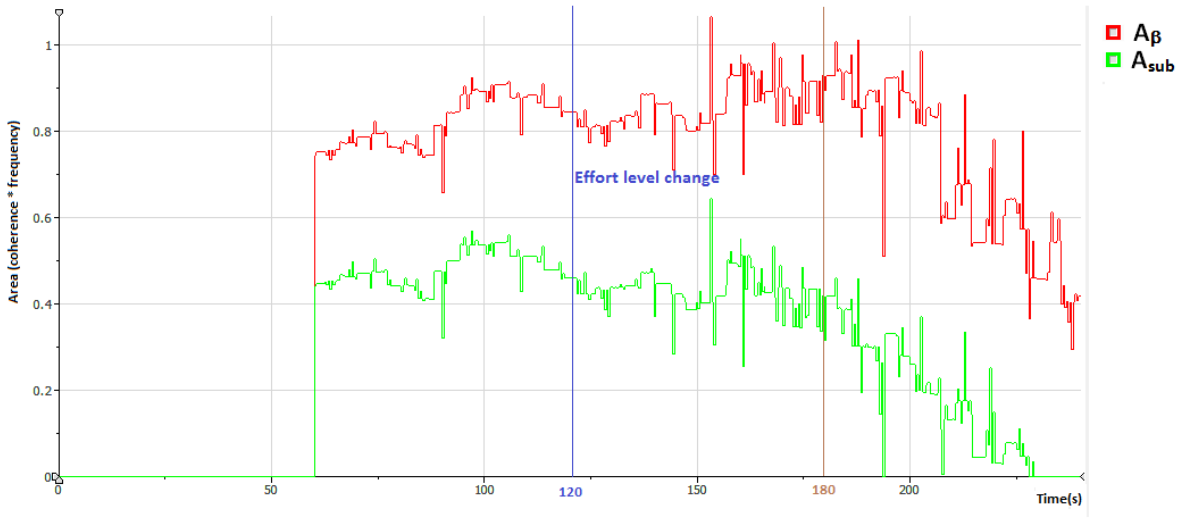

Figure 7. 10: Results from subject C under the same conditions.

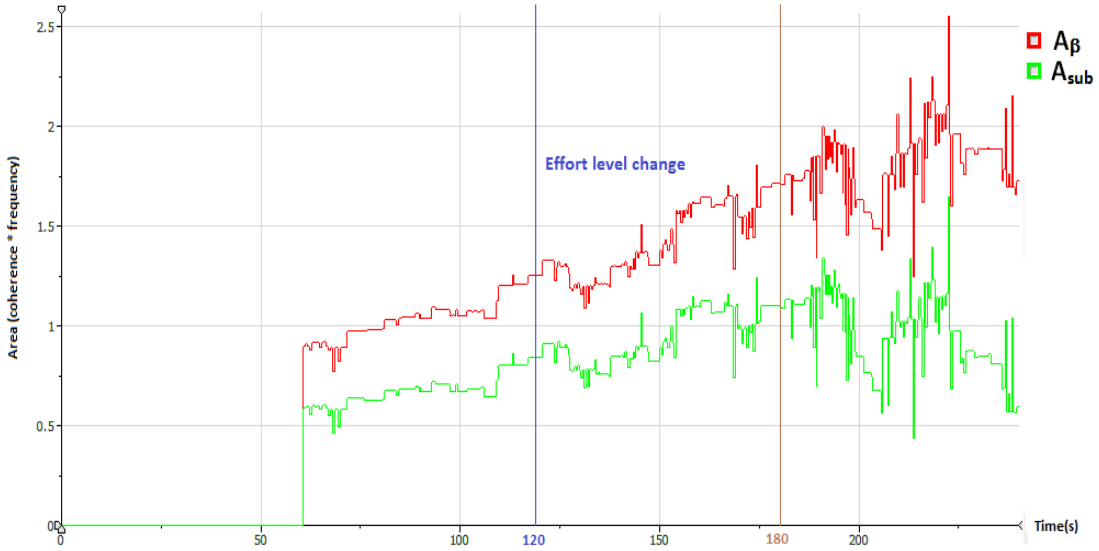

Figure 7. 11: Results from subject D under the same conditions.

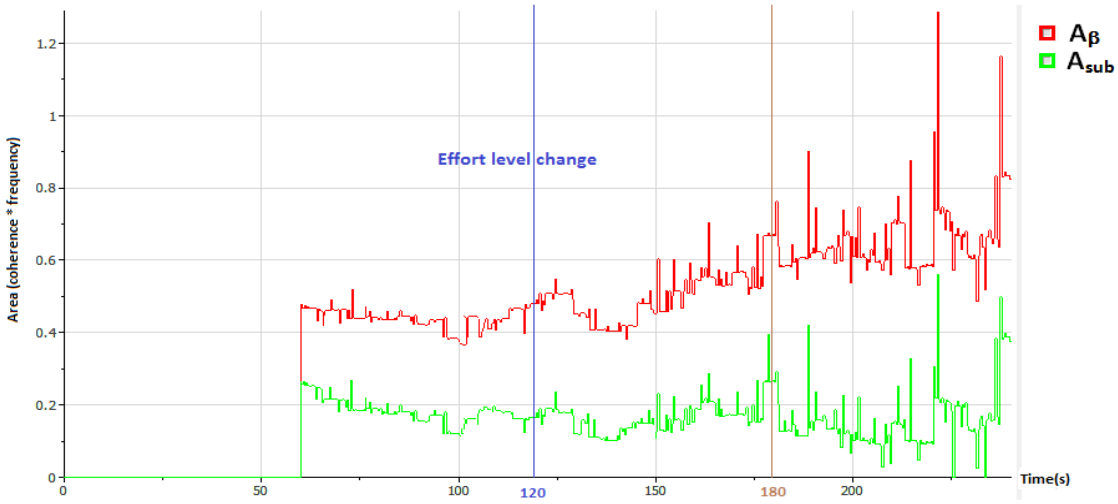

Figure 7. 12: Results from subject E under the same conditions.

Table 7. 1: Increment of mean A_β from selected windows before and after the effort level change (the blue line)

Subject	Mean of Aβ calculated using 10s of data before the effort level change	Mean of Aβ calculated using 10s of data after the effort level change	Increment (%)	Mean of Aβ calculated using 20s of data before the effort level change	Mean of Aβ calculated using 20s of data after the effort level change	Increment (%)
A	0.71	1	40.8	0.74	1	35.1
B	1.13	1.53	35.4	1.13	1.59	40.7
C	0.87	0.92	5	0.88	0.9	2
D	1.22	1.74	42.6	1.15	1.77	53.9
E	0.46	0.62	34.8	0.43	0.63	46.5

7.5.4 Summary

- The LABVIEW program allows real time processing of the data. There is an observed delay in the coherence calculation of around 0.3s, which is considered satisfactory considering that the area is refreshed every 0.5s.

- For the 1st minute of coherence calculation, A_β and A_{sub} remain relatively constant.

- Between 120-180s, A_β and A_{sub} have an increasing trend.

- After 180s and dominantly after 200s, A_β has increased in unexpected way for subjects A, B and D. This increment is not very visible for Subject E with some random spikes. For Subject C, a decreasing trend was seen.

- After 180s and dominantly after 200s, A_{sub} has stayed relatively flat for subjects B and E. The same trend is also seen in Subject A until around 230s, A_{sub} begins to rise with a high plateau. The same decreasing pattern was found in A_{sub} for Subject C. The pattern of A_{sub} is very similar to that of A_β only with lower amplitudes.

- These results are discussed further in 7.7 with the results from Experiment 2.

7.6 Experiment 2

7.6.1. Aims

The results from Experiment 1 show that A_β and A_{sub} both show some unexpected patterns after the first three minutes of the experiments. To further investigate this, a second experiment is conducted in which a longer recording time was used without effort level change. In so doing, we hope to see that if the effort level change is the reason of the events or if they are time related (i.e. fatigue related).

7.6.2. Procedures

In this experiment, 5 subjects were asked to cycle for five minutes at a constant cadence of 60rpm. Two effort levels were used in two separate trials, levels 3 and 7. There was no effort level change during the experiment. Note only A_β is plotted here as the results from Experiment 1 show that two areas are equally affected by the unknown effect.

7.6.3. Results

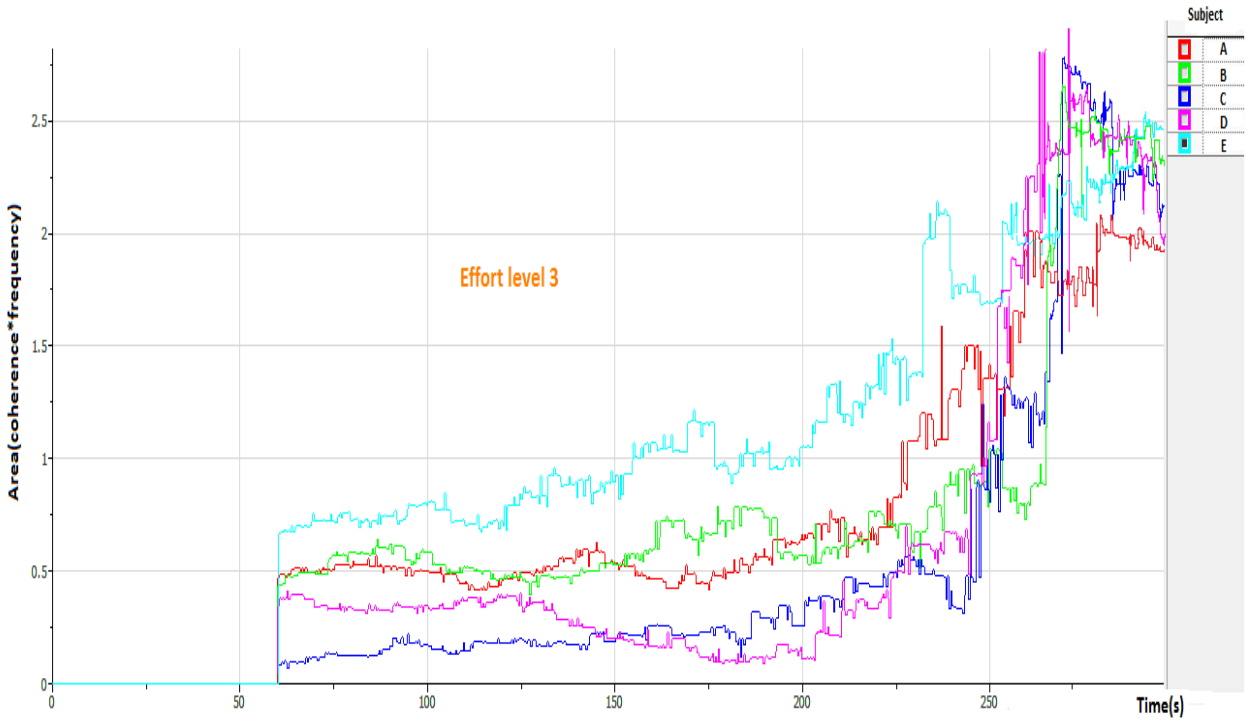

Figure 7. 13: A_β for five minutes of cycling at Level 3 for 5 subjects.

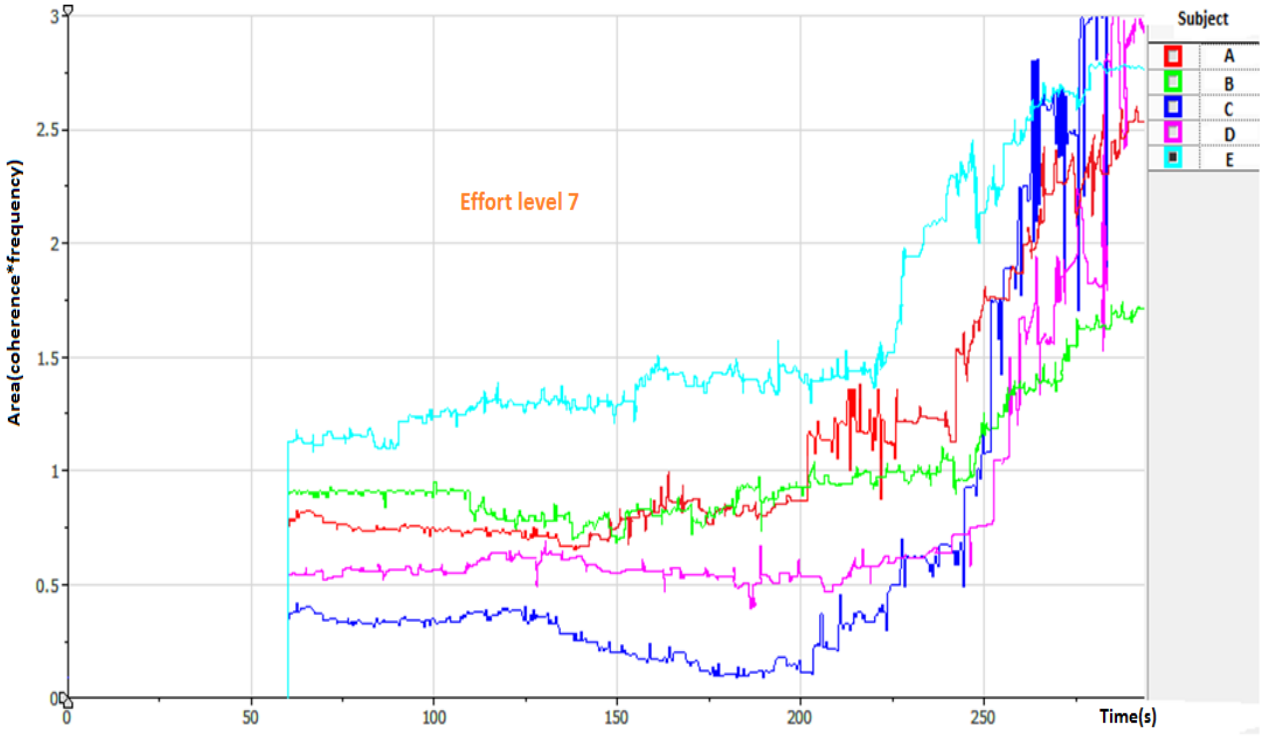

Figure 7. 14: A_β for five minutes of cycling at Level 7 for 5 subjects.

7.6.4. Summary

Level 3

- A_β is quite stable for the first 120s for all subjects.
- Subject D shows a decreasing trend from 120s to 200s.
- Subject E showing a clear increasing trend from 120s to 200s.
- All five subjects begin to show an increasing trend from 200s and the slopes rise after 230s.
- The variations of A_β are large for the five subjects at the same effort level

Level 7

- The first 120s are fairly similar to that of Level 3 but with a higher amplitude.
- Subjects B and D maintain their levels well from 120s to 250s.
- Subject A and E become the irregular earlier than the others at 200s and 225s respectively.
- Subject C shows a decreasing trend from 125s onwards and gradually increases after 200s.

Comparing the two levels:

- A_β is stable in the first 120s
- From 120s-200s, the variations in A_β differs for different subjects. For some subjects, A_β stays relatively constant for some subjects (for example subjects D and E of Level 7); for the others, it begins to show some variations (slightly decreasing or increasing trend).
- Same subjects can behave differently in different trials, the level of A_β varies.
- A sudden increase in A_β after around 235-245s was observed for all subjects at both effort levels.

7.7 Discussion

Two experiments were described in this chapter. Experiment 1 aimed to test A_β and A_{sub} against two effort level change. The two areas (A_β and A_{sub}) follow the same pattern for the first minute of the coherence calculation (60-120s) for all subjects although A_{sub} has lower amplitude than A_β. This is understandable as A_β covers more area than A_{sub}. From the 2nd minute onwards, where we expect to see the linear increase from Level 3 to 7, the two areas begin to show some difference. The increasing trend is much clearer for A_β than A_{sub} for subjects A, B, C and E. For subject C, the two areas do not differ much. In the last minute from 180s to 240s, where the coherence calculation was completely dependent on the EMG obtained at effort Level 7, we expected to see a relatively stable line similar to that of the 2nd minute but only with a higher value. However, this was not the

case. The two areas diverge in the last minute for Subjects A and B. A_β continuous to increase for a reason that is unclear while A_{sub} stays at the same level with some spikes.

In conclusion, A_β and A_{sub} are equally stable in short experiment time and they are equally affected by the unknown event after 3 minutes, which is most likely to be fatigue. Therefore there is no preference in choosing one over the other, and A_β is chosen to be used in Experiment 2.

The coherence calculation is based on long data clips. A_β might indeed be reflecting the effort level change, but is it doing so quickly enough? One of the characteristics we are looking for as a control signal for FES cycling is that it has to reflect the change fairly quickly for a prompt control. As introduced in 6.5.6, the coherence calculation is based on at least 1 minute of data recording. So does it mean we need to wait for a minute to see a significant change in A_β after an effort level change? For example in Experiment 1, when changing the effort level from 3 to 7 at the 2nd minute, the area shows an increasing trend starting from the second minute. Table 7. 1 evaluates the change of mean A_β in 10s and 20s windows before and after the effort level change. Four out of the five subjects show a significant increase in mean A_β between 34.8-42.8 for 10s and 35.1-53.9% for 20s. There is not much increment by doubling the time. Therefore A_β changes respond to the effort level change in around 10s after the change. Subject C is the only one that has a different pattern and his increment after effort level change is small (2% and 5%) compare to the other 4 subjects.

Subject C was new to the experiment and it is quite difficult for people who are unfamiliar with the experiment to keep a constant cadence especially when there is an effort level change. Therefore several trials were performed until we could get a relatively stable cadence. However, since we were doing this at high cycling speed against high resistance levels for long periods, the subjects got tired very quickly despite the breaks given between the sessions. In the experiments of Chapter 6, A_β was calculated for shorter periods of time (3 minutes and 1.5 minutes) compared to the two experiments here. Therefore the time-dependency of the area was never explored, which means it is possible that the coherence not only depends on the effort level but also on some other time-related factors.

A second experiment was conducted trying to find the cause of the increase in area in the 4^{th} minute and whether it was due to the change in the effort level at the second minute. The results from experiment 2 showed that the unexpected trend in the 4^{th} minute is not due to an effort level change, as it still exists when there is no effort level change. Whatever causes this should be time-dependent.

One possible explanation of the reason for the increase at 4 minute could be muscle fatigue (see 3.9). However, shouldn't we see this pattern earlier in the Level 7 results (Figure 7. 14) than the Level 3's (Figure 7. 13)? In the Level 3 result, we could say that the rise began around 235-245s for all subjects. The range for the Level 7 trials is slightly later than that (around 245-250s). In both cases, subject E led the other four subjects by around 5s. A design flaw of experiment 2 is that all the subjects were asked to do the Level 7 trials first as it was more tiring. Therefore it is difficult to tell if the slight lead we found in the Level 3 results is meaningful. It could be the subjects were not

completely recovered although a 10 minutes of break was given. Proper randomised tests should be planned to understand this further.

In conclusion, A_{β} (and similarly A_{sub}) cannot be used as a control signal of the proposed FES cycling system as its characteristic is only predictable for around 3 minutes. The cycling system aims to work as part of a function recovery routine for SCI patients and therefore it should provide a reliable cycling session of reasonable duration (say 20 minutes). It is possible that reducing the cycling speed could extend the predictable pattern of the area longer. The cycling speed used in the experiments was 60rpm which was quite fast even for healthy subjects. The reason of choosing such high speed is to see the maximum possible muscle activity at the chosen effort levels. Such a high speed should only be used in the experimental phase and it is not suitable for SCI patients.

CHAPTER 8 GENERAL DISCUSSIONS, CONCLUSIONS AND FUTURE WORK

8.1 The research question

People with ISCI have paretic muscles and retain reduced voluntary control of these muscles. Below the lesion, the inactive motor units in the muscles can still be stimulated to contract artificially. FES is used together with traditional physiotherapy for the rehabilitation of ISCI patients. Recovery of lost functions or reduction in disability is sometimes found in some patients after FES treatment. The recovery of lost function, which can be short-lasting or long-lasting, is called "carry-over effect". The exact mechanism of carry over effect remains an enigma. Rushton's hypothesis suggests that the carry-over effect is due to the combination of the voluntary effort and the artificial AP which makes the muscle contract, bringing about a re-learning process. However, this hypothesis has never been tested and a first step to the testing would be the measurement of the voluntary drive. During the course of this research only AB subjects were used.

The research questions investigated are:

1. *Can we find a signal to represent the subject's voluntary drive during FES cycling?*
2. *Can this signal be used as a control signal to modulate the stimulation of FES cycling?*

At this stage of the project, we are able to answer both questions.

1. Yes. We have successfully found signals that relate to the subject's voluntary drive in both time domain and the frequency domain. In the time domain, it is the RMS EMG amplitude measured from selected time windows after the stimulation. In the frequency domain, it is the area under the coherence curve between synergistic muscles.

2. No. When evaluating these signals against different effort levels (power output), it was found neither of them was appropriate as a control signal for the FES cycling system. The signal either showed excessive variation for the same effort level, or, its relation with the effort level alters with exercise time.

8.2 Summary of the findings

This section discusses the findings of this thesis in terms of two important contributions made, namely:

1. The development of the assorted hardware for an FES cycling system.

2. The estimation of voluntary drive in the time domain and the frequency domain;

8.2.1 The FES cycling system

Assorted apparatus were designed and constructed for this project, including the commutator, the stimulator, the EMG amplifiers, isolation amplifiers, and the control box. Some other apparatus were adapted and modified to be used with the FES cycling system, like the CC EMG amplifier, the biphasic stimulator, the shaft encoder and the ergotrainer. If we refer back to Figure 21, the block diagram of the planned FES cycling system, the development of all the illustrated devices has been completed. The FES cycling system provides a platform used to carry out all the experiments described in Chapters 4-7 and enables the testing of the proposed methodologies of the voluntary drive estimation.

8.2.2 The voluntary drive estimation in the time domain

This method was based on research conducted in 2004 by our group (the IDG group, UCL). A method of simple EMG control of FES cycling was described (Norton et al. 2004) where RMS EMG from pre- and post-stimulus windows were plotted and compared. This project expanded on their idea by looking at a larger number of windows as well as the comparison of the RMS EMG with the effort levels.

A major difficulty of the time domain method is the elimination of the stimulation artefacts and other reflexes. With the aid of blanking amplifiers, we were able to record RMS EMG amplitudes in a range of post-stimulus windows soon after the stimulation. These amplitudes were compared to the pre-stimulus amplitude measured just before the stimulation which was considered to be a good representation of the voluntary drive. High correlations were found between the post-stimulus amplitude and pre, which proves that it is possible to extract a signal from the recorded EMG during stimulation to represent the subject's voluntary drive. However, further tests show that these amplitudes suffer from huge variations in each subject and effort levels. Therefore it was decided that the time domain method was not suitable for the estimation of the voluntary drive.

8.2.3 The voluntary drive estimation in the frequency domain

In the time domain analysis, the presence of the stimulus artefact made it difficult to analyse the data to determine the voluntary drive. However, this problem was eliminated by performing an analysis in the frequency domain. This was because the frequency spectrum of the stimulus artefact and other reflexes, has a different frequency range as compared to that of the signal of interest, namely the coherence frequency. Consequently it is easy to filter out the stimulus artefact. This following findings are summarised from the experiments:

1) Significant coherence can be found between synergetic muscles during cycling. The calculation of the coherence requires at least one minute of EMG data which are selected during coactivation of the muscles.

2) The area below the coherence curve was found to be increasing with the increasing effort levels. However, it was noticed that the intra-subject variability of the area is large, which means one cannot use the area to predict the effort level without knowing the baseline of the subjects for at least one effort level.

3) The two areas, A_{β} and A_{sub} can be used to represent a change in effort level, provided the duration is short

4) The two areas are both found to be unsatisfactory after roughly three minutes of cycling, as their relation to the effort level become unpredictable.

5) Further experiments show that the effort level change is not the cause of the characteristic change after 3 minutes.

6) The most likely cause of such findings is muscle fatigue.

8.3 The major achievements

The major achievements of this project have been:

- Development of the essential apparatus that constitute the FES cycling system as well as realisation of the angle triggered stimulation using developed hardware.
- Proof that using the post-stimulus EMG amplitudes to predict the pre-stimulus EMG amplitude is reliable.
- Show that the averaged RMS EMG amplitude can reflect in change in effort level (power output).
- Successfully measured EMG-EMG coherence during FES without the influence of stimulation artefacts in the coherence spectrum.
- Comparison of the two areas under the coherence curve, A_{sub} and A_{β}, and how these areas can be used to reflect a change in effort level.
- Observation of time/fatigue related change in the area under coherence curve in the β band during cycling.
- Development of the real-time recording, process and control program in LABVIEW.

8.4 General discussions

What are the shortcomings with the two voluntary drive measurement methods?

1. Time to get a reliable reading is long.

Time domain method

The method of using RMS EMG in short windows to predict effort level change will work, providing that the EMG is averaged over many revolutions. In chapter 5, when averaging the RMS EMG over roughly 30s (30 revolutions), the mean amplitude can reflect the corresponding effort level but with a shallow slope. Therefore there is a tradeoff between the number of revolutions to average over and the accuracy of the estimation.

Frequency domain method

The coherence is calculated using a moving window of 1min, refreshed every 0.5s. Therefore any change in the coherence also takes time to become evident, as the data after the change is only a small proportion of the 1 minute data in the beginning. This method will work better if we could find a way to identify the change more quickly (i.e. not waiting for a minute after the change). A possible way to enhance the signal is to record coherence from multiple synergistic muscles. For example, we have done this with the RF, VM & VL combinations in 6.4, and found coherence between each pair. It is possible that coherence from the combinations of these muscles be used together to infer a change in the effort level more quickly; hence making the coherence method more effective.

2. Both methods are affected by fatigue

Fatigue seems to influence both of our methods. In the time domain method, when the subjects begin to fatigue, their RMS EMG amplitudes also decrease, which results in the RMS EMG amplitude not representing the correct effort level the subject was cycling at. However, this would not be a problem if we do not use the effort level but use the corresponding power output as a reference. Thereby the subjects can change their cadence and power output freely, and the RMS EMG amplitude can be calculated with the output power. This should provide a more accurate evaluation of the time domain method.

In the coherence plot, an anomaly occurred in the signal after three minutes of cycling. This anomaly was considered to be related to fatigue. It is reasonable to suspect that when the subjects start to fatigue, their intention to maintain the constant cadence may result in higher voluntary drive to the muscles. This may be the reason of the dramatic increase in the results. Further analysis is needed to provide more information. It may have been better to use lower effort levels and/or lower cycling speed for the experiments. In so doing the effect of fatigue would have been reduced and the exercise duration extended.

8.5 Critical evaluation of the experiments

A few design flaws have been noticed for Chapter 7 Experiment 2:

- By using effort Level 7 before level 3 (where level 7 required more effort to pedal against, hence increasing the rate of fatigue as compared with level 3), the results were biased and it was impossible to conclude the influence of higher effort level (hence earlier fatigue) on the coherence calculation.
- A 10 minute rest interval between experiments may not have been sufficient for the subjects to fully recover from the exercise. A longer break may have yielded better results.
- To achieve real time recording, processing and control of the system, the LABVIEW program was written to save data to the hard disk, representing only the area and the relative timing information. Therefore, it is not possible to do any further analysis on the same data set. For example, it would be informative to see if the frequency shift described in 3.9.1, which is often

found with muscle fatigue, existed in the data captured during the 4th minute of cycling, where irregularities were seen.

The subjects

A small number of subjects were used in this project. For most of the experiments, five subjects were used, and, in some occasions four. The results from the time domain method were consistent for the five subjects. However, for the frequency domain method, the results were diverse, especially during the last minute of cycling. Therefore it is difficult to draw a conclusion about the general pattern seen for the subjects, as the sample size was too small.

The FES cycling system is designed for rehabilitation of ISCI patients. Prior to the experiments with the ISCI patients, the methods and the apparatus were tested with AB subjects. The EMG signals measured from ISCI patients will have much lower amplitude and would therefore be more difficult to detect and to interpret. It is reasonable to think that if the measured voluntary drive cannot be used as a reliable control signal for AB subjects, there is no need to test them on ISCI patients.

8.6 Future work

8.6.1 Measure the power output with O-tec power transducer

The effort levels used as an indication of power output, throughout the thesis, were measured using the cycling computer connected to the ergotrainer. It would be more accurate and informative if we could measure the power output with a more suitable apparatus. An O-tec power transducer could be used for this purpose. The O-tec transducer enables the simultaneous measurement the force applied to the pedals as well as the power output, while cycling. It can improve the time domain method by replacing the effort levels with more accurate assessment of the power output. It will also be used in the future experiments as planned in 8.6.2.

8.6.2 Further investigation of the change in coherence spectrum and its relationship with fatigue

The exercise time related coherence change seen in this thesis, has not been previously reported on. We expect that this change occurs due to fatigue. A proposed experiment to investigate this is:

Aims

1. Can this change in coherence be delayed by using lower effort level and/or lower cadence?
2. How does the frequency spectrum of the EMG signals change when the change in coherence happens?

Procedures

1. Subjects are recruited to cycle at constant cadence at 30rpm under constant load level 3.
2. Recording raw EMG from VM, VL and RF, as well as power output from the power transducer.
3. Monitor the change in A_β, until an abnormal change (event) is seen.

4. Post processing could involve relating the event to changes in frequency shift (compared to the frequency spectrum when there is no fatigue, see 3.9.1, e.g. first a few minutes of cycling could be used as a reference).

Expectations

The change in the area plot is expected to be delayed by the reduced cadence and the load. Such a delay would indicate that the event is truly fatigue-related. It will also be informative to know how the power output changes when the event happens. We also expect to see changes in the frequency spectrum for the EMG signals.

8.6.3 Alternative ways of measuring the voluntary drive

As the use of EMG to estimate the voluntary drive, both in the time domain and the frequency domain, was found to be an unreliable control signal for the FES cycling system, an alternative method should be considered. One possibility is the use of EEG measurements as an estimation of the voluntary drive. It has been shown that EEG can be used to detect a patient's motor intention to activate a paralyzed limb. This types of EEG measurements have been used in so called Brain Computer Interfaces (BCI), to control FES systems (Do et al., 2011; Wang et al., 2010).

A BCI is a technology that provides a communication platform for patients with motor impairments. The range of real world applications of BCIs have increased in recent years due to the development of more technically reliable systems, and the successful testing of different applications with patients (Machado et al., 2010). The basic mechanism of a BCI is shown in Figure 8. 1. Signals from the brain are acquired by electrodes on the scalp or in the head and processed to extract specific signal features that reflect the user's intent. An event-related desynchronisation (ERD), which is a specific EEG signal from the motor area is often chosen to represent the motor intentions. The detection of ERD is then translated into commands that operate a device.

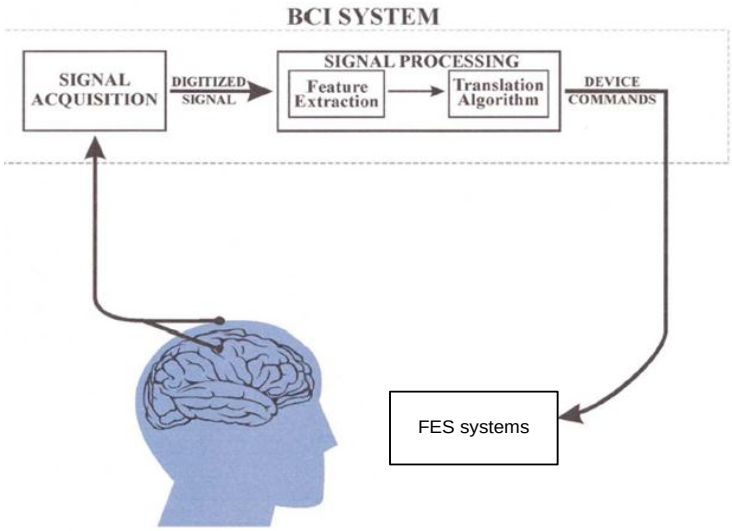

Figure 8. 1: Basic design and operation of a BCI-controlled FES system.

Recent studies have demonstrated that subjects can control a cursor on a computer screen using EEG (Wolpaw & Birbaumer, 2002). However, such a system will require training of the subjects. Without training, many subjects cannot extract ERD when they are engaged in motor imagery (McFarland et al., 2000). It has been reported that ERD can be extracted after a few months of real-time feedback training (Müller-Putz et al., 2005). So far there is no reported literature on BCI with FES cycling.

A possible way of initiating the EEG signal for cycling could be playing a visual game in front of a subject, showing a cyclist cycling with detailed leg movements on the screen. The subject will be asked to imagine himself being the cyclist and try to match the leg movements. In this way we might be able to record an ERD that represents the subject's intention to pedal and is phase-locked to the pedalling sequence. The ERD might be used as a control signal to the FES cycling system. Such a system might provide an alternative to EMG-controlled FES cycling and would have the added benefit of making enhanced functional recovery available to patients with both complete and incomplete spinal cord injury.

APPENDIX

Appendix A: Information Sheet for Participants in Research Studies

You will be given a copy of this information sheet.
Title of Project: Can the voluntary drive to a paretic muscle be estimated from the myoelectric signal during stimulation?

This study has been approved by the UCL Research Ethics Committee [Project ID Number]: 0900/001
Name, Address and Contact Details of Investigators: Runhan Luo
Medical Physics and Bioengineering Department
UCL Gower Street
London WC1E 6BT
You are being invited to take part in a research study. Before you decide it is important for you to understand why the research is being done and what will involve. Please take time to read the following information carefully and discuss it with others if you wish. Ask us if there is anything that is not clear or if you would like more information. Take time to decide whether or not you wish to take part. Thank you for reading this.

What is the purpose of the study?
We would like you to consider taking part in a research project that investigates the relationship between voluntary effort and the electrically recorded muscle signal, during electrical muscle stimulation. We wish to see if we can use this signal to control the stimulation in a cycling system to benefit partially paralyzed patients, and therefore we are asking you to take part in 2 experiments which the procedures are stated afterwards.

Why have I been chosen?
Participants to be chosen will be required to be physically active, neurologically normal and healthy with no current medication.

Do I have to take part?
It is up to you to decide whether or not to take part. If you choose not to participate it will involve no penalty or loss of benefits to which you are otherwise entitled. If you decide to take part you will be given this information sheet to keep and be asked to sign a consent form. If you decide to take part you are still free to withdraw at any time and without giving a reason.

What will happen to me if I take apart?
The study will involve attending the laboratory on one day only. On that day we will ask you to sit on a semi-recumbent static tricycle. Stimulation and recording electrodes will be placed on your leg. You will be asked to cycle with a constant power which will be displayed to you using a simple

display screen. The tricycle will have a motor to help you maintain a constant speed of revolution. At fixed points in the cycle we will stimulate your leg using a simple stimulator.
Procedures:
Upon selection to participate in this study the subject will be asked to undergo 2 trails, each taking about 5 minutes. They are going to pedal a stationary tricycle. Surface electrodes will be stick on their skin and record the Electromyography （EMG） signals from the various muscles.
For the two trials:
Trial 1: The subject will be required to relax all his/ her leg muscle during the stimulation.
Trial 2: The subject will be required to consciously want to use his/her muscles during the stimulation.

Possible side-effects and risks

The electrical stimulation may produce a tingling sensation underneath the electrodes. This is normally unpleasant but not painful, please tells us if it is and we will reduce or stop the stimulation. The stimulation may also produce some reddening of the skin underneath the electrodes. This normally disappears within a couple of hours.
What are the possible benefits of taking part?
The study will be of no direct benefit; however the information we get from this study may help us to treat future patients with incomplete spinal injury better and develop novel treatments for them.

What if something goes wrong?

If you are harmed by taking part in this research project, there are no special compensation arrangements. If you are harmed due to someone's negligence, then you may have grounds for a legal action but you may have to pay for it. Regardless of this, if you wish to complain, or have any concerns regarding this study, the UCL ethics committee should be available to you.

Will my taking part in this study be kept confidential?

All information which is collected about you during the course of the research will be kept strictly confidential. Any information about you which leaves the university will have your name and address removed so that you cannot be recognized from it. The data we collect from you will include your name, age and sex. Miss Runhan Luo will be responsible for the data throughout the study and the "data controller" will be UCL.

What will happen to the results of the research study?

The research from the study will be published on completion of the study. You will not be identified in any report or publication.
Contact for further information
If you have further questions for concerns regarding participation in this research study you may contact:
Miss Runhan Luo on 020 7679 0296
Prof. Nick Donaldson on 020 7679 0265
(from 9am to 5pm)

All data will be collected and stored in accordance with the Data Protection Act 1998.

Appendix B: A summary of onset determination criteria

Author	Burst	Baseline	Signal processing	Method
Neafsey et al. (1978)	Two consecutive 50 ms bins >2 SD from baseline activity	Initial 500 ms of 2s before stimulus	Averaged in 50 ms epochs	Computer-based
Greenisen et al. (1979)	RMS>RMS threshold for >2 windows of 50 ms (threshold criteria not stated)	–	1000 Hz low pass filter	Computer-based
Nashner et al. (1983)	First deviation >1.5 SD from baseline	100 ms prior to stimulus	40 Hz low pass filter	Not stated
DiFabio (1987)	>3 SD beyond baseline for 25 ms	50 ms prior to stimulus	50 Hz low pass filter	Computer-based
Lee et al. (1987)	>2 SD beyond baseline for 40 ms (both mean and median of sample)	500 ms quiet standing prior to stimulus	10–100 Hz band pass filter	Computer-based
Chanaud and Macpherson (1991)	>2.5 SD beyond baseline	100 ms quiet stance	? Hz low pass filter	Not stated
Studenski et al. (1991)	3 × baseline for 8 of 16 ms	100 ms quiet standing	?	Not stated
Happee (1992)	Segment of *n* samples>previous segment at 5% significance level and following sample>previous at 5% significance level and current sample and following sample>30% maximal signal (n = 20% of movement duration)	?	500 Hz low pass filter	Not stated
Bullock-Saxton et al. (1993)	15% maximal contraction for cycle of gait	?	?	Not stated
Bullock-Saxton (1994)	5% of peak magnitude of burst	500 ms prior to burst	Low pass filter, subtraction of baseline mean	Computer-based
Steele (1994)	>1 SD beyond baseline for 80 ms (not below for >16 ms)	240 ms prior to signal to move	6 Hz low pass filter	Computer-based
Karst and Willet (1995)	>1 SD beyond baseline, visually verified on computer screen and modified if inaccurate	First 15 ms of sampling window	Ensemble average of four trials	Computer-based
Thompson and McKinley (1995)	>95% confidence interval for >10 ms	–	10–500 Hz band pass filter	Not stated

Appendix C: Regions of on-off muscle activity for individual test subjects for the same experimental setups (Jorge & Hull, 1986)

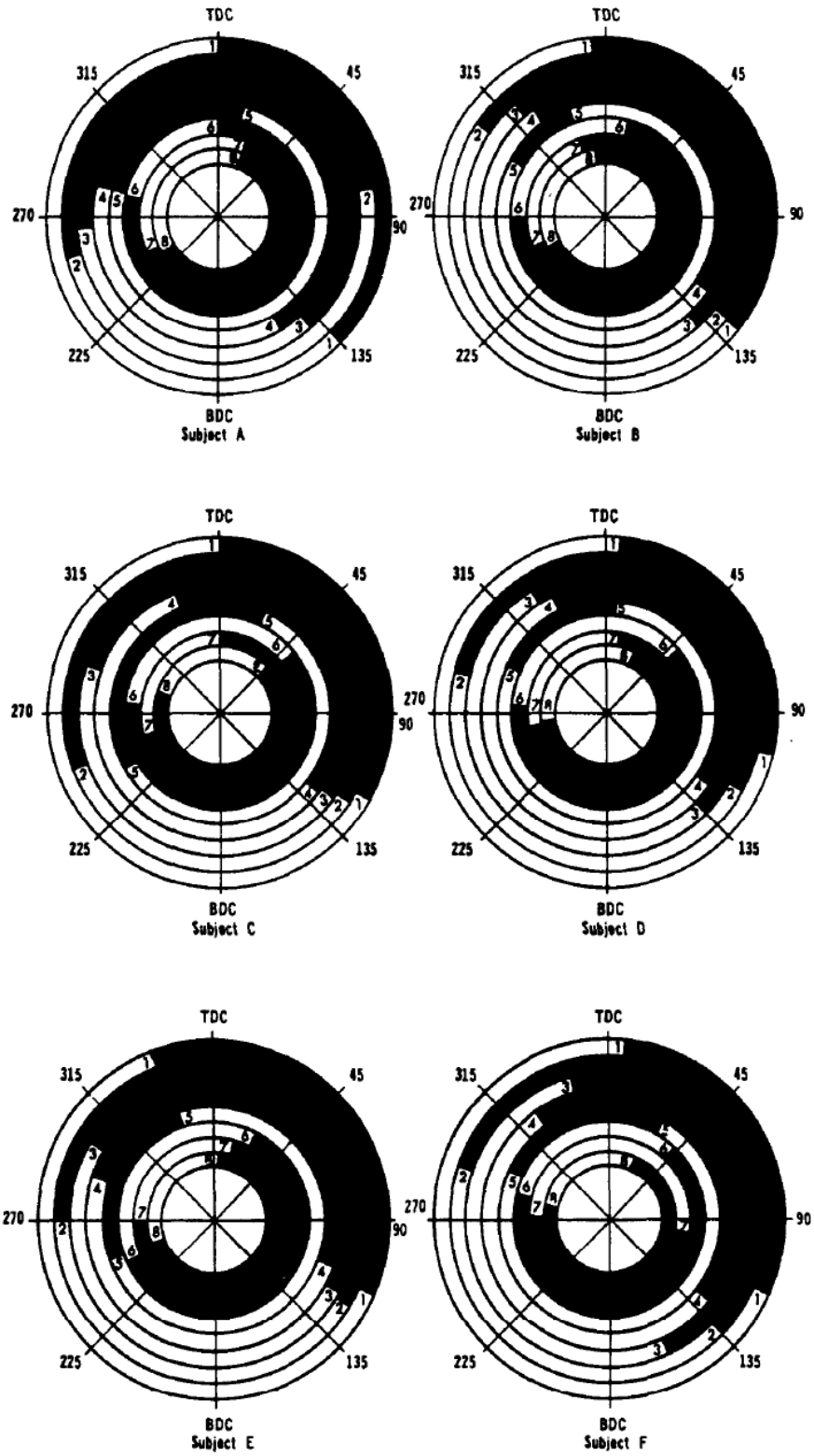

Appendix D: Guidelines of electrode placement for the 4 muscles used in this project (SENIAM, 2010)

Muscle	
Name	Quadriceps Femoris
Subdivision	rectus femoris
Muscle Anatomy	
Origin	Straight head from anterior inferior iliac spine. Reflected head from groove above rim of acetabulum.
Insertion	Proximal border of the patella and through patellar ligament.
Function	Extension of the knee joint and flexion of the hip joint.
Recommended sensor placement procedure	
Starting posture	Sitting on a table with the knees in slight flexion and the upper body slightly bend backward.
Electrode placement	
- location	The electrodes need to be placed at 50% on the line from the anterior spina iliaca superior to the superior part of the patella
- orientation	In the direction of the line from the anterior spina iliaca superior to the superior part of the patella.
- fixation on the skin	(Double sided) tape / rings or elastic band.
- reference electrode	On / around the ankle or the proc. spin. of C7.
Clinical test	Extend the knee without rotating the thigh while applying pressure against the leg above the ankle in the direction of flexion.
Remarks	The SENIAM guidelines include also a separate sensor placement procedure for the vastus medialis and the vastus lateralis muscle.

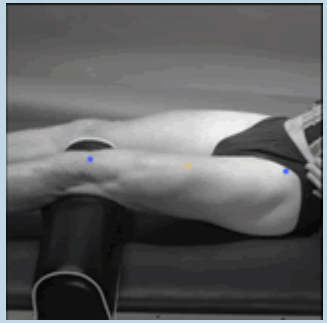

Click on image for larger view

Muscle	
Name	Quadriceps Femoris
Subdivision	vastus medialis
Muscle Anatomy	
Origin	Distal half of the intertrochanteric line, medial lip of line aspera, proximal part of medial supracondylar line, tendons of adductor longus and adductor magnus and medial intermuscular septum.
Insertion	Proximal border of the patella and through patellar ligament.
Function	Extension of the knee joint.
Recommended sensor placement procedure	
Starting posture	Sitting on a table with the knees in slight flexion and the upper body slightly bend backward.
Electrode placement	
- location	Electrodes need to be placed at 80% on the line between the anterior spina iliaca superior and the joint space in front of the anterior border of the medial ligament.
- orientation	Almost perpendicular to the line between the anterior spina iliaca superior and the joint space in front of the anterior border of the medial ligament.
- fixation on the skin	(Double sided) tape / rings or elastic band.
- reference electrode	On / around the ankle or the proc. spin. of C7.
Clinical test	Extend the knee without rotating the thigh while applying pressure against the leg above the ankle in the direction of flexion.
Remarks	The SENIAM guidelines include a separate sensor placement procedure for the vastus lateralis and the rectus femoris muscle.

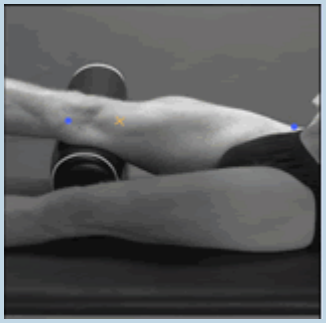

Click on image for larger view

Muscle	
Name	Quadriceps Femoris
Subdivision	vastus lateralis
Muscle Anatomy	
Origin	Proximal parts of intertrochanteric line, anterior and inferior borders of greater trochanter, lateral lip of gluteal tuberosity, proximal half of lateral lip of linea aspera, and lateral intermuscular septum.
Insertion	Proximal border of the patella and through patellar ligament.
Function	Extension of the knee joint.
Recommended sensor placement procedure	
Starting posture	Sitting on a table with the knees in slight flexion and the upper body slightly bend backward.
Electrode placement	
- location	Electrodes need to be placed at 2/3 on the line from the anterior spina iliaca superior to the lateral side of the patella.
- orientation	In the direction of the muscle fibres
- fixation on the skin	(Double sided) tape / rings or elastic band.
- reference electrode	On / around the ankle or the proc. spin. of C7.
Clinical test	Extend the knee without rotating the thigh while applying pressure against the leg above the ankle in the direction of flexion.
Remarks	The SENIAM guidelines include also a separate sensor placement procedure for the vastus medialis and the rectus femoris muscle.

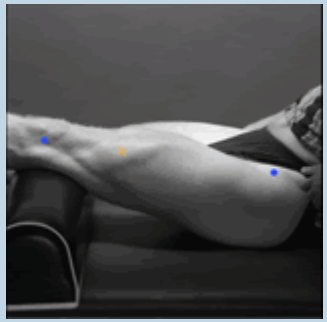

Click on image for larger view

Muscle	
Name	Biceps femoris
Subdivision	Long head and short head
Muscle Anatomy	
Origin	Long head: distal part of sacrotuberous ligament and posterior part of tuberosity Short head: lateral lip of linea aspera, proximal 2/3 of supracondylar line and lateral intermuscular septum.
Insertion	Lateral side of head of fibula, lateral condyle of tibia, deep fascial on lateral side of leg.
Function	Flexion and lateral rotation of the knee joint. The long head also extends and assists in lateral rotation of the hip joint.
Recommended sensor placement procedure	
Starting posture	Lying on the belly with the face down with the thigh down on the table and the knees flexed (to less than 90 degrees) with the thigh in slight lateral rotation and the leg in slight lateral rotation with respect to the thigh.
Electrode placement	
- location	The electrodes need to be placed at 50% on the line between the ischial tuberosity and the lateral epicondyle of the tibia.
- orientation	In the direction of the line between the ischial tuberosity and the lateral epicondyle of the tibia.
- fixation on the skin	(Double sided) tape / rings or elastic band.
- reference electrode	On / around the ankle or the proc. spin. of C7.
Clinical test	Press against the leg proximal to the ankle in the direction of knee extension.
Remarks	

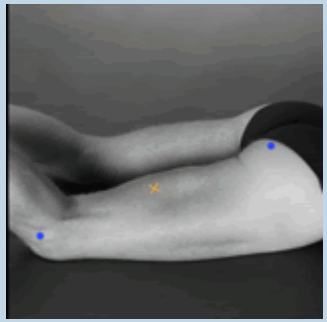

Click on image for larger view

Appendix E: Effort level detection

Effort level change is an important factor that was used in both time domain and frequency domain methods. In the previous experiments, the effort levels were set for in a certain trial, which means there is no need to monitor the change of it. However, when it came to the real-time feedback control loop tests, the effort level was altered during a session of the experiment. Problems were found when trying to detect when the change happened. The ergotrainer used is a TACX Grand Excel (model T1640) which was discontinued. Without its original CD & cable to connect to the control unit, we were unable to monitor the effort level change or speed which is shown on the cycling computer. Two attempts were made to detect the timing of the effort level change.

1. When changing the effort level, there is a series of buttons that needed to be pressed. The change is not effective until it is stored, & the sound of the “store” button is at a higher frequency (around 4200Hz) and amplitude (about 25 times higher) than the other buttons (mainly at low frequencies around 200Hz) after passing through a FFT function. It also has a narrow bandwidth which is quite easy to identify. Therefore, a real-time signal detection program was written in LABVIEW to allocate this unique sound with a microphone taped to the speaker of the control unit. This signal was treated as the indication of effort level change. The features we were looking for are the amplitude and the bandwidth.

However, this method is quite sensitive to the environmental noise and for some reason the amplitude as well as the bandwidth of the ”store” button sound signal is not very stable and in some rare cases, a change in effort level might be missed because of the criteria we set. Therefore this method is not appropriate.

2. To be 100% sure of capturing the change, the control unit was taken apart and the PCB was studied trying to identify the trace representing the effort level change. Wires were then soldered to the tracks and connected to the digital input channels of the DAC. Therefore the detection is much more reliable in this manner.

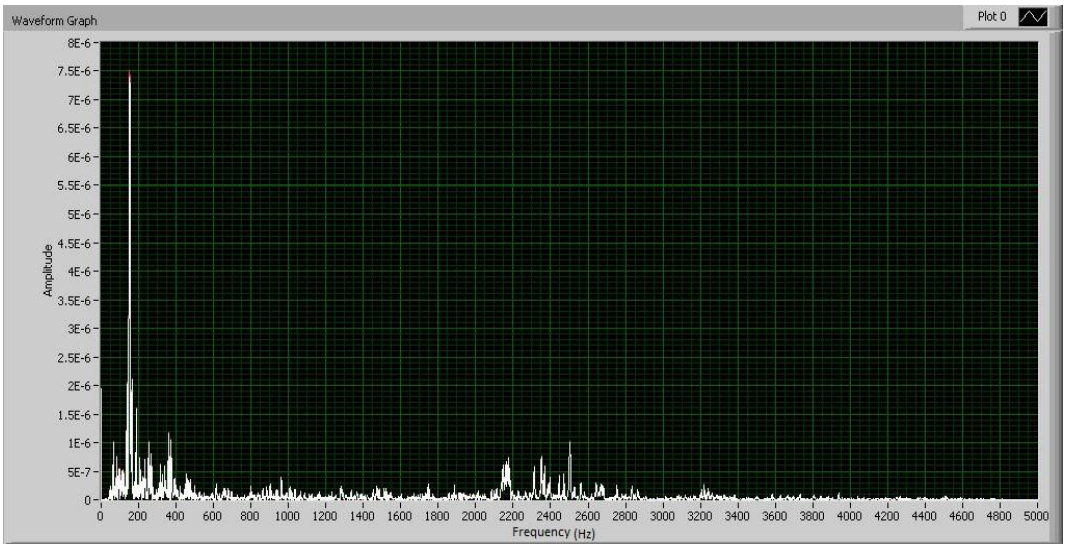

Figure A. 1: FFT of the other button sound

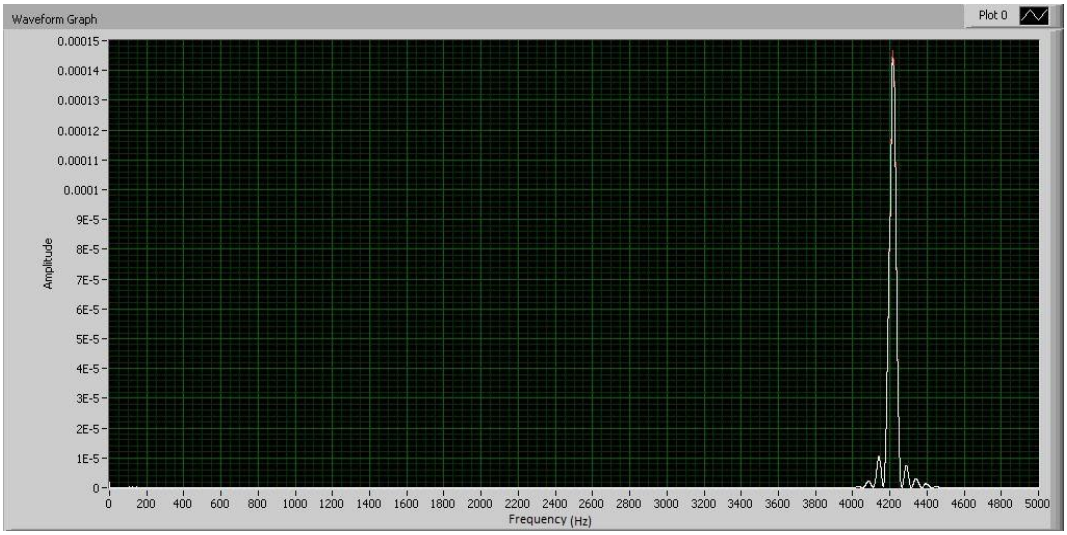

Figure A. 2: FFT of the “store” button sound

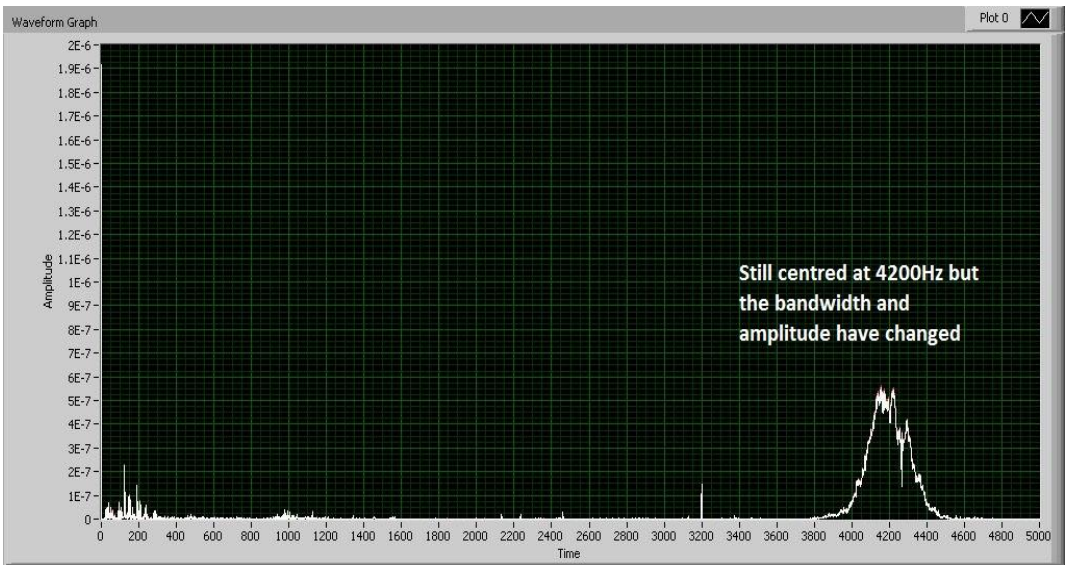

Figure A. 3: FFT of the “store” button sound in very rare cases

References

Allum, J. H. J., & Pfaltz, C. R. (1985). Visual and vestibular contributions to pitch sway stabilization in the ankle muscles of normals and patients with bilateral peripheral vestibular deficits. *Experimental Brain Research*, *58*(1), 82–94–94.

Amjad, A. M., Halliday, D. M., Rosenberg, J. R., & Conway, B. A. (1997). An extended difference of coherence test for comparing and combining several independent coherence estimates: Theory and application to the study of motor units and physiological tremor. *Journal of Neuroscience Methods*.

Analog Devices Inc. (1999). (2009). *Data Sheets (AD620, ADG419, OP200, OP07).* (p. http://www.analog.com).

Apparelyzed spinal cord injury peer support. (2010). Spinal Cord Injury Statistics. Retrieved February 27, 2011, from http://www.apparelyzed.com/statistics.html

ASIA. (2010). ASIA | American Spinal Injury Association. Retrieved January 28, 2011, from http://www.asia-spinalinjury.org/publications/store.php

Babb, T. L., Mariani, E., Strain, G. M., Lieb, J. P., Soper, H. V, & Crandall, P. H. (1978). A sample and hold amplifier system for stimulus artifact suppression. *Electroencephalography and clinical neurophysiology*, *44*(4), 528–31.

Baker, S. N., Olivier, E., & Lemon, R. N. (1996). 20 Hz coherent oscillations in cortical and EMG recordings from a monkey performing a precision grip task. In *Journal of Physiology-London* (Vol. 494P, pp. 64–65). Cambridge University Press.

Başar, E. (1998). *Brain Function and Oscillations: Integrative Brain Function. Neurophysiology and Cognitive Processes* (p. 293). the University of Michigan: Springer.

Basmajian, J. V. (1962). Muscles alive. Their functions revealed by electromyography. *Academic Medicine*, *37*(8), 802.

Bellemare, F., & Grassino, A. (1982). Evaluation of human diaphragm fatigue. *Journal of Applied Physiology*, *53*(5), 1196–1206.

Bendat, J. S., & Piersol, A. G. (2011). *Random Data: Analysis and Measurement Procedures (Google eBook)* (p. 640). John Wiley & Sons.

Benton, Baker, Bowman, & Waters. (1981). *Functional Electrical Stimulation - A Practical Clinical Guide* (Second.). Rancho Los Amigos Rehabilitation Engineering Center.

BerkelBike. (2011). BerkelBike. Retrieved March 13, 2011, from http://www.berkelbike.com/

Bigland-Ritchie, B. (1981a). EMG/force relations and fatigue of human voluntary contractions. *Exercise and sport sciences reviews*, *9*, 75–117.

Bigland-Ritchie, B. (1981b). Conduction velocity and EMG power spectrum changes in fatigue of sustained maximal efforts. *Journal of Applied physiology*, *51*(5), 1300–1305.

Bliss, T. V, & Lomo, T. (1973). Long-lasting potentiation of synaptic transmission in the dentate area of the anaesthetized rabbit following stimulation of the perforant path. *The Journal of physiology*, *232*(2), 331–56.

Bracken, M. B. (2012). Steroids for acute spinal cord injury. *Cochrane database of systematic reviews (Online)*, *1*, CD001046.

Brazier, M. A. B., & Casby, J. U. (1952). Cross-correlation and autocorrelation studies of electroencephalographic potentials. *Electroencephalography and clinical neurophysiology*, *4*(2), 201–11.

Brown, J. E., & Frank, J. S. (1987). Influence of event anticipation on postural actions accompanying voluntary movement. *Experimental brain research. Experimentelle Hirnforschung. Expérimentation cérébrale*, *67*(3), 645–50.

Brown, J., & Frank, J. (1987). Influence of event anticipation on postural actions accompanying voluntary movement. *Experimental Brain Research*, *67*(3), 645–50.

Brown, P. (2000). Cortical drives to human muscle: the Piper and related rhythms. *Progress in Neurobiology*, *60*(1), 97–108.

Bruun, E., & Haxthausen, E. (1991). Current conveyor based EMG amplifier with shutdown control. *Electronics letters*, *27*(23), 2172–2174.

Cambridge, N. A. (1977). Electrical apparatus used in medicine before 1900. *Proceedings of the Royal Society of Medicine*, *70*(9), 635–41.

Camic, C. L., Housh, T. J., Johnson, G. O., Hendrix, C. R., Zuniga, J. M., Mielke, M., & Schmidt, R. J. (2010). An EMG frequency-based test for estimating the neuromuscular fatigue threshold during cycle ergometry. *European journal of applied physiology*, *108*(2), 337–45.

Carr, J., & Shepherd, R. (1987). *A motor relearning programme for stroke*. *Key Issues in Neurological Physiotherapy*. Aspen Systems Corporation.

Carr, J., & Shepherd, R. (1990). A motor learning model for rehabilitation of the movementdisabled. In L. Ada & C. C (Eds.), *Key Issues in Neurological Physiotherapy.* (pp. 1–24). Oxford: Butterworth Heinemann.

Carr, J., & Shepherd, R. (1997). Task-related training improves performance of seated reaching tasks after stroke: a randomized controlled trial. *Stroke*, *28*(4), 722–8.

Cash, M. (2000). *Pocket atlas of the moving body: for all students of human biology, medicine, sports and physical therapy* (p. 68). Ebury.

Cerna, M., & Harvey, A. (2000). The fundamentals of FFT-based signal analysis and measurement. *National Instruments Application Note 041*.

Chae, J. (2008). Neuromuscular electrical stimulation for motor restoration in hemiplegia. *Topics in Stroke Rehabilitation*, *15*(5), 412–26.

Chae, J., & Fang, Z. (2001). Intramuscular electromyographically controlled neuromuscular electrical stimulation for upper limb recovery in chronic hemiplegia. *American Journal of Physical Medicine & Rehabilitation*, *80*(12), 935–41.

Challis, R. E., & Kitney, R. I. (1990). Biomedical signal processing (in four parts). *Medical & Biological Engineering & Computing*, *28*(6), 509–524.

Chapin, J., & Moxon, K. (1999). Real-time control of a robot arm using simultaneously recorded neurons in the motor cortex. *Nature Neuroscience*, *2*(7), 664–70.

Chen, CC, Hsueh, Y., & He, Z. (2008). A Novel EMG Feedback Control Method in Functional Electrical Stimulation Cycling System for Stroke Patients. In *World Academy of Science, Engineering …* (pp. 186–189). World Academy of Science, Engineering and Technology.

Chen, Chien-chih, Hsueh, Y., & He, Z. (2008). A Novel EMG Feedback Control Method in Functional Electrical Stimulation Cycling System for Stroke Patients, 186–189.

Cifrek, M., Medved, V., Tonković, S., & Ostojić, S. (2009). Surface EMG based muscle fatigue evaluation in biomechanics. *Clinical biomechanics (Bristol, Avon)*, *24*(4), 327–40. doi:10.1016/j.clinbiomech.2009.01.010

Close, R. (1972). Dynamic properties of mammalian skeletal muscles. *Physiological Reviews*, *52*(1), 129.

Conn, M. (2003). *Neuroscience in Medicine* (p. 201). Humana Press.

Conway, B., Halliday, D., & Farmer, S. (1995). Synchronization between motor cortex and spinal motoneuronal pool during the performance of a maintained motor task in man. *The Journal of Physiology*, *489*(3), 917–924.

Coombs, J. (1965). Some methods of reducing interference caused by stimulus artifacts. *Studies in physiology: presented to John C. Eccles*, *17*(5), 29–33.

Cordivari, C., Lees, A., & Misra, V. (2002). EMG-EMG coherence in writer's cramp. *Movement Disorders*, *17*(5), 1011–6.

Cozean, C., Pease, W., & Hubbell, S. (1988). Biofeedback and functional electric stimulation in stroke rehabilitation. *Arch Phys Med Rehabil*, *69*(6), 401–5.

Crago, P., Nakai, R., & Chizeck, H. (1991). Feedback regulation of hand grasp opening and contact force during stimulation of paralyzed muscle. *IEEE transactions on bio-medical engineering*, *38*(1), 17–28.

Crenna, P., Frigo, C., Massion, J., & Pedotti, A. (1987). Forward and backward axial synergies in man. *Experimental Brain Research*, *65*(3), 538–548.

CS., S. (1906). *Integrative Actions of the Nervous System.* Yale University Press.

De Luca, C J. (1984). Myoelectrical manifestations of localized muscular fatigue in humans. *Critical reviews in biomedical engineering*, *11*(4), 251–79.

De Luca, C J, & Merletti, R. (1988). Surface myoelectric signal cross-talk among muscles of the leg. *Electroencephalography and clinical neurophysiology*, *69*(6), 568–75.

De Luca, C. (2002). Surface electromyography: Detection and recording. *DelSys Incorporated*.

De Luca, C., & Adam, A. (2006). Decomposition of surface EMG signals. *Journal of Physiology*, *96*(3), 1646–1657.

De Luca, Carlo J, Adam, A., Wotiz, R., Gilmore, L. D., & Nawab, S. H. (2006). Decomposition of surface EMG signals. *Journal of neurophysiology*, *96*(3), 1646–57.

Desipres, M. (1974). An electromyographic study of competetive road cycling conditions simulated on a treadmill. In *Biomechanics IV: proceedings* (pp. 349–355). Baltimore.

Dibner, B. (1971). *Luigi Galvani: an expanded version of a biography prepared for the forthcoming edition of the Encyclopaedia Britannica : with a supplement reproducing three of the four original drawings illustrating the 1791 edition of De viribus electricitatis* (p. 24). Burndy Library.

Do, A. H., Wang, P. T., King, C. E., Abiri, A., & Nenadic, Z. (2011). Brain-computer interface controlled functional electrical stimulation system for ankle movement. *Journal of neuroengineering and rehabilitation*, *8*, 49.

Donaldson, N., Perkins, T., Fitzwater, R., Wood, D., & Middleton, F. (2000). FES cycling may promote recovery of leg function after incomplete spinal cord injury. *Spinal cord: the official journal of the International Medical Society of Paraplegia*, *38*(11), 680.

Dorel, S., & Drouet, J. (2009). Changes of pedaling technique and muscle coordination during an exhaustive exerciseb *in Sports+ Exercise*, *41*(6), 1277–86.

Drude, P. (1902). *The theory of optics* (p. 1). Longmans, Green, and Co.

Duc, S., Betik, A., & Grappe, F. (2005). EMG activity does not change during a time trial in competitive cyclists. *International journal of sports medicine*, *26*(2), 145–150.

Eberstein, A., & Beattie, B. (1985). Simultaneous measurement of muscle conduction velocity and EMG power spectrum changes during fatigue. *Muscle & nerve*, *8*(9), 768–773.

Edelstein, J. E., & Bruckner, J. (2002). *Orthotics: a comprehensive clinical approach* (p. 178). SLACK Incorporated.

Eisenstadt, M., Goldman, J. E., Kandel, E. R., Koike, H., Koester, J., & Schwartz, J. H. (1973). Intrasomatic injection of radioactive precursors for studying transmitter synthesis in identified neurons of Aplysia californica. *Proceedings of the National Academy of Medical Sciences*, *70*(12), 3371–5.

Fara, P. (2003). *An entertainment for angels: electricity in the Enlightenment* (p. 177). Icon.

Faria, I., & Cavanagh, P. R. (1978). *The physiology and biomechanics of cycling* (p. 179). Wiley.

Farina, D, Merletti, R., Indino, B., & Graven-Nielsen, T. (2004). Surface EMG crosstalk evaluated from experimental recordings and simulated signals. Reflections on crosstalk interpretation, quantification and reduction. *Methods of information in medicine*, *43*(1), 30–5.

Farina, Dario, Merletti, R., Indino, B., Nazzaro, M., & Pozzo, M. (2002). Surface EMG crosstalk between knee extensor muscles: experimental and model results. *Muscle & nerve*, *26*(5), 681–95.

Farmer, S., Gibb, J., Halliday, D., Harrison, L., James, L., Mayston, M., & Stephens, J. (2007). Changes in EMG coherence between long and short thumb abductor muscles during human development. *The Journal of Physiology*, (579), 389–402.

FESTIVAL Project (Bristol University). (1995). *Festival: EMG Amplifier Final Report* (p. D4).

Fields, R. (1987). Electromyographically triggered electric muscle stimulation for chronic hemiplegia. *Archives of physical medicine and rehabilitation*, *68*(7), 407–14.

Francisco, G., Chae, J., & Chawla, H. (1998). Electromyogram-triggered neuromuscular stimulation for improving the arm function of acute stroke survivors: a randomized pilot study. *Archives of physical medicine and rehabilitation*, *79*(5), 570–5.

Frazier, W. (1967). Morphological and functional properties of identified neurons in the abdominal ganglion of Aplysia californica. *Journal of neurophysiology*, *30*(6), 1288–1351.

Freeman, J. (1971). An electronic stimulus artifact suppressor. *Electroencephalography and Clinical Neurophysiology*, *31*(2), 170–172.

Futami, R., Seki, K., & Kawanishi, T. (2005). Application of local EMG-Driven FES to incompletely paralyzed lower extremities. In *10th Annual Conference of the International Functional Electrical Stimulation Society*.

Garcia, M. a C., Catunda, J. M. Y., Lemos, T., Oliveira, L. F., Imbiriba, L. a, & Souza, M. N. (2010). An alternative approach in muscle fatigue evaluation from the surface EMG signal. In *2010 Annual International Conference of the IEEE Engineering in Medicine and Biology* (Vol. 0, pp. 2419–2422). Ieee.

González-Izal, M., Malanda, A., Gorostiaga, E., & Izquierdo, M. (2012). Electromyographic models to assess muscle fatigue. *Journal of Electromyography and Kinesiology*, *22*(4), 501–512.

Gracanin, F. (1984). Functional electrical stimulation in external control of motor activity and movements of paralysed extremities. Research and clinical practice and applied technology in Yugoslavia. *International rehabilitation medicine*, *6*(1), 25–30.

Graupe, D. (1988). Above-and below-lesion EMG pattern mapping for controlling electrical stimulation of paraplegics to facilitate unbraced walker-assisted walking. *Journal of biomedical engineering*, *10*(4), 305–11.

Gregor, R., Green, D., & Garhammer, J. (1981). An electromyographic analysis of selected muscle activity in elite competitive cyclists. In A. Moercki, K. Fidelus, K. Kedzior, & A. Wit (Eds.), *Biomechanics VII-B* (eds., pp. 537–41). Baltimore: University Park Press.

Greig, G., Hortobayi, T., & Sargeant, A. (1985). Quadriceps surface E.M.G. and fatigue during maximal dynamic exercise in man. *Journal of physiology London*, *369*, 180.

Grieve, R, Parker, P. A., Hudgins, B., & Englehart, K. (2000). Nonlinear adaptive filtering of stimulus artifact. *IEEE transactions on bio-medical engineering*, *47*(3), 389–95.

Grieve, RCW. (1995). Adaptive stimulus artifact cancellation in biological signals using neural networks. *Engineering in Medicine and Biology Society*, *1*, 801–802.

Grosse, P., Cassidy, M., & Brown, P. (2002). EEG-EMG, MEG-EMG and EMG-EMG frequency analysis: physiological principles and clinical applications. *Clinical neurophysiology*, *113*(10), 1523–31.

Grundy, D., & Russell, J. (1986). ABC of spinal cord injury. Urological management. *British Medical Journal*, *292*(6515), 249.

Guld, C. (1959). Use of screened power transformers and output transformers to reduce stimulus artefacts. In *Proceedings of the 2nd International Medical Electronics* (pp. 24–27).

Hakansson, N. a., & Hull, M. L. (2005). Functional Roles of the Leg Muscles When Pedaling in the Recumbent Versus the Upright Position. *Journal of Biomechanical Engineering*, *127*(2), 301.

Halliday, D. (2008). Introduction to NeuroSpec. Retrieved October 19, 2010, from http://www.neurospec.org/background.html

Halliday, D. M., Conway, B. A., Farmer, S. F., & Rosenberg, J. R. (1999). Load-independent contributions from motor-unit synchronization to human physiological tremor. *Journal of neurophysiology*, *82*(2), 664–75.

Halliday, DM, & Rosenberg, J. (1999). Time and frequency domain analysis of spike train and time series data. In U. Windhorst & H. Johansson (Eds.), *Modern techniques in neuroscience research* (eds., pp. 503–543). Springer.

Halliday, DM, & Rosenberg, J. (2000). On the application, estimation and interpretation of coherence and pooled coherence. *Journal of Neuroscience Methods*, *100*(2000), 173–174.

Halliday, DM, Rosenberg, J., Amjad, A., Breeze, P., Conway, B., & Farmer, S. (1995). A framework for the analysis of mixed time series/point process data–theory and application to the study of physiological tremor, single motor unit discharges and electromyograms. *Progress in Biophysics and molecular Biology*, *64*(2-3), 237.

Hamm, T., & McCurdy, M. (1995). The use of coherence spectra to determine common synaptic inputs to motoneurone pools of the cat during fictive locomotion. In A. Taylor, M. Gladden, & R. Durbaba (Eds.), *Alpha and Gamma Motor Systems* (1st ed., pp. 309–315). New York: Springer.

Harding, G. W. (1991). A method for eliminating the stimulus artifact from digital recordings of the direct cortical response. *Computers and biomedical research, an international journal*, *24*(2), 183–95.

Harms, K., & Rioult-Pedotti, M. (2008). Transient spine expansion and learning-induced plasticity in layer 1 primary motor cortex. *The Journal of Neuroscience*, *28*(22), 5686–5690.

Harris, F. (1978). On the use of windows for harmonic analysis with the discrete Fourier transform. *Proceedings of the IEEE*, *66*(1), 51–83.

Harvey, L. (2008). *Management of spinal cord injuries: a guide for physiotherapists* (p. 297). Elsevier Health Sciences.

Hashimoto, T. (2002). A template subtraction method for stimulus artifact removal in high-frequency deep brain stimulation. *Journal of neuroscience methods*, *113*(2), 181–6.

Hausdorff, J. M., & Durfee, W. K. (1991). Open-loop position control of the knee joint using electrical stimulation of the quadriceps and hamstrings. *Medical & biological engineering & computing*, *29*(3), 269–80.

Hautier, C A, Arsac, L. M., Deghdegh, K., Souquet, J., Belli, A., & Lacour, J. R. (2000). Influence of fatigue on EMG/force ratio and cocontraction in cycling. *Medicine and science in sports and exercise*, *32*(4), 839–43.

Hautier, C.A., Arsac, L., Deghdegh, K., Souquet, J., Belli, A., & Lacour, J. R. (2000). Influence of fatigue on EMG/force ratio and cocontraction in cycling. *Medicine & Science in Sports & Exercise*, *32*(4), 839.

Hebb, D. (1950). Organization of behavior. *Journal of Clinical Psychology*, *6*(3), 307–307.

Henneman, E., Somjen, G., & Carpenter, D. (1965). Functional significance of cell size in spinal motoneurons. *Journal of neurophysiology*, *28*(3), 560–580.

Hines, A. E., Crago, P. E., Chapman, G. J., & Billian, C. (1996). Stimulus artifact removal in EMG from muscles adjacent to stimulated muscles. *Journal of neuroscience methods*, *64*(1), 55–62.

Hodges, P., & Bui, B. (1996). A comparison of computer-based methods for the determination of onset of muscle contraction using electromyography. *Electroencephalography and Clinical Neurophysiology/Electromyography and Motor Control*, *101*(6), 511–519.

Horak, F. B., & Nashner, L. M. (1986). Central programming of postural movements: adaptation to altered support-surface configurations. *Journal of neurophysiology*, *55*(6), 1369–81.

Horak, F., & Nashner, L. (1986). Central programming of postural movements: adaptation to altered support-surface configurations. *Journal of Neurophysiology*, *55*(6), 1369–81.

Housh, T. J., Perry, S. R., Bull, A. J., Johnson, G. O., Ebersole, K. T., Housh, D. J., & devries, H. A. (2000). Mechanomyographic and electromyographic responses during submaximal cycle ergometry. *European journal of applied physiology*, *83*(4), 381–387.

Houtz, S. J., & Fischer, F. J. (1959). An analysis of muscle action and joint excursion during exercise on a stationary bicycle. *The Journal of Bone and Joint Surgery*, *41*(1), 123–131.

Hsu, J., Michael, J., & Fisk, J. (2008). *AAOS atlas of orthoses and assistive devices* (p. 652). Elsevier Health Sciences.

Inglis, J. T., Horak, F., Shupert, C., & Jones-Rycewicz, C. (1994). The importance of somatosensory information in triggering and scaling automatic postural responses in humans. *Experimental Brain Research*, *101*(1), 159–164.

Jorge, M., & Hull, M. L. (1986). Analysis of EMG measurements during bicycle pedalling. *Journal of Biomechanics*, *19*(9), 683–694.

Karni, A., Meyer, G., Jezzard, P., & Ungerleider, L. (1995). Functional MRI evidence for adult motor cortex plasticity during motor skill learning. *Nature*, *377*(6545), 155–158.

Karu, Z., Durfee, W., & Barzilai, A. (1995). Reducing muscle fatigue in FES applications by stimulating with N-let pulse trains. *IEEE Transactions on Biomedical Engineering*, *42*(8), 809–817.

Kattla, S., & Lowery, M. M. (2010). Fatigue related changes in electromyographic coherence between synergistic hand muscles. *Experimental brain research. Experimentelle Hirnforschung. Expérimentation cérébrale*, *202*(1), 89–99.

KEITH, M., & PECKHAM, P. (1988). Functional neuromuscular stimulation neuroprostheses for the tetraplegic hand. *Clinical orthopaedics and related research*, *233*(Aug), 25–33.

Khaslavskaia, S., & Sinkjaer, T. (2005). Motor cortex excitability following repetitive electrical stimulation of the common peroneal nerve depends on the voluntary drive. *Experimental brain research*, *162*(4), 497–502.

Kilner, J. M., Baker, S. N., Salenius, S., Hari, R., & Lemon, R. N. (1999). 15-30 Hz coherence between rectified EMGs from human hand muscles has task-dependent modulation. *Journal of Physiology*, *516*(pt 2), 559–570.

Kilner, J. M., Baker, S. N., Salenius, S., Jousmaki, V., Hari, R., & Lemon, R. N. (1999). Task-dependent modulation of 15-30 Hz coherence between rectified EMGs from human hand and forearm muscles. *Journal of Physiology*, *516*(2), 559–570.

Kilner, J. M., Salenius, S., Baker, S. N., Jackson, A., Hari, R., & Lemon, R. N. (2003). Task-dependent modulations of cortical oscillatory activity in human subjects during a bimanual precision grip task. *Neuroimage*, *18*(1), 67–73.

Kirsch, R., & Rymer, W. (1987). Neural compensation for muscular fatigue: evidence for significant force regulation in man. *Journal of neurophysiology*, *57*(6), 1893.

Kjaer, M. (2000). Why exercise in paraplegia? *British Journal of Sports Medicine*, *34*(5), 322–323.

Klein, M., & Kandel, E. R. (1978). Presynaptic modulation of voltage-dependent Ca2+ current: mechanism for behavioral sensitization in Aplysia californica. *Proceedings of the National Academy of Sciences of the United State of America*, *75*(7), 3512–3516.

Knaflitz, M., & Molinari, F. (2003). Assessment of muscle fatigue during biking. *IEEE Transaction on Neural Systems and Rehabilitation Engineering*, *11*(1), 17–23.

Knaflitz， M, Merletti， R, & Catani， F. (1988). Crosstalk assessment in human thigh muscles. *"Electrophysiological Kinesiology*, (Elsevier Science Publishers B. V. (Biomedical Division)), 261–264.

Koh, T. J., & Grabiner, M. D. (1993). Evaluation of methods to minimize cross talk in surface electromyography. *Journal of biomechanics*, *26 Suppl 1*, 151–7.

Kriegstein, A. R., Castellucci, V., & Kandel, E. R. (1974). Metamorphosis of Aplysia californica in laboratory culture. *Proceedings of the National Academy of Sciences of the United States of America*, *71*(9), 3654–3658.

Kuiken, T. A., Lowery, M. M., & Stoykov, N. S. (2003). The effect of subcutaneous fat on myoelectric signal amplitude and cross-talk. *Prosthetics and orthotics international*, *27*(1), 48–54.

Lawrence, J. H., & De Luca, C. J. (1983). Myoelectric signal versus force relationship in different human muscles. *Journal of applied physiology: respiratory, environmental and exercise physiology*, *54*(6), 1653–9.

Lenman, J. A. R., & Ritchie, A. E. (1987). *Clinical electromyography* (p. 218). Churchill Livingstone.

Lindsay, K. W., Bone, I., & Fuller, G. (2010). *Neurology and Neurosurgery Illustrated* (p. 612). Churchill Livingstone.

Lippold, O. (1952). The relation between integrated action potentials in a human muscle and its isometric tension. *The Journal of physiology*, *117*(4), 492.

Liverman, C. (2005). *Spinal cord injury: progress, promise, and priorities* (p. 343). National Academies Press.

Luft, A. R., & Buitrago, M. M. (2005). Stages of motor skill learning. *Molecular neurobiology*, *32*(3), 205–216.

Lyon, D. (2009). The Discrete Fourier Transform, Part 4: Spectral Leakage. *Journal of Object Technology*, *8*(7).

Machado, S., Araújo, F., Paes, F., Velasques, B., Cunha, M., Budde, H., … Ribeiro, P. (2010). EEG-based brain-computer interfaces: an overview of basic concepts and clinical applications in neurorehabilitation. *Reviews in the neurosciences*, *21*(6), 451–68.

MacIntosh, B. R., Gardiner, P. F., & McComas, A. J. (2006). *Skeletal muscle: form and function* (2, illustr., p. 423). Human Kinetics.

MAGLADERY, J. W., PORTER, W. E., PARK, A. M., & TEASDALL, R. D. (1951). Electrophysiological studies of nerve and reflex activity in normal man. IV. The two-neurone reflex and identification of certain action potentials from spinal roots and cord. *Bulletin of the Johns Hopkins Hospital*, *88*(6), 499–519.

Mangold, S., Keller, T., & Dietz, V. (2005). Transcutaneous functional electrical stimulation for grasping in subjects with cervical spinal cord injury. *Spinal Cord*, *43*(1), 1–13.

Marple, S., & Marino, C. (2005). Coherence in signal processing: a fundamental redefinition. In *Conference Record of the Thirty-Eighth Asilomar Conference* (Vol. 1, pp. 1035–1038).

McCallum, R. W. (1998). *Adaptive stimulus artifact cancellation in gastric myoelectrical signals*. *Proceedings of the 20th Annual International Conference of the IEEE Engineering in Medicine and Biology Society. Vol.20 Biomedical Engineering Towards the Year 2000 and Beyond (Cat. No.98CH36286)* (pp. 1636–1639). IEEE.

McDonald, J., & Becker, D. (2002). Late recovery following spinal cord injury: case report and review of the literature. *Journal of Neurosurgery: Spine*.

McDonald, J. W. (2004). Repairing the damaged spinal cord: from stem cells to activity-based restoration therapies. *Clinical neurosurgery*, *51*, 207–27.

McFarland, D. J., Miner, L. A., Vaughan, T. M., & Wolpaw, J. R. (2000). Mu and beta rhythm topographies during motor imagery and actual movements. *Brain topography*, *12*(3), 177–86.

McGill, K., & Cummins, K. (2007). On the nature and elimination of stimulus artifact in nerve signals evoked and recorded using surface electrodes. *IEEE transactions on bio-medical engineering*, *29*(2), 1239–137.

Merletti, R, Knaflitz, M., & De Luca, C. J. (1990). Myoelectric manifestations of fatigue in voluntary and electrically elicited contractions. *Journal of applied physiology (Bethesda, Md. : 1985)*, *69*(5), 1810–20.

Merletti, R., Knaflitz, M., & De Luca, C. (1992). Electrically evoked myoelectric signals. *Crit Rev Biomed Eng*, *19*(4), 293–340.

Merletti, Roberto, & Parker, P. A. (2004). *Electromyography: Physiology, Engineering, and Noninvasive Applications* (p. 494). IEEE/John Wiley & Sons.

Müller-Putz, G. R., Scherer, R., Pfurtscheller, G., & Rupp, R. (2005). EEG-based neuroprosthesis control: a step towards clinical practice. *Neuroscience letters*, *382*(1-2), 169–74.

Myers, L. (2003). Rectification and non-linear pre-processing of EMG signals for cortico-muscular analysis. *Journal of Neuroscience Methods*, *124*(2), 157–165.

Nakamura, M., Shibasaki, H., & Nishida, S. (1990). Method for recording short latency evoked potentials using an EKG artifact elimination procedure. *Journal of biomedical engineering*, *12*(1), 51–56.

Nashner, L M, Shumway-Cook, A., & Marin, O. (1983). Stance posture control in select groups of children with cerebral palsy: deficits in sensory organization and muscular coordination. *Experimental brain research. Experimentelle Hirnforschung. Expérimentation cérébrale*, *49*(3), 393–409.

Nashner, L. M., & Forssberg, H. (1986). Phase-dependent organization of postural adjustments associated with arm movements while walking. *J Neurophysiol*, *55*(6), 1382–1394.

National Institute of Neurological Disorders and Stroke (NINDS). (n.d.). Retrieved June 12, 2010, from http://www.ninds.nih.gov/

Nidd Valley Medical website. (n.d.). Nidd Valley Medical website. Retrieved February 17, 2011, from http://www.niddvalley.co.uk/index.asp

Nielsen, J. (2002). Motoneuronal drive during human walking. *Brain research reviews*, *40*(1-3), 192–201.

Nigg, B., MacIntosh, B., & Mester, J. (2000). *Biomechanics and biology of movement* (p. 468). Human Kinetics .

Norton, J., Fry, M., Day, B., & Donaldson, N. (2004). Simple EMG Control for FES-Cycling. In *9th Annual Conference of the International Functional Electrical Stimulation Society*.

Norton, J., Gorassini, M., & Gorassini, M. A. (2006). Changes in cortically related intermuscular coherence accompanying improvements in locomotor skills in incomplete spinal cord injury. *Journal of neurophysiology*, *95*(4), 2580–2589.

Norton, J., Wood, D., & Day, B. (2004). Is the spinal cord the generator of 16-Hz orthostatic tremor? *Journal of Neurology*, *62*(4), 632–634.

Norton, J., Wood, D., & Marsden, J. (2003). Spinally generated electromyographic oscillations and spasms in a low-thoracic complete paraplegic. *Movement Disorders: Offical Journal of the Movement Disorder Society*, *18*(1), 101–106.

O'Keeffe, D., Lyons, G., Donnelly, A., & Byrne, C. (2001). Stimulus artifact removal using a software-based two-stage peak detection algorithm. *Journal of Neuroscience Methods*, *109*(2), 137–145.

Ounjian, M., Roy, R., Eldred, E., Garfinkel, A., Payne, J., Armstrong, A., … Edgerton, V. (1991). Physiological and developmental implications of motor unit anatomy. *Journal of Neurobiology*, *22*(5), 547–559.

Peasgood, W., Whitlock, T., Bateman, A., & Fry, M. (2000). EMG-controlled closed loop electrical stimulation using a digital signal processor. *Electronic Letters*, *36*(22), 1832–1933.

Perkins, T., Donaldson, N., Fitzwater, R., Phillips, G., & Wood, D. (2001). Leg powered paraplegic cycling system using surface functional electrical stimulation. In *7 th Vienna internationnal workshop on functional eleectrical stimulation* (pp. 36–39).

Petrofsky, J. (1979). Frequency and amplitude analysis of the EMG during exercise on the bicycle ergometer. *European Journal of Applied Physiology and Occupational Physiology*, *41*(1), 1–15.

Pockett, S., & Figurov, A. (1993). Long-term potentiation and depression in the ventral horn of rat spinal cord in vitro. *Neuroreport*, *4*(1), 97–99.

Polgar, J., & Johnson, M. (1973). Data on fibre size in thirty-six human muscles: an autopsy study. *Journal of the Neurological Science*, *19*(3), 307–318.

Popovic, M., Keller, T., Pappas, I., Dietz, V., & Morari, M. (2001). Surface-stimulation technology for grasping and walking neuroprostheses. *IEEE Engineering in Medicine and Biology Magazine*, *20*(1), 82–93.

Popovic, M., Thrasher, T., & Adams, M. (2006). Functional electrical therapy: retraining grasping in spinal cord injury. *Spinal cord*, *44*(3), 143–151.

Psek, J. a, & Cafarelli, E. (1993). Behavior of coactive muscles during fatigue. *Journal of applied physiology (Bethesda, Md. : 1985)*, *74*(1), 170–5.

Ramon y Cajal, S. (1893). Neue Darstellung vom Histologischen Bau des Centralnervensystem. *Arch. Anat. Entwick*, 319–428.

RANDOM.ORG - Sequence Generator. (2010). Retrieved June 05, 2010, from http://www.random.org/sequences/?min=3&max=7&col=1&format=html&rnd=new

Restorative therapies website, R. (2011). Restorative Therapies FES powered systems. Retrieved March 13, 2011, from http://www.restorative-therapies.com/home

Rioult-Pedotti, M., Donoghue, J., & Dunaevsky, A. (2007). Plasticity of the synaptic modification range. *Journal of Neurophysiology*, *98*(6), 3688–3695.

Roby, R., & Lettich, E. (1975). A simplified circuit for stimulus artifact suppression. *Electroencephalography and Clinical Neurophysiology*, *39*(1), 85–87.

Routh, G., & Durfee, W. (2003). Doublet stimulation to reduce fatigue in electrically stimulated muscle during controlled leg lifts. In *Engineering in Medicine and Biology Society, 2003. Proceedings of the 25th Annual International Conference of the IEEE* (pp. 1531–1534 Vol.2).

Rushton, D. (2003). Functional electrical stimulation and rehabilitation–an hypothesis. *Medical engineering & physics*, *25*(1), 75–78.

Ryan, M. M., & Gregor, R. J. (1992). EMG profiles of lower extremity muscles during cycling at constant workload and cadence. *Journal of Electromyography and Kinesiology*, *2*(2), 69–80.

Sanderson, D., & Black, A. (2003). The effect of prolonged cycling on pedal forces. *Journal of sports sciences*, *21*(3), 191–199.

Sarre, G., & Lepers, R. (2005). Neuromuscular function during prolonged pedalling exercise at different cadences. *Acta physiologica scandinavica*, *185*(4), 321–328.

Saunders, M. J., EVANS, E. M., ARNGRIMSSON, S. A., ALLISON, J. D., WARREN, G. L., & others. (2000). Muscle activation and the slow component rise in oxygen uptake during cycling. *Medicine & Science in Sports & Exercise*, *32*(12), 2040.

Scott, T., Peckham, P., & Kilgore, K. (1996). Tri-state myoelectric control of bilateral upper extremity neuroprostheses for tetraplegic individuals. *IEEE Transactions on Rehabilitation Engineering*, *4*(4), 251–263.

Sedra, A. S., & Smith, K. C. (1997). *Microelectronic Circuits (Oxford Series in Electrical Engineering)* (p. 1360). Oxford University Press, USA.

SENIAM. (2010). SENIAM: surface EMG for non-invasive assessment of muscles. Retrieved March 08, 2011, from http://www.seniam.org/

Sennels, S., Biering-Sorensen, F., Andersen, O., & Hansen, S. (1997). Functional neuromuscular stimulation controlled by surface electromyographic signals produced by volitional activation of the same muscle: adaptive removal of the stimulation artefact. *IEEE Transactions on Rehabilitation Engineering*, *5*(2), 195–206.

Shaw, C., & McEachern, J. (2013). *Toward a Theory of Neuroplasticity* (p. 468). Psychology Press.

Sherrington, C. (1906). The integrative action of the nervous system. *compendium of Sherrington's Silliman lectures, delivered at Yale University*, 150–180.

Shin, J. O. (2003). *Clinical electromyography: nerve conduction studies* (p. 848). Lippincott Williams & Wilkins.

Shumway-Cook, A., & Woollacott, M. H. (2007). *Motor control: translating research into clinical practice* (p. 612). Lippincott Williams & Wilkins.

So, R. C. H., Ng, J. K.-F., & Ng, G. Y. F. (2005). Muscle recruitment pattern in cycling: a review. *Physical Therapy in Sport*, *6*(2), 89–96.

Solomonow, M., Baratta, R., Bernardi, M., Zhou, B., Lu, Y., Zhu, M., & Acierno, S. (1994). Surface and wire EMG crosstalk in neighbouring muscles. *Journal of electromyography and kinesiology : official journal of the International Society of Electrophysiological Kinesiology*, *4*(3), 131–42.

Solomonow, M., Baratta, R., & Miwa, T. (1985). A technique for recording the EMG of electrically stimulated skeletal muscle. *Orthopedics*, *8*(4), 492–495.

Steel, R. G. D., & Torrie, J. H. (1960). *Principles and procedures of statistics: with special reference to the biological sciences* (p. 481). McGraw-Hill.

Stulen, F. B., & DeLuca, C. J. (1981). Frequency parameters of the myoelectric signal as a measure of muscle conduction velocity. *IEEE transactions on bio-medical engineering*, *28*(7), 515–23.

Tanzi, E. (1893). I fatti e le induzione nell'odierna istologia del sistema nervoso. Riv. sper. *Freniat. Med. leg Alien. ment*, *19*, 419–472.

Tator, C. (1995). Update on the pathophysiology and pathology of acute spinal cord injury. *Brain Pathology*, *5*(4), 407–413.

Tator, C. H. (1996). Experimental and clinical studies of the pathophysiology and management of acute spinal cord injury. *The journal of spinal cord medicine*, *19*(4), 206–14.

Tator, C. H. (1998). Biology of neurological recovery and functional restoration after spinal cord injury. *Neurosurgery*, *42*(4), 696–707; discussion 707–8.

Taylor, P., Burridge, J., Dunkerley, A., Wood, D., Norton, J., Singleton, C., & Swain, I. (1999). Clinical use of the Odstock dropped foot stimulator: its effect on the speed and effort of walking. *Archives of physical medicine and rehabilitation*, *80*(12), 1577–1583.

Taylor, P. N., Burridge, J. H., Dunkerley, A. L., Lamb, A., Wood, D. E., Norton, J. A., & Swain, I. D. (1999). Patients‘ perceptions of the Odstock Dropped Foot Stimulator (ODFS). *Clinical Rehabilitation*, *13*(5), 439–446.

Therapeutic Alliances Inc website, I. (2011). Therapeutic Alliances Inc. Retrieved March 13, 2011, from http://www.musclepower.com/

Thorsen, R. (2002). An artefact suppressing fast-recovery myoelectric amplifier. *Biomedical Engineering, IEEE Transactions on*, *46*(6), 764–766.

Thorsen, Rune. (1997). *Restoration of Hand Function in Tetraplegics Using Myoelectrically Controlled Functional Electrical Stimulation of the Controlling Muscle*. Technical University of Denmark, Department of Mathematical Modeling.

Vodovnik, L., & Long, C. (2008). Myo-electric control of paralyzed muscles. *IEEE Transactions on Biomedical Engineering*, *12*(3-4), 169–172.

Von Tscharner, V. (2002). Time-frequency and principal-component methods for the analysis of EMGs recorded during a mildly fatiguing exercise on a cycle ergometer. *Journal of electromyography and kinesiology : official journal of the International Society of Electrophysiological Kinesiology*, *12*(6), 479–92.

Vredenbregt, J., & Rau, G. (1973). Surface electromyography in relation to force, muscle length and endurance. *New developments in electromyography and clinical neurophysiology*, *1*, 607–622.

Walker, D., & Kimura, J. (1978). A fast-recovery electrode amplifier for electrophysiology. *Electroencephalography and Clinical Neurophysiology*, *45*(6), 789–792.

Wang, P., King, C., Chui, L., Nenadic, Z., & Do, A. (2010). BCI controlled walking simulator for a BCI driven FES device. In *RESNA Annual Conference*. Las Vegas.

Watson, C., Paxinos, G., & Kayalioglu, G. (2008). *The spinal cord: a Christopher and Dana Reeve Foundation text and atlas* (p. 387). Academic Press.

Website, A. C. (2011). FES Cycling - Active FES Fitness for spinal cord injured. Retrieved March 13, 2011, from http://fescycling.com/

Whittington, R., Giovangrandi, L., & Kovacs, G. (2005). A closed-loop electrical stimulation system for cardiac cell cultures. *IEEE Transactions on Biomedical Engineering*, *52*(7), 1261–1270.

Wichmann, T. (2000). A digital averaging method for removal of stimulus artifacts in neurophysiologic experiments. *Journal of neuroscience methods*, *98*(1), 57–62.

Wolpaw, J., & Birbaumer, N. (2002). Brain-computer interfaces for communication and control. *Clinical neurophysiology*, *113*, 767–791.

Woollacott, M. H., von Hosten, C., & Rösblad, B. (1988). Relation between muscle response onset and body segmental movements during postural perturbations in humans. *Experimental brain research. Experimentelle Hirnforschung. Expérimentation cérébrale*, *72*(3), 593–604.

Xu, T., Yu, X., Perlik, A., & Tobin, W. (2009). Rapid formation and selective stabilization of synapses for enduring motor memories. *Nature*, (462), 915–919.

Yeom, H. J., Park, Y. C., Yoon, Y. R., Shin, T. M., & Yoon, H. R. (2004). An adaptive M-wave canceler for the EMG controlled functional electrical stimulator and its FPGA implementation. In *Conference proceedings : Annual International Conference of the IEEE Engineering in Medicine and Biology Society. IEEE Engineering in Medicine and Biology Society.* (Vol. 6, pp. 4122–5).

Yvonnes neuropsychology pictures, P. (2011). Yvonnes neuropsychology pictures. Retrieved March 16, 2011, from http://www.glittra.com/yvonne/neuropics.html

Zsolt L. Kovacs, Timothy L. Johnson, D. S. S. (1979). Estimation of the distribution of conduction velocities in peripheral nerves. *Computers in Biology and Medicine*, *9*(4), 281–293.

Zuniga, E. N., & Simons, E. G. (1969). Nonlinear relationship between averaged electromyogram potential and muscle tension in normal subjects. *Archives of physical medicine and rehabilitation*, *50*(11), 613–20.